Izadian, Jamaledin

TWO-DIMENSIONAL EM-SCATTERING BY BURIED PENETRABLE NON-CIRCULAR CYLINDERS USING THE METHOD OF MOMENTS

The Ohio State University PH.D. 1983

PLEASE NOTE:

In all cases this material has been filmed in the best possible way from the available copy. Problems encountered with this document have been identified here with a check mark __√__.

1. Glossy photographs or pages _____
2. Colored illustrations, paper or print _____
3. Photographs with dark background _____
4. Illustrations are poor copy _____
5. Pages with black marks, not original copy _____
6. Print shows through as there is text on both sides of page _____
7. Indistinct, broken or small print on several pages __✓__
8. Print exceeds margin requirements _____
9. Tightly bound copy with print lost in spine _____
10. Computer printout pages with indistinct print __✓__
11. Page(s) _____ lacking when material received, and not available from school or author.
12. Page(s) _____ seem to be missing in numbering only as text follows.
13. Two pages numbered _____. Text follows.
14. Curling and wrinkled pages _____
15. Other _____

TWO DIMENSIONAL EM-SCATTERING BY BURIED PENETRABLE NON-CIRCULAR CYLINDERS USING THE METHOD OF MOMENTS

Dissertation

Presented in Partial Fulfillment of the Requirement for the Degree Doctor of Philosophy in the Graduate School of The Ohio State University

By

Jamaledin Izadian, B.S.E.E., M.S.E.E.

The Ohio State University

1982

Reading Committee:

Leon Peters, Jr.
Jack H. Richmond
W.D. Burnside

Approved By

Leon Peters Jr.
Advisor

Department of Electrical Engineering

ACKNOWLEDGEMENT

The author wishes to thank his graduate advisor Professor Leon Peters, Jr. for his guidance, many useful suggestions and his critical review of the dissertation draft. A very special gratitude is due to Professor Jack H. Richmond for giving so generously of his valuable time, and many stimulating discussions which proved to be priceless. Much credit is due to Professor Richmond for his special skill in setting up the problem and putting everything in perspective, and for his expertise in numerical techniques which provided a solid foundation for this effort.

The author also wishes to thank Dr. Jonathan D. Young for suggesting the problem, for his continuous support and interest, and for bringing about a continuous financial support for the project. Additionally, many thanks go to Professor Walter D. Burnside for his participation in the reading committee, and his review of the dissertation draft.

Finally, the professional quality of the draftings by Jim Gibson and Bob Davis, and the technical typing by Pat Wassmuth is gratefully acknowledged.

VITA

April ,1955 . . . . . Born - Meshed, Iran

1980 . . . . . M.S.E.E., Ohio State University, Columbus, Ohio

1978 . . . . . B.S.E.E., University of Kentucky, Lexington, Kentucky

PUBLICATIONS

"Computation of Scattering from Penetrable Cylinders with Improved Numerical Efficiency", to be published in the October issue of the IEEE Transactions on Geoscience and Remote Sensing.

"Two Dimensional EM-Scattering by Buried Penetrable Noncircular Cylinders Using the Method of Moments", The Ohio State University ElectroScience Laboratory, Department of Electrical Engineering. Ph.D. Dissertation, March 1983.

"Measurement of Surface Coupled Antennas for Subsurface Radar Probing", Proceedings of the 1982 Antenna Measurement Techniques Association meeting, held at Physical Sciences Laboratory, New Mexico State University, Las Cruces, New Mexico (Also an oral presentation).

"Coal Pile Electromagnetic Sensing Research", co-author, The Ohio State University ElectroScience Laboratory, Department of Electrical Engineering. Report No. 712861-4, June 1981. Prepared under Contract No. TVA-53983A for Tennessee Valley Authority.

"An Underground Near Field Antenna Pattern Range", a master's thesis. Also Report No. 529081-3, July 1980, The Ohio State University ElectroScience Laboratory, Department of Electrical Engineering. Prepared under Contract No. 5014-352-0234 for Gas Research Institute.

"An Efficient Computational Model for Calculating the EM-Scattering from Penetrable Cylinders of Infinite Length", to be presented at the 1983 International IEEE/AP-S Symposium and National Radio Science (URSI) meeting at the University of Houston, May 23-26.

FIELDS OF STUDY

Major Field: Electromagnetics

Professor Jack H. Richmond

Professor Leon Peters, Jr.

Professor R.G. Kouyoumjian

Professor C. Levis

Minor Fields:

Communications:

Professor C.W. Warren

Professor Dean Davis

Digital Systems:

Professor W. Olson

Mathematics:

Professor Colson

Professor J.T. Scheick

TABLE OF CONTENTS

LIST OF FIGURES

CHAPTER I

INTRODUCTION

Rigorous solutions for scattering problems may be obtained if there exists a coordinate system in which the field components can be separated. In practice, these cases are few, and occur only for special scatterers, i.e., spheres, circular cylinders, etc. To solve problems of more general nature, an integral equation formulation may be used. A numerical technique such as the moment method is then used to solve the integral equation. In this work the attention is focused on the penetrable non-circular cylinders of infinite length, and the Plane Wave Expansion Galerkin (PWEG) is employed to solve the integral equations.

A basic introduction to the moment method is given by Harrington [1] and various examples and numerical results are presented. Richmond [2-3] introduced solutions for scattering by dielectric cylinders of infinite length, where he employed the Pulse Basis Point Matching (PBPM) technique.

Although a variety of conventional techniques has been used by geophysicists for many years as suggested by Ward [4], many improvements are being made and various EM-techniques are being introduced. Ward [4]

provides an excellent historical overview of geophysical methods and their future developments.

Parry et al. [5] treat the problem of EM-scattering from cylinders of arbitrary cross-section in a conducting half space by obtaining some integral equations in terms of the surface currents and solving them by expanding the unknown currents in terms of some quadradic algebraic functions and point matching.

D'Yakonov [6] treated the problem of a circular cylinder in a homogeneous half space. This paper is rather involved and difficult to follow. This problem was later considered by Howard [7], and some numerical solutions were given. Ogunade [8] also considered D'Yakonov's [6] problem and provided some numerical results, however, there seems to have been an incorrect symmetry in equation (21) in this paper (Richmond, Peters [9]). Ogunade and Dosso present more numerical results in [10].

During the past decade, considerable research and development effort has been devoted to underground radar at the ElectroScience Laboratory. Most efforts have been concentrated on system design [16-19] propagation and scattering [20-26], experimental measurement and data collection [27-29] identification and imaging [30-35] and computational modeling [36].

The purpose of this dissertation is to develop an efficient computational model for EM-scattering by lossy dielectric cylinders of infinite length buried in the earth. It is hoped that a frequency spectrum obtained from the computational model and a future extension of

the model would enable obtaining transient EM-scattering results for the underground radar targets. It is believed that an unwanted filled trench response in the transient echo of a buried target may be identified and ultimately eliminated which in turn would help to enhance the desired echo. An effort, however, has been made to provide a formulation for general cases, but specific examples are given for rectangular cylinders.

Additionally, it is hoped that the numerical results given here will provide additional insight and lead to a simple explanation of the effect of the air-earth interface so that some simple approximations may be employed. One such an approximation is the use of the plane wave reflection and transmission coefficients at the air-earth interface to account for most of the interface effects. This, in turn, would eliminate the costly evaluation of Sommerfeld integrals.

The formulation of the integral equations are based on the polarization current representation for dielectric bodies proposed by Rhodes [37], wherein a scatterer may be replaced by a volume of polarization currents which produce the correct scattered field everywhere. The integral equations obtained involve the electric field inside the scatterer as the unknown function. These integral equations are then solved by expanding the unknown fields in terms of some plane waves with unknown coefficients. Galerkin's method is used to obtain a set of N simultaneous linear equations with N unknowns, where the N unknowns are the coefficients of the plane waves in the expansion. A simple matrix inversion and multiplication then gives the solution for

the unknown coefficient. The problem of scattering by cylindrical inhomogeneities in a lossy medium is presented by Peters and Richmond [38], volume polarization currents are used to obtain an E-integral equation and an H-integral equation which then are solved by the moment method. The same approach is taken here except that all the integral equations in this dissertation are based on the electric field. This proved to be more stable for obtaining a convergent solution.

A. THE STRUCTURE OF THE DISSERTATION

This dissertation is basically composed of two parts: The first part deals only with the scatterers in a homogeneous ambient medium in the absence of the air-earth interface. The second part deals with buried scatterer where a Sommerfeld integral is used to account for the effects of the air-earth interface.

Chapter II gives a general formulation for the EM-scattering by lossy dielectric cylinder immersed in a homogeneous lossy medium for an electric and a magnetic line source excitations. In Chapter III, the plane wave expansion is introduced, the E-wave scattering formulation derived in Chapter II are specialized to rectangular cylindrical scatterers. In addition, some numerical results are given and discussed. In Chapter IV, a similar treatment of the H-wave scattering model is given and some specific results are provided for a rectangular cylindrical scatterer.

In Chapter V, a basic introduction to the air-earth interface effect is made for both an electric and a magnetic line source on the interface. Some radiation patterns are included and discussed. In addition, some helpful hints are given for evaluating the Sommerfeld type integrals encountered in this dissertation. In Chapter VI, a general moment method formulation is given for the EM-scattering by buried cylindrical geometries for an electric and a magnetic line source excitations. These scattering models are then specialized for buried rectangular cylindrical geometries for an electric line source excitation in Chapter VII, and a magnetic line source excitation in Chapter VIII. In Chapter IX, a discussion of the computer time required is given. A comparison is made with the computation time for a Pulse Basis Point Matching (PBPM) and a Plane Wave Expansion Galerkin (PWEG) solutions for the same target.

The time harmonic convention $e^{j\omega t}$ is assumed throughout this work and suppressed.

CHAPTER II

FORMULATION OF MOMENT METHOD

A. INTRODUCTION

A two-dimensional moment method formulation is to be developed in this chapter for the scattered fields of a lossy dielectric cylinder immersed in a homogeneous lossy ambient medium. Both electric and magnetic line currents are to be used as sources. The solution will have the capability of treating a cylinder of rather general cross section. Figure 1(a) shows the general geometry whereas Figure 1(b) shows the special case of most interest herein, i.e., a rectangular cylinder. This is because the target of interest at present happens to be the refilled trench in which a pipe has been placed. The region inside the cylinder is designated as Region I with electrical parameters ε_1, μ_0, and σ_1, and the region outside the cylinder is designated as Region II with constituative parameters ε_2, μ_0, and σ_2. In the rectangular model it is assumed that x-dimension is greater than or equal to y-dimension, and that the length and width of the rectangular cylinder are 2a and 2b meters, respectively. The

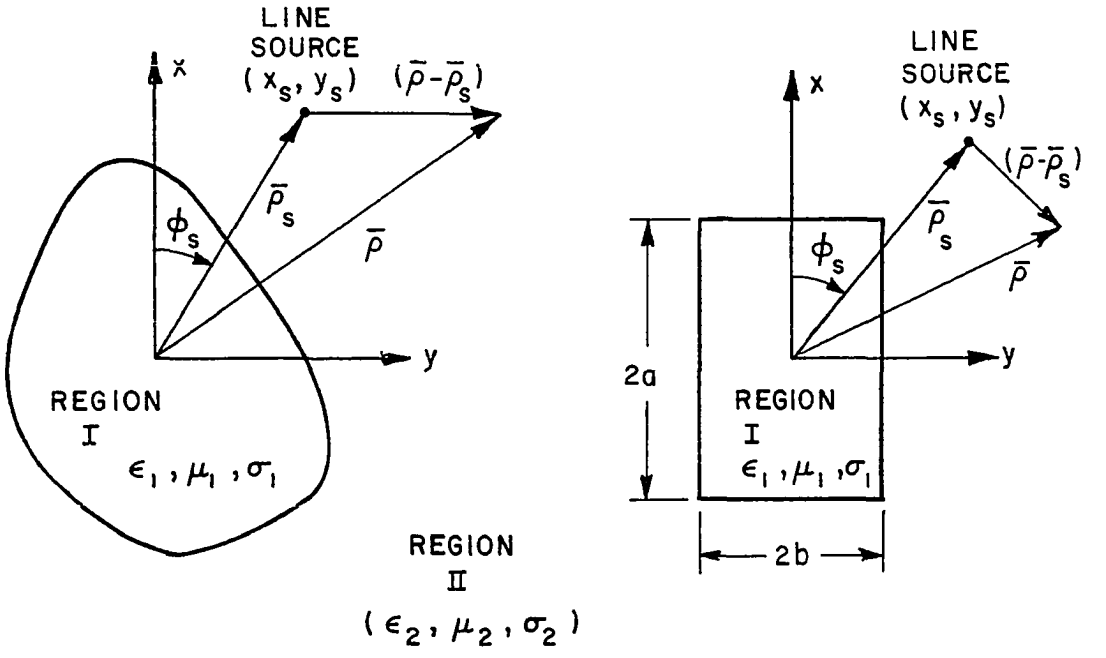

(a) ARBITRARY CROSS SECTION (b) RECTANGULAR CROSS SECTION

Figure 2-1. Electromagnetic scattering model for two-dimensional lossy dielectric rectangular cylinders (region I) immersed in a lossy homogeneous ambient medium (region II).

coordinates of the line source are designated by (x_s,y_s). Region I is considered to be homogeneous and source-free.

Peters, et al. [9], has presented a two-dimensional moment method formulation for both parallel and perpendicular polarizations of the incident field. When the incident electric field is in the z direction, the formulation to be used follows directly from Peters, et al. [9]. This shows a great numerical stability and convergence. This solution for the orthogonal excitation proved to be unstable. Thus for the TE_z case, a new formulation is introduced which does exhibits improved numerical stability and convergence.

The purposes of this chapter are basically the presentation of the theory for the electromagnetic scattering models and the formulation of numerical technique to solve these mathematical formulas. In this chapter the general model of Figure 2-1a is treated for any arbitrarily shaped cross-section of a two-dimensional cylinder. This will be specialized for the model of Figure 2-1b in the next chapter.

B. E-WAVE SCATTERING BY TWO-DIMENSIONAL LOSSY DIELECTRIC CYLINDERS

1. Electric Line Source Excitation

An infinitely long time harmonic electric line source with uniform current of 1 ampere is radiating in a homogeneous medium II with complex propagation constant γ_2, produces a field

$$\overline{E}^i = \frac{-j\omega\mu_0}{2\pi} K_0(\gamma_2|\overline{\rho}-\overline{\rho}_s|)\,\hat{z} \tag{2.1}$$

where K_0 is the modified Bessel function

$$\gamma_2 = j\omega\sqrt{\hat{\varepsilon}_2\mu_0} \quad , \tag{2.2a}$$

$$\omega = 2\pi f \quad , \tag{2.2b}$$

$$\hat{\varepsilon}_2 = \varepsilon_0\left(\varepsilon_{r_2} - j\frac{\sigma_2}{\omega\varepsilon_0}\right) \quad , \tag{2.2c}$$

$$|\bar{\rho}-\bar{\rho}_s| = \sqrt{(x-x_s)^2 + (y-y_s)^2} \quad , \quad \text{and} \tag{2.3}$$

(x_s, y_s) is the coordinate of the location of the line source. When the above line source is radiating in the presence of the scatterer, the total field everywhere is the sum of the incident field and the scattered field. This field is given by

$$\bar{E}(x,y) = \bar{E}^i(x,y) + \bar{E}^s(x,y) \quad , \tag{2.4}$$

where $\bar{E}^i(x,y)$ is the field radiated by the source in the ambient homogeneous medium II (see Figure 2) in the absence of the scatterer given by Eq. (2.1),

$\bar{E}(x,y)$ is the total field observed when the source radiates in the presence of the scatterer.

Both $\bar{E}^i(x,y)$ and $\bar{E}(x,y)$ are measurable quantities, and difference of these two fields renders the scattered field $\bar{E}^s(x,y)$.

To calculate $\bar{E}^s(x,y)$, one may replace the scatterer by a volumetric equivalent polarization current $\bar{J}_{eq}$ which when radiating in a homogeneous ambient medium gives the correct scattered field. The equivalent volume polarization current is given by Harrington [39].

$$\bar{J}_{eq}(x,y) = j\omega(\hat{\varepsilon}_1-\hat{\varepsilon}_2)\bar{E}^I(x,y) \quad , \tag{2.5}$$

where $\hat{\varepsilon}_1$ and $\hat{\varepsilon}_2$ are assumed to be constant throughout each respective region (homogeneous), and

$\underline{E}^{I}_{(x,y)}$ is the total unknown field in region I.

$E^{s}_{z}(x,y)$ is given by

$$E^{s}_{z}(x,y) = \frac{-j\omega\mu_0}{2\pi} \iint_{cs} J_{eq}(x',y') K_0(\gamma_2 |\bar{\rho}-\bar{\rho}'|) ds' \quad , \tag{2.6a}$$

where ds' is the differential cross sectional area of the cylinder, and

$$|\bar{\rho}-\bar{\rho}'| = \sqrt{(x-x')^2 + (y-y')^2} \quad . \tag{2.6b}$$

From Eq. (2.5), (2.6) and (2.4), the following integral equation is obtained

$$E^{i}_{z}(x,y) = E^{I}_{z}(x,y) - \frac{\omega^2\mu_0(\hat{\varepsilon}_1-\hat{\varepsilon}_2)}{2\pi} \iint_{cs} E^{I}_{z}(x',y') K_0(\gamma_2 |\bar{\rho}-\bar{\rho}'|) ds' \quad . \tag{2.7}$$

The unknown function in the above integral equation is $E^{I}_{z}(x,y)$ or the field inside the scatterer. The unknown function appears both inside and outside the integral, thus this is a Fredholm integral equation of the second kind. To obtain a solution, E^{I}_{z} is expanded in terms of some known basis function $F_{n(x,y)}$ with unknown coefficient C_n's.

$$E^{I}_{z(x,y)} = \sum_{n=1}^{N} C_n F_{n(x,y)} \quad . \tag{2.8}$$

Substituting the above expansion in Equation (2.7) gives

$$E^{i}_{z(x,y)} = \sum_{n=1}^{N} C_n \left[F_{n(x,y)} - \frac{\omega^2\mu_0(\hat{\varepsilon}_1-\hat{\varepsilon}_2)}{2\pi} \iint_{cs} F_{n(x',y')} K_0(\gamma_2 |\bar{\rho}-\bar{\rho}'|) ds' \right] , \tag{2.9}$$

where the C_n's are unknown. To evaluate C_n a set of simultaneous linear equations may be obtained by choosing a set of suitable testing functions, multiplying the above equation by these testing functions and then integrating over the cross-section of the scatterer. Various choices of testing methods exist. However, the two most common ones are point matching and Galerkin. The first involves use of delta function, and the latter makes use of basis function used in the expansion of unknown function in Eq. (2.8) as a testing function. It is desired to apply a testing which makes use of reciprocity theorem in electromagnetic theory, this theorm states

$$\iint_{S_m} \bar{J}_m \cdot \bar{E}_n \, dS_m = \iint_{S_n} \bar{J}_n \cdot \bar{E}_m \, dS_n \quad . \tag{2.10}$$

where

$\bar{J}_m$ and $\bar{J}_n$ are $_m{}^{th}$ and $_n{}^{th}$ current modes, $\bar{E}_m$ and $\bar{E}_n$ are field generated by these current modes, and S_m and S_n are the cross-section areas of $_m{}^{th}$ and $_n{}^{th}$ current elements. A major advantage of implementing a solution involving the above theorm is that a symmetric impedance matrix is generated. The Galerkin method is used to take advantage of the above properties, also, it provides a great numerical stability and convergence. To apply Galerkin testing, both sides of Eq. (2.9) are multiplied by the testing function $F_{m(x,y)}$ and integrated over the cross-section. One obtains the following set of simultaneous linear equations;

$$V_m = \sum_{n=1}^{N} C_n Z_{mn} \qquad m = 1,2,\ldots, N \ , \tag{2.11}$$

where

$$V_m = \iint_{cs} F_{m(x,y)} E^i_z(x,y)ds \qquad m = 1,2,\ldots, N \ , \tag{2.12}$$

and

$$Z_{mn} = \iint_{cs} F_{n(x,y)} F_{m(x,y)} ds - \frac{\omega^2 \mu_o (\hat{\varepsilon}_1 - \hat{\varepsilon}_2)}{2\pi} \iiiint_{cscs} F_{n(x',y')} F_{m(x,y)} K_o(\gamma_2 |\bar{\rho} - \bar{\rho}'|) ds' ds. \tag{2.13}$$

The matrix form of Equation (2.11) can be written as

$$[Z_{mn}][C_n] = [V_m] \ , \tag{2.14}$$

where $[Z_{mn}]$ is a (NxN) impedence matrix, $[C_n]$ is the unknown column matrix, and $[V_m]$ is a known voltage column matix. For a nonsingular $[Z_{mn}]$ the above matrix equation can be solved numerically with the aid of a digital computer. Thus

$$[C_n] = [Z_{mn}]^{-1}[V_m] \ . \tag{2.15}$$

Once the $[C_n]$ matrix has been determined, $\bar{J}_{eq}$ is evaluated by Equations (2.5) and (2.8). In turn $E^s_z(x,y)$ can be calculated from Eq. (2.6a) to obtain

$$E^s_{z(x,y)} = \frac{\omega^2 \mu_o (\hat{\varepsilon}_1 - \hat{\varepsilon}_2)}{2\pi} \sum_{m=1}^{N} C_m \iint_{cs} F_{m(x',y')} K_o(\gamma_2 |\bar{\rho} - \bar{\rho}'|) ds' \ . \tag{2.16}$$

The above equation is valid for all scattering angles. However for backscattered case some computation time may be saved by using the following

$$E^{B.S.}_{z(x_s,y_s)} = j\omega(\hat{\varepsilon}_1-\hat{\varepsilon}_2) \sum_{n=1}^{N} C_n V_n \quad . \tag{2.17}$$

The pertinent numerical values (V_n) may be stored when setting up the voltage column matrix. These values are then retrieved when the above equation is used to calculate the backscattered field. This result can be obtained by reciprocity. Considering Figure 1, the line source has a current distribution $\overline{J}_{L.S.} = \delta(x-x_s)\delta(y-y_s)$, and radiates a field $\overline{E}^i(x,y)$ given by Equation (2.1). A particular current mode $\overline{J}_n$ in the scatterer is given by $\overline{J}_n=j\omega(\hat{\varepsilon}_1-\hat{\varepsilon}_2)\overline{E}^I_n$, where $\overline{E}^I_n$ is the total field of mode n in the scatterer. $\overline{J}_n$ generates the n^{th} mode of the scattered field $\overline{E}^s_n$, where the total scattered field due to the scatterer is $\overline{E}^s(x,y) = \sum_{n=1}^{N} \overline{E}^s_n$. Applying reciprocity to a typical current mode $\overline{J}_n$ in the scatterer and $\overline{J}_{L.S.}$ on the line source gives

$$\int_{L.S.}\int \overline{J}_{L.S.} \cdot \overline{E}^s_n \, ds = \int_{C.S.}\int \overline{J}_n \cdot \overline{E}^i(x,y) \, ds \quad . \tag{2.18}$$

or

$$\begin{aligned} E^s_n(x_s, y_s) &= j\omega(\hat{\varepsilon}_1-\hat{\varepsilon}_2) \iint_{cs} \overline{E}^I_n(x,y) \cdot \overline{E}^i(x,y) \, ds \\ &= j\omega(\hat{\varepsilon}_1-\hat{\varepsilon}_2)C_n \iint_{cs} F_n(x,y)E^i_z(x,y) \, ds \\ &= j\omega(\hat{\varepsilon}_1-\hat{\varepsilon}_2)C_nV_n \quad . \end{aligned} \tag{2.19}$$

Thus, Equation (2.17) is obtained.

All of the single cross-section integration encountered so far are easy to evaluate numerically. The double cross-section integration of Equation (2.13) is rather tedious because of the singular point (x=x', y=y'). Richmond [40] has given an integration technique for evaluation of the inner most cross-section integration of Equation (2.13). A careful reapplication of the same technique can also be used to evaluate the outer most integration. This is especially useful for considering scattering by cylinders with arbitrary cross section. For the rectangular cross-section shaped cylinders, these integrations are evaluated in a closed form as will be illustrated in future chapters for specific cases.

2. E_z-plane Wave Incidence

The fields of a z-polarized incident plane wave are given by

$$E_z^i = E_0 e^{-\gamma_2 \hat{p}\cdot\hat{r}} . \qquad (2.20)$$

where E_0 is amplitude of the incidence plane wave which is to be set to unity, $\hat{p} = -\hat{x}\cos\phi_i - \hat{y}\sin\phi_i$ is the unit vector in direction of propagation, $\hat{r} = \hat{x}x + \hat{y}y$ is radial position vector, and ϕ_i is the angle of incidence as shown in Figure 2-2.

The incident field can now be written in the form

$$E_z^i = e^{\gamma_2(x\cos\phi_i + y\sin\phi_i)} . \qquad (2.21)$$

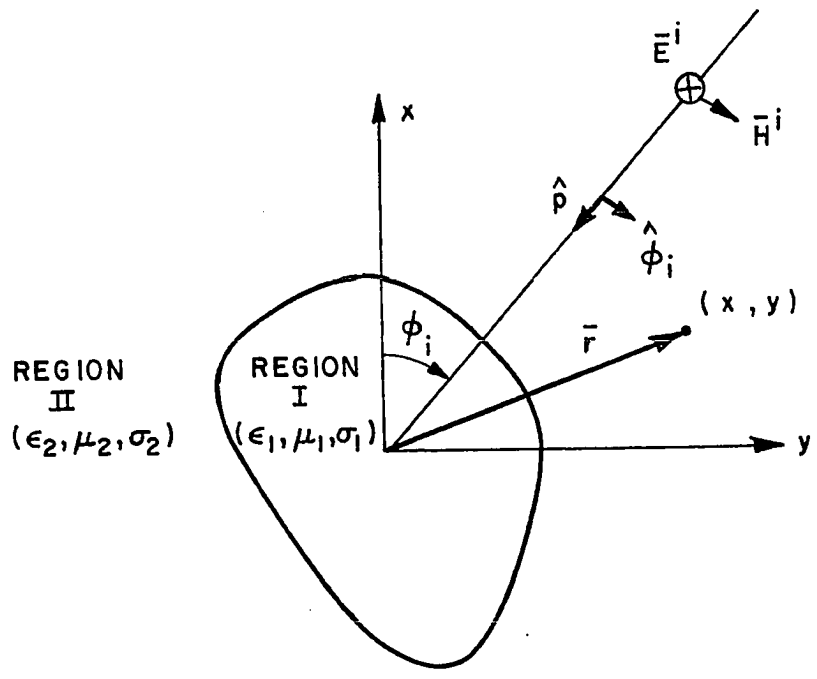

Figure 2-2. E_z-plane wave incident on the scatterer.

From Eq. (2.12)

$$V_m = \iint_{cs} F_{m(x,y)} e^{\gamma_2(x\cos\phi_i + y\sin\phi_i)}\, ds \quad . \tag{2.22}$$

In the far zone, the scattered field can be obtained by using asymptotic form of $K_0(\gamma_2|\bar{\rho}-\bar{\rho}'|)$ in Equation (2.16)

$$E_z^s(\rho,\phi) = \frac{\omega^2\mu_o(\hat{\varepsilon}_1-\hat{\varepsilon}_2)}{2\pi}\sqrt{\frac{\pi}{2\gamma_2}}\sum_{m=1}^{N} C_m \iint_{cs} F_m(x,y)\, e^{\gamma_2(x\cos\phi_s+y\sin\phi_s)}\, ds.$$

$$\frac{e^{-\gamma_2\rho}}{\sqrt{\rho}} \quad . \tag{2.23}$$

The far field approximation has been used as illustrated in Figure 2-3. where

$$|\bar{\rho}-\bar{\rho}'| = \rho - \rho'\cos(\phi_s-\phi')$$
$$= \rho - (x'\cos\phi_s+y'\sin\phi_s) \quad . \tag{2.24}$$

When $\phi_i = \phi_s$ (Backscattered case)

$$E_z^{B.S.}(\rho,\phi_s) = \frac{\omega^2\mu_o(\hat{\varepsilon}_1-\hat{\varepsilon}_2)}{2\pi}\sqrt{\frac{\pi}{2\gamma_2}}\sum_{m=1}^{N} C_m V_m \frac{e^{-\gamma_2\rho}}{\sqrt{\rho}} \quad . \tag{2.25}$$

Where V_m is now given in Equation (2.22).

C. H-WAVE SCATTERING BY TWO DIMENSIONAL LOSSY DIELECTRIC CYLINDERS

1. Magnetic Line Source Excitation

An infinite magnetic line source with uniform current M_o located at (x_s,y_s) when radiating in the homogeneous medium $(\varepsilon_2,\mu_o,\sigma_2)$ generates the field given by

$$\underline{H}^i = -\frac{j\omega\hat{\varepsilon}_2}{2\pi} K_o(\gamma_2|\bar{\rho}-\bar{\rho}_s|)\hat{z} \quad . \tag{2.26}$$

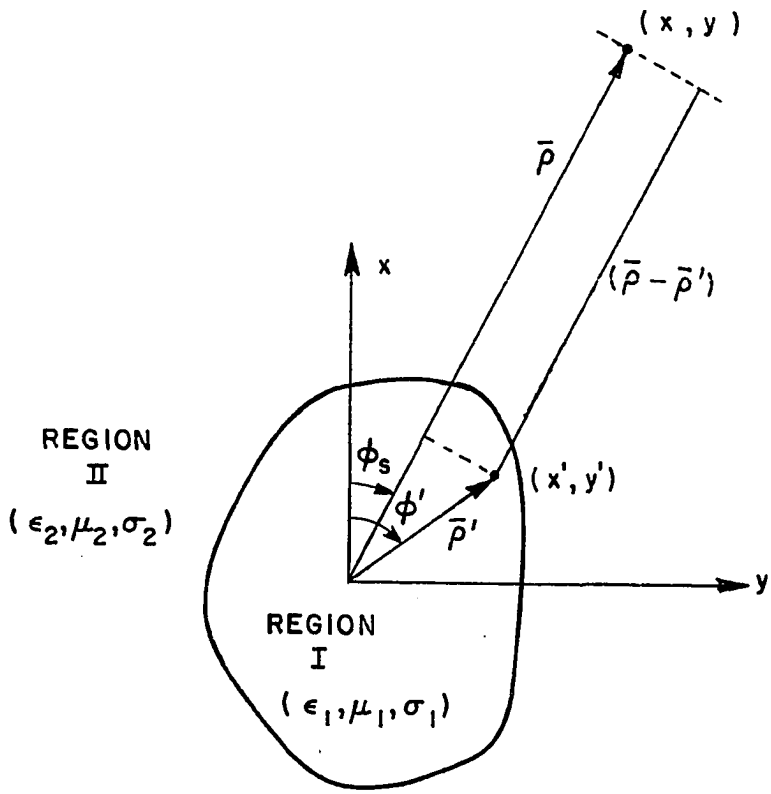

$$\rho = \sqrt{x^2 + y^2}$$

$$\rho' = \sqrt{x'^2 + y'^2}$$

IN FAR ZONE

$$|\bar{\rho} - \bar{\rho}'| \approx \rho - \rho' \cos(\phi_s - \phi')$$

Figure 2-3. Illustration of the far field approximation for the scattered field.

The corresponding electric field generated by the above magnetic current is

$$\bar{E}^i = \frac{\gamma_2}{2\pi} K_1(\gamma_2|\bar{\rho}-\bar{\rho}_s|)\,\hat{\phi}_{LS} \quad , \tag{2.27a}$$

where

$$\hat{\phi}_{LS} = -\hat{x}\sin\phi_{LS} + \hat{y}\cos\phi_{LS} \; ; \text{ and} \tag{2.27b}$$

$$\phi_{LS} = \tan^{-1}\left(\frac{y-y_s}{x-x_s}\right) \quad .$$

where $\hat{\phi}_{LS}$ is the unit vector is direction of ϕ_{LS} as shown in Figure 2-4 and K_1 is the modified Bessel function of order one.

The field scattered by the dielectric cylinder is given by

$$\bar{E}^s(x,y) = -j\omega\bar{A}^s(x,y) - \nabla V^s(x,y) \quad . \tag{2.28}$$

where $\bar{A}^s$ is the electric vector potential given by

$$\bar{A}^s(x,y) = \frac{\mu_0}{2\pi}\iint_{cs} \bar{J}_{eq}(x',y')K_0(\gamma_2|\bar{\rho}-\bar{\rho}'|)\,ds' \quad , \tag{2.29}$$

$V_{(x,y)}$ is the scalar potential given by

$$V_{(x,y)} = \frac{1}{2\pi\hat{\epsilon}_2}\int_{\ell} \rho_s(\ell')K_0(\gamma_2|\bar{\rho}-\bar{\rho}'|)d\ell' \quad . \tag{2.30}$$

$\rho_s(\ell')$ is the surface charge density on the surfaces of the scatterer. $d\ell'$ is the differential linear element on the contour of the scatterer as shown in Figure 2-4. (The prime designates integration over the source region.)

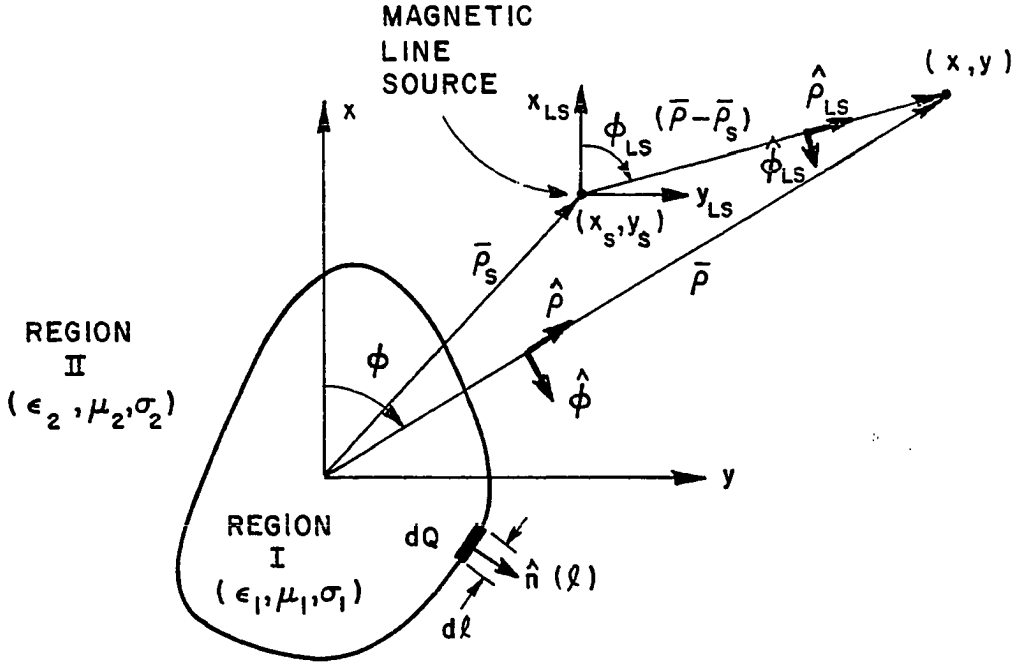

$$\phi_{LS} = \tan^{-1}\left(\frac{y - y_s}{x - x_s}\right)$$

$$\hat{\phi}_{LS} = -\hat{x}\sin\phi_{LS} + \hat{y}\cos\phi_{LS}$$

Figure 2-4. Electromagnetic scattering model for magnetic line source excitation.

Region I is source free thus

$$\rho_v = 0. \tag{3.31}$$

The incremental current dI in an elemental length at the perimeter is obtained from the normal component of $\bar{J}_{eq}$ as

$$dI = [\bar{J}_{eq}(\ell)\cdot\hat{n}(\ell)]d\ell \quad . \tag{2.32}$$

where $\hat{n}(\ell)$ a unit normal out of region I as illustrated in Figure 2-4.

For a time harmonic source,

$$dI = j\omega dQ \quad . \tag{2.33}$$

where dQ is the total charge in element $d\ell$. From Equations (2.32) and (2.33), and knowing $\rho_s = \frac{dQ}{d\ell}$,

$$\rho_s(\ell) = \frac{J_{eq}(\ell).\hat{n}\ (\ell)}{j\omega} \quad . \tag{2.34}$$

Substituting Equation (2.34) in Equation (2.30) yields

$$V_{(x,y)} = \frac{1}{j\omega 2\pi\hat{\varepsilon}_2} \int_{\ell} [\bar{J}_{eq}(\ell')\cdot\hat{n}(\ell')]K_0(\gamma_2|\bar{\rho}-\bar{\rho}'|)d\ell' \quad . \tag{2.35}$$

Noting that only ρ in the integration is dependent on (x, y), taking the gradient of v(x,y) gives

$$\nabla V_{(x,y)} = -\frac{\gamma_2}{j\omega 2\pi\hat{\varepsilon}_2} \int_{\ell} [\bar{J}_{eq}(\ell')\cdot\hat{n}(\ell')]K_1(\gamma_2|\bar{\rho}-\bar{\rho}'|)\hat{\rho}d\ell' \tag{2.36a}$$

where

$$\hat{\rho} = \cos\phi\hat{x} + \sin\phi\hat{y}, \quad \text{and} \tag{2.36b}$$

$$\phi = \tan^{-1}\left(\frac{y-y'}{x-x'}\right) .$$

Now $\bar{E}^s_{(x,y)}$ can be written as (from Equations (2.28), (2.29) and (2.36)

$$\bar{E}^s_{(x,y)} = -\frac{j\omega\mu_0}{2\pi}\iint_{cs} \bar{J}_{eq}(x',y')K_0(\gamma_2|\bar{\rho}-\bar{\rho}'|)ds'$$

$$+\frac{\gamma_2}{j\omega 2\pi\hat{\varepsilon}_2}\int_{\ell}[\bar{J}_{eq}(\ell')\cdot\hat{n}(\ell')]K_1(\gamma_2|\bar{\rho}-\bar{\rho}'|)\hat{\rho}d\ell' . \tag{2.37}$$

The integral equation is formed by substituting for $\bar{J}_{eq}$ from Equation (2.5) in Equation (2.37), transposing Equation (2.4) and substituting from Equation (2.37) to obtain

$$\bar{E}^i_{(x,y)} = \bar{E}^I_{(x,y)} - \frac{\omega^2\mu_0(\hat{\varepsilon}_1-\hat{\varepsilon}_2)}{2\pi}\iint_{cs}\bar{E}^I(x',y')K_0(\gamma_2|\bar{\rho}-\bar{\rho}'|)ds'$$

$$-\frac{\gamma_2(\hat{\varepsilon}_1-\hat{\varepsilon}_2)}{2\pi\hat{\varepsilon}_2}\int_{\ell}[\bar{E}^I(x',y')\cdot\hat{n}(\ell')]K_1(\gamma_2|\bar{\rho}-\bar{\rho}'|)\hat{\rho}d\ell' . \tag{2.38}$$

The unknown function in the above integral equation is $\bar{E}^I(x,y)$, the field in region I. The unknown function appears both inside and outside the integral. To solve this integral equation, it is convenient to expand the total magnetic field inside the scatterer (region I) in terms of a set of basis function $F_n(x,y)$, thus

$$\bar{H}^{I}_{(x,y)} = \sum_{n=1}^{N} C_n F_n(x,y)\hat{z} \quad , \tag{2.39}$$

Where the unknowns are the C_n's.

Using Maxwell's equation we obtain the expansion for total electric field in Region I.

$$\bar{E}^{I}_{(x,y)} = p \sum_{n=1}^{N} C_n \bar{F}_n(x,y) \quad . \tag{2.40a}$$

where

$$\bar{F}_{n(x,y)} = \hat{x} \frac{\partial F_n(x,y)}{\partial y} - \hat{y} \frac{\partial F_n(x,y)}{\partial x} \quad . \tag{2.40b}$$

$$p = \frac{1}{j\omega\hat{\varepsilon}_1} \quad . \tag{2.40c}$$

It will be shown in future chapters that $\bar{F}_n(x,y)$ and p will be simplified for a proper choice of basis function.

Substituting Equation (2.40a) in Equation (2.38) yields

$$\bar{E}^{i}_{(x,y)} = p \sum_{n=1}^{N} C_n \left[\bar{F}_n(x,y) - \frac{\omega^2 \mu_o(\hat{\varepsilon}_1 - \hat{\varepsilon}_2)}{2\pi} \iint_{cs} \bar{F}_n(x,y) K_o(\gamma_2 |\bar{\rho} - \bar{\rho}'|) ds' \cdot \right.$$

$$\left. - \frac{(\hat{\varepsilon}_1 - \hat{\varepsilon}_2)\gamma_2}{2\pi\hat{\varepsilon}_2} \int_{\ell} [\bar{F}_n(\ell') \cdot \hat{n}(\ell')] K_1(\gamma_2 |\bar{\rho} - \bar{\rho}'|) \hat{\rho} \, d\ell' \right] \quad . \tag{2.41}$$

and again the C_n's are the unknowns.

It is desired to obtain a set of simultaneous linear equations given by Equation (2.11) by implementing the reciprocity theorem of Equation (2.10), thus the Galerkin testing is used in above equation. The inner product of $\bar{F}_m(x,y)$ is formed with both sides of Equation (2.41), and integrated over the cross section of the scatterer.

Using Eq. (2.27), this yields

$$V_m = \iint_{cs} \bar{F}_{m(x,y)} \cdot \bar{E}^i_{(x,y)} ds \qquad m=1,2,3,\ldots, N$$

$$= \frac{\gamma_2}{2\pi} \iint_{cs} \left(\frac{\partial F_m(x,y)}{\partial y} \sin\phi_{LS} + \frac{\partial F_m(x,y)}{\partial x} \cos\phi_{LS} \right) K_1(\gamma_2 |\bar{\rho}-\bar{\rho}_s|) ds \,, \tag{2.42}$$

and

$$Z_{mn} = p\iint_{cs} \bar{F}_{n(x,y)} \cdot \bar{F}_{m(x,y)} ds - \frac{\omega^2 \mu_o (\hat{\varepsilon}_1 - \hat{\varepsilon}_2)}{2\pi} p\iiint\iint_{cscs} \bar{F}_{n(x',y')}$$

$$\cdot \bar{F}_{m(x,y)} K_o(\gamma_2 |\bar{\rho}-\bar{\rho}'|) ds' ds - \frac{(\hat{\varepsilon}_1 - \hat{\varepsilon}_2)\gamma_2}{2\pi\hat{\varepsilon}_2} p\iiint_{cs\ell} F_{m(x,y)}$$

$$\cdot \hat{\rho}[\bar{F}_n(\ell').\hat{n}(\ell')] K_1(\gamma_2 |\bar{\rho}-\bar{\rho}'|) d\ell' ds \,. \tag{2.43}$$

where ϕ_{LS} is defined in Equation (2.27b) and $\hat{\rho}$ is defined in Equation (2.36b).

The difficulty encountered in evaluating the above integrals is dependent upon the choice of the basis functions. The integration in the first term is rather straight forward since there is no singular points involved in the region. The integrals of second term of Equation

(2.43) involve a singular point (when x=x' and y=y') but it can be evaluated in the same manner discussed for Equation (2.13). Perhaps the most difficult term in Equation (2.43) to integrate is the third term. This term involves a set of singular points on the cross-section contour for the inner most integration around the cross-section contour, and another set of singular points in the cross-section for the outer most integration over the cross-section. It is suggested that when approximating the scatterer by a set of overlapping small circular cylinders, the surface charge density due to all cells be included and summed. For a rectangular cross-section, however, all the integrals of the Equations (2.42) and (2.43) can be evaluated in closed form for a proper choice of testing function. This will be illustrated in future chapters.

After numerically solving for C_n's the scattered field can be found by

$$\overline{H}^s = \frac{1}{\mu_0} \nabla X \overline{A}^s \quad . \tag{2.44}$$

where $\overline{A}_s$ is given by Equation (2.29) and $\overline{J}_{eq}$ is given by Equations (2.5) and (2.40a).

$$\overline{H}^s_{(x,y)} = \frac{j\omega\gamma_2(\hat{\varepsilon}_1-\hat{\varepsilon}_2)_p}{2\pi} \sum_{m=1}^{N} C_m \left[\int\int_{cs} \overline{F}_m(x',y') x\hat{\rho} K_1(\gamma_2|\overline{\rho}-\overline{\rho}'|) ds' \right] \hat{z} \quad . \tag{2.45a}$$

where

$$\overline{F}_n(x',y') x\hat{\rho} = \hat{z}\left(\frac{\partial F_m(x',y')}{\partial y'} \sin\phi + \frac{\partial F_m(x',y')}{\partial x'} \cos\phi \right) \quad . \tag{2.45b}$$

Thus

$$\bar{H}^s_{(x,y)} = \frac{j\omega\gamma_2 p(\hat{\varepsilon}_1-\hat{\varepsilon}_2)}{2\pi} \sum_{m=1}^{N} C_m \left[\iint_{cs} \left(\frac{\partial F_m(x',y')}{\partial y'} \sin\phi + \frac{\partial F_m(x',y')}{\partial x'} \cos\phi \right) K_1(\gamma_2 |\bar{\rho}-\bar{\rho}'|) ds' \right] \hat{z} \quad . \tag{2.46}$$

The above is valid for all scattering angles. However for backscattering, some computation time may be saved by using

$$\bar{H}^{B.S.}_{(x_s,y_s)} = -j\omega p^2(\hat{\varepsilon}_1-\hat{\varepsilon}_2) \sum_{m=1}^{N} C_m V_m \hat{z} \quad . \tag{2.47}$$

where V_m is given by Equation (2.42).

2. H_z-Plane Wave Incidence

Using expansions similar to those involving the E_z-Plane Wave incidence case, one may analyze a z-polarized plane magnetic field incident on the scatterer as shown in Figure 2-5. The incident fields are given by

$$\bar{H}^i = \hat{z} H_0 e^{\gamma_2(x\cos\phi_i + y\sin\phi_i)}$$

$$\bar{E}^i = \eta_2(\bar{H}^i \times \hat{\rho}) = -\eta_2 e^{\gamma_2(x\cos\phi_i + y\sin\phi_i)} \hat{\phi}_i \quad . \tag{2.48a}$$

where $H_0 = 1$ is assumed and

$$\text{where } \hat{\phi}_i = -\hat{x}\sin\phi_i + \hat{y}\cos\phi_i \ , \tag{2.48b}$$

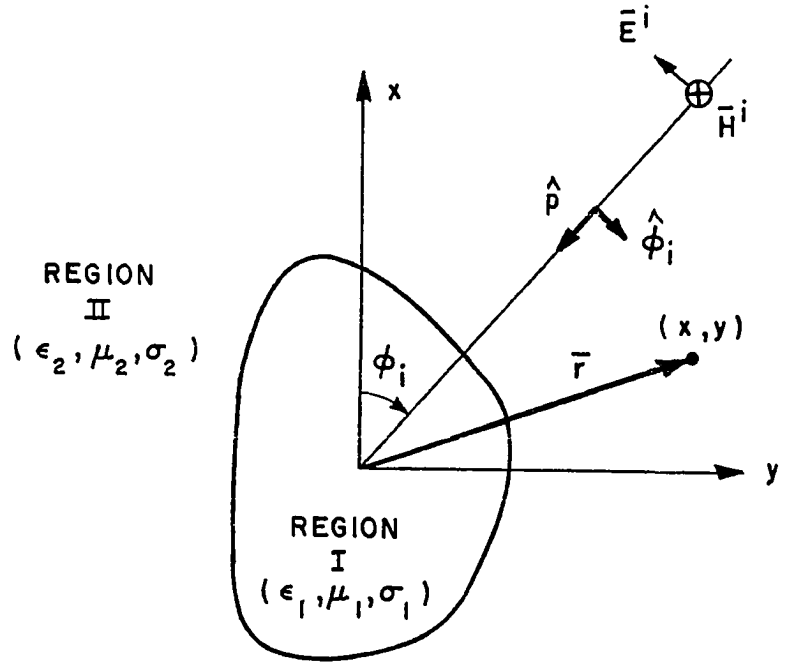

Figure 2-5. H_z-plane wave incident on the scatterer.

$n_2 = \sqrt{\frac{\mu_0}{\hat{\epsilon}_2}}$ is the the intrinsic impedance of homogeneous Region II.

From Equation (2.42).

$$V_m = n_2 \iint_{cs} \left(\frac{\partial F_m(x,y)}{\partial y} \sin\phi_i + \frac{\partial F_m(x,y)}{\partial x} \cos\phi_i \right) e^{\gamma_2 (x\cos\phi_i + y\sin\phi_i)} \, ds \, . \tag{2.49}$$

To calculate the far zone scattered field, Equation (2.46) can be utilized where $K_1(\gamma_2|\bar{\rho}-\bar{\rho}'|)$ is replaced by its asymptotic form and using a similar far field approximation as in Figure 2-3 and Equations (2.23) and (2.24) yields

$$\underline{H}^{s}(\rho,\phi)= \frac{j\omega\gamma_2 p(\hat{\varepsilon}_1-\hat{\varepsilon}_2)}{2\pi}\sqrt{\frac{\pi}{2\gamma_2}}\sum_{m=1}^{N} C_m\left[\iint_{cs}\left(\frac{\partial F_m(x',y')}{\partial y'}\sin\phi_s+\frac{\partial F_m(x',y')}{\partial x'}\cos\phi_s\right)\right.$$

$$\left. e^{-\gamma_2(x'\cos\phi_s+y'\sin\phi_s)}\, ds'\right]\frac{e^{-\gamma_2\rho}}{\sqrt{\rho}}\,\hat{z}\ . \qquad (2.59)$$

ϕ_s is the angle of scattered field as shown in Figure 2-3. When $\phi_s=\phi_i$ the backscattered far field is given by

$$\underline{H}^{B.S.}(\rho,\phi_s) = \frac{j\omega\gamma_2 p(\hat{\varepsilon}_1-\hat{\varepsilon}_2)}{2\pi}\sqrt{\frac{\pi}{2\gamma_2}}\sum_{m=1}^{N} C_m V_m \frac{e^{-\gamma_2\rho}}{\sqrt{\rho}}\ . \qquad (2.60)$$

V_m is given by Equation (2.49).

In this chapter all the derivations have been very general and can be applied directly to any suitable two dimensional electromagnetic model by simply chosing a suitable expansion function. It is however essential that a stable convergence be obtained. Thus the first test to be made is a convergence test. In the following chapters these theories are applied to scattering by a two dimensional lossy dielectric rectangular cylinders hereafter referred to as rectangular cylinders. In each case a convergence test is included which exhibits the reliability of the numerical solution.

CHAPTER III

E-WAVE SCATTERING BY LOSSY DIELECTRIC RECTANGULAR CYLINDERS OF INFINITE LENGTH IN A LOSSY HOMOGENEOUS MEDIUM

A. INTRODUCTION

In this chapter, the plane wave expansion is introduced and an example of the convergence properties is given. Examples of typical scattered field patterns are presented for the cases of a lossy rectangular cylinder in a free space environment and for an air cylinder in a lossy ambient medium.

B. PLANE WAVE EXPANSION

The expansion of the field inside the cylinder in terms of a set of basis function F_n is given in Equation (2.8). The choice of F_n as a spectrum of plane waves is such that each F_n satisfies the Helmholtz wave equation inside the cylinder. Since the electric fields are z-directed, it is only necessary to treat the scalar problem. Thus the basis function equals

$$F_n(x,y) = e^{-jf_n x} e^{-jg_n y} \quad . \tag{3.1a}$$

From Equation (2.40b)

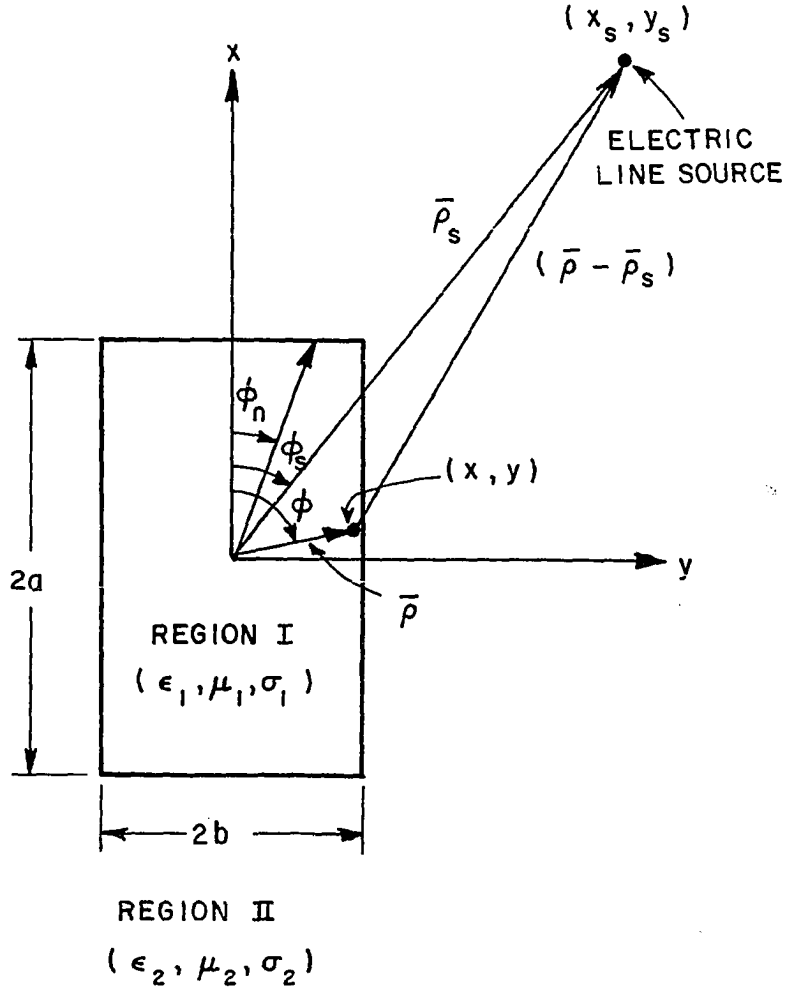

Figure 3-1. E-wave, electromagnetic scattering model for a lossy, dielectric rectangular cylinder of infinite length immersed in a lossy medium.

$$\bar{F}_n = -jk_1(\cos\phi_n\,\hat{x} - \sin\phi_n\,\hat{y})\, e^{-jf_n x}\, e^{-jg_n y}$$

$$= -jk_1(\cos\phi_n\,\hat{x} - \sin\phi_n\,\hat{y})\, F_n(x,y) \quad . \tag{3.1b}$$

From the wave equation and Equation (3.1)

$$f_n^2 + g_n^2 = k_1^2 \quad , \tag{3.2a}$$

where

$$f_n = k_1\cos\phi_n \quad , \tag{3.2b}$$

$$g_n = k_1\sin\phi_n \quad , \tag{3.2c}$$

$$\phi_n = \frac{(n-1)}{N}\,2\pi \quad , \tag{3.2d}$$

$$k_1 = \omega\sqrt{\mu_o\hat{\varepsilon}_1} \quad , \tag{3.2e}$$

$$\hat{\varepsilon}_1 = \varepsilon_o\left(\varepsilon_{r_1} - j\,\frac{\sigma_1}{w\varepsilon_o}\right) \quad , \tag{3.2f}$$

where ϕ_n is shown in Figure 3-1. Observe that once the number of terms N retained in this plane wave expansion is given, the individual F_n's are completely specified, thus Equation (2.8) becomes .

$$E^I_{z(x,y)} = \sum_{n=1}^{N} C_n e^{-jf_n x}\, e^{-jg_n y} \quad . \tag{3.3}$$

To obtain a set of simultaneous linear equations such as Equation (2.11), Equation (3.1) is substituted in Equations (2.12) and (2.13). The terms of the excitation column matrix now take the form

$$V_m = -\frac{j\omega\mu_o}{2\pi}\int_{-a}^{a}\int_{-b}^{b} e^{-jf_m x} e^{-jg_m y} k_o(\gamma_2|\bar{\rho}-\bar{\rho}_s|)dxdy \; ; \; m = 1,2,\ldots,N \; . \tag{3.4}$$

The impedance matrix

$$Z_{mn} = \int_{-a}^{a}\int_{-b}^{b} e^{-jf_m x} e^{-jg_m y} e^{-jf_n x} e^{-jg_n y} dxdy - \frac{\omega^2\mu_o(\hat{\varepsilon}_1-\hat{\varepsilon}_2)}{2\pi} \int_{-a}^{a}\int_{-b}^{b}\int_{-a}^{a}\int_{-b}^{b}$$

$$e^{-jf_n x'} e^{-jg_n y'} e^{-jf_m x} e^{-jg_m y} K_o(\gamma_2|\bar{\rho}-\bar{\rho}'|)dx'dy'dxdy$$

$$= R_{mn} + S_{mn} \quad . \tag{3.5a}$$

The first integral may be integrated in closed form to obtain

$$R_{mn} = \frac{4\sin[(f_m+f_n)a]\,\sin[(g_m+g_n)b]}{(f_m+f_n)(g_m+g_n)} \quad . \tag{3.5b}$$

The second term of Equation (3.5a) is

$$S_{mn} = C_1 \int_{-a}^{a}\int_{-b}^{b}\int_{-a}^{a}\int_{-b}^{b} e^{-jf_n x'} e^{-jg_n y'} e^{-jf_m x} e^{-jg_m y} K_o(\gamma_2|\bar{\rho}-\bar{\rho}'|)dx'dy'dxdy \; , \tag{3.5c}$$

where

$$C_1 = -\frac{\omega^2\mu_o(\hat{\varepsilon}_1-\hat{\varepsilon}_2)}{2\pi} \quad . \tag{3.5d}$$

To evaluate Equations (3.4) and (3.5c) we utilized the spectral transform of $K_o(\gamma_2|\bar{\rho}-\bar{\rho}'|)$ is utilized

$$K_o(\gamma_2|\rho-\rho'|) = \int_0^\infty \frac{e^{-f|x-x'|}}{f} \cos[g(y-y')]\, dg \quad . \tag{3.6a}$$

From the wave equation

$$f^2 - g^2 = \gamma_2^2 \quad . \tag{3.6b}$$

Note that f and g should not be mistaken with f_n and g_n in Equation (3.2a).

This transform is easily obtained by redefining some parameters in the form given by Tyras [41].

Substituting Equation (3.6a) in Equation (3.4) with $x'=x_s$ and $y'=y_s$ and changing the order of integration one obtains

$$V_m = -\frac{j\omega\mu_o}{2\pi} \int_o^\infty \left[\frac{1}{f} \int_{-a}^{a} \int_{-b}^{b} e^{-jf_m x} e^{-jg_m y} e^{-f|x-x_s|} \cos g[(y-y_s)]\, dx\, dy \right] dg \quad . \tag{3.7}$$

The integration over the cross-section is easily evaluated in a closed form to obtain.

$$V_m = -\frac{j\omega\mu_o}{\pi} \int_o^\infty \frac{1}{f} (F_m \cdot GE_m^v)\, dg \quad . \tag{3.8a}$$

where

$$F_m = \begin{cases} \dfrac{\sin[(f_m+jf)a]}{(f_m+jf)} e^{-fx_s} & x_s > a \\ \dfrac{je^{-fx_s}}{2(f_m+jf)} \left(e^{-j(f_m+jf)xs} - e^{j(f_m+jf)a}\right) & \\ \qquad + \dfrac{je^{+fx_s}}{2(f_m-jf)} \left(e^{-j(f_m-jf)a} - e^{-j(f_m-jf)x_s}\right) & -a \leq x_s \leq a \\ \dfrac{\sin[(f_m-jf)a]}{(f_m-jf)} e^{fx_s} & x_s < -a \end{cases} \quad (3.8b)$$

and

$$GE_m^v = e^{-jgy_s} \frac{\sin[(g_m-g)b]}{(g_m-g)} + e^{jgy_s} \frac{\sin[(g_m+g)b]}{(g_m+g)} \quad . \quad (3.8c)$$

Thus the only remaining integration is the $\int_0^\infty dg$ which will be encountered frequently throughout this dissertation. This integration must be evaluated rather carefully, and it will be fully discussed in Chapter V.

To evaluate S_{mn} in Equation (3.5c), Equation (3.6a) is substituted into Equation (3.5c). Rearranging the order of integrations yields

$$S_{mn} = C_1 \int_0^\infty \frac{1}{f} \left[\int_{-a}^{a} \int_{-b}^{b} \int_{-a}^{a} \int_{-b}^{b} e^{-jf_n x'} e^{-jg_n y'} e^{-jf_m x} e^{-jg_m y} e^{-f|x-x'|} \cos g[(y-y')] dx' dy' dx dy \right] dg. \quad (3.9)$$

The integrations on y and y' are easily evaluated. The integration on x can be evaluated by integrating first, from -a to x' where $|x'-x|=(x'-x)$, and then from x' to a, where $|x-x'|=(x-x')$. The result, dependent only on x', is readily evaluated to obtain

$$S_{mn} = 4C_1 \int_0^{\infty} \frac{1}{f} (FE_{mn} \cdot GE_{mn}) dg \quad , \tag{3.10a}$$

where

$$FE_{mn} = j \left[\frac{\sin[(f_m+f_n)a]}{(f_n+jf)(f_m+f_n)} - e^{j(f_n+jf)a} \frac{\sin[(f_m-jf)a]}{(f_n+jf)(f_m-jf)} \right.$$

$$\left. + e^{-j(f_n-jf)a} \frac{\sin[(f_m+jf)a]}{(f_n-jf)(f_m+jf)} - \frac{\sin[(f_m+f_n)a]}{(f_n-jf)(f_m+f_n)} \right] \quad , \tag{3.10b}$$

and

$$GE_{mn} = \frac{\sin[(g_n+g)b]\sin[(g_m-g)b]}{(g_n+g)(g_m-g)} + \frac{\sin[(g_n-g)b]\sin[g_m+g)b]}{(g_n-g)(g_m+g)} \quad . \tag{3.10c}$$

The scattered field can be obtained by substituting Equations (3.1) and (3.6) in Equation (2.16) and evaluating the integrals.

$$E^s_{z(x,y)} = \frac{\omega^2 \mu_o (\hat{\varepsilon}_1 - \hat{\varepsilon}_2)}{\pi} \sum_{m=1}^{N} C_m \int_0^{\infty} \frac{1}{f} (F_m \cdot GE^V_m) dg \cdot \tag{3.11}$$

where F_m is given by Equation (3.8b) and ${}_{G}E_m^v$ is given by Equation (3.8c) by replacing y_s by y. The above equation is valid for all scattering angles. For the backscattered case, i.e., $(x,y)=(x_s,y_s)$, the following may also be used.

$$E_{z(x_s,y_s)}^{B.S.} = \frac{\omega^2 \mu_0 (\hat{\varepsilon}_1 - \hat{\varepsilon}_2)}{\pi} \sum_{m=1}^{N} C_m V_m \quad . \tag{3.12}$$

V_m is given by Equation (3.8a). The far zone scattered field can be calculated using Equation (2.23), and Equation (3.1). In addition, Equations (2.25) and (3.8a) may be used to calculate the far zone backscattered field.

C. CONVERGENCE

Two computer programs were developed based on the moment method formulation given above. These programs are included in the Appendices A and B. To evaluate the number of plane waves required in the expansion of Equation (3.3), the program is run for increasing values of N. A typical result is given in Figure 3-2. This example gives the relative backscattered field in the form of the scattering attenuation function (SAF) [42]. The SAF is the normalized scattered field obtained by dividing the scattered field by the fields of an imaged line source in a ground plane positioned at the center of the scatterer. For the rectangular scatterer under consideration, the pictorial definition of the ground plane is shown in Figure 3-3a for backscattered case, and Figure 3-3b for bistatic case. In these figures, the ground plane is

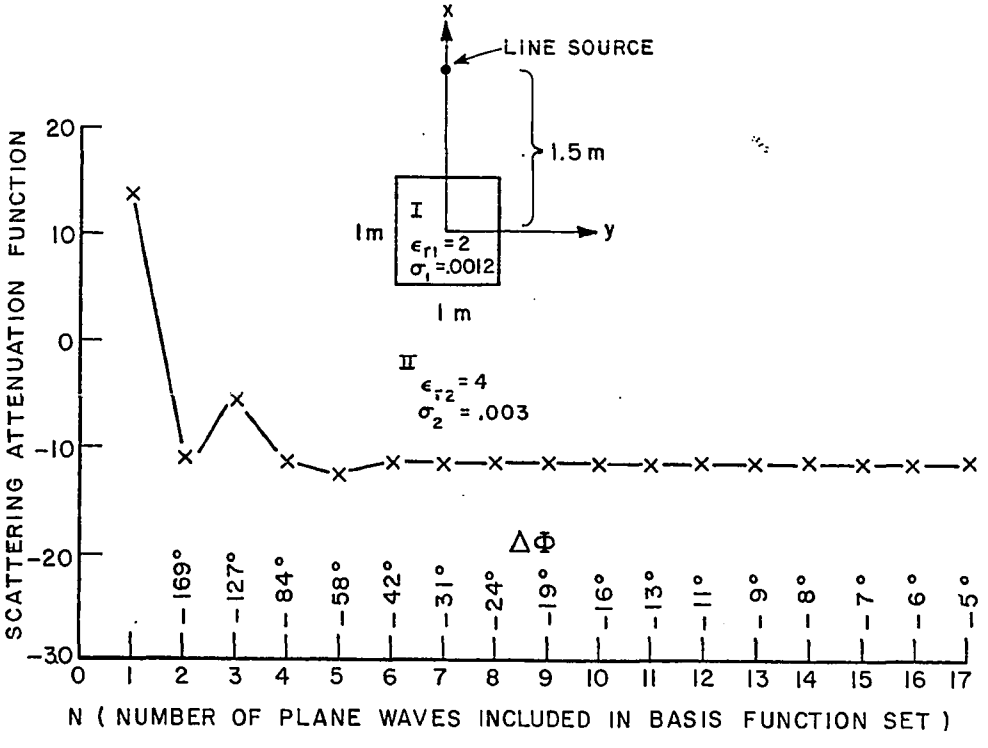

Figure 3-2. Convergence Curve for the RTUNLE or RCYLEGP computer program which uses plane wave expansion Galerkin method at 100MHz. Scattering Attenuation Function is plotted as a function of N the number of plane waves in the expansion.

specified by the plane which includes the z-axis, and is normal to the bisector of the angle between $\bar{\rho}_s$ and $\bar{\rho}$, $(\phi-\phi_s)$.

The scatterer is a 1m square cylinder with relative permittivity of $\varepsilon_{r_1}=2$ and conductivity of .0012 s/m. A line source is located at $x_s=1.5$m and $y_s=0$m in a homogeneous medium with $\varepsilon_{r_2}=4.$ and $\sigma_2=.003$ s/m. As the number of plane waves N, used to represent the field inside the cylinder is increased, the solution converges to a single value. Figure 3-2 indicates that N=6 is sufficient to obtain a reasonably accurate solution for the particular case.

A convenient way to determine N at which convergence may occur can be based on the phase difference between the plane wave traveling in the x-direction (i.e., $\phi_i=0$ direction. See Equations (3.1) to (3.3)), and its neighboring plane wave traveling in $\phi_2=2\pi/N$ direction. This may be expressed as follows

$$E_1 = e^{-j\beta_1(x\cos\phi_1+y\sin\phi_1)}\Big|_{\phi_1=0} = e^{-j\beta_1 x} \tag{3.13a}$$

and

$$E_2 = e^{-j\beta_1(x\cos\phi_2+y\sin\phi_2)}\Big|_{\substack{y=0\\ \phi_2=\frac{2\pi}{N}}} = e^{-j\beta_1 x\cos(\frac{2\pi}{N})} \tag{3.13b}$$

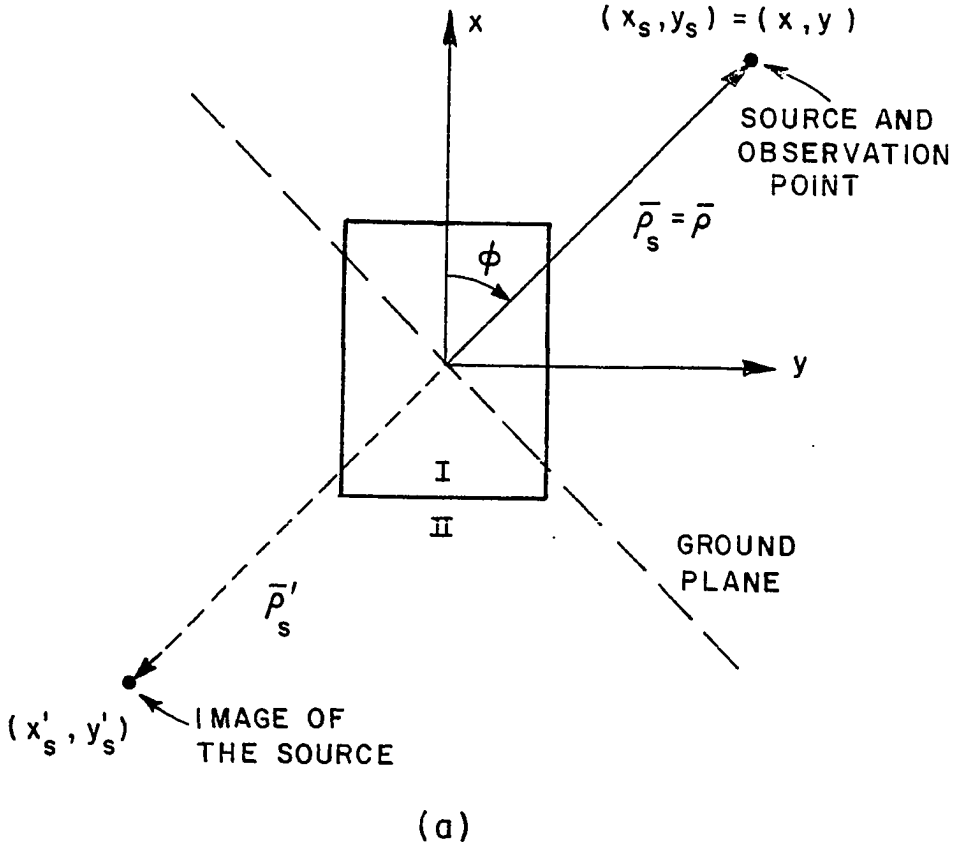

Figure 3-3. Pictorial definition for the Scattering Attenuation Function a) backscattered, b) bistatic scattering.

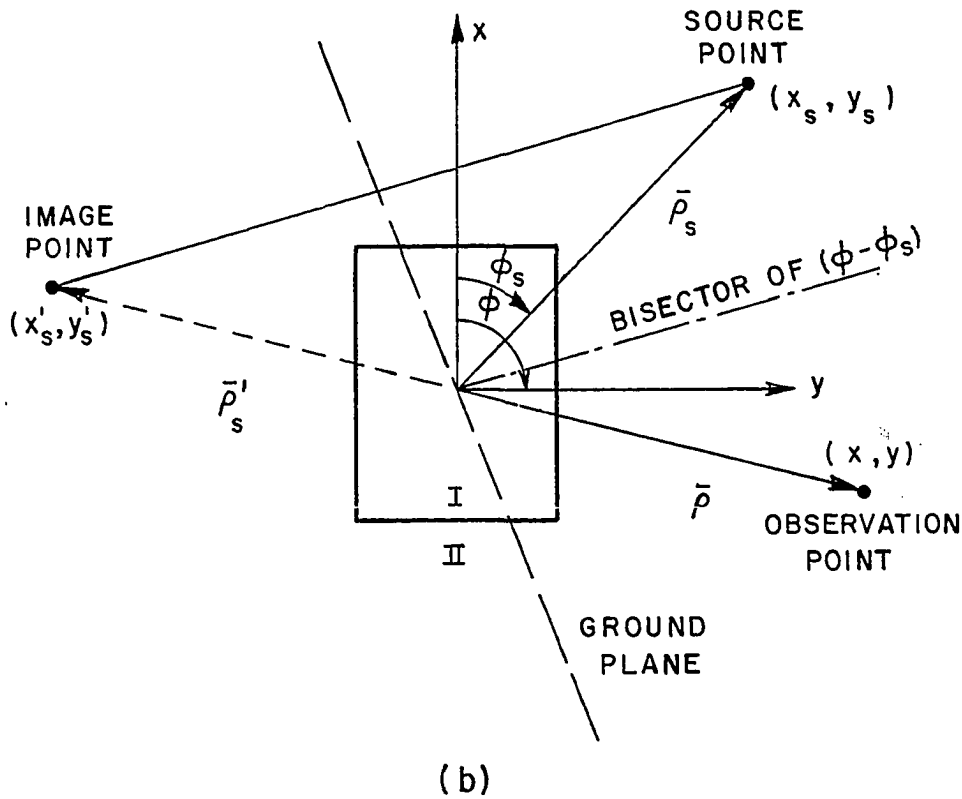

(b)

Figure 3-3. (continued)

where $\gamma_1=\alpha_1+j\beta_1$ and $\alpha_1=0$ is assumed without loss of generality. The phase difference between E_1 and E_2 at x=a($a \geq b$ is assumed as shown in Figure 3-1) is

$$\Delta\Phi = -\beta_1 a\left(1 - \cos\left(\frac{2\pi}{N}\right)\right) \quad . \tag{3.14}$$

This phase difference may be arbitrarily chosen, thus, a value for N can be calculated. Experimentally, it was determined that $\Delta\Phi=-\pi/5$ is an initial suitable phase difference. N is now given by

$$N = \text{Integer}\left[\frac{2\pi}{\cos^{-1}\left[1-\frac{\pi}{5\beta_1 a}\right]}\right] \geq 4 \quad . \tag{3.15}$$

Determination of N from Equation (3.15) is dependent on "a" and "β_1" the phase constant inside the cylinder. The "≥ 4" in Equation (3.15) suggests that there should be at least four plane waves in the expansion. For various values of N, $\Delta\Phi$ is calculated from Equation (3.14) and is plotted in Figure 3-2.

D. BACKSCATTERED FIELD

1. Far Zone

The first example for which the backscattered fields are to be computed is a 1m by .5m rectangular scatterer with $\varepsilon_{r_1}=4$, $\sigma_1=.3$ms/m which is located in a free space environment. A z-polarized plane wave is incident on this scatterer at an angle ϕ_i, as is shown in Figure 3-4. The echo width pattern is given in Figure 3-4. The frequency used is

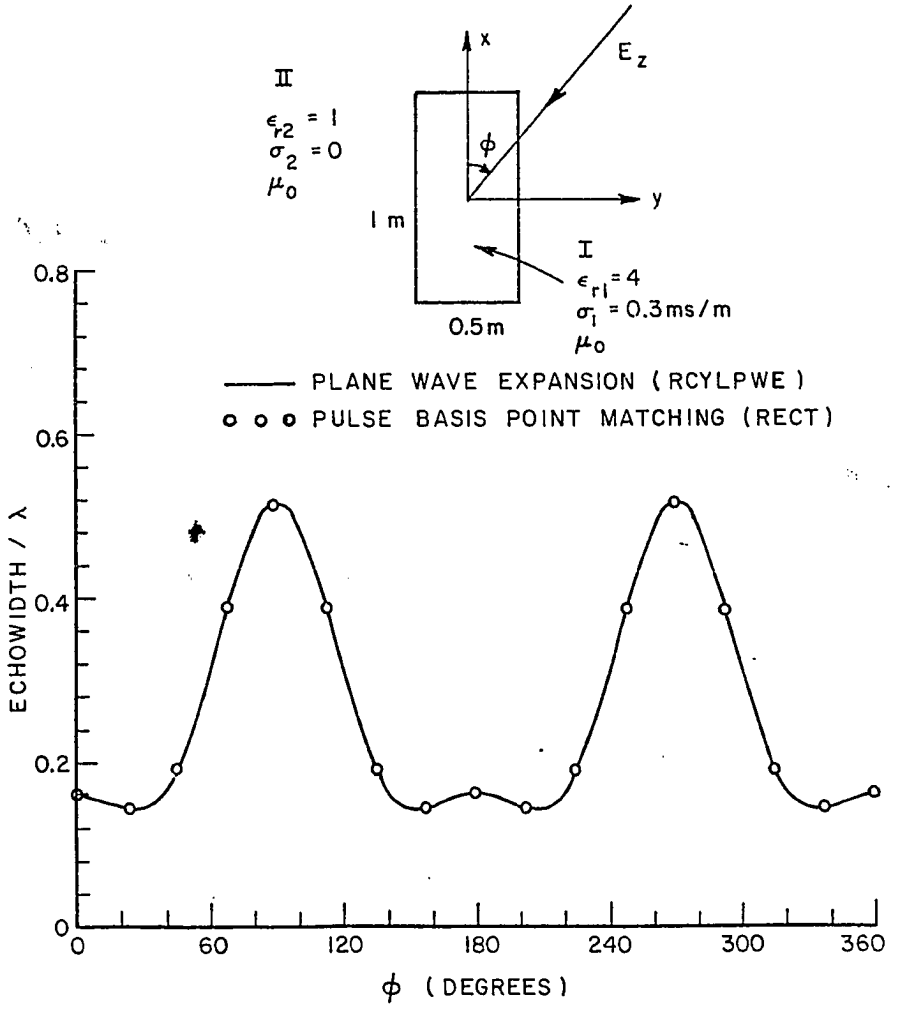

Figure 3-4. Far zone backscattered pattern for plane wave incidence at 100 MHz.

100MHz and is used throughout the remainder of this section unless specified otherwise. The maximum backscattered field is obtained when the plane wave is incident along y or -y axis (ϕ_i=90° or ϕ_i=270°). There is comparatively smaller backscattering at x and -x direction (ϕ_i=0° and 180°). The results of pulse basis point matching program [43] is also included for comparison which shows excellent agreement with the plane wave expansion result.

2. Near Zone

As a second example, consider a 1.m by .5m air filled rectangular cylinder located in a homogeneous dielectric medium with ε_{r_2} =4. and σ_2=.3ms/m as shown in the model of Figure 3-5. The electric line source is placed at the radial distance of ρ=2m and the relative backscattered field is calculated as a function of ϕ_i. The SAF versus ϕ_i is shown in Figure 3-5. The result of an alternative computer program (RCYLPWE) is also included which shows a 1db descripancy. The program RCYLPWE is included in Appendix A along with a complete description.

E. BISTATIC SCATTERING

1. Far Zone

The complete scattering patterns for three cases of plane wave incidences at ϕ_i=0°, 45°, and 90°, and for a 1m by .5m rectangular

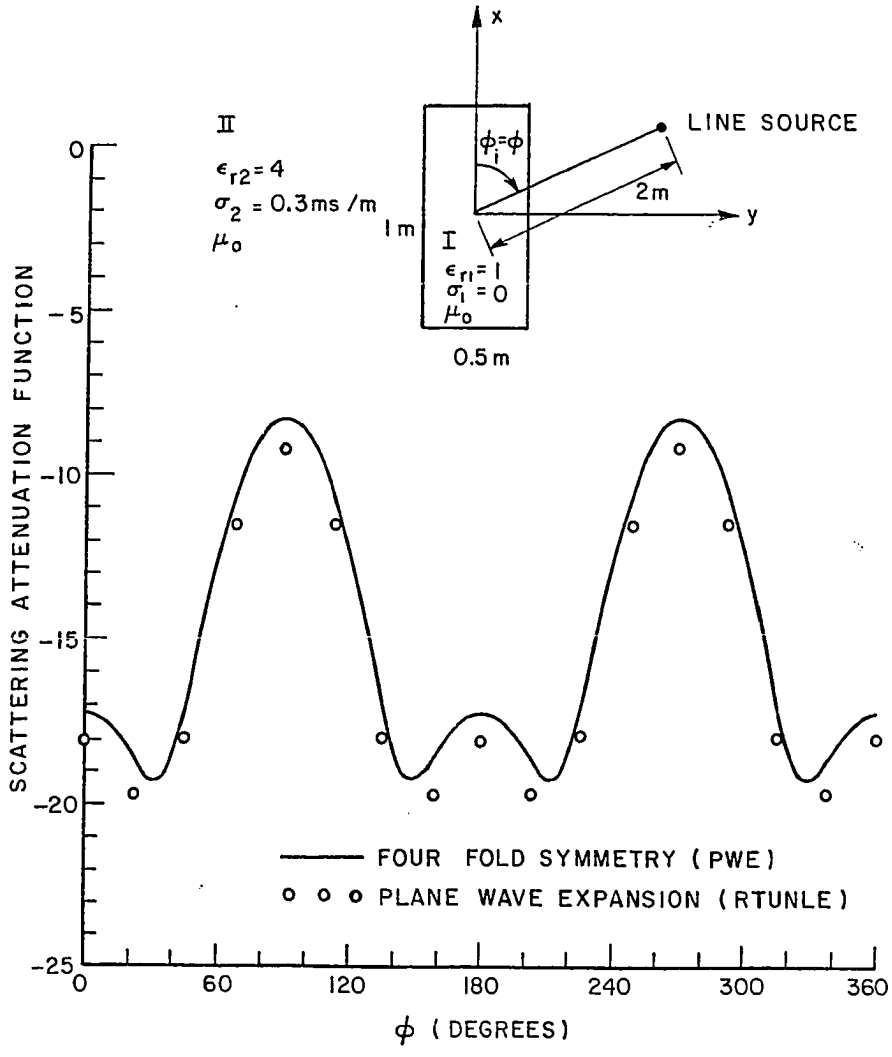

Figure 3-5. Near zone backscattering pattern for the model shown above. The line source is placed at ρ_s=2m. the frequency is 100 MHz.

cylinder have been computed and given in Figures 3-6, 3-7, and 3-8, respectively. The bistatic pattern for a z-polarized plane wave incident along x-axis (ϕ_i=0°)is shown in Figure 3-6. A strong forward scattered lobe is indicated at ϕ=180°. This lobe will shift and the symmetry will be altered if ϕ_i is changed. For example, at ϕ_i=45° (see Figure 3-7) the symmetry is no longer maintained because of the none symmetric physical situation. The maximum is now obtained around ϕ=210°. Initially, this result seemed suspicious since the maximum value of the scattered field is not in the forward direction and thus prompted further investigations. Some approximate methods were considered and proved not useful. Some of these methods will be discussed in a future section. Richmond's pulse basis point matching showed excellent agreement and is also shown in Figure 3-7. If we further increase the incidence angle to 90° so that now the plane wave is incident along y-axis, the symmetry is obtained about ϕ=270° where the main forward lobe is maximum. This is shown in Figure 3-8 along with the pulse basis point matching result which indicates excellent agreement.

2. Near Zone

The three cases considered here place the line source at (ρ_s,ϕ_s)=(2m,0°), (ρ_s,ϕ_s)=(2m, 45°), and (ρ_s,ϕ_s)=(2m, 90°) which are analogeous to ϕ_i=0°, 45°, and 90° considered in the previous section. A 1m by .5m air filled rectangular cylinder is located in a homogeneous

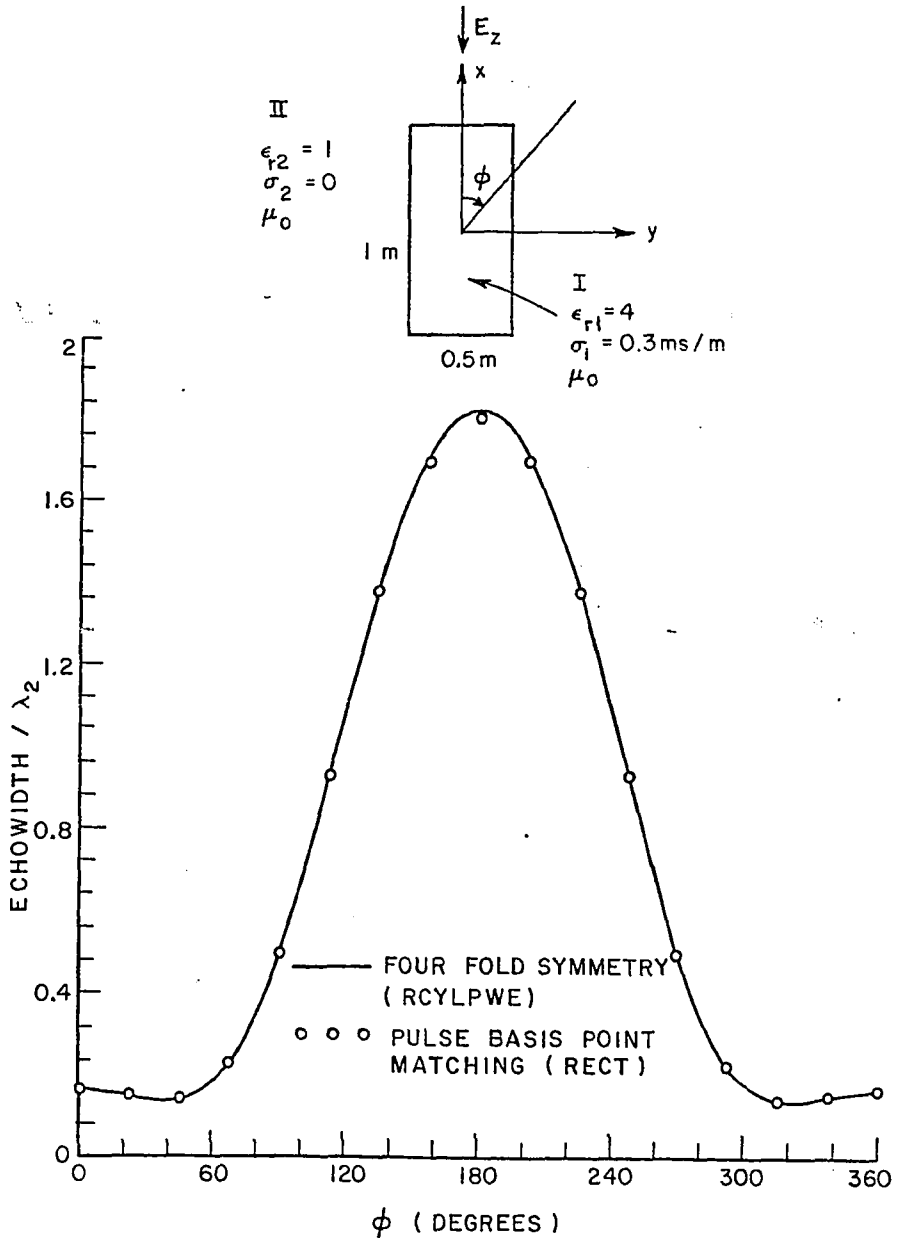

Figure 3-6. Far zone bistatic scattering pattern for a plane wave incident at $\phi_i=0°$, at 100 MHz.

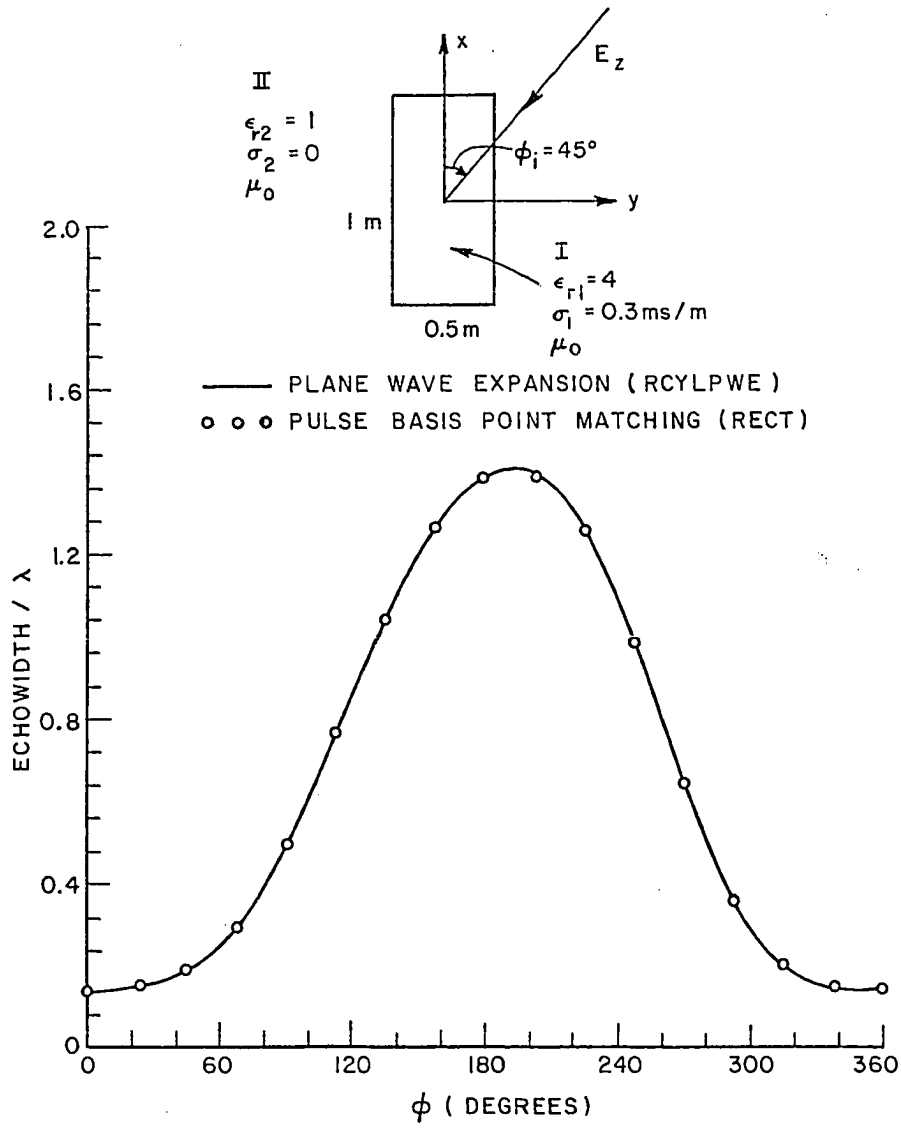

Figure 3-7. Far zone bistatic scattering pattern for a plane wave incident at ϕ_i=45°, at 100 MHz.

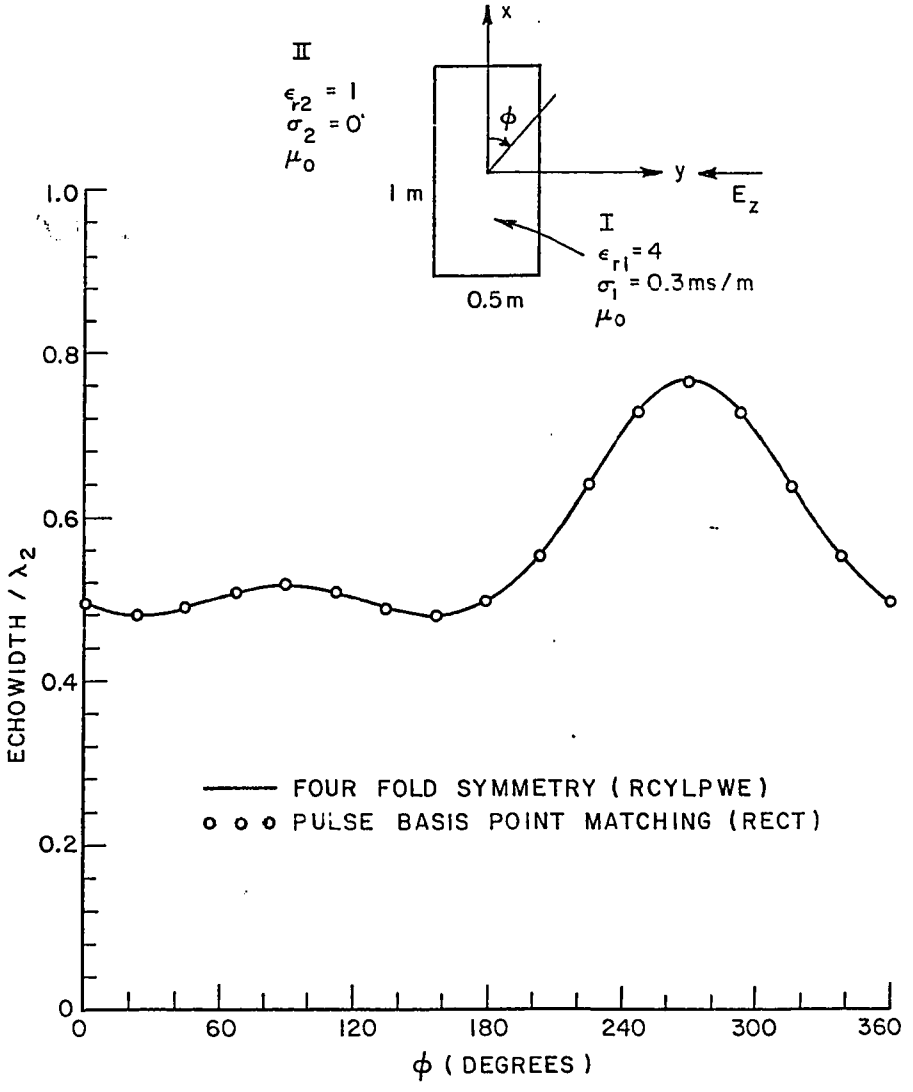

Figure 3-8. Far zone bistatic scattering pattern for a plane wave incident at ϕ_i=90°, at 100 MHz.

medium of ε_{r_2} =4. and σ_2=.3ms/m. The results are shown in Figure 3-9, 3-10, and 3-11.

The field is observed at a radial distance of ρ=2m. Figure 3-9 shows the bistatic pattern when the line source is located at (ρ_s, ϕ_s)=(2m,0°) as a function of observation angle ϕ. This pattern shows large forward scattering and small backlobe. The pattern is symmetric about ϕ=180° as expected. When the line source is moved to (ρ_s, ϕ_s) = (2m, 45°), the shape of the pattern is changed and the symmetry is no longer maintained, and the main lobe is shifted to around ϕ=240° as may be observed in Figure 3-10. Figure 3-11 shows the bistatic pattern for the line source at (ρ_s, ϕ_s)=(2m, 90°). A strong forward lobe and a smaller back lobe is observed (ϕ=270° and ϕ=90° respectively). The pattern is now symmetric about ϕ=270°. Also included in Figures 3-9, 3-10, and 3-11 are the results of RCYLPWE which show good agreement in each case. The slight descripancy is due to the nature of the numerical techniques used.

F. SCATTERING VERSUS FREQUENCY

In this section three line source locations are considered. In each case the frequency is varied from 10MHz up to 300MHz and the Scattering Attenuation Function is calculated.

A 1.m by .5m air filled rectangular cylinder is immersed in a homogeneous medium with ε_{r_2}=4. and σ_2=.003s/m. Figure 3-12 shows backscattered SAF versus frequency for three line source locations. The

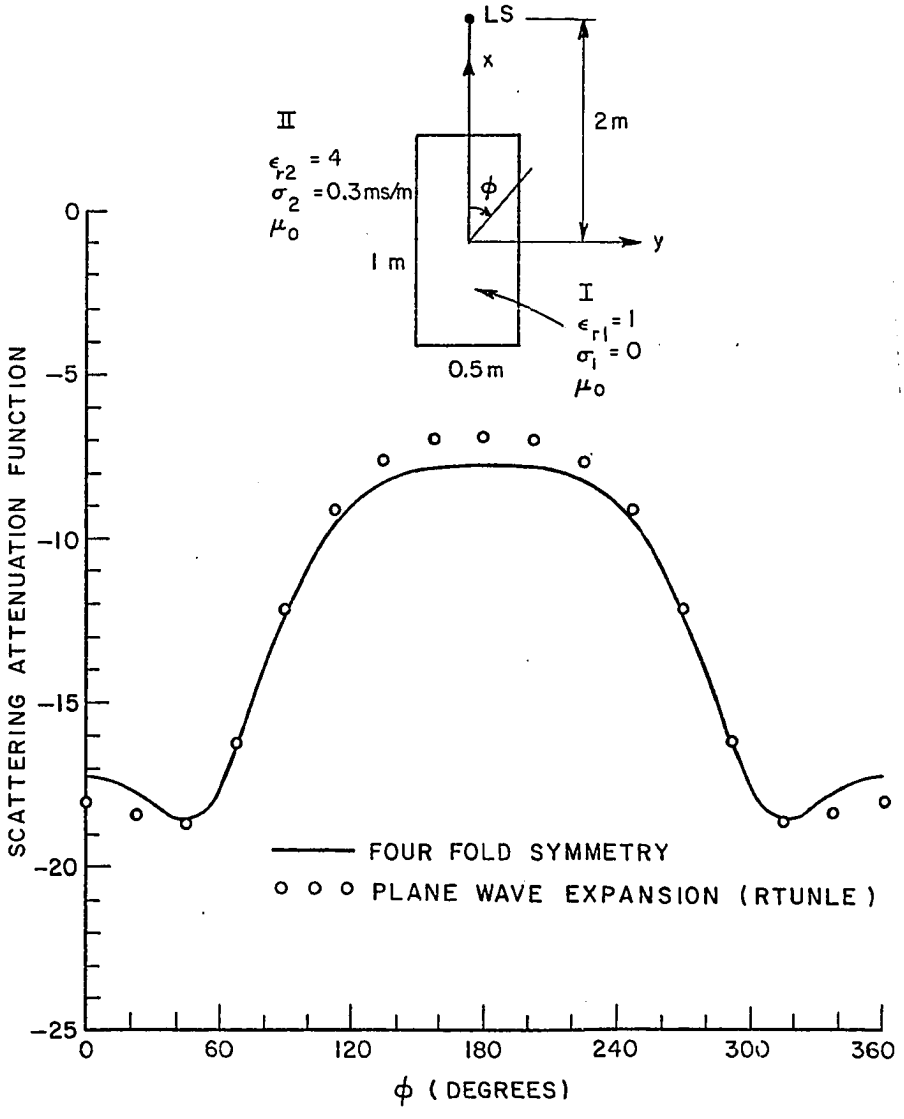

Figure 3-9. Near zone bistatic scattering pattern for an electric line source excitation placed at $(\rho_S, \phi_S)=(2m, 0°)$ and at 100 MHz. The observation point is at $\rho=2m$.

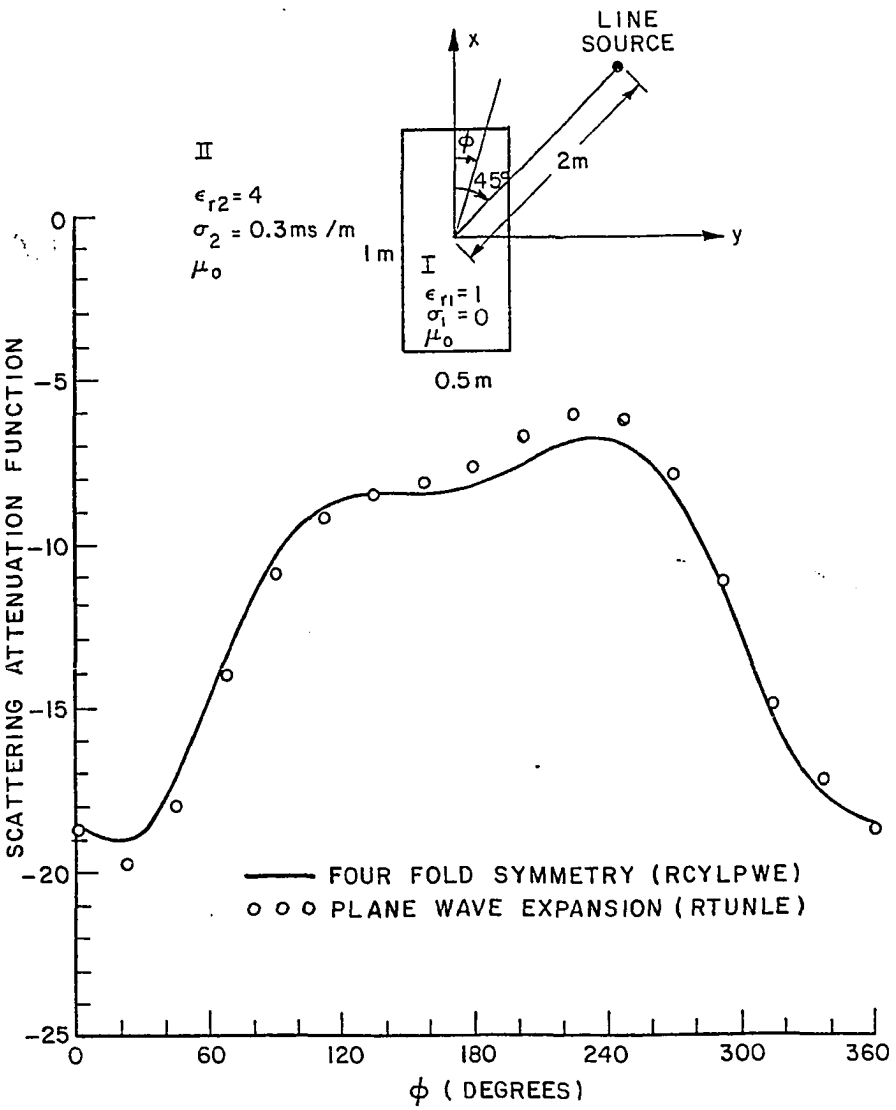

Figure 3-10. Near zone bistatic scattering pattern for an electric line source excitation placed at $(\rho_s, \phi_s)=(2m, 45°)$ and at 100 MHz. The observation point is at $\rho=2m$.

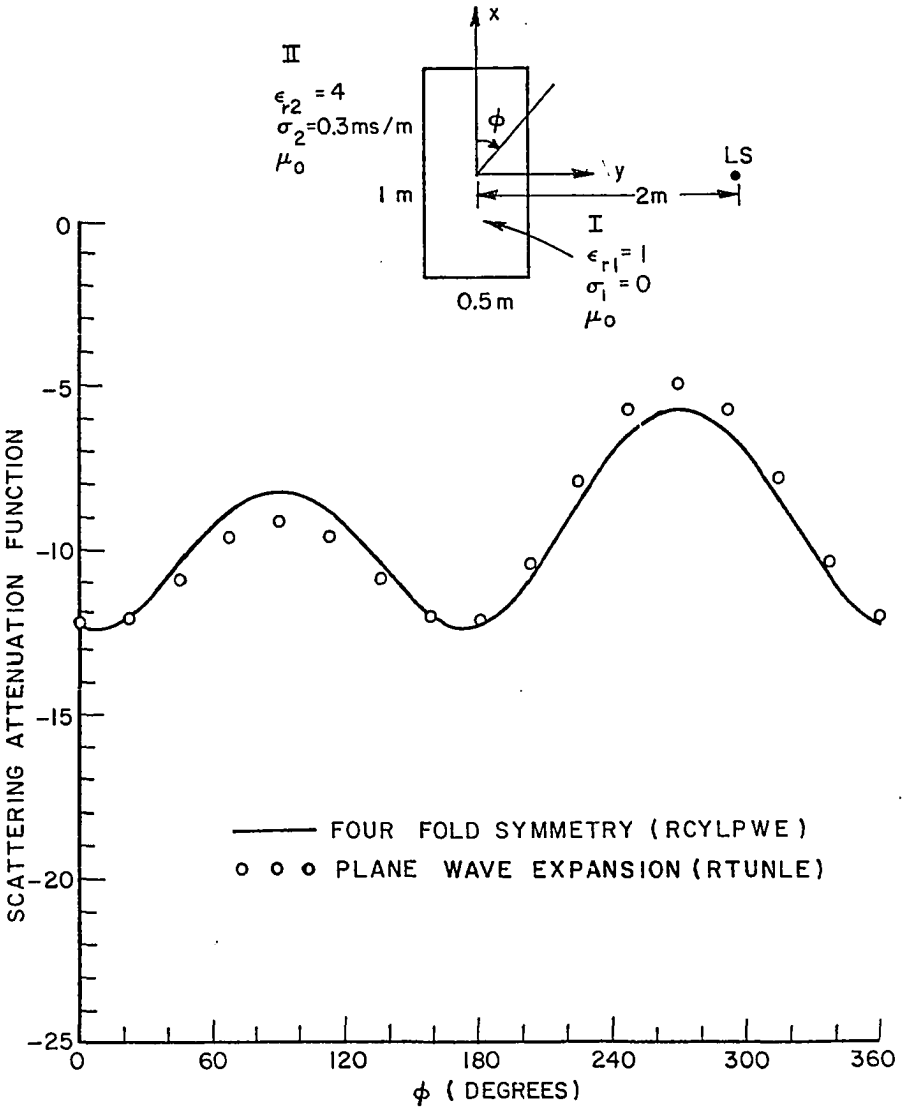

Figure 3-11. Near zone bistatic scattering pattern for an electric line source placed at $(\rho_s, \phi_s)=(2m, 90°)$ and at 100 MHz. The observation point is at ρ=2m.

dashed line shows the SAF versus frequency for a line source located at $(\rho_s, \phi_s)=(2m, 0°)$. The solid line shows the SAF versus frequency for a line source located at $(\rho_s, \phi_s)=(2m, 45°)$, and the dash-dot line shows the SAF versus frequency for a line source located at $(\rho_s, \phi_s)=(2m, 90°)$. at low frequencies the rectangular scatterer looks the same to an observer at the observation point. This is the so called Rayleigh region.

In addition to moment method, two approximate methods were investigated consisting of an aperture integration solution and physical optics type of solution for dielectrics. For aperture integration approach, an aperture is defined, the Equivalence currents J_e densities are determined [44] and integrated to give the scattered field. To calculate the far zone backscattered field using this approach the aperture is defined as shown in Figure 3-13. The aperture field is the total reflected field evaluated at the aperture and the equivalent currents are $\overline{J}_e = 2\hat{n} \times \overline{H}$. The scattered field obtained by this method is shown in Figure 3-13. This does not agree with the moment method results. The physical optics approximation assumes the field in the scatterer is the same as that of a infinite slab of the same thickness (i.e., dielectric slab with thickness of 2b) [45]. Using the physical optics, a volumetric polarization current is defined and integrated to give the scattered field. The far zone backscattered field obtained by physical optics is given in Figure 3-13. This result agrees well with the aperture integration result, but does not agree with the moment method solution.

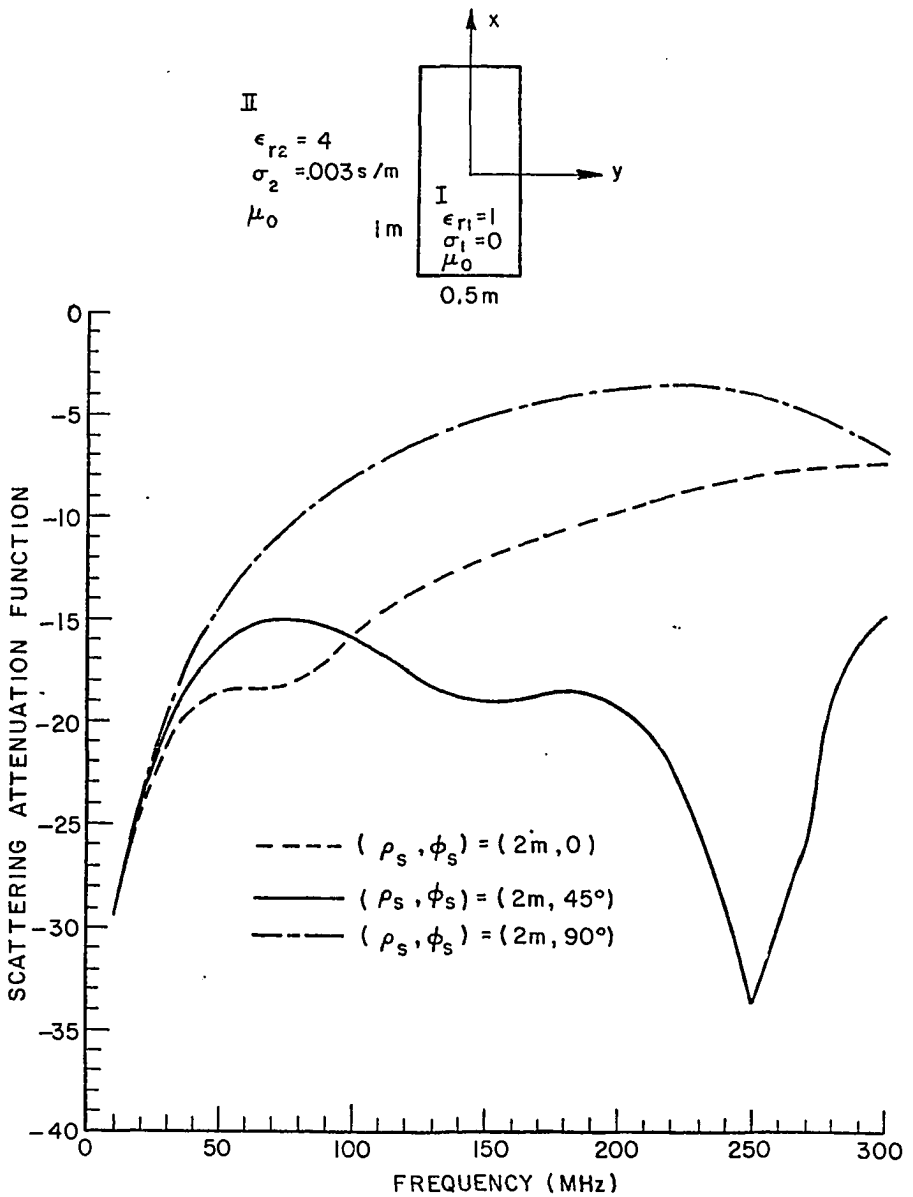

Figure 3-12. Near zone backscattering versus frequency for electric line source excitations placed at $(\rho_s, \phi_s)=(2m, 0°)$, $(2m, 45°)$, and $(2m, 90°)$.

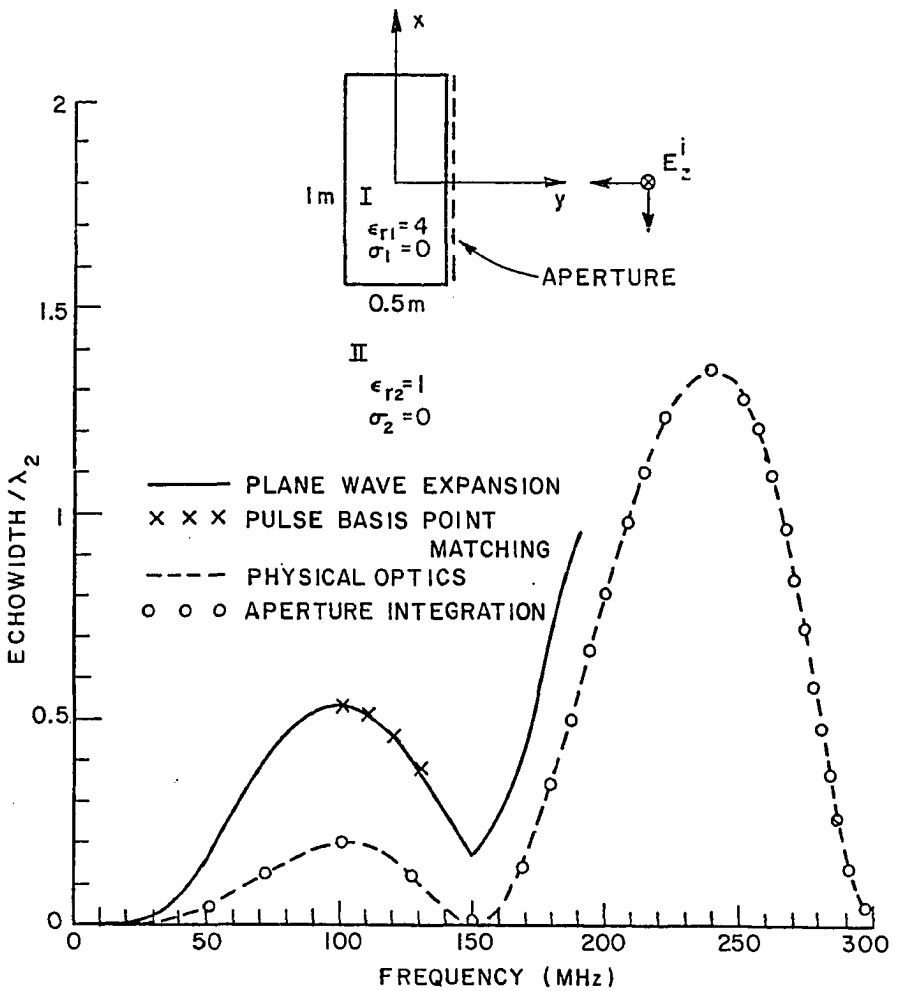

Figure 3-13. Far zone backscattering versus frequency for a plane wave incident at $\phi_i=90°$.

An anologous set of curves as Figure 3-13 is obtained for the forward scattering case, and is shown in Figure 3-14. The aperture defined for forward scattering is also shown in Figure 3-14. The aperture field is the difference of the total transmitted field and the incident field evaluated at the aperture. The aperture field and physical optics results for forward scattering shown in Figure 3-14 agree more closely with the moment method solution than the analogous results for backscattering.

Finally, a comparison is given in Figure 3-15 between a moment method solution for scattering by a 1.m-square air filled cylinder immersed in a homogeneous medium with $\varepsilon_{r_2}=4.$ and $\sigma_2=.003$s/m and an exact solution for an equivalent (equal cross-sectional areas) air-filled circular cylinder immersed in the homogeneous medium of the same electrical parameters as given above. These geometries are shown in Figure 3-15. For low frequencies as one may expect the two scatterers are not distinguished. This provides a good check on the validity of the moment method solution.

G. SUMMARY

In this chapter, the mathematical formulation for E-wave scattering by a two-dimensional lossy dielectric rectangular cylinder immersed in a lossy homogeneous medium was presented. A convergence curve was included and some numerical results were presented and discussed. A comparison between a moment method solution for a square cylinder and an exact solution for an equivalent circular cylinder was included.

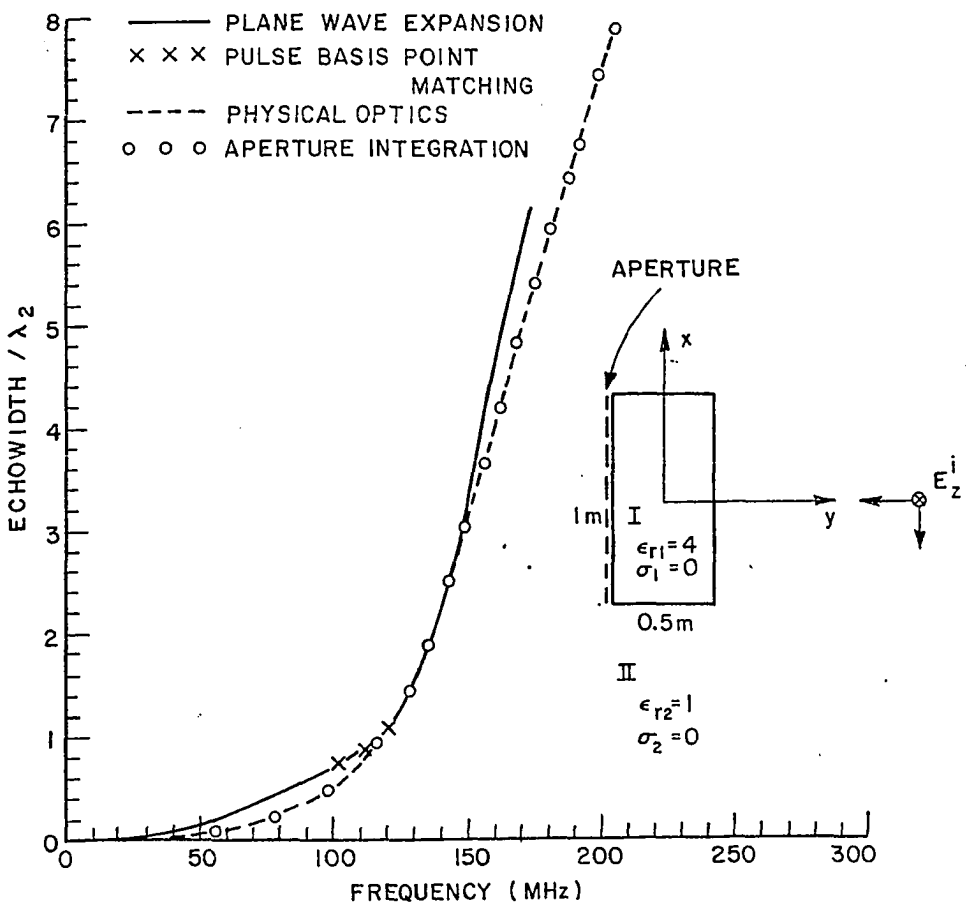

Figure 3-14. Far zone forward scattering versus frequency for a plane wave incident at $\phi_i=90°$.

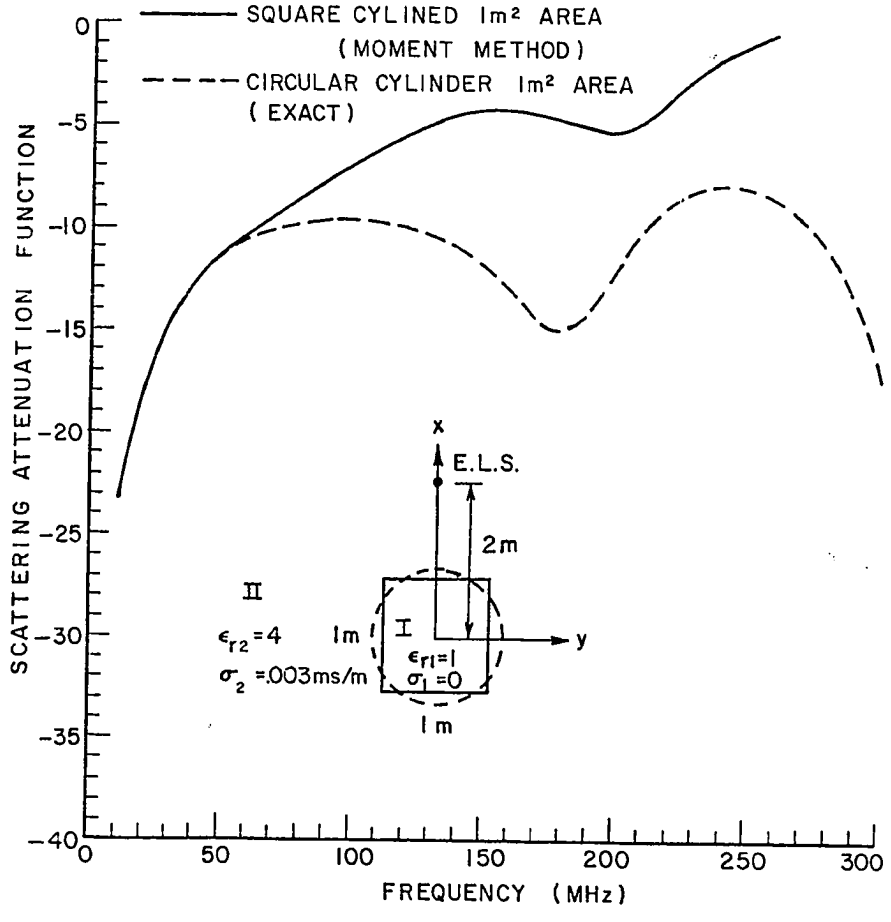

Figure 3-15. Comparison of backscattering versus frequency for a 1 m square cylinder and an equivalent cross-section area circular cylinder. The electric line source is located at $(\rho_s, \phi_s)=(2m, 0°)$.

In the next chapter, the H-wave scattering by a two-dimensional lossy dielectric rectangular cylinder is treated.

CHAPTER IV

H-WAVE SCATTERING BY LOSSY, DIELECTRIC RECTANGULAR CYLINDERS OF INFINITE LENGTH, IN A LOSSY HOMOGENEOUS MEDIUM

A. INTRODUCTION

In this chapter, the plane wave expansion is applied to the H-wave scattering formulation presented in Chapter II. Some examples of the convergence properties are given. Examples of typical scattered field patterns are presented for cases of a lossy rectangular cylinder in a free space environment and for an air cylinder in a lossy ambient medium.

B. PLANE WAVE EXPANSION

The general moment method formulation for H-wave scattering by dielectric cylinders presented in Chapter II is specialized to analyze the geometry depicted in Figure 4-1, where, a (2a) by (2b) lossy dielectric rectangular cylinder of infinite length with the electrical parameters ε_1, σ_1, μ_1 is immersed in homogeneous medium whose electrical parameters are ε_2, σ_2, μ_2. The source is a time harmonic, infinite magnetic line source placed at (x_s, y_s) or (ρ_s, ϕ_s).

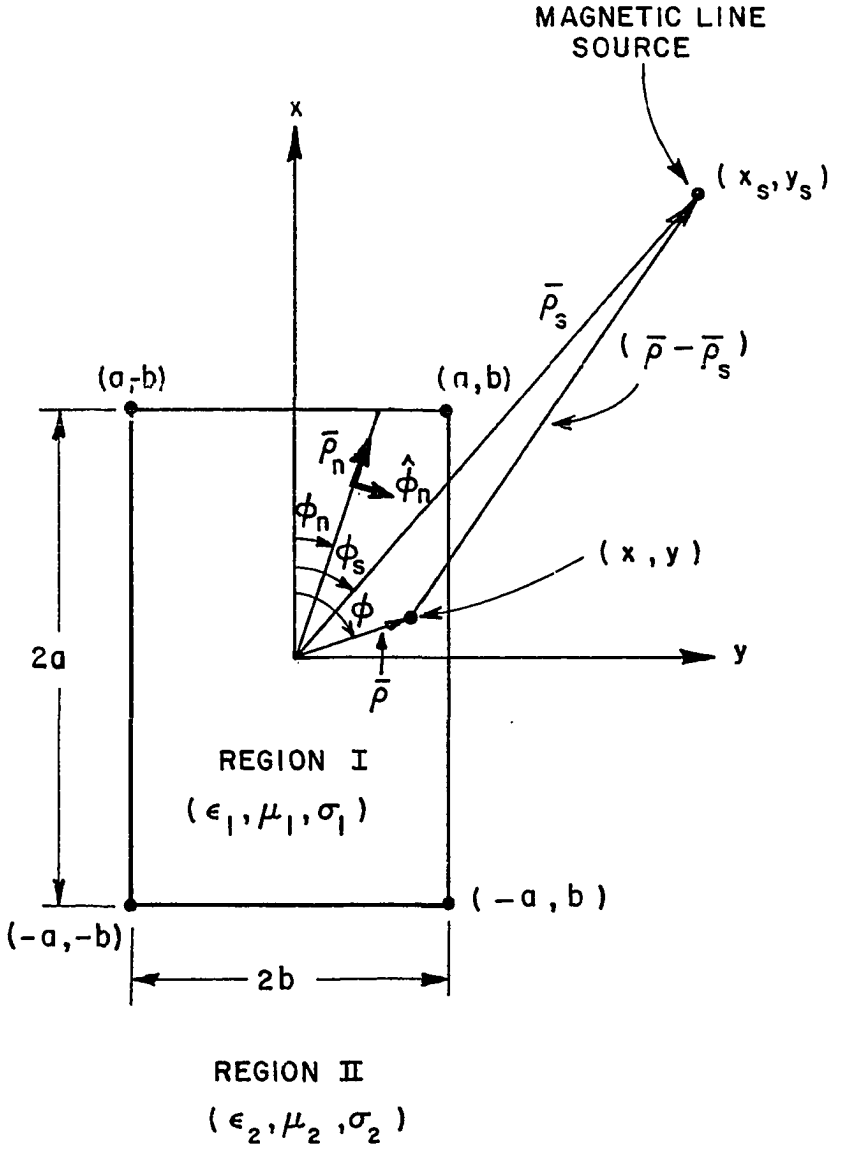

Figure 4-1. H-wave electromagnetic scattering model for a lossy dielectric rectangular cylinder of infinite length immersed in a lossy homogeneous medium.

As shown in Figure 4-1, the z-axis constitutes the cylinder axis. The magnetic fields inside this cylinder are expanded in terms of a set of basis function $F_m(x,y)$ similar to Equation (3.3). Choosing the plane wave basis function given in Equation (3.1) one obtains

$$H^I_{z(x,y)} = \sum_{n=1}^{N} C_n e^{-jf_n x} e^{-jg_n y} \quad . \tag{4.1}$$

For this plane wave expansion,

$$\bar{E}^I_{(x,y)} = \eta_1 \sum_{n=1}^{N} C_n e^{-jf_n x} e^{-jg_n y} \hat{\phi}_n \quad , \tag{4.2}$$

where

$$\hat{\phi}_n = -\hat{x}\sin\phi_n + \hat{y}\cos\phi_n \quad . \tag{4.3}$$

$\hat{\phi}_n$ is the unit vector associated with n^{th} plane wave traveling in direction of $\hat{\rho}_n = \hat{x}\cos\phi_n + \hat{y}\sin\phi_n$ as shown in Figure 4-1 and η_1 is the interinsic impedance of Medium I.

It is desired to obtain a set of simultaneous linear equations as given by Equation (2.11). To obtain the elements of the voltage matrix column (V_m). Equations (3.1b) and (2.27a) are substituted in Equation (2.42) to obtain

$$V_m = \frac{-\gamma_2}{2\pi\eta_1} \int_{-a}^{a}\int_{-b}^{b} e^{-jf_m x} e^{-jg_m y} K_1(\gamma_2|\bar{\rho}-\bar{\rho}_s|)\cos(\phi_m-\phi_{LS})dxdy \quad , \tag{4.4}$$

where ϕ_{LS} is defined in Figure 2-4.

Equation (2.43) for Z_{mn} may be expressed as the sum of three terms

$$Z_{mn} = R'_{mn} + S'_{mn} + T_{mn} \quad . \tag{4.5a}$$

The evaluation of R'_{mn} and S'_{mn} is similar to Equations (3.5b) and (3.5c) respectively. Using Equations (3.1b) and (2.43), the equations for R'_{mn} and S'_{mn} are reduced to

$$R'_{mn} = \cos(\phi_m - \phi_n) R_{mn} \quad , \tag{4.5b}$$

and

$$S'_{mn} = \cos(\phi_m - \phi_n) S_{mn} \quad . \tag{4.5c}$$

R_{mn} and S_{mn} are given by Equations (3.5b) and (3.10a) respectively. The remaining term in Equation (4.5a) is obtained using Equation (3.16) in the last term of Equation (2.43)

$$T_{mn} = C_2 \int_{-a}^{a} \int_{-b}^{b} \int_{\ell} \left[e^{-jf_n x'} e^{-jg_n y'} \left((\hat{\phi}_n \cdot \hat{n}(\ell')) \right) \right] e^{-jf_m x} e^{-jg_m y} (\hat{\phi}_m \cdot \hat{\rho}) K_1(\gamma_2 |\bar{\rho} - \bar{\rho}'|) d\ell' dx dy \quad . \tag{4.5d}$$

where

$$C_2 = - \frac{(\hat{\varepsilon}_1 - \hat{\varepsilon}_2)\gamma_2}{2\pi \hat{\varepsilon}_2} \quad , \tag{4.5e}$$

and V_m and Z_{mn} have been normalized by $(-jk_1\eta_1)$.

Integrations in Equations (4.4) and (4.5d) are evaluated to a closed form by using the transform of the modified Bessel function

$K_1(\gamma_2|\bar{\rho}-\bar{\rho}'|)$. Taking the gradient of both sides of Equation (3.6a) yields

$$K_1(\gamma_2|\bar{\rho}-\bar{\rho}'|)\cos\phi = \frac{1}{\gamma_2}\int_0^\infty \frac{f\,\mathrm{sgn}(x-x')e^{-f|x-x'|}\cos[g(y-y')]}{f}\,dg \quad . \tag{4.6a}$$

$$K_1(\gamma_2|\bar{\rho}-\bar{\rho}'|)\sin\phi = \frac{1}{\gamma_2}\int_0^\infty \frac{g e^{-f|x-x'|}\sin[g(y-y')]}{f}\,dg \quad . \tag{4.6b}$$

f and g are given in Equation (3.6b).

To evaluate Equation (4.4), the above two relations are used with $\phi=\phi_{LS}$, $\rho'=\rho_s$ $x'=x_s$ and $y'=y_s$. Changing the order of integrations yields

$$V_m = \frac{-1}{2\pi\eta_1}\int_0^\infty \frac{1}{f}\Big[f\cos\phi_m \int_{-a}^{a}\int_{-b}^{b} e^{-jf_m x} e^{-jg_m y}\,\mathrm{sgn}(x-x_s)\, e^{-f|x-x_s|}\cos[g(y-y_s)]\,dx\,dy + g\sin\phi_m \int_{-a}^{a}\int_{-b}^{b} e^{-jf_m x} e^{-jg_m y} e^{-f|x-x_s|}\sin[g(y-y_s)]\,dx\,dy\Big]\,dg \quad . \tag{4.7}$$

$$V_m = \frac{-1}{2\pi\eta_1} \int_0^\infty \frac{1}{f} \sin\phi_m \left\{ \int_{-a}^{a} e^{-jf_m x} e^{-f|x-x_s|} dx \left[g \int_{-b}^{b} e^{-jg_m y} \sin[g(y-y_s)]dy \right] \right.$$

$$\left. + \cos\phi_m \int_{-a}^{a} \mathrm{sgn}(x-x_s) e^{-f_m x} e^{-f|x-x_s|} dx \left[f \int_{-b}^{b} e^{-jg_m y} \cos[g(y-y_s)]dy \right] \right\} dg \quad , \tag{4.8}$$

$$V_m = \frac{-1}{\pi\eta_1} \int_0^\infty \frac{1}{f} \left[F_m(g\sin\phi_m)\, GO_m^V + G_m(f\cos\phi_m)\, GE_m^V \right] dg \quad , \tag{4.9a}$$

where

F_m and GE_m^V are given in Equations (3.8b) and (3.8c) respectively,

$$GO_m^V = -j\left(e^{-jgy_s} \frac{\sin[(g_m-g)b]}{(g_m-g)} - e^{jgy_s} \frac{\sin[g_m+g)b]}{(g_m+g)} \right) , \tag{4.9b}$$

and

$$G_m = \left\{ \begin{array}{ll} -e^{-fx_s} \dfrac{\sin[(f_m+jf)a]}{(f_m+jf)} & x_s > a \\ \dfrac{-j\, e^{-fx_s}}{2(f_m+jf)} e^{-j(f_m+jf)x_s} - e^{j(f_m+jf)a} & -a \leq x_s \leq a \\ + \dfrac{j\, e^{fx_s}}{2(f_m-jf)} e^{-j(f_m-jf)a} - e^{-j(f_m-jf)x_s} & \\ e^{fx_s} \dfrac{\sin[(f_m-jf)a]}{(f_m-jf)} & x_s < -a \end{array} \right\} . \tag{4.9c}$$

To evaluate the integrals in T_{mn}, (Equation (4.5d)) the two useful transforms of Equations (4.6a) and (4.6b) are used, but first, the integration path ℓ is broken into four segments and defined as follows; considering Figure 4-1

$$\ell = \begin{cases} \ell_1 \text{ ; from } (a,-b) \text{ to } (a,b) \text{ , } \hat{n}(\ell_1) = \hat{x} \\ \ell_2 \text{ ; from } (-a,b) \text{ to } (a,b) \text{ , } \hat{n}(\ell_2) = \hat{y} \\ \ell_3 \text{ ; from } (-a,-b) \text{ to } (-a,b) \text{ , } \hat{n}(\ell_3) = -\hat{x} \\ \ell_4 \text{ ; from } (-a,-b) \text{ to } (a,-b) \text{ , } \hat{n}(\ell_4) = -\hat{y} \end{cases} \tag{4.10}$$

Also, the inner-product $(\hat{\phi}_n \cdot \hat{n}(\ell'))$ in Equation (4.5d) is found from Equations (4.3) and (4.10) as

$$(\hat{\phi}_n \cdot \hat{n}(\ell')) = \begin{cases} -\sin\phi_n \text{ ; for } \ell_1 \quad . \\ \cos\phi_n \text{ ; for } \ell_2 \quad . \\ \sin\phi_n \text{ ; for } \ell_3 \quad . \\ -\cos\phi_n \text{ ; for } \ell_4 \quad . \end{cases} \tag{4.11}$$

Substituting Equations (4.11) in (4.5d), T_{mn} is now given by

$$T_{mn} = C_2 \int_{-a}^{a}\int_{-b}^{b} e^{-jf_m x} e^{-jg_m y} \left\{ -\sin\phi_n \left[\int_{-b}^{b} e^{-jf_n a} e^{-jg_n y'} \right.\right.$$

$$\left.\left. (\cos\phi_m K_1(\gamma_2|\bar{\rho}-\bar{\rho}_1|)\sin\alpha_1 + \sin\phi_m K_1(\gamma_2|\bar{\rho}-\bar{\rho}_1|)\cos\alpha_1)dy' \right] \right.$$

$$\left. + \left[\cos\phi_n \int_{-a}^{a} e^{-jf_n x'} e^{-jg_n b} (\cos\phi_m K_1(\gamma_2|\bar{\rho}-\bar{\rho}_2|)\sin\alpha_2 \right. \right.$$

$$
\left.
\begin{aligned}
&- \sin\phi_m K_1(\gamma_2|\bar{\rho}-\bar{\rho}_2|)\cos\alpha_2)dx'\Big] + \\
&\Big[\sin\phi_n \int_{-b}^{b} e^{jf_n a}\, e^{-jg_n y'} (\cos\phi_m K_1(\gamma_2|\bar{\rho}-\bar{\rho}_3|)\sin\alpha_3 \\
&- \sin\phi_m K_1(\gamma_2|\bar{\rho}-\bar{\rho}_3|)\cos\alpha_3)dy'\Big] \\
&- \Big[\cos\phi_n \int_{-a}^{a} e^{-jf_n x'}\, e^{jg_n b} (\cos\phi_m K_1(\gamma_2|\bar{\rho}-\bar{\rho}_4|)\sin\alpha_4 \\
&- \sin\phi_m K_1(\gamma_2|\bar{\rho}-\bar{\rho}_4|)\cos\alpha_4)dx'\Big]\Big\}\, dxdy \quad .
\end{aligned}
\right. \tag{4.12}
$$

where $(\hat{\phi}_m \cdot \hat{\rho}) = \sin(\phi-\phi_m)$ was used above ($\hat{\rho}$ is the unit vector in the direction of $\bar{\rho}$). To avoid confusion with ϕ_m and ϕ_n, ϕ is changed to α and subscripted according to the path of integration.

$$
\left\{
\begin{aligned}
&|\bar{\rho}-\bar{\rho}_1| = \sqrt{(x-a)^2 + (y-y')^2} \quad ; \quad \alpha_1 = \tan^{-1}\left(\frac{y-y'}{x-a}\right) \\
&|\bar{\rho}-\bar{\rho}_2| = \sqrt{(x-x')^2 + (y-b)^2} \quad ; \quad \alpha_2 = \tan^{-1}\left(\frac{y-b}{x-x'}\right) \\
&|\bar{\rho}-\bar{\rho}_3| = \sqrt{(x+a)^2 + (y-y')^2} \quad ; \quad \alpha_3 = \tan^{-1}\left(\frac{y-y'}{x+a}\right) \\
&|\bar{\rho}-\bar{\rho}_4| = \sqrt{(x-x')^2 + (y+b)^2} \quad ; \quad \alpha_4 = \tan^{-1}\left(\frac{y+b}{x-x'}\right)
\end{aligned}
\right\} \quad . \tag{4.13}
$$

The relations given in Equations (4.6a) and (4.6b) may now be used in Equation (4.12), and the integrals are rearranged so that the line and cross sectional integrals are evaluated to a closed form. After some regrouping T_{mn} is now given by

$$T_{mn} = \frac{C_2}{\gamma_2} \int_0^{\infty} \frac{1}{f} \Big[- \sin\phi_n \cos\phi_m g(S1-S5) + \sin\phi_n \sin\phi_m f(S2-S6) + \cos\phi_n \cos\phi_m g(S3-S7) - \cos\phi_n \sin\phi_m f(S4-S8) \Big] \, dg \quad . \tag{4.14}$$

where

$$S1 = 4e^{-j(f_n-jf)a} \; F1 \cdot G1 \quad . \tag{4.15a}$$

$$S2 = -4e^{-j(f_n-jf)a} \; F2 \cdot G2 \quad . \tag{4.15b}$$

$$S3 = 2e^{-jg_n b} \; F3 \cdot G3 \quad . \tag{4.15c}$$

$$S4 = 2e^{-jg_n b} \; F4 \cdot G4 \quad . \tag{4.15d}$$

$$S5 = 4e^{-j(f_n+jf)a} \; F5 \cdot G5 \quad . \tag{4.15e}$$

$$S6 = 4e^{-j(f_n+jf)a} \; F6 \cdot G6 \quad . \tag{4.15f}$$

$$S7 = 2\,e^{jg_n b} \; F7 \cdot G7 \quad . \tag{4.15g}$$

$$S8 = 2e^{jg_n b} \; F8 \cdot G8 \quad . \tag{4.15h}$$

where

$$F1 = F2 \ \frac{2\sin[(f_m+jf)a]}{(f_m+jf)} \quad . \tag{4.16}$$

$F3 = F7 = 2FE_{mn}$ (FE_{mn} is given in Equation (3.10b))

$$F4 = F8 = 2j\left(\frac{\sin[(f_m+f_n)a]}{(f_n+jf)(f_m+f_n)} - e^{j(f_m+jf)a}\frac{\sin[(f_m-jf)a]}{(f_n+jf)(f_m-jf)}\right.$$

$$\left. - e^{-j(f_n-jf)a}\frac{\sin[(f_m+jf)a]}{(f_n-jf)(f_m+jf)} + \frac{\sin[(f_m+f_n)a]}{(f_n-jf)(f_m+f_n)}\right) \quad . \tag{4.17}$$

$$F5 = F6 = \frac{2\sin[(f_m-jf)a]}{(f_m-jf)} \quad . \tag{4.18}$$

$G1 = G5 = 2GO_{mn}$ where

$$GO_{mn} = -j\left(\frac{\sin[(g_n+g)b]\sin[(g_m-g)b]}{(g_n+g)(g_m-g)} - \frac{\sin[(g_n-g)b]\sin[(g_m+g)b]}{(g_n-g)(g_m+g)}\right) \quad . \tag{4.19}$$

$G2 = G6 = 2GE_{mn}$; (GE_{mn} is given in Equation (3.10c))

$$G3 = -j\left(e^{-jgb}\frac{\sin[(g_m-g)b]}{(g_m-g)} - e^{jgb}\frac{\sin[(g_m+g)b]}{(g_m+g)}\right) \quad . \tag{4.20}$$

$$G4 = e^{-jgb}\frac{\sin[(g_m-g)b]}{(g_m-g)} + e^{jgb}\frac{\sin[(g_m+g)b]}{(g_m+g)} \quad . \tag{4.21}$$

$$G7 = -j\left(e^{jgb}\frac{\sin[(g_m-g)b]}{(g_m-g)} - e^{-jgb}\frac{\sin[(g_m+g)b]}{(g_m+g)}\right) \quad . \tag{4.22}$$

$$G8 = e^{jgb}\frac{\sin[(g_m-g)b]}{(g_m-g)} + e^{-jgb}\frac{\sin[(g_m+g)b]}{(g_m+g)} \quad . \tag{4.23}$$

These steps now completely fill the matrix elements of Equation (2.14). Now the matrix can be inverted to solve for the response matrix $[C_n]$. The scattered field can be calculated by substituting Equation (3.1) into Equation (2.46)

$$H^s_{z(x,y)} = \frac{\gamma_2 j\omega(\hat{\varepsilon}_1-\hat{\varepsilon}_2)p(-jK_1)}{2\pi}\sum_{m=1}^{N}$$

$$C_m\left[\int_{-a}^{a}\int_{-b}^{b} e^{-jf_m x'}\, e^{-jg_m y'}\left(\sin\phi_m \sin\phi K_1(\gamma_2|\bar{\rho}-\bar{\rho}'|)\right.\right.$$

$$\left.\left. + \cos\phi_m \cos\phi K_1(\gamma_2|\bar{\rho}-\bar{\rho}'|)\right)\right]dx'dy' \quad , \tag{4.24}$$

where Equations (3.2b) and (3.2c) have been used. Constant p is defined by Equation (2.40c).

Using Equation (4.6) in Equation (4.24) and simplifying yields

$$H^s_{z(x,y)} = -\frac{j\omega\eta_1(\hat{\varepsilon}_1-\hat{\varepsilon}_2)}{2\pi}\sum_{m=1}^{N}$$

$$\left[C_m \int_{-a}^{a}\int_{-b}^{b}\left[e^{-jf_m x'}\, e^{-jg_m y'}\left(\sin\phi_m \int_0^\infty \frac{g e^{-f|x-x'|}\sin[g(y-y')]}{f}dg\right.\right.\right.$$

$$\left.\left.\left. + \cos\phi_m \int_0^\infty \frac{\mathrm{sgn}(x-x')f e^{-f|x-x'|}\cos[g(y-y')]dg}{f}\right)\right]\right]dx'dy' \quad . \tag{4.25}$$

Interchanging the order of integrations and rearranging terms gives

$$H^s_{z(x,y)} = \frac{j\omega\eta_1(\hat{\varepsilon}_1-\hat{\varepsilon}_2)}{2\pi} \sum_{m=1}^{N}$$

$$C_m \int_0^\infty \frac{1}{f}\Bigg[\cos\phi_m f \iint_{cs} e^{-jf_m x'} e^{-jg_m y'} \operatorname{sgn}(x'-x) e^{-f|x'-x|} \cos[g(y'-y)]dx'dy'$$

$$+ \sin\phi_m g \iint_{cs} e^{-jf_m x'} e^{-jg_m y'} \sin[g(y'-y)]dx'dy'\Bigg] dg \quad , \qquad (4.26)$$

where the arguments of the functions have been rearranged so that the results of Equation (4.7) may be used to simplify the above complicated relation.

Comparing Equations (4.26) and (4.7), and evaluating the cross-sectional integrations to a closed form, the scattered field is finally given by

$$H^s_{z(x,y)} = \frac{j\omega\eta_1(\hat{\varepsilon}_1-\hat{\varepsilon}_2)}{\pi} \sum_{m=1}^{N} C_m \int_0^\infty \frac{1}{f}\left[F_m(\sin\phi_m g)GO^V_m + (\cos\phi_m f)GE^V_m\right] dg \cdot \qquad (4.27)$$

F_m, G_m, GE^V_m, and GO^V_m are given by Equations (3.8b), (4.9c), (3.8c), and (4.9b) respectively, with (x_s, y_s) replaced by (x,y).

The above equation gives the bistatic and backscattered fields. Additionally, when the backscattered field is needed, i.e., $(x,y) = (x_s,y_s)$, some calculation time may be saved by using the following

$$H_z^{B.S.}(x_s,y_s) = -j\omega\eta_1^2(\hat{\varepsilon}_1-\hat{\varepsilon}_2)\sum_{m=1}^{N} C_m V_m \quad . \tag{4.28}$$

This was obtained by replacing (x,y) with (x_s,y_s) in Equation (4.26) and (4.27) and comparing the resulting equations with Equations (4.8) and (4.9a).

The far zone scattered fields may be found by using Equation (3.1) in Equation (2.50), and evaluating the resulting integrals.

C. CONVERGENCE

Two computer programs RTUNLH and RCYLHGP were developed based on the formulation given in this chapter. RTUNLH and RCYLHGP programs are included and fully discussed in Appendices C and D. RCYLHGP was developed to enable the calculation of far zone, near zone, and back and bistatic scattering patterns, whereas, RTUNLH was developed to include all the above capabilities but was restricted so that x and $x_s > a$. This restriction is made so that the effect of an air-earth interface may be modeled. The air-earth interface is discussed extensively in the following chapter.

Two examples of convergence are shown in Figure 4-2. The backscattered field is calculated and plotted for increasing numbers of plane waves (N) in the expansion. In Figure 4-2a, a 1m by 1m square air filled cylinder immersed in a homogeneous dielectric medium with $\varepsilon_{r_2} = 4$ and $\sigma_2 = .001$s/m is modeled. The line source is located at $(x_s,y_s) =$

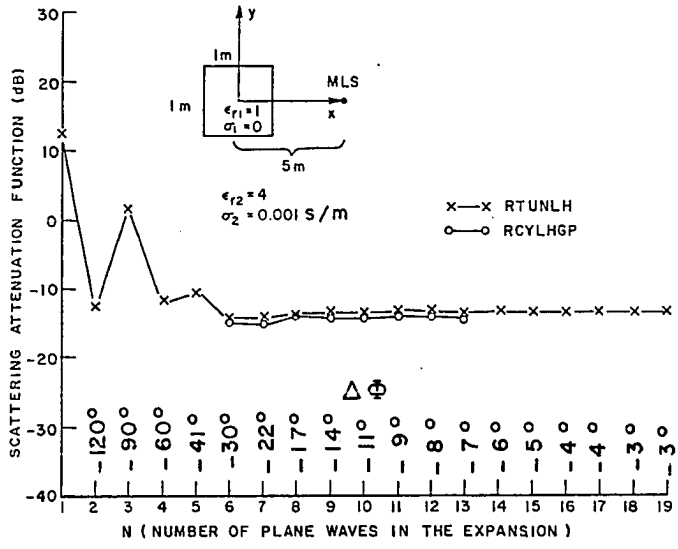

(a)

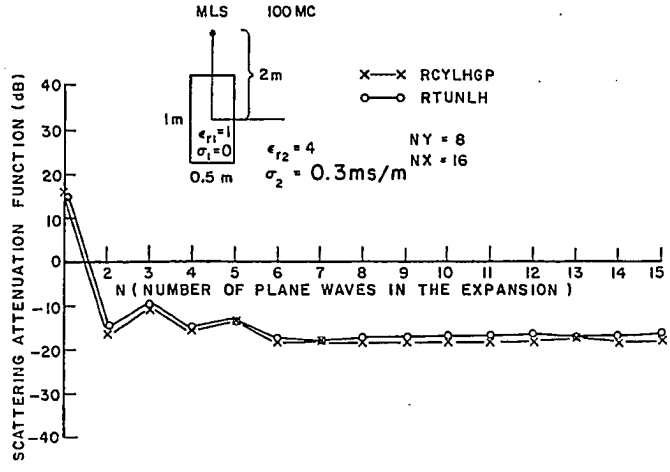

(b)

Figure 4-2. Convergence curves for RTUNLH and RCYLHGP computer programs which use plane wave expansion Galerkin method at 100 MHz. (a) for square air filled cylinder, (b) for a rectangular air filled cylinder. Scattering attenuation function is plotted as a function of N the number of plane waves in the expansion.

(5m,0m). The curves of Figure 4-2a suggest that the solution converges to a single value for N > 6 for RTUNLH computer program. Several points are also calculated by RCYLHGP computer program to confirm the convergence. The frequency used is 100 MHz.

The second example is shown is Figure 4-2b. A 1m by .5m, air-filled rectangular cylinder immersed in a homogeneous medium with ε_{r_2} = 4 and σ_2 = .3ms/m illuminated by a magnetic line source placed at (x_s, y_s) = (2m,0m). The curve for both programs seems to have converged to a single value at N > 6.

To get an idea about how many plane waves must be included in the expansion, a similar estimate as discussed for E-waves in Chapter III may be used for the expanded H-wave in the cylinder. In Figure 4-2a the $\Delta\Phi$ from Equation (3.14) corresponding to each N is also included.

D. BACKSCATTERED PATTERNS

1. Far Zone

The first example for which the backscattered fields are to be computed is a 1m by .5m lossy dielectric rectangular cylinder with ε_{r_1} = 4. and σ_1=.3ms/m immersed in a free space environment. An H_z-polarized plane wave is incident on this scatterer at an angle ϕ_i as shown in Figure 4-3. The far zone backscattered pattern is plotted and is shown in Figure 4-3. The frequency used is 100 MHz. The maxima of backscattered field are obtained at incidence angles of 90° and 270° at which E_x is incident on the larger faces of the cylinder, and the minima

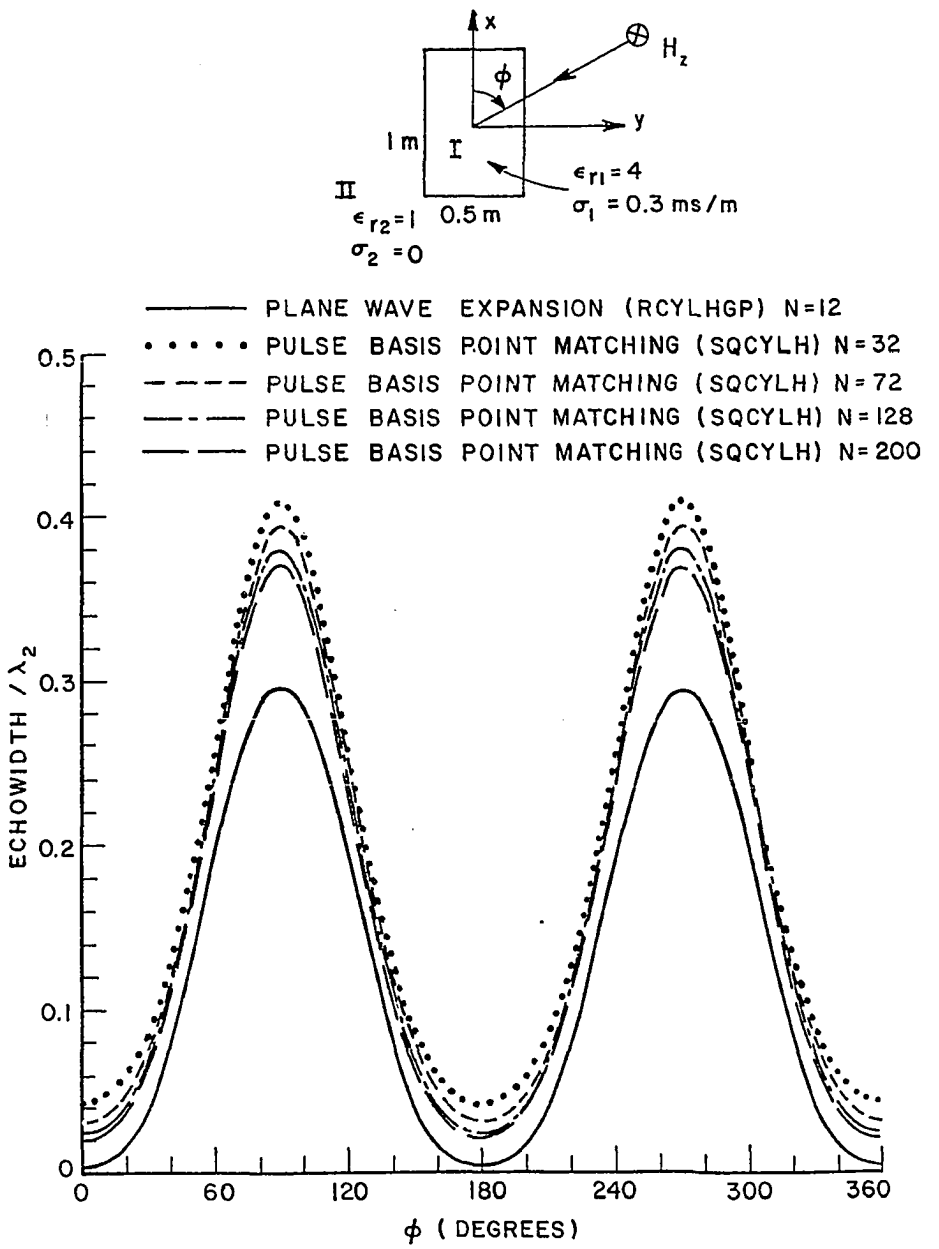

Figure 4-3. Far zone backscattered pattern for a z-polarized magnetic plane wave incidence at 100 MHz.

of scattered field are obtained at incidence angles of 0° and 180° for which E_y is incident on the smaller faces of the cylinder. In addition, some results of a pulse basis point matching program is also included which indicate that, if enough equations are included, the solution approaches that of the plane wave expansion. Four incremental cases for the pulse basis point matching shown in Figure 4-3 are for N = 32, 72, 128, and 200. It is apparent that the pulse basis method has not yet converged for N = 200, but the plane wave expansion has already converged for N = 12.

2. Near Zone

As a second example, consider an air filled, 1m by .5m rectangular cylinder immersed in a lossy homogeneous medium with $\epsilon_{r_2} = 4$ and σ_2=.3ms/m. A magnetic line source is placed at $(\rho_s,\phi_s)=(2m,\phi_s)$. This model is shown at top of the Figure 4-4. Scattering Attenuation Function versus ϕ is shown in Figure 4-4 for backscatter for increasing values of N; 6, 7, 8, and 9. For N=8 and 9, the pattern is exactly the same, this suggests that the solution has converged at N=8. The result of the pulse basis point matching shows excellent agreement with the plane wave expansion at the maxima, but, more equations are needed (i.e., N > 200) to obtain better agreement at minima. This is because the pulse basis point matching solution has not yet converged at minima regions. This was investigated by using N = 32, 72, 128, and 200 and comparing the patterns. Only N = 200 case is included in Figure 4-3.

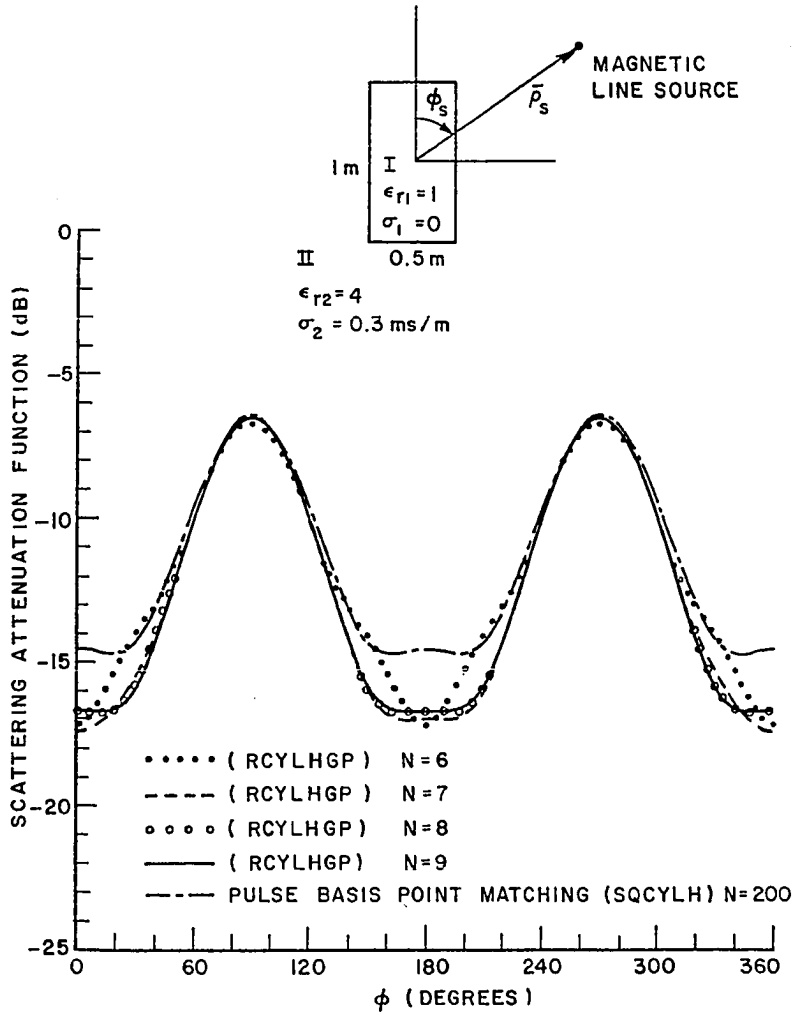

Figure 4-4. Near zone backscattered pattern for the model shown above. The line source is palaced at a radial distance ρ_S=2m, and the frequency is 100 MHz. (RCYLHP) is the Plane Wave Expansion Computer program used to obtain the above results.

(The frequency used is 100 MHz.) Obtaining a converged solution by the pulse basis method is costly and has not been carried out.

E. BISTATIC SCATTERING PATTERNS

1. Far Zone

The complete scattering patterns for three cases of plane wave incidences at ϕ_i = 0°, 45°, and 90°, and for a 1m by .5m lossy dielectric rectangular cylinder with $\varepsilon_{r_1}=4$ and $\sigma_1=.3$s/m located in a free space environment have been computed and given in Figures 4-5, 4-6, and 4-7, respectively. A H_z-polarized plane wave is incident on the scatterer at $\phi_i=0°$ as shown in Figure 4-5. The bistatic scattering pattern shown in Figure 4-5 shows a strong forward scattering and comparatively weak backscattering, and as expected the pattern is symmetrical about 180°. (The frequency used in this section is 100 MHz.) Also included in Figure 4-5, is the pulse basis point matching result for N=200. As discussed in Figure 4-3, better agreement would be obtained by increasing N in the point matching solution. For a plane wave incident along 45°-axis, the bistatic scattering pattern is shown in Figure 4-6. A small lobe is observed at about 70° and a greater lobe is observed at approximately 230°. The pattern does not have a point about which it is symmetric. For a plane wave incident nearly at $\phi_i=90°$, the bistatic scattering pattern of Figure 4-7 is obtained. This indicates a small backscattered lobe and a large forward scattered lobe. As expected, the pattern is symmetrical about approximately 270°. The

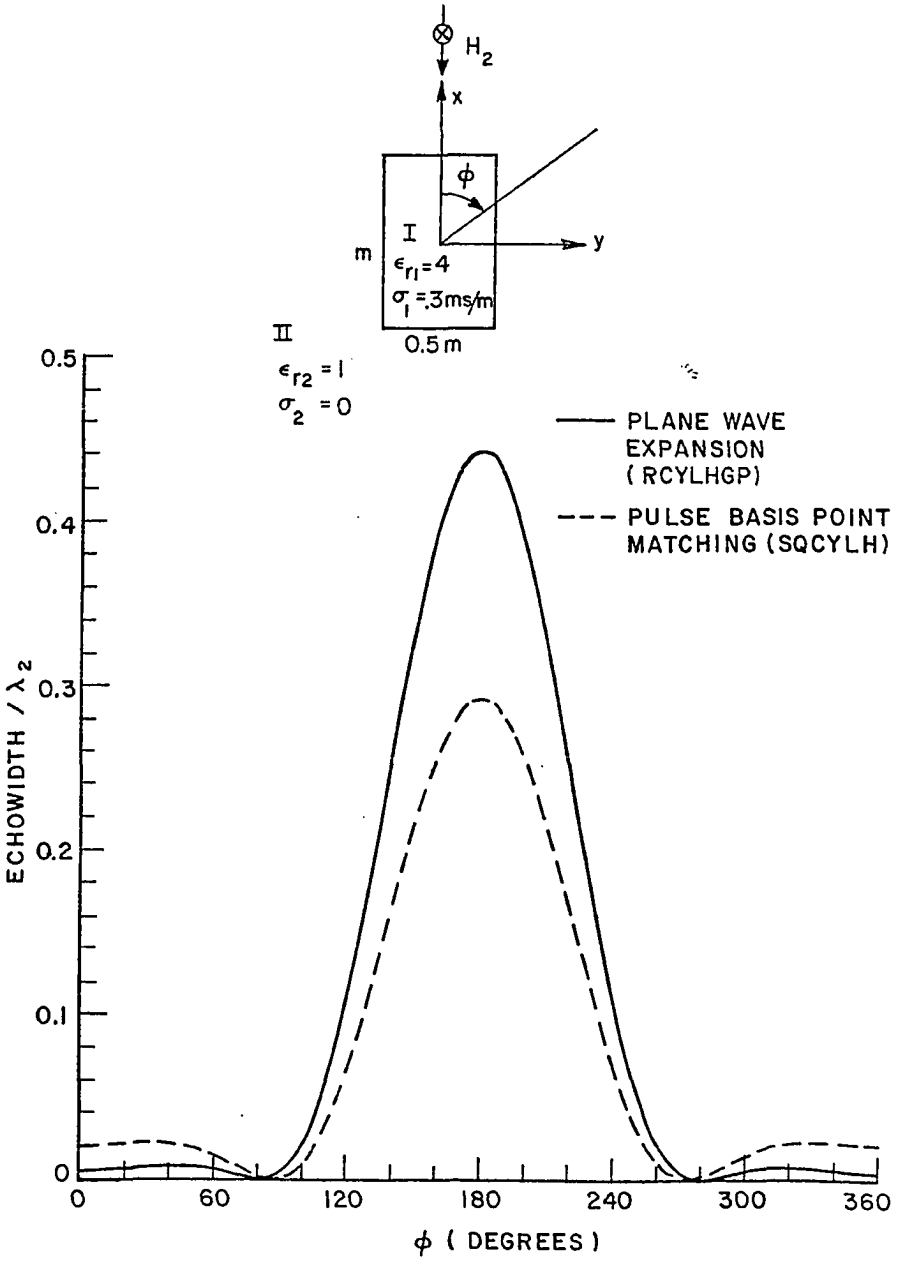

Figure 4-5. Far zone bistatic scattering pattern for a H_z-polarized plane wave incident at $\phi_i=0°$, and at 100 MHz.

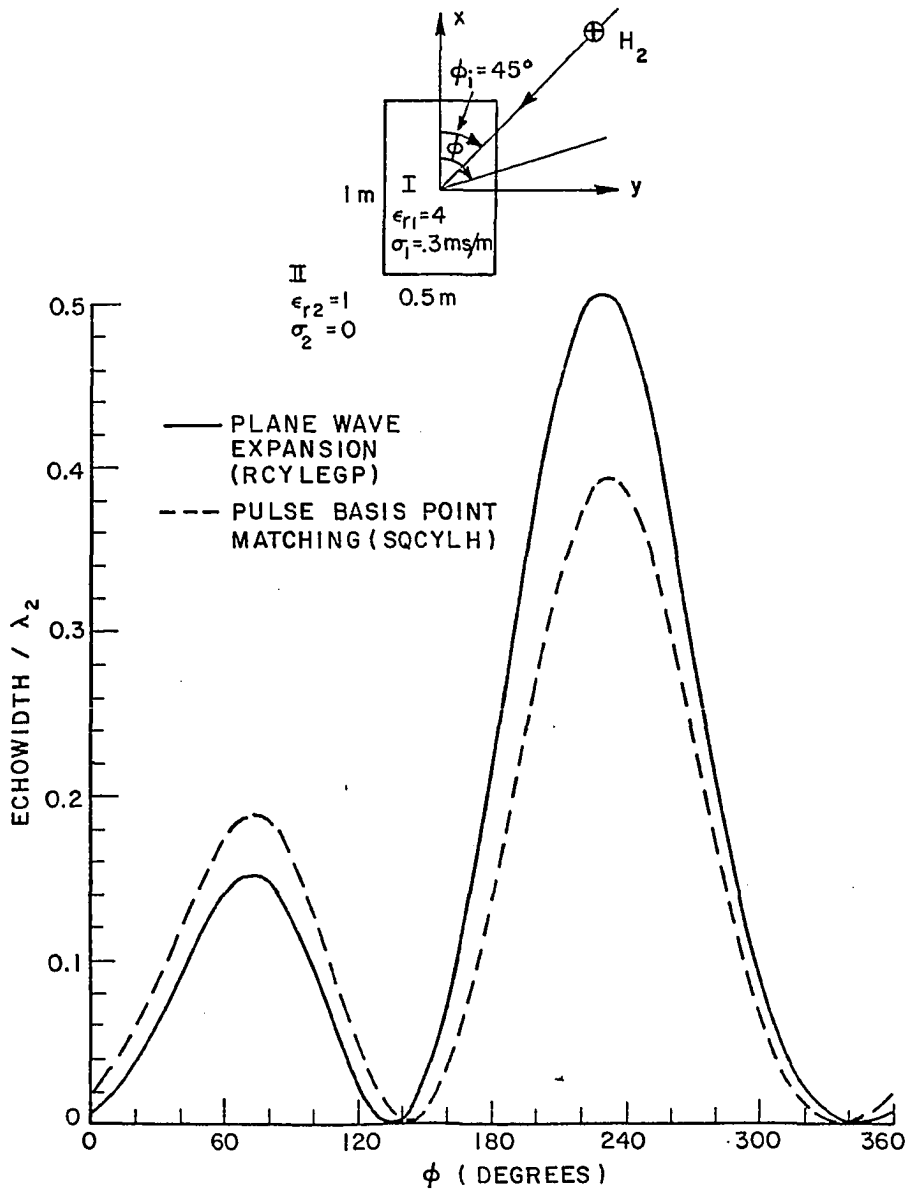

Figure 4-6. Far zone bistatic scattering pattern for a H_z-polarized plane wave incident at ϕ_i=45°, and at 100 MHz.

pulse basis point matching solutions included in Figures 4-6, and 4-7 show a 5° descrepancy in the position of the maxima and minima as compared to the plane wave expansion solutions. In part, this is caused by numerical approximations of the trigonometric functions by the computer.

2. Near Zone

The three cases considered include line sources at $(\rho_s,\phi_s)=(2m,0°)$, $(\rho_s,\phi_s)=(2m,45°)$, and $(\rho_s,\phi_s)=(2m,90°)$ which are analogous to $\phi_i=0°$, 45°, and 90° as considered in previous section for a 1m by .5m air filled rectangular cylinder immersed in a lossy homogeneous medium with $\varepsilon_{r_2}=4$ and $\sigma_2=.3ms/m$. The scattering patterns are given in Figures 4-8, 4-9, and 4-10. The field is observed at a radial distance $\rho=2m$, and the frequency of excitation source is 100 MHz. In each case, a pulse basis point matching solution is provided for comparison. The bistatic scattering pattern for a line source placed at $(\rho_s,\phi_s)=(2m,0°)$ is shown in Figure 4-8. This pattern shows a strong forward scattering and significantly smaller backscattering. The pattern is symmetric about 180° as expected. For a magnetic line source located at $(\rho_s,\phi_s)=(2m,45°)$, the bistatic scattering pattern is shown in Figure 4-9. The pattern is no longer symmetric and the lobes are offset accordingly. When the magnetic line source is moved to $(\rho_s,\phi_s)=(2m,90°)$, the bistatic scattering pattern of Figure 4-10 is obtained. The pattern is symmetric about 270° where the maximum of the forward scattering lobe is obtained. In each case, the pulse basis

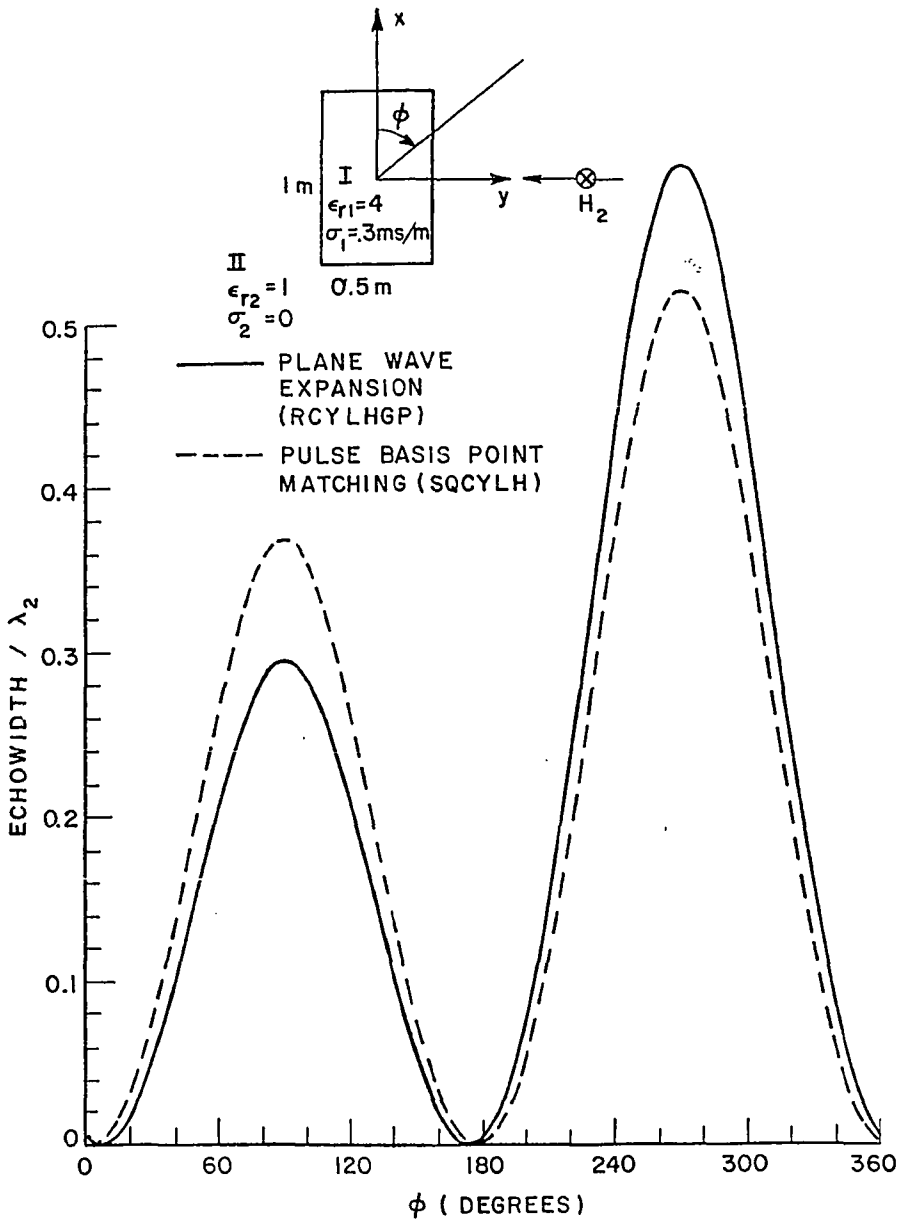

Figure 4-7. Far zone bistatic scattering pattern for a H_z-polarized plane wave incident at ϕ_i=90°, and at 100 MHz.

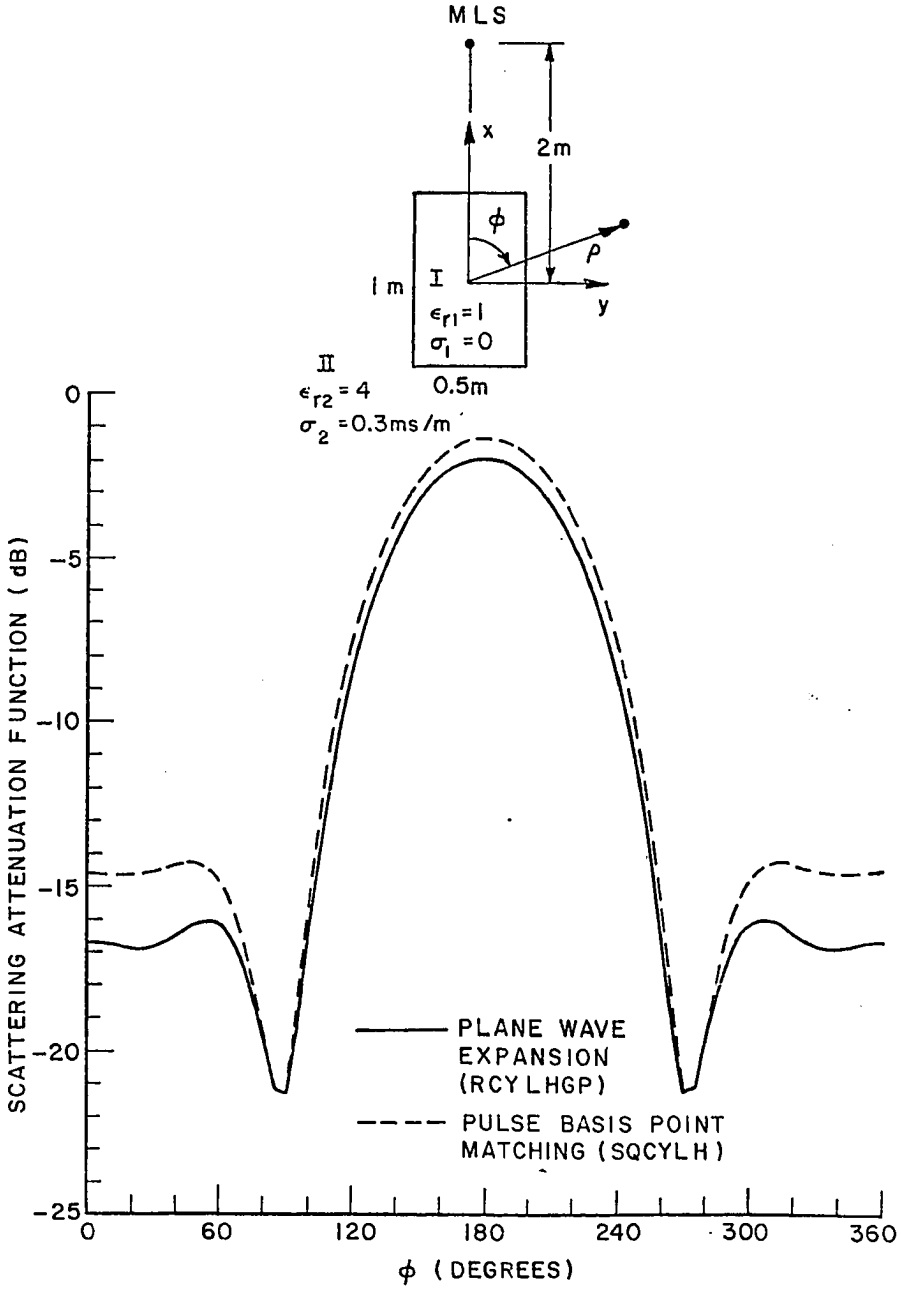

Figure 4-8. Near zone bistatic scattering pattern for a magnetic line source excitation placed at $(\rho_S,\phi_S)=(2m,0°)$ and at 100 MHz. The field is observed at a radial distance $\rho=2m$.

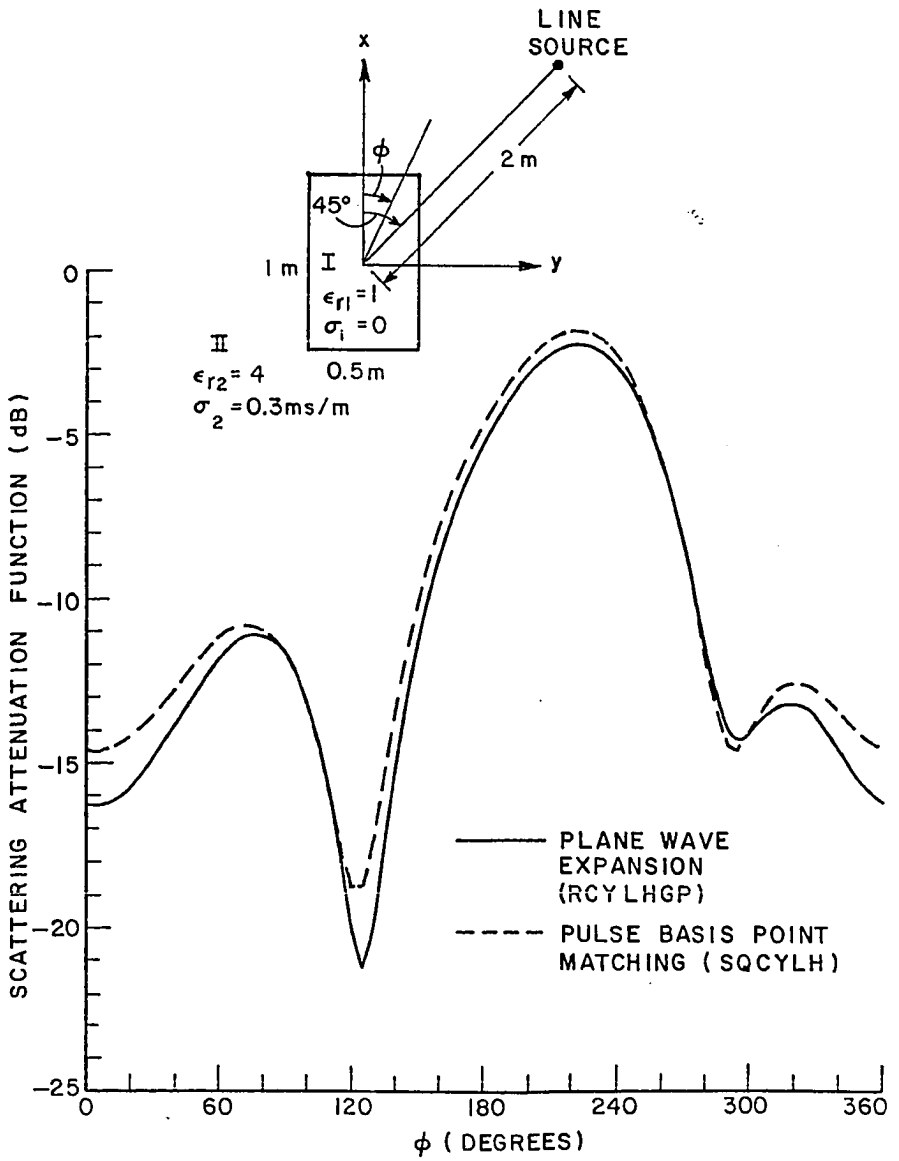

Figure 4-9. Near zone bistatic scattering pattern for a magnetic line source excitation placed at $(\rho_s, \phi_s)=(2m, 45°)$ and at 100 MHz. The field is observed at a radial distance $\rho=2m$.

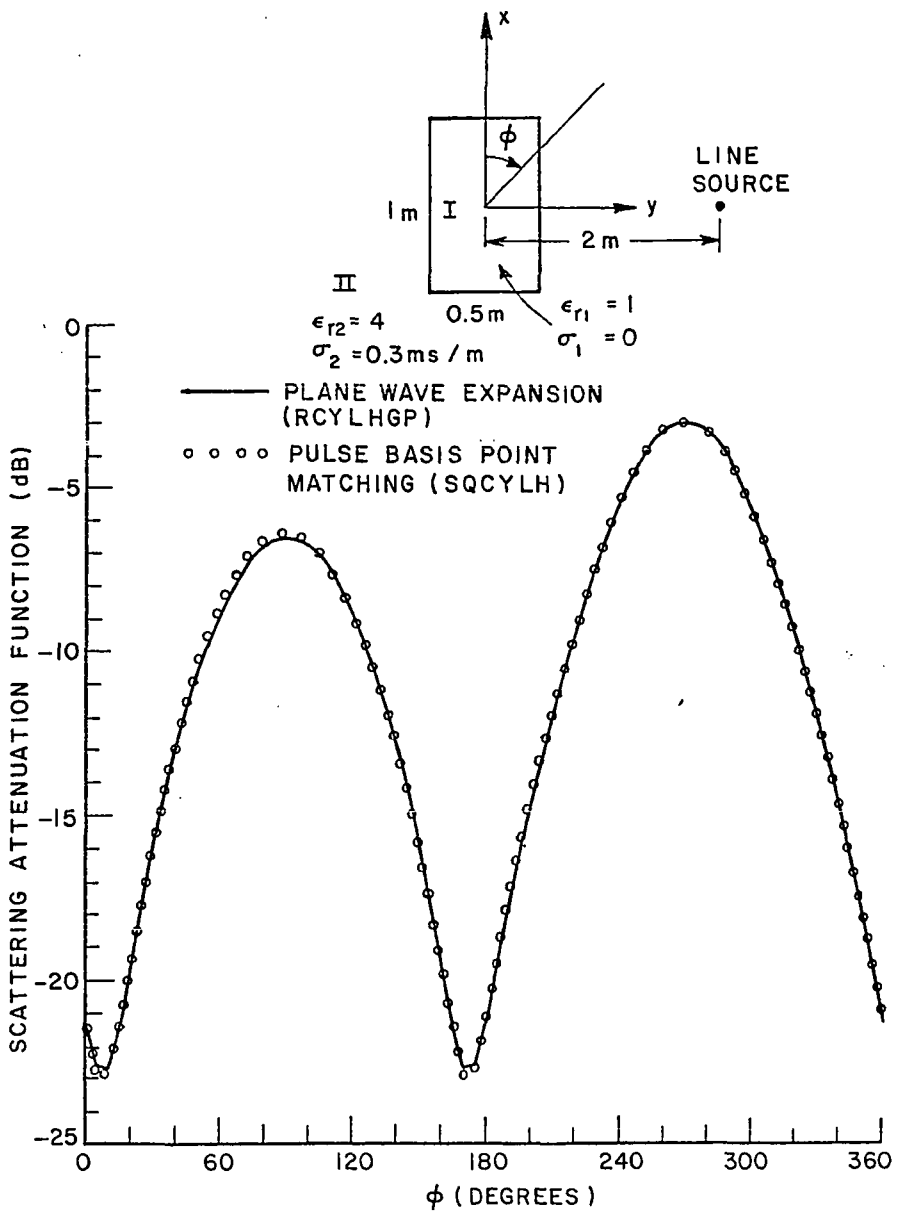

Figure 4-10. Near zone bistatic scattering pattern for a magnetic line source excitation placed at $(\rho_s, \phi_s)=(2m, 90°)$ and at 100 MHz. The field is observed at a radial distance $\rho=2m$.

point matching solution shows reasonable agreement for the number of equations N utilized. For the region off the main beam, i.e., the backlobe region, the match may be improved by increasing N in the Pulse Basis Point Matching.

F. BACKSCATTERING VERSUS FREQUENCY

In this section, three excitation examples are given for a 1m by .5m air filled rectangular cylinder immersed in a lossy homogeneous medium with $\varepsilon_{r_2}=4$ and $\sigma_2=.3$s/m. For these three locations of the excitation line source, backscattered fields are calculated for various frequencies. These curves are shown in Figure 4-11. It is apparent that at low frequencies, i.e., <40MHz, where the dimensions of the scatterer are small as compared to the wavelength, there seems to be no distinction between the three curves. This is the so called Rayleigh region. However, when the frequency is increased, the scattering is different for the three excitations shown in Figure 4-11.

To check the reliability of the moment method formulation given in this chapter, the frequency plots of Figure 4-12 is presented. First an air filled, 1m square cylinder immersed in a lossy homogeneous medium of $\varepsilon_{r_2}=4.$ and $\sigma_2=.003$s/m is considered. A magnetic line source located at $(\rho_s,\phi_s)=(2m,0°)$ is the source of excitation. This model is shown in Figure 4-12. The relative backscattered curve versus frequency is shown as the solid line in Figure 4-12. An equivalent scattering model for an air-filled circular cylinder of the same cross-sectional area as the

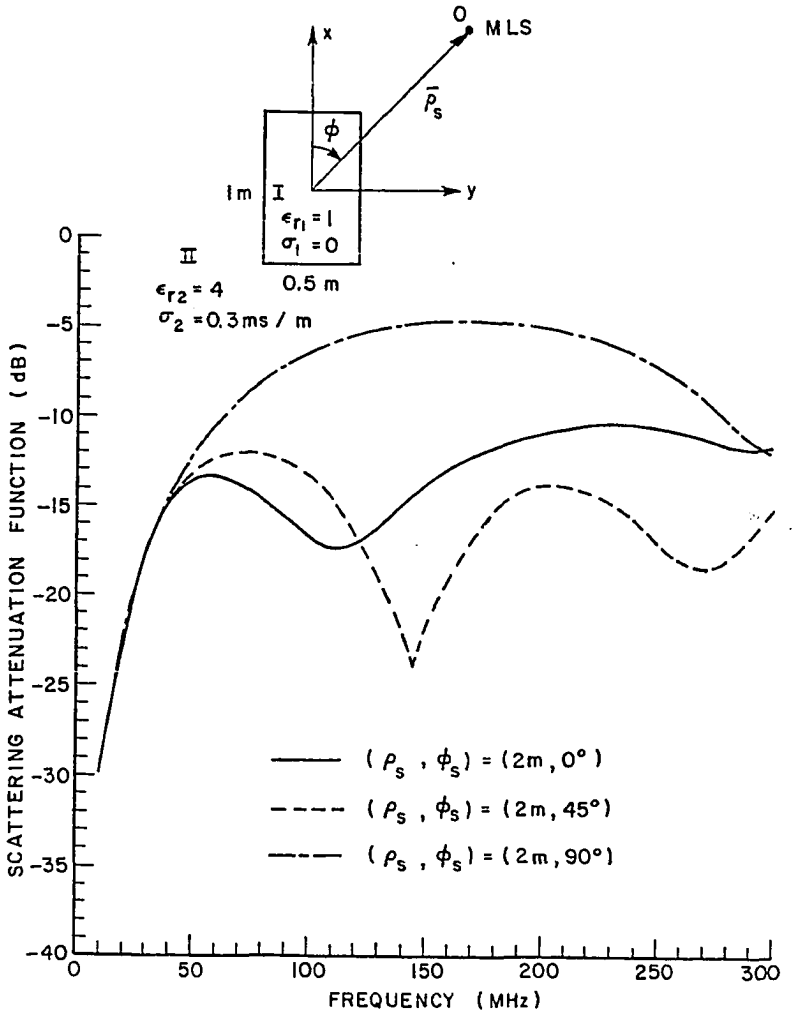

Figure 4-11. Near zone backscattering versus frequency for magnetic line source excitations placed at $(\rho_s, \phi_s)=(2m, 0°)$, $(2m=45°)$, and $(2m, 90°)$.

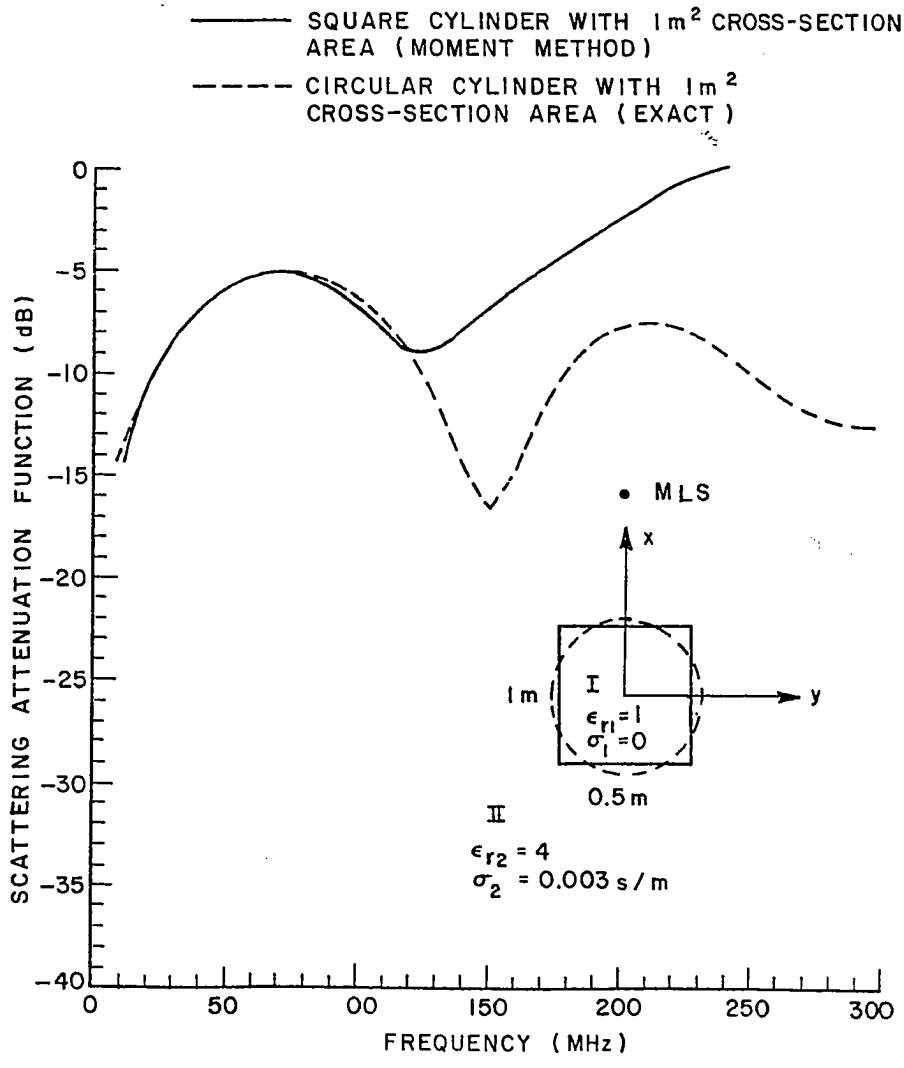

Figure 4-12. Comparison of backscattering versus frequency for a 1m square cylinder and an equivalent cross-section area air filled circular cylinder. The magnetic line source is located at $(\rho_s, \phi_s)=(2m, 0°)$.

square cylinder immersed in the same lossy homogeneous medium as before is considered. This model is also shown in Figure 4-12. The dash line shows the exact relative backscattered field as a function of frequency for the circular cylinderical model. At low frequencies where the dimensions of the square are small with respect to the wavelengths, the two scatterers are indistinguishable to the observer and the current moment is the same and appears to be identically distributed in both models. However, at larger frequencies where the electrical dimensions are larger, the current distribution is different, and the two scatter curves are no longer identical.

G. SUMMARY

In this chapter the H-wave scattering by lossy rectangular cylinders immersed in a lossy homogeneous medium was considered. The moment method formulation presented in Chapter II was specialized here, and some numerical results were presented.

In the next chapter a basic introduction of the effects of air-earth interface, and the solution of the Sommerfeld integral is presented.

CHAPTER V

AIR-EARTH INTERFACE AND THE SOMMERFELD INTEGRAL

A. INTRODUCTION

The parallel and perpendicular plane wave reflection coefficients for the air-earth interface are given. These coefficients are then used to obtain radiation patterns for a magnetic line source and an electric line source when they are located directly on the interface. It will be shown that the line source radiation patterns can be reasonably approximated by (1+R), where R is $R_{\perp}$ for an electric line source and $R_{\parallel}$ for a magnetic line source. Finally, some recommendations are included for evaluating the Sommerfeld type integrals encountered in this dissertation.

B. REFLECTION COEFFICIENTS

The simple model of Figure 5-1 is used for deriving a plane wave reflection coefficient. As shown, the yz-plane constitutes the interface between Region I (free space) and II (earth), and the x-axis is

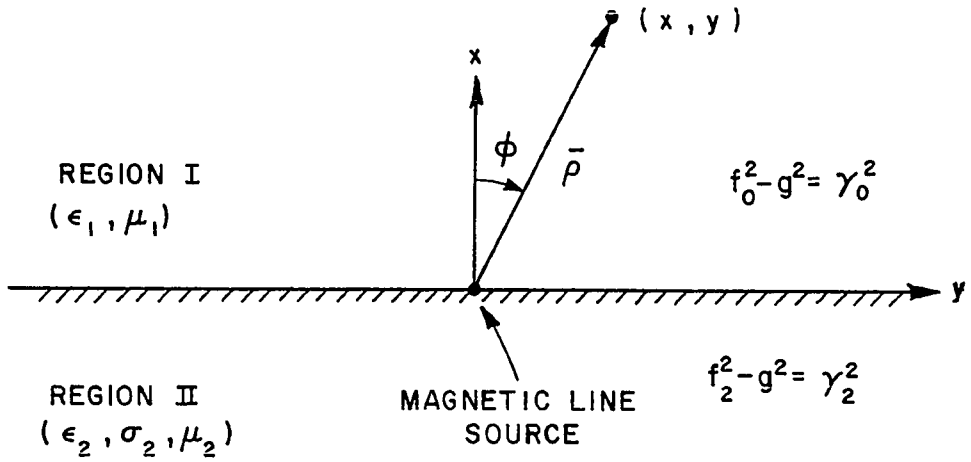

Figure 5-1. The magnetic line source, and interface model used to derive the reflection and transmission coefficients.

normal to this interface. Consider a magnetic line source with a $\hat{z}$ directed magnetic current M_0, located on the interface along z-axis. This line source radiates a field in the homogeneous earth region given by

$$H_z^i = - \frac{j\omega\hat{\epsilon}_2 M_0}{2\pi} K_0(\gamma_2 |\bar{\rho} - \bar{\rho}_s|) \quad , \tag{5.1}$$

or

$$H_z^i = - \frac{j\omega\hat{\epsilon}_2 M_0}{2\pi} \int_0^\infty \frac{e^{-f|x|}\cos(gy)dg}{f} \quad , \tag{5.2}$$

where Equation (3.6) was used.

The boundary conditions at the interface are

$$\hat{n} \times (\bar{H}^I - \bar{H}^{II}) = \bar{J}_S \quad , \tag{5.3a}$$

and

$$\hat{n} \times (\bar{E}^{I} - \bar{E}^{II}) = -\bar{M}_S \quad , \tag{5.3b}$$

where

$$\hat{n} = \hat{x} \quad . \tag{5.3c}$$

For the situation depicted in Figure 5-1, the electric surface current density $\bar{J}_S$ is zero and the magnetic surface current density $\bar{M}_S$ on the interface can be expressed as

$$\bar{M}_S = \hat{z} M_0 \delta(y) = \frac{\hat{z} M_0}{\pi} \int_0^{\infty} \cos(gy)dg \quad . \tag{5.4}$$

From Equation (5.2), and for the earth region where $x<0$

$$H_z^i = \frac{-j\omega\hat{\varepsilon}_2 M_0}{2\pi} \int_0^{\infty} \frac{e^{fx}\cos(gy)dg}{f} \quad x<0 \quad . \tag{5.5a}$$

Applying Maxwell's equation to above yields

$$E_y^i = \frac{M_0}{2\pi} \int_0^{\infty} e^{fx}\cos(gy)dg \quad ; \quad x<0 \quad . \tag{5.5b}$$

From Equation (5.5a) the reflected magnetic field may be expressed as

$$H_z^r = \frac{-j\omega\hat{\varepsilon}_2 M_0}{2\pi} \int_0^{\infty} \frac{R_{\parallel} e^{fx}\cos(gy)dg}{f} \quad x<0 \, , \tag{5.6a}$$

When the observation point is below the line source , the reflected electric field has the form.

$$E_y^r = \frac{M_0}{2\pi} \int_0^{\infty} R_{\parallel}\, e^{fx}\cos(gy)dg \quad x<0 \quad . \tag{5.6b}$$

From Equation (5.2) the transmitted field is obtained for x>0 as

$$H_z^T = -\frac{j\omega\hat{\varepsilon}_2 M_o}{2\pi} \int_o^\infty T_{\parallel} \frac{e^{-f_o x}\cos(gy)dg}{f} \quad ; \quad x>0 \ . \tag{5.7a}$$

Again applying Maxwell's equation to above in Region I

$$E_y^T = -\frac{M_o\hat{\varepsilon}_2}{2\pi\hat{\varepsilon}_1} \int_o^\infty f\, T_{\parallel} \frac{e^{-f_o x}\cos(gy)dg}{f} \quad ; \quad x>0 \ . \tag{5.7b}$$

Now the fields are matched at the boundary. From Equations (5.3a), (5.5a), (5.6a), and (5.7a) it follows that

$$-\frac{j\omega\hat{\varepsilon}_2 M_o}{2\pi} \int_o^\infty \frac{1}{f} (1+R_{\parallel}) - T_{\parallel} \cos(gy)dg = 0 \ . \tag{5.8}$$

Thus

$$T_{\parallel} = 1+R_{\parallel} \ . \tag{5.9}$$

Also, from Equations (5.3b), (5.4), (5.5b), (5.6b), and (5.7b)

$$-\frac{M_o\hat{\varepsilon}_2}{2\pi\hat{\varepsilon}_1} \int_o^\infty \frac{f_o T_{\parallel}}{f}\cos(gy)dy - \frac{M_o}{2\pi}\int_o^\infty (1+R_{\parallel})\cos(gy)dg$$

$$= -\frac{M_o}{\pi}\int_o^\infty \cos(gy)dg \ . \tag{5.10}$$

Thus, from Equation (5.9) and (5.10), it can be shown that

$$T_{\parallel} = \frac{2\hat{\varepsilon}_1 f}{\hat{\varepsilon}_1 f+\hat{\varepsilon}_2 f_o} \ . \tag{5.11a}$$

$$R_{\parallel} = \frac{\hat{\varepsilon}_1 f-\hat{\varepsilon}_2 f_o}{\hat{\varepsilon}_1 f+\hat{\varepsilon}_2 f_o} \ . \tag{5.11b}$$

where

$$f^2 - g^2 = \gamma_2^2 = jk_2 = j\omega\sqrt{\mu_o\hat{\varepsilon}_2} \quad . \tag{5.11c}$$

$$f_o^2 - g^2 = \gamma_o^2 = jk_o = j\omega\sqrt{\mu_o\hat{\varepsilon}_o} \quad . \tag{5.11d}$$

$$\hat{\varepsilon}_1 = \varepsilon_o \quad , \tag{5.11e}$$

and

$$\hat{\varepsilon}_2 = \varepsilon_o\left(\varepsilon_{r_2} - j\frac{\sigma_2}{\omega\varepsilon_o}\right) . \tag{5.11f}$$

An analogous consideration for an electric line source renders $R_\perp$ and $T_\perp$, or, a simple application of duality to Equations (5.11a) and (5.11b) gives

$$T_\perp = \frac{2\mu_1 f}{\mu_1 f + \mu_2 f_o} \quad . \tag{5.12a}$$

$$R_\perp = \frac{\mu_1 f - \mu_2 f_o}{\mu_1 f + \mu_2 f_o} \quad . \tag{5.12b}$$

$R_\parallel$ and $R_\perp$ are Fresnel's plane wave reflection coefficients and $T_\parallel$ and $T_\perp$ are the corresponding transmission coefficients.

Substituting

$$f = \gamma_2 \cos\phi_i \quad , \tag{5.13a}$$

$$f_o = \gamma_o \cos\phi_i \quad , \tag{5.13b}$$

and

$$g = j\gamma_2 \operatorname{sinc}\phi_i = j\gamma_o \sin\phi_t \quad , \tag{5.13c}$$

in $T_\parallel$, $R_\parallel$, $T_\perp$, and $R_\parallel$ gives the familiar forms of T and R as

The above equations are in complete agreement with Equation (5.11c) and (5.11d), and are compatible with the Snell's law.

$$T_{\parallel} = \frac{2\eta_2 \cos\phi_i}{\eta_2 \cos\phi_i + \eta_1 \cos\phi_i} \quad . \tag{5.14a}$$

$$R_{\parallel} = \frac{\eta_2 \cos\phi_i - \eta_1 \cos\phi_t}{\eta_2 \cos\phi_i + \eta_1 \cos\phi_t} \quad . \tag{5.14b}$$

$$T_{\perp} = \frac{2\eta_1 \cos\phi_i}{\eta_1 \cos\phi_i + \eta_2 \cos\phi_t} \quad . \tag{5.14c}$$

$$R_{\perp} = \frac{\eta_1 \cos\phi_i - \eta_2 \cos\phi_t}{\eta_1 \cos\phi_i + \eta_2 \cos\phi_t} \quad . \tag{5.14d}$$

where η_2 and η_1 are intrinsic impedances of media II and I respectively.

C. LINE SOURCE RADIATION ON THE AIR-EARTH INTERFACE

Consider the situation depicted in Figure 5-3, where an air-earth interface (parallel to yz-plane) is located at x=d. A line source is placed below the interface at point (x',y'). The fields at any point (x,y) below the interface is the sum of the direct and the reflected waves. A typical direct and reflected ray is shown in Figure 5-3.

$$E_z^{II}(x,y) = -\frac{j\omega\mu_2 I_o}{2\pi} \int_0^{\infty} \frac{\cos[g(y-y')]}{f} \left[e^{-f|x-x'|} + R_{\perp} e^{-f(2d-x-x')} \right] dg \quad ; \quad x \leq d \ , \tag{5.15}$$

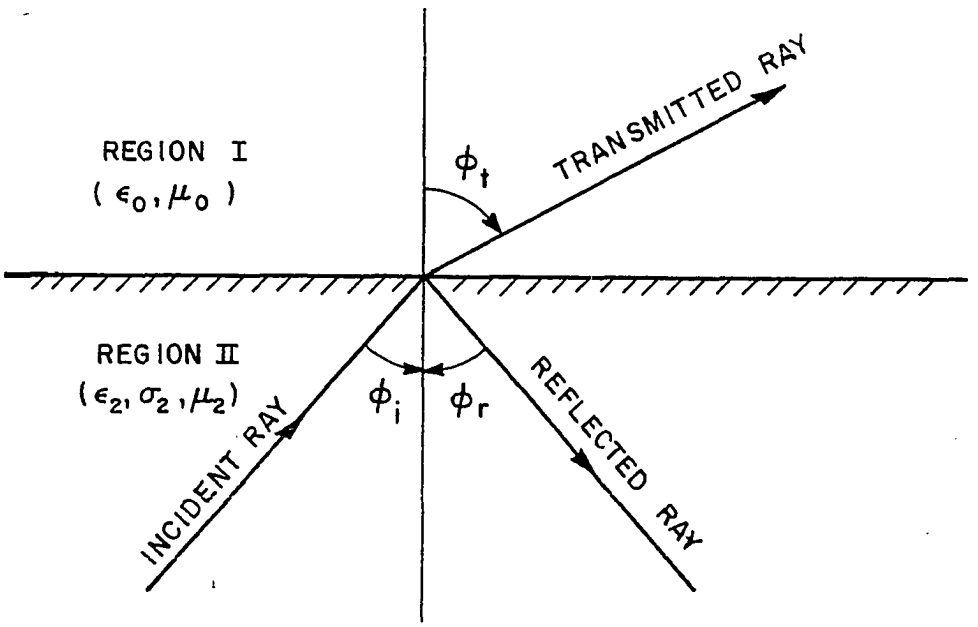

Figure 5-2. Typical ray geometry for reflection and transmission at a plane boundary between Regions I and II.

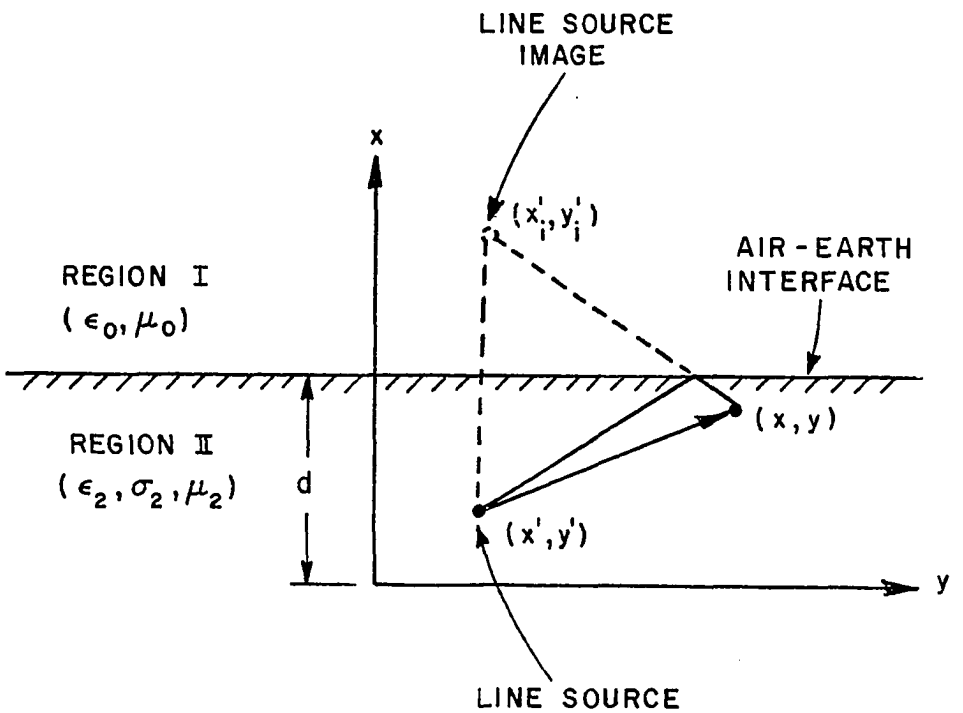

Figure 5-3. Definition of a general coordinate system and the air-earth interface and the line source. The plane interface is parallel to yz-plane and is located at x=d.

where I_0 is the electric current on the line source

The field observed at a point (x,y) in air may be expressed as

$$E_z^I(x,y) = -\frac{j\omega\mu_2 I_0}{2\pi}\int_0^\infty \frac{T_\perp}{f} e^{-f(d-x')} e^{-f_0(x-d)} \cos[g(y-y')]\, dg \quad ; x>d \,. \tag{5.16}$$

where $T_\perp$ and $R_\perp$ are given by Equations (5.12a) and (5.12b), and f and f_0 by Equations (5.11c) and (5.11d).

For a buried magnetic line source the corresponding magnetic field observed at a point (x,y) below the interface is

$$H_z^{II}(x,y) = -\frac{j\omega\hat{\epsilon}_2 M_0}{2\pi}\int_0^\infty \frac{\cos[g(y-y')]}{f}\left(e^{-f|x-x'|} + R_\parallel e^{-f(2d-x-x')}\right)dg \quad ; x \leq d \,, \tag{5.17}$$

and the magnetic field observed at a point (x,y) above the interface is

$$H_z^I(x,y) = -\frac{j\omega\hat{\epsilon}_2 M_0}{2\pi}\int_0^\infty \frac{T_\parallel}{f} e^{-f(d-x')} e^{-f_0(x-d)} \cos[g(y-y')]dg \quad ; x > d \,. \tag{5.18}$$

Using Equations (5.15) and (5.16) a near zone pattern is obtained for an electric line source harmonic at 100MHz, and located on the interface (i.e., d=x'=0). The earth medium is represented by $\epsilon_{r_2}=4$ and $\sigma_2=0$, and the field is observed at a radial distance $\rho=2m$. This pattern is shown in Figure 5-4, where the earth region is between $\phi=90°$ and

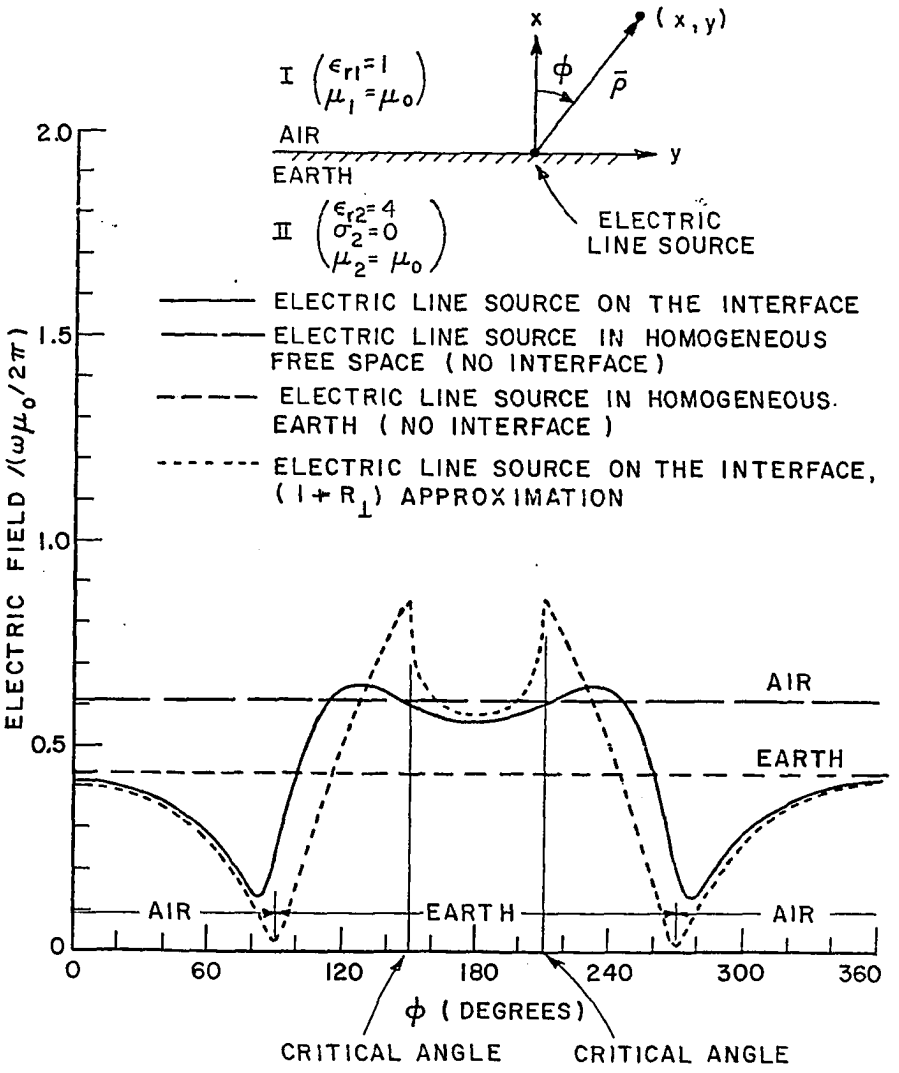

Figure 5-4. Near zone radiation pattern of an electric line source placed on the air-earth interface field is observed at a radial distance ρ=2m, and the frequency is 100 MHz.

ϕ=270°. The two additional curves in Figure 5-4 are the radiation pattern of an electric line source radiating in a homogeneous earth on interface and radiation pattern of an electric line source radiating in homogeneous free space. The current is kept constant in all line source cases. Note that the far field of a line source in a lossless homogeneous medium is proportional to $\varepsilon_r^{-1/4}$. Thus, the difference in these two levels is caused by the change in ε_r. For the case where the electric line source is placed at the interface, one can use reciprocity and a test current source far from the interface to show that the radiated field is modified by a factor $(1+R_\perp)$. For the example of Figure 5-4 at ϕ=180°, $R_\perp$=1/3 and the electric field from the line source is increased accordingly. It is also observed that the power from the electric line source on the interface is radiated primarily into the earth medium. A plot of $(1+R_\perp)$ is also included in Figure 5-4 which indicates that the approximation is very good in air region and at normal incidence in earth region. The approximation may be improved by including the effects of the lateral waves. This is illustrated by the solid curve in Figure 5-4. For a lossy earth however, the radiated energy into the earth region is attenuated. A typical case is shown in Figure 5-5 for σ_2=3ms/m.

Using Equations (5.17) and (5.18) some near zone patterns were obtained for a magnetic line source (harmonic at 100 MHz) located on interface. Figure 5-6 shows the radiation patterns for a magnetic line source on the interface, in homogeneous earth, and in homogeneous air. The far zone magnetic field for the magnetic line source is proportional to $\varepsilon_r^{3/4}$. For the case where the interface is introduced the approximate

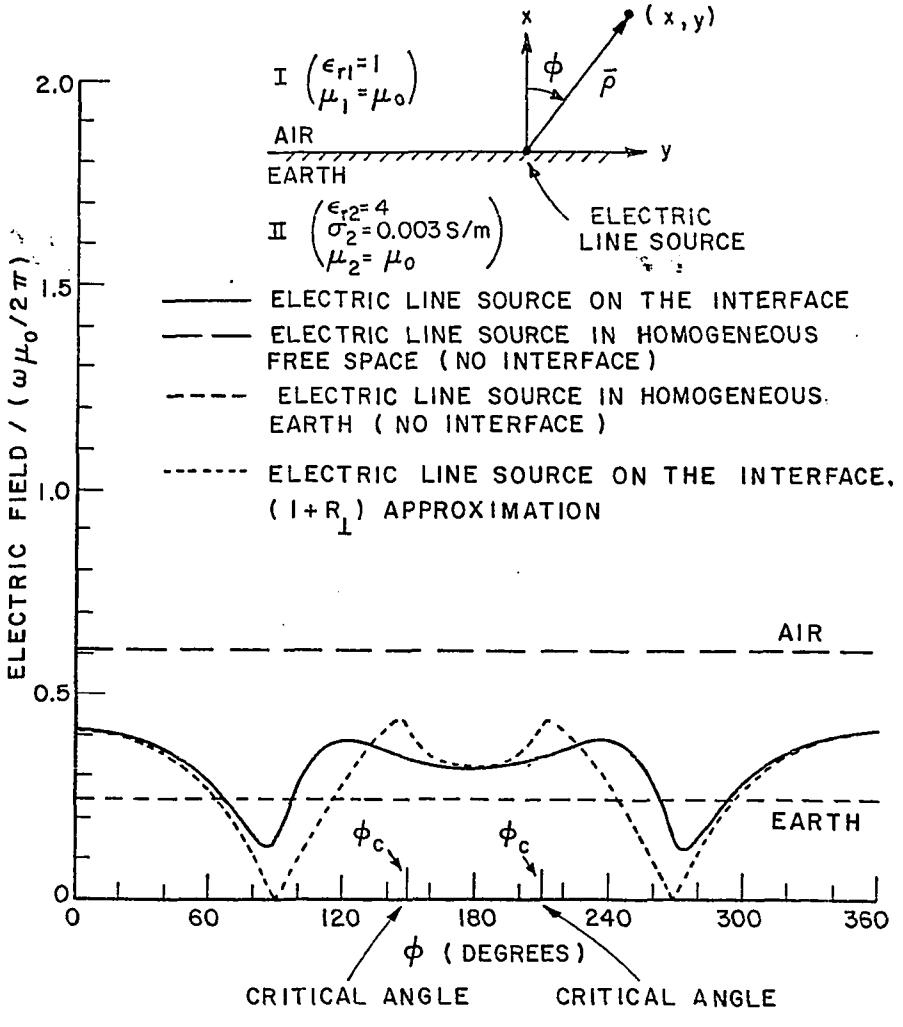

Figure 5-5. The same as Figure 5-4, except the earth is lossy (σ_2=.003s/m).

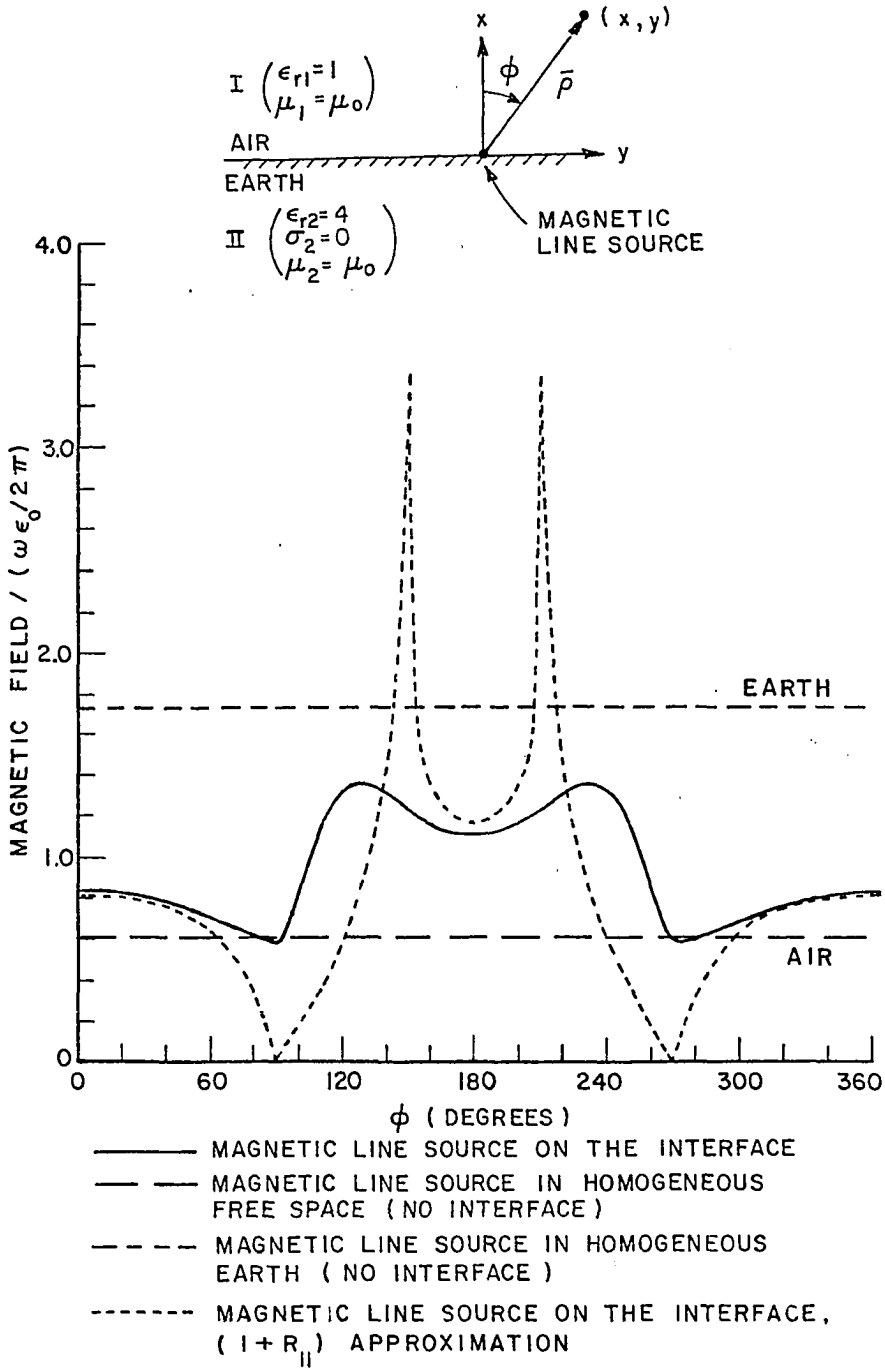

Figure 5-6. Near zone radiation pattern of a magnetic line source placed on the air-earth interface field is observed at a radial distance ρ=2m, and the frequency is 100 MHz.

solution is obtained by introducing a factor given by $(1+R_{\parallel})$ which is also plotted in Figure 5-6. As shown, this approximation is not as good as the electric line source case. This suggests that the effects of the lateral waves are more important in this case. For a lossy earth, the energy radiated into the earth is attenuated. A typical case is shown Figure 5-7 for σ_2=3sm/m.

D. LIMITING CASE

The limit is examined here as the line source approaches the interface. Let us consider Figure 5-8a where an electric line source is placed at (x',y') above the interface in the free space region. The field observed at (x,y) above the interface is

$$E_z(x,y) = -\frac{j\omega\mu_0}{2\pi}\left[\int_0^{\infty}\frac{e^{-f_0|x-x'|}\cos[g(y-y')]}{f_0}\,dg + \int_0^{\infty}\frac{R_{\perp}'\, e^{-f_0|x+x'|}\cos[g(y-y')]}{f_0}\,dg\right] . \tag{5.19}$$

the line source is then moved towards the interface until it is directly placed on it, i.e., x'=0

$$\lim_{x'\to 0}(E_z(x,y)) = -\frac{j\omega\mu_0}{2\pi}\int_0^{\infty}\frac{(1+R_{\perp}')\, e^{-f_0|x|}\cos[g(y-y')]}{f_0}\,dg . \tag{5.20}$$

where $R_{\perp}' = -R_{\perp}$, and $R_{\perp}$ is given by Equation (5.12b). Using this in Equation (5.20) and further simplifying gives

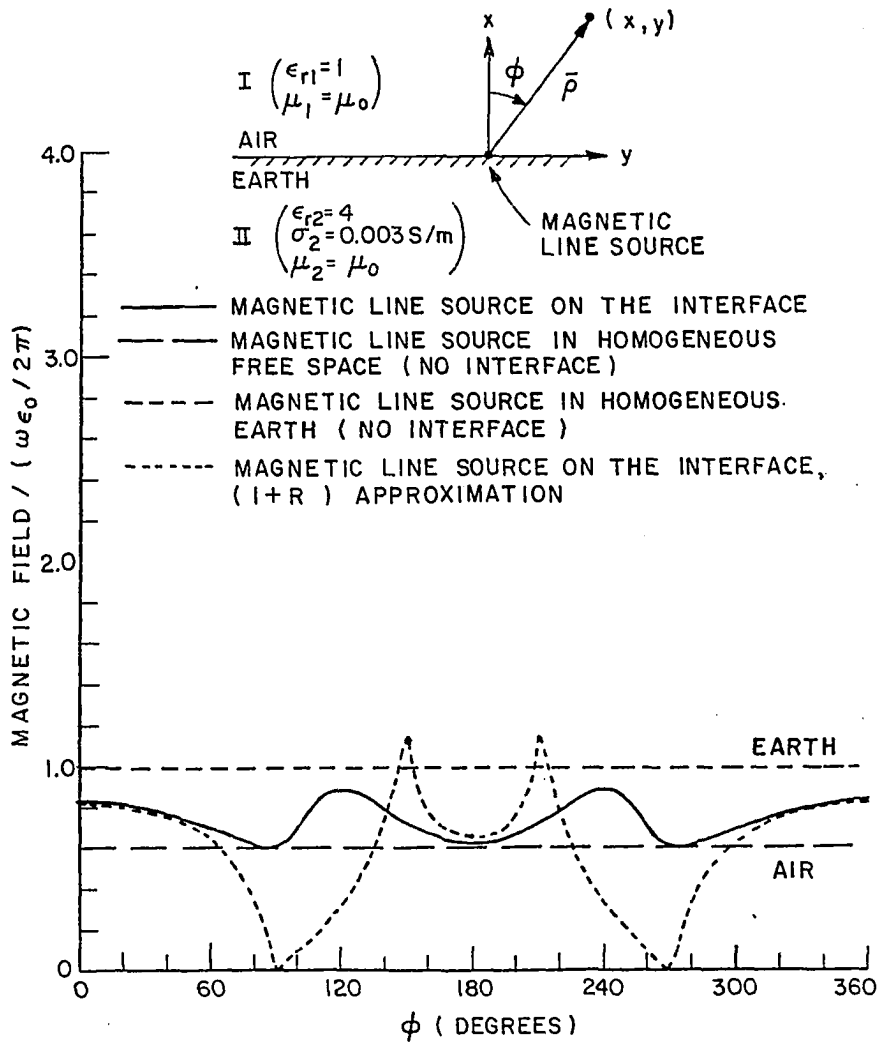

Figure 5-7. The same as Figure 5-6, except the earth lossy (σ_2=.003s/m).

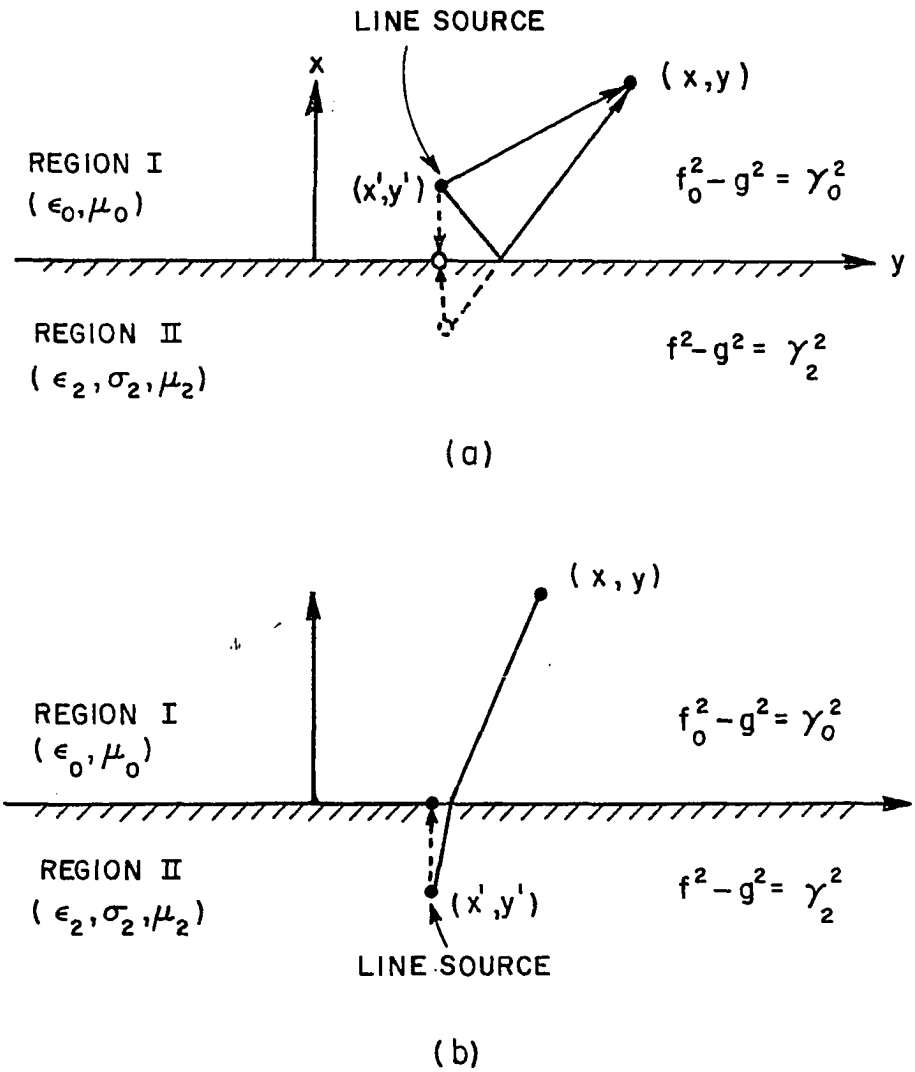

Figure 5-8. (a) An electric line source placed at (x',y') above the interface and moved towards the interface. (b) The same electric line source placed at (x',y') below the interface and moved towards the interface. In each case, the field is observed at (x,y).

$$E_z(x,y) = -\frac{j\omega\mu_0\mu_2}{\pi}\int_0^\infty \frac{e^{-f_0 x}\cos[g(y-y')]}{\mu_0 f + \mu_2 f_0}\,dy \quad ; x > 0 \ . \tag{5.21}$$

Now, let us consider Figure 5-8b where the same electric line source is placed below the interface. The field observed at (x,y) above the interface can be expressed as

$$E_z(x,y) = -\frac{j\omega\mu_2}{2\pi}\int_0^\infty \frac{T_\perp\, e^{fx'-f_0 x}\cos[g(y-y')]}{f_0}\,dg \quad ; \quad x'<0 \ . \tag{5.22}$$

moving the line source towards the interface implies

$$\lim_{x'\to 0}(E_z(x,y)) = -\frac{j\omega\mu_2}{2\pi}\int_0^\infty \frac{T_\perp\, e^{-f_0 x}\cos[g(y-y')]}{f}\,dg \ . \tag{5.23}$$

substituting for $T_\perp$ from Equation (5.12a) and simplifying give

$$E_z(x,y) = -\frac{j\omega\mu_0\mu_2}{\pi}\int_0^\infty \frac{e^{-f_0 x}\cos[g(y-y')]}{\mu_0 f + \mu_2 f_0}\,dy \quad ; x > 0 \ . \tag{5.24}$$

which is exactly the same as Equation (5.21). This can also be proved by using reciprocity theorem which is not included here.

The procedure is the same for a magnetic line source.

E. SOME REMARKS ON THE EVALUATION OF THE SOMMERFELD INTEGRAL

The Sommerfeld type integrals encountered in this dissertation are in general of the form

$$I = \int_0^\infty \frac{F(f,g)}{f}\, dg \; ; \; f^2 = \gamma_2^2 + g^2 \quad . \tag{5.25}$$

The integrand may be singular depending on f, which can be expressed as

$$f^2 = -\omega^2 \mu_o \varepsilon'_2 + j\omega\mu_o\sigma + g^2 \quad . \tag{5.26}$$

where ε'_2 is the real part of the $\hat{\varepsilon}_2$.

It can be seen from Equation (5.26) that for a lossy case, the above integrand does not have any singularities, thus, it can easily be evaluated numerically. For a lossless case, however, the integrand is singular when

$$g = g_c = \omega\sqrt{\mu_o \varepsilon_2'} \quad . \tag{5.27}$$

To get around this problem, the integration path can be chosen as follows

$$I = \underbrace{\left[\int_0^{g_1} \frac{F}{f}\, dg\right]}_{I_1} + \underbrace{\left[\int_{g_1}^{g_c} \frac{F}{f}\, dg\right]}_{I_2} + \underbrace{\left[\int_{g_c}^{\infty} \frac{F}{f}\, dg\right]}_{I_3} \tag{5.28}$$

where

$$g_1 = g_c/\sqrt{2} \quad .$$

I_1 is easy to evaluate. I_2 is evaluated by introducing the following transformation.

$$\beta^2 = g_c^2 - g^2 = -f^2 \; ; \quad \sigma = 0 \; . \tag{5.29a}$$

$$dg = -\frac{\beta}{g}\, d\beta \quad . \tag{5.29b}$$

$$I_2 = -j \int_0^{g_1} \frac{F}{g}\, d\beta \quad . \tag{5.30}$$

To evaluate I_3 the transformation

$$\alpha^2 = g^2 - g_c^2 = f^2 \quad ; \quad \sigma = 0. \tag{5.31a}$$

$$d_g = \frac{\alpha d\alpha}{g} \quad . \tag{5.31b}$$

$$I_3 = \int_0^{\infty} \frac{F}{g}\, d\alpha \quad . \tag{5.32}$$

May be used, thus the integral of Equation (5.25) takes the form

$$I = \int_0^{g_1} \frac{F}{f}\, dg + \begin{cases} \displaystyle\int_0^{g_1} \frac{F\beta d\beta}{fg} + \int_0^{\infty} \frac{F\alpha d\alpha}{fg} \quad ; \quad \sigma \neq 0 \\ \\ \displaystyle -j \int_0^{g_1} \frac{F}{g}\, d\beta + \int_0^{\infty} \frac{F d\alpha}{g} \quad ; \quad \sigma = 0 \quad . \end{cases} \tag{5.33}$$

The $\int_0^{\infty} d\alpha$ may be approximated by $\int_0^{\alpha_1} d\alpha$, and a sufficiently large α_1 may be chosen for a good approximation. The value of α_1 is dependent on how fast or how slow the integrand is decaying. For the integrands encountered in this work $\alpha_1 = 10x[\text{maximum}(|\sigma_2|, |K_o|, g_c)]$ proved to be sufficient.

The above integrals have been programmed using Simpson's integration method and the program is included in Appendix E. F can be any nonsingular function of g.

F. SUMMARY

In this chapter the reflection coefficients for parallel and perpendicular polarizations were presented, some pattern were given for radiation by line sources on an air-earth interface. Finally, some remarks were made about the integration of Sommerfeld integral. In the next chapter, moment method formulation of E_z and H_z scattering by buried cylindrical geometries is presented.

CHAPTER VI

MOMENT METHOD FORMULATION FOR SCATTERING BY BURIED, LOSSY DIELECTRIC CYLINDERS OF INFINITE LENGTH

A. INTRODUCTION

In this chapter an electromagnetic scattering model for buried cylindrical geometries is introduced. The integral equations for E-Wave and H-wave scatterings are presented, and the moment method is used to solve these integral equations. Two sets of simultaneous linear equations obtained here are a modification of the system of linear equations obtained in Chapter II. This modification is introduced to incorporate the reflection at the air-earth interface into the solution.

Figure 6-1 shows a plane cut of the electromagnetic scattering model. The z-axis is parallel to the axis of the cylinder, and x=d plane constitutes the air-earth interface. The region inside the scatterer is designated by I (ε_1, μ_1, σ_1), and earth region external to the scatterer is designated by II (ε_2, μ_2, σ_2). The source of excitation is a line source at (x_s,y_s) or (ρ_s, ϕ_s). For this model $x_s \leq d$

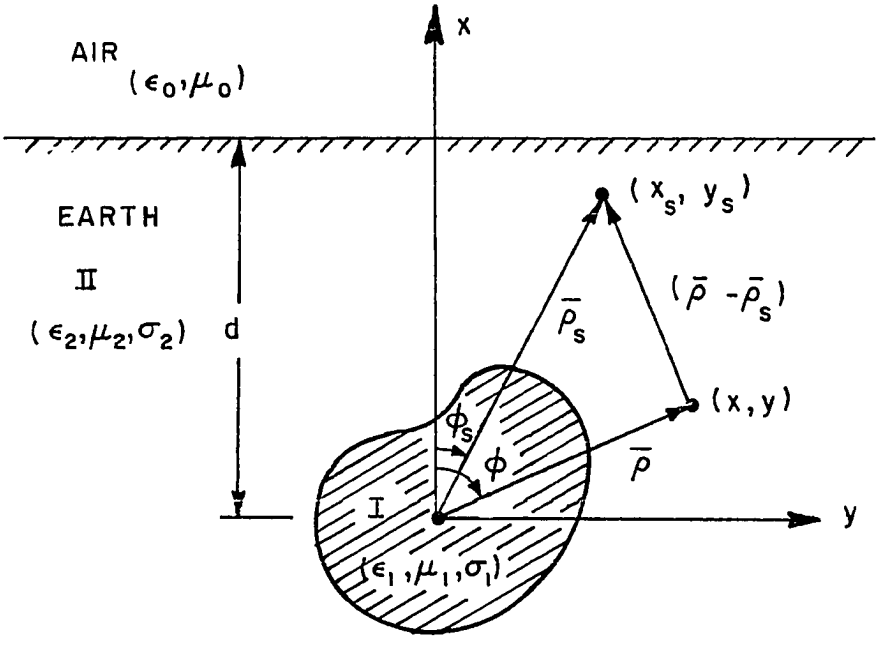

Figure 6-1. Electromagnetic scattering model for a lossy dielectric cylinder of infinite length buried in earth.

is considered without loss of generality. Thus the line source can be placed either on the interface or within the earth medium.

B. E-WAVE SCATTERING BY BURIED, LOSSY DIELECTRIC CYLINDERS OF INFINITE LENGTH

A uniform time harmonic, infinite electric line source is placed at (x_s,y_s) as shown in Figure 6-1. In homogeneous Medium II, this line source radiates a field given by Equation (2.1). For the model of Figure 6-1, the total field incident on the scatterer is the sum of the direct incident wave and the wave reflected at the interface and then incident toward the scatterer.

$$E_z^i = E_z^{id} + E_z^{ir} \quad . \tag{6.1a}$$

where from Equation (5.15) one may obtain

$$E_z^{id} = -\frac{j\omega\mu_o}{2\pi} \int_o^\infty \frac{e^{-f|x-xs|}}{f} \cos[g(y-y_s)]\, dg \quad , \tag{6.1b}$$

and

$$E_z^{ir} = -\frac{j\omega\mu_o}{2\pi} \int_o^\infty \frac{R_\perp\, e^{-f(2d-x-xs)}}{f} \cos[g(y-y_s)]\, dg \quad , \tag{6.1c}$$

where $I_o=1$ is assumed and $R_\perp$ is the reflection coefficient given by Equation (5.12b).

In the presence of the scatterer and the interface the field at any point is given by

$$E_z(x,y) = E_z^{id} + E_z^{ir} + E^{sd} + E^{sr} \quad . \tag{6.2}$$

where E_z^{id} and E_z^{ir} are direct and reflected incident fields due to the line source given by Equation (6.1). E_z^{sd} and E_z^{sr} are direct and reflected scattered fields. A typical ray geometry demonstrating these quantities are shown in Figure 6-2 for an elemental scatterer. Note that multiple reflections between the interface and the scatterer are implicitly contained in this solution. E_z^{sd} and E_z^{sr} are expressed

$$E_z^{sd} = -\frac{j\omega\mu_o}{2\pi} \iint_{cs} J_{eq}(x',y') \left[\int_o^\infty \frac{e^{-f|x-x'|}}{f} \cos[g(y-y')]\, dg \right] ds' \quad , \tag{6.3a}$$

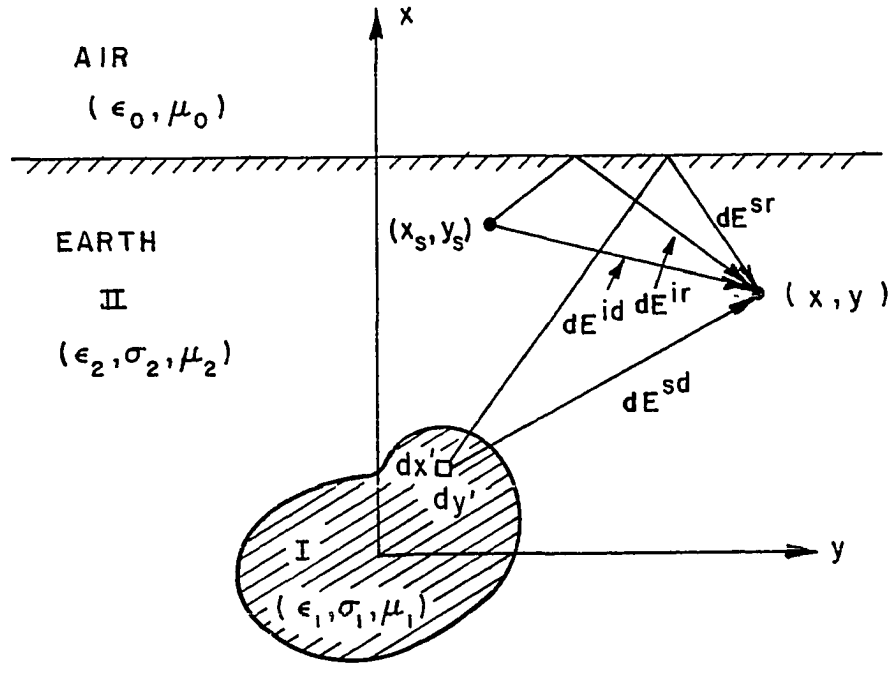

Figure 6-2. Illustration of typical direct incident and reflected incident fields, and direct scattered and reflected scattered fields for an element of the scatterer.

and

$$E_z^{sr} = -\frac{j\omega\mu_0}{2\pi} \iint_{cs} J_{eq}(x',y') \left[\int_0^{\infty} \frac{R_\perp e^{-f(2d-x-x')} \cos[g(y-y')]}{f} \, dg \right] ds' \quad . \tag{6.3b}$$

where J_{eq} is the equivalent volume polarization current placed at the position of the scatterer given by Equation (2.5). Using Equation (2.5) in Equation (6.3) yields

$$E_z^{sd} = \frac{\omega^2\mu_0(\hat{\epsilon}_1-\hat{\epsilon}_2)}{2\pi} \iint_{cs} E_z^I(x',y') \left[\int_0^{\infty} \frac{e^{-f|x-x'|} \cos[g(y-y')]}{f} \, dg \right] ds' \, , \tag{6.4a}$$

and

$$E_z^{sr} = \frac{\omega^2 \mu_o (\hat{\varepsilon}_1 - \hat{\varepsilon}_2)}{2\pi} \iint_{cs} E_z^I(x',y') \left[\int_0^\infty \frac{R_\perp e^{-f(2d-x-x')} \cos[g(y-y')]}{f} dg \right] ds'. \quad (6.4b)$$

$E_z^I(x,y)$ is the field inside the scatterer to be obtained by evaluating Equation (6.2) in Region I. After rearranging Equation (6.2) and using Equations (6.4a) and (6.4b), the following integral equation is obtained.

$$E_z^{id}(x,y) + E_z^{ir}(x,y) = E_z^I(x,y) - \frac{\omega^2 \mu_o (\hat{\varepsilon}_1 - \hat{\varepsilon}_2)}{2\pi} \iint_{cs} E_z^I(x',y')$$

$$\left[\int_0^\infty \frac{e^{-f|x-x'|} \cos[g(y-y')]}{f} dg + \int_0^\infty \frac{R_\perp e^{-f(2d-x-x')} \cos[g(y-y')]}{f} dg \right] ds'. \quad (6.5)$$

The unknown function in the above integral equation is the field in Region I (E_z^I). This unknown appears both in the integral and out of the integral, thus, it is a Fredholmz integral equation of the second kind. The above integral equation is a modified form of integral equation given by Equation (2.7). The two additional terms are E^{ir} and E^{sr} due to the reflection at the interface. The present integral equation is solved in the same way as Equation (2.7) was solved. To avoid repetition, the attention is directed to the two new terms. The unknown function $E_z^I(x,y)$ is expanded in terms of some known functions with unknown coefficients as in Equation (2.8), then substituted in the integral Equation (6.5). After the Galerkin testing is carried out

(discussed in Chapter II), the following system of linear equations is obtained

$$(V_m + \Delta V_m) = \sum_{n=1}^{N} C_n (Z_{mn} + \Delta Z_{mn}) \qquad m=1,2,3,\ldots, N \ . \tag{6.6}$$

where V_m and Z_{mn} are given by Equations (2.12) and (2.13) respectively. ΔV_m and ΔZ_{mn} are given by

$$\Delta V_m = - \frac{j\omega\mu_o}{2\pi} \iint_{cs} F_m(x,y) \left[\int_0^\infty \frac{R_\perp e^{-f(2d-x-x_s)} \cos g(y-y_s)}{f} \, dg \right] ds \ , \tag{6.7}$$

and

$$\Delta Z_{mn} = - \frac{\omega^2 \mu_o (\hat{\varepsilon}_1 - \hat{\varepsilon}_2)}{2\pi} \iint_{cs} \iint_{cs} F_n(x',y') F_m(x,y) \left[\int_0^\infty \frac{R_\perp e^{-f(2d-x-x')} \cos[g(y-y')]}{f} dg \right] ds' ds. \tag{6.8}$$

After solving the system of linear Equation (6.6), the scattered field is obtained as

$$E_z^s(x,y) = E_z^{sd}(x,y) + E_z^{sr}(x,y) \tag{6.9}$$

where $E_z^{sd}(x,y)$ is given by Equations (2.16) or (2.17), From Equations (6.4b) and (2.8), $E_z^{sr}(x,y)$ is obtained.

$$E_z^{sr}(x,y) = \frac{\omega^2 \mu_o (\hat{\varepsilon}_1 - \hat{\varepsilon}_2)}{2\pi} \sum_{m=1}^{N} C_m \iint_{cs} F_m(x',y') \left[\int_0^\infty \frac{R_\perp e^{-f(2d-x-x')} \cos[g(y-y')]}{f} dg \right] ds'. \tag{6.10}$$

For the backscattered case where $(x,y) = (x_s,y_s)$, $E_z^{sr}(x,y)$ can also be obtained by

$$E_z^{sr}(x_s,y_s) = j\omega(\hat{\varepsilon}_1-\hat{\varepsilon}_2) \sum_{m=1}^{N} C_m \Delta V_m \quad . \tag{6.11}$$

ΔV_m is given by Equation (6.7).

C. H-WAVE SCATTERING BY BURIED, LOSSY DIELECTRIC CYLINDERS OF INFINITE LENGTH

The electromagnetic scattering model of Figure 6-1 is used with the electric line source replaced by a magnetic line source. In homogeneous medium II, the magnetic field radiated by this magnetic line source is given by Equation (2.26). In the presence of the interface, the total field incident on the scatterer due to the line source is the sum of direct incident and reflected incident fields

$$H_z^i = H_z^{id} + H_z^{ir} \quad . \tag{6.12}$$

Substituting from Equation (3.6) into Equation (2.26) yields

$$H_z^{id} = -\frac{j\omega\hat{\varepsilon}_2}{2\pi} \int_0^{\infty} \frac{e^{-f|x-x_s|}\cos[g(y-y_s)]}{f}\, dg \quad , \tag{6.13a}$$

and the reflected incident field is

$$H_z^{ir} = -\frac{j\omega\hat{\varepsilon}_2}{2\pi} \int_0^{\infty} \frac{R_{\parallel} e^{-f(2d-x-x_s)}\cos[g(y-y_s)]}{f}\, dg \quad , \tag{6.13b}$$

where $R_{\parallel}$ is the plane wave reflection coefficient given by Equation (5.11b). The scattered magnetic field at any point is the sum of direct scattered fields and scattered reflected fields

$$\bar{H}^{s} = \bar{H}^{sd} + \bar{H}^{sr} \quad , \tag{6.14}$$

where

$$\bar{H}^{sd} = \frac{1}{\mu_0} \nabla \times \bar{A}^{sd} \quad . \tag{6.15}$$

$\bar{A}^{sd}$ is the electric vector potential given by Equation (2.29). From Equations (3.6), (2.29), and (6.15) the direct scattered field is obtained as

$$\bar{H}^{sd} = \frac{1}{2\pi} \nabla \times \iint_{cs} \bar{J}_{eq}(x',y') \left[\int_0^{\infty} \frac{e^{-f|x-x'|}}{f} \cos[g(y-y')] \, dg \right] ds' \quad . \tag{6.16}$$

Interchanging the order of differentiation and integration and using a well known vector identity yields

$$H_z^{sd} = -\frac{1}{2\pi} \iint_{cs} \bar{J}_{eq}(x',y') \times \left[\left(\hat{x} \frac{\partial}{\partial x} + \hat{y} \frac{\partial}{\partial y} \right) \int_0^{\infty} \frac{e^{-f|x-x'|}}{f} \cos[g(y-y')] \, dg \right] ds. \tag{6.17}$$

$\bar{J}_{eq}$ is the equivalent electric volume polarization current in the scatterer given by Equation (2.5).

Using the reflection coefficient $R_{\parallel}$ as given by Equation (5.11b) in above equation, the scattered reflected magnetic field is obtained as

$$\bar{H}^{sr} = -\frac{1}{2\pi}\iint_{cs} \bar{J}_{eq}(x',y') \times \left[\hat{x}\int_0^{\infty} \frac{fR_{\parallel}\, e^{-f(2d-x-x')}\cos[g(y-y')dy]}{f} - \hat{y}\int_0^{\infty} \frac{gR_{\parallel}\, e^{-f(2d-x-x')}\sin[g(y-y')dg]}{f}\right] ds' \quad . \tag{6.18a}$$

Thus

$$H_z^{sr} = \frac{1}{2\pi}\iint_{cs} \left[J_x(x',y')\int_0^{\infty} \frac{gR_{\parallel}\, e^{-f(2d-x-x')}\sin[g(y-y')dy]}{f} + J_y(x',y')\int_0^{\infty} \frac{fR_{\parallel}\, e^{-f(2d-x-x')}\cos[g(y-y')dg]}{f}\right] ds' \quad . \tag{6.18b}$$

where J_x and J_y are the x and y components of the equivalent electric volume polarization current.

The total magnetic field at any point is the sum of the direct incident and the reflected incident fields due to the magnetic line source and direct scattered and scattered reflected fields due to the scatterer. A typical ray geometry describing this situation for an elemental section of the scatterer is shown in Figure 6-2, where the E-field may be replaced by H field for the case under consideration.

Thus

$$\bar{H} = \bar{H}^{id} + \bar{H}^{ir} + \bar{H}^{sd} + \bar{H}^{sr} \quad . \tag{6.19}$$

As it was discussed in Chapter II, it is preferred to obtain an integral equation involving the electric field as the unknown function. This choice improved the convergence of the solution significantly (see Chapter II). To obtain an integral equation involving $\bar{E}^{I}$, Maxwell's equation is used to find $\bar{E}^{id}$, $\bar{E}^{ir}$, $\bar{E}^{sd}$, and $\bar{E}^{sr}$ in Region II from $\bar{H}^{id}$, $\bar{H}^{ir}$, $\bar{H}^{sd}$, and $\bar{H}^{sr}$ respectively. Then the resulting equation is evaluated in Region I.

Thus, one may write

$\bar{E}^{id} + \bar{E}^{ir} = \bar{E}^{I} - \bar{E}^{sd} - \bar{E}^{sr}$;in Region I, where $\bar{E}^{id}$ is given by Equation (2.27a), and from Equation (6.13b) (6.20)

$$\begin{aligned} \bar{E}^{ir} &= \frac{1}{j\omega\hat{\varepsilon}_2} \nabla \times \bar{H}^{ir} \\ &= \frac{1}{2\pi}\left[\hat{x}\int_0^{\infty} \frac{gR_{\parallel}\, e^{-f(2d-x-x_s)}}{f}\sin[g(y-y_s)]\,dg \right. \\ &\quad \left. + \hat{y}\int_0^{\infty} \frac{fR_{\parallel} e^{-f(2d-x-x_s)}}{f}\cos[g(y-y_s)]\,dg\right] . \end{aligned} \tag{6.21}$$

$\bar{E}^{sd}$ is given by Equation (2.37), which is found by using Maxwell's equation in Equation (6.15) and using lorentz condition. $\bar{E}^{sr}$ is found from Equation (6.18a) as follows

$$\underline{E}^{sr} = \frac{1}{j\omega\hat{\varepsilon}_2} \nabla \times \underline{H}^{sr}$$

$$= \frac{-1}{2\pi j\omega\hat{\varepsilon}_2} \iint_{cs} \nabla \times \left\{ \bar{J}_{eq}(x',y') \times \left[\hat{x} \int_0^\infty \frac{fR_{\parallel}\, e^{-f(2d-x-x')} \cos[g(y-y')]}{f}\, dg \right.\right.$$

$$\left.\left. - \hat{y} \int_0^\infty \frac{gR_{\parallel}\, e^{-f(2d-x-x')} \sin[g(y-y')]}{f}\, dg \right] \right\} ds. \tag{6.22}$$

Using the above quantities in Equation (6.20) and substituting for $\bar{J}_{eq}$ from Equation (2.5) yields the following integral equation.

$$\underline{E}^{id}(x,y) + \underline{E}^{ir}(x,y) = \underline{E}^{I}(x,y) - \frac{\omega^2\mu_0(\hat{\varepsilon}_1-\hat{\varepsilon}_2)}{2\pi} \iint_{cs} \underline{E}^{I}(x,y) K_0(\gamma_2|\bar{\rho}-\bar{\rho}'|) ds'$$

$$- \frac{\gamma_2(\hat{\varepsilon}_1-\hat{\varepsilon}_2)}{2\pi\hat{\varepsilon}_2} \int_{\ell} \left[\underline{E}^{I}(x',y') \cdot \hat{n}(\ell') \right] K_1(\gamma_2|\bar{\rho}-\bar{\rho}'|)\hat{\rho}\, d\ell'$$

$$+ \frac{(\hat{\varepsilon}_1-\hat{\varepsilon}_2)}{2\pi\hat{\varepsilon}_2} \iint_{cs} \nabla \times \left\{ \underline{E}^{I}(x',y') \times \left[\hat{x} \int_0^\infty \frac{fR_{\parallel}\, e^{-f(2d-x-x')} \cos[g(y-y')]}{f}\, dg \right.\right.$$

$$\left.\left. - \hat{y} \int_0^\infty \frac{gR_{\parallel}\, e^{-f(2d-x-x')} \sin[g(y-y')]}{f}\, dg \right] \right\} ds' \quad . \tag{6.23}$$

The unknown function in the above integral equation is $\bar{E}^{I}(x,y)$ which appears inside and outside of the integrals, thus, this may be viewed as a Fredholm integral equation of the second kind. $\bar{E}^{id}$ and $\bar{E}^{ir}$ have been defined previously. The above integral equation is basically

the same as the integral equation in Equation (2.38b) except here two additional terms due to the reflection at the interface are added. This integral equation is solved in the same way as Equation (2.38b) was solved. To avoid repetition, the attention is focused on the reflected terms. After expansion and testing (see Chapter II) the new system of linear equations is as follows

$$(V_m + \Delta V_m) = \sum_{n=1}^{N} C_n (Z_{mn} + \Delta Z_{mn}) \quad . \tag{6.24a}$$

where V_m and Z_{mn} are given by Equations (2.42) and (2.43) respectively and,

$$\Delta V_m = \iint_{cs} \bar{F}_m(x,y) \cdot \underline{\bar{E}}^{ir}(x,y)\, ds \qquad m=1,2,..,N \quad . \tag{6.24b}$$

Substituting from Equations (2.40b) and (6.21) in Equation (6.24b) yields

$$\Delta V_m = \frac{1}{2\pi} \iint_{cs} \left[\frac{\partial F_m(x,y)}{\partial y} \int_0^{\infty} \frac{gR_{\parallel} e^{-f(2d-x-x_s)} \sin[g(y-y_s)]}{f}\, dg \right.$$

$$\left. - \frac{\partial F_m(x,y)}{\partial x} \int_0^{\infty} \frac{fR_{\parallel} e^{-f(2d-x-x_s)} \cos[g(y-y_s)]}{f}\, dg \right] ds \quad . \tag{6.24c}$$

Testing the last term in the integral equation (6.23)

$$\Delta Z_{mn} = -\frac{(\hat{\varepsilon}_1-\hat{\varepsilon}_2)P}{\hat{\varepsilon}_2} \iint_{cs}\iint_{cs} \overline{F}_m(x,y) \cdot \left\{ \nabla x \left[\overline{F}_n(x',y') x \left(\hat{x} \int_0^\infty \frac{f R_{\parallel} e^{-f(2d-x-x')} \cos[g(y-y')]dg}{f} - \hat{y} \int_0^\infty \frac{g R_{\parallel} e^{-f(2d-x-x')} \sin[g(y-y')]}{f} dg \right) \right] \right\} 2\pi\varepsilon_2 \, ds'ds \quad . \tag{6.25}$$

where $\overline{F}_m(x,y)$ and P are given by Equations (2.40b) and (2.40c) respectively.

A further simplified form of ΔZ_{mn} is given by

$$\Delta Z_{mn} = -\frac{(\hat{\varepsilon}_1-\hat{\varepsilon}_2)P}{2\pi\hat{\varepsilon}_2} \iint_{cs}\iint_{cs} \left[\frac{\partial F_m(x,y)}{\partial y} \frac{\partial F_n(x',y')}{\partial y'} \int_0^\infty \frac{g^2 R_{\parallel} e^{-f(2d-x-x')} \cos[g(y-y')]dg}{f} + \left(\frac{F_m(x,y)}{\partial y} \frac{\partial F_n(x',y')}{\partial x'} + \frac{\partial F_m(x,y)}{\partial x} \frac{\partial F_n(x',y')}{\partial y'} \right) \int_0^\infty \frac{fg R_{\parallel} e^{-f(2d-x-x')} \sin[g(y-y')]dg}{f} - \frac{\partial F_m(x,y)}{\partial x} \frac{\partial F_n(x',y')}{\partial x'} \int_0^\infty \frac{f^2 R_{\parallel} e^{-f(2d-x-x')} \cos[g(y-y')]dg}{f} \right] ds'ds \quad . \tag{6.26}$$

After solving the system of linear equations (6.24), the scattered field is obtained by

$$H_z^s(x,y) = H_z^{sd}(x,y) + H_z^{sr}(x,y) \quad . \tag{6.27}$$

$H_z^{sd}(x,y)$ is given by Equation (2.46) or Equation (2.47). To calculate H_z^{sr} Equation (2.40) is substituted in Equation (2.5), from which J_x and J_y are determined. Substituting for J_x and J_y in Equation (6.18b) yields

$$H_z^{sr}(x,y) = + \frac{j\omega(\hat{\varepsilon}_1-\hat{\varepsilon}_2)P}{2\pi} \sum_{m=1}^{N} C_m \iint_{cs} \left[\frac{\partial F_m(x',y')}{\partial y'} \int_0^{\infty} \frac{gR_{\parallel} e^{-f(2d-x-x')} \sin[g(y-y')]}{f} dg \right.$$

$$\left. - \frac{\partial F_m(x',y')}{\partial x'} \int_0^{\infty} \frac{fR_{\parallel} e^{-f(2d-x-x')} \cos[g(y-y')]}{f} dg \right] ds' \quad . \tag{6.28}$$

P is given by Equation (2.40c).

The above equation in general may be used to calculate the bistatic or backscattered fields. However, for backscattered case, i.e., $(x,y) = (x_s,y_s)$, a comparison of Equation (6.28) with Equation (6.24) reveals that the following can be written

$$H_z^{B.sr.}(x_s,y_s) = \frac{j\omega(\hat{\varepsilon}_1-\hat{\varepsilon}_2)P}{} \sum_{m=1}^{N} C_m \Delta V_m \quad , \tag{6.29}$$

where ΔV_m is given by Equation (6.24c).

D. SUMMARY

In this chapter, an electromagnetic scattering model for buried two-dimensional, cylindrical geometries was presented. Integral equations involving the unknown electric field inside the scatterer for

parallel and perpendicular polarization were derived. To solve these integral equations the moment method was used and corresponding linear equations were derived.

In the next chapter, the E-wave scattering model is specialized to buried rectangular cylinders and the moment method formulation presented here is applied by choosing a set of basis and testing functions.

CHAPTER VII

E-WAVE SCATTERING BY BURIED, LOSSY DIELECTRIC RECTANGULAR CYLINDER OF INFINITE LENGTH

A. INTRODUCTION

An E-wave scattering model for lossy dielectric rectangular cylinders buried in earth is presented. This model may be used to simulate a tunnel or a trench geometry. The moment method formulations are presented. Then the number of plane waves in the expansion to obtain convergence is considered. Some numerical results are presented and discussed.

Figure 7-1 shows a plane cut of the electromagnetic scattering model. A (2a) by (2b) rectangular dielectric cylinder is buried in earth region designated by II (ε_2, μ_2, σ_2). The z-axis is along the axis of the cylinder and x=d plane constitutes the air-earth interface. For the sake of simplicity, $a \leq x_s \leq d$ is assumed. If d>a, the tunnel geometry is modeled (Figure 7-1a), and if d=a, the trench geometries is modeled (Figure 7-1b). Most of the geometries considered in this chapter are for filled trenches and tunnels. This reflects the interest of one of the supporting agencies but does not restrict the applicability of the techniques.

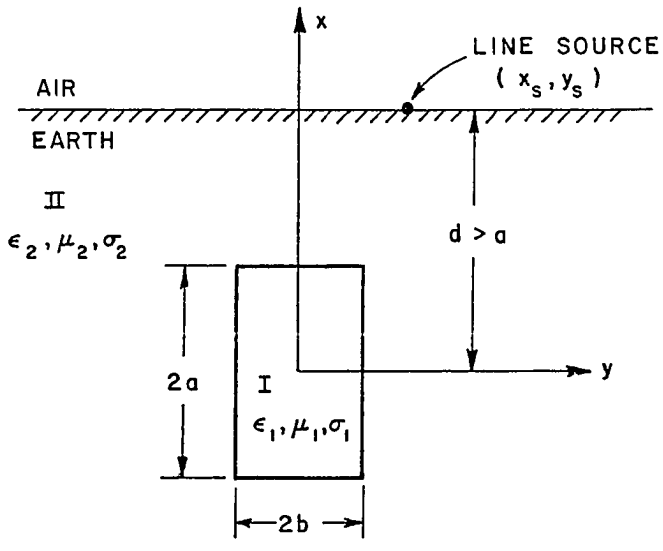

(a) TUNNEL GEOMETRY

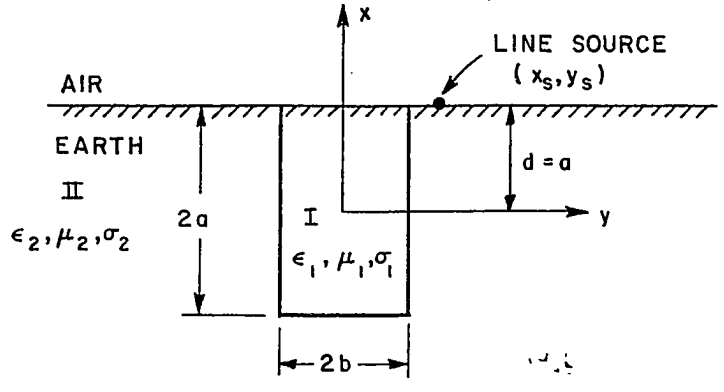

(b) TRENCH GEOMETRY

Figure 7-1. The electromagnetic scattering model for (a) a buried tunnel, and (b) a trench geometry.

B. PLANE WAVE EXPANSION

The system of linear Equation (6.6) has already been discussed for an infinite-length cylinder of arbitrary cross-section shape and for general basis functions. Here it suffices to choose the basis functions and evaluate the cross-sectional integrations in a closed form in the same manner as discussed in Chapter III. The set of simultaneous linear equations obtained are

$$(V_m + \Delta V_m) = \sum_{n=1}^{N} C_n (Z_{mn} + \Delta Z_{mn}) \; ; \; m = 1,2,3,\ldots,N \quad . \tag{7.1}$$

V_m and Z_{mn} are now given by Equations (3.8)and (3.5) respectively, and from Equations (6.7) and (3.1).

$$\Delta V_m = -\frac{j\omega\mu_o}{2\pi} \int_{-a}^{a}\int_{-b}^{b} e^{-jf_m x} e^{-jg_m y} \left[\int_0^{\infty} \frac{R_\perp e^{-f(2d-x-x_s)} \cos[g(y-y_s)]}{f} dg \right] dxdy \quad . \tag{7.2}$$

From Equations (6.8) and (3.1)

$$\Delta Z_{mn} = C_1 \int_{-a}^{a}\int_{-b}^{b}\int_{-a}^{a}\int_{-b}^{b} e^{-jf_n x'} e^{-jg_n y'} e^{-jf_m x} e^{-jg_m y} \left[\int_0^{\infty} \frac{R_\perp e^{-f(2d-x-x')} \cos[g(y-y')]}{f} dg \right] dx'dy'dxdy \quad . \tag{7.3}$$

C_1 is given by Equation (3.5d).

Interchanging the order of the integrations in Equation (7.2) and rearranging terms, one obtains

$$\Delta V_m = -\frac{j\omega\mu_o}{2\pi}\int_o^\infty \frac{R_\perp e^{-f(2d-x_s)}}{f}\left[\int_{-a}^{a} e^{-jf_m x} e^{fx}\,dx \int_{-b}^{b} e^{-jg_m y}\cos[g(y-y_s)]\,dy\right] dg \ ,$$

or

$$\Delta V_m = -\frac{j\omega\mu_o}{\pi}\int_o^\infty \frac{R_\perp e^{-f(2d-x_s)}}{f}\ (F_m \cdot GE_m^V)\ dg \ , \qquad (7.4a)$$

where

$$F_m = \frac{\sin[(f_m+jf)a]}{(f_m+jf)} \ . \qquad (7.4b)$$

GE_m^V is given by Equation (3.8c).

Changing the order of integration and rearranging terms in Equation (7.3) yields

$$\Delta Z_{mn} = C_1 \int_o^\infty \frac{R_\perp e^{-2fd}}{f}\left[\int_{-a}^{a} e^{-jf_n x'} e^{fx'}\,dx' \int_{-a}^{a} e^{-jf_m x} e^{fx}\,dx \int_{-b}^{b}\int_{-b}^{b} e^{-jg_n y'} e^{-g_m y}\cos[g(y-y')]\,dy'dy\right] \ ,$$

or

$$= 8C_1 \int_o^\infty \frac{R_\perp e^{-2fd}}{f}\ (F_n \cdot F_m \cdot GE_{mn})\ dg \ . \qquad (7.5)$$

F_m and F_n are given by Equation (7.4b), and GE_{mn} is given by Equation (3.10c).

After solving the system of linear equations (7.1) for C_n's, the scattered field is calculated by

$$E_z^s(x,y) = E_z^{sd} + E_z^{sr} \quad , \tag{7.6}$$

where E_z^{sd} is given by Equations (3.11) or (3.12), and E_z^{sr} is found from Equations (6.10) and (3.1) as

$$E_z^{sr}(x,y) = \frac{\omega^2 \mu_o (\hat{\varepsilon}_1 - \hat{\varepsilon}_2)}{\pi} \sum_{m=1}^{N} C_m \int_o^{\infty} \frac{R_{\perp} e^{-f(2d-x)}}{f} (F_m \cdot GE_m^V)\, dg \quad . \tag{7.7}$$

F_m is given by Equation (7.4b) and GE_m^V is given by Equation (3.8c) with y_s replaced by y. An additional way to obtain the backscattered field ($(x,y) = (x_s,y_s)$) is by comparing Equations (7.7) and (7.4) which yields

$$E_z^{sr}(x_s,y_s) = -j\omega(\hat{\varepsilon}_1 - \hat{\varepsilon}_2) \sum_{m=1}^{N} C_m \Delta V_m \quad . \tag{7.8}$$

ΔV_m is given by Equation (7.4).

C. CONVERGENCE

Two computer programs were developed to model the air-earth interface and buried scatterers. These programs are called RTUNLE and RCYLEGP. The former uses the closed form evaluation for the cross-sectional integrals, whereas, the latter uses numerical integration for

the cross-sectional integrals. These computer programs are included and fully discussed in the Appendices B and F.

To test the convergence of the solution, a typical convergence test is made. The scattered field is calculated for increasing number of plane waves in the expansion (N). For this purpose, a 1 m square tunnel with $\varepsilon_{r_1}=2$ and $\sigma_1=.0012$ s/m buried 1 m below the interfere in an earth with $\varepsilon_{r_2}=4$ and $\sigma_2=.003$ s/m, is considered. The source of excitation is an electric line source located on the interface directly above the tunnel. Figure 7-2 shows the resulting backscattered field versus increasing number of plane waves spanning the field inside the tunnel. The solution is converged for N>6. After convergence the solution seems to be very stable and the curve is smooth for the range shown. Using Equation (3.14), a value for $\Delta\Phi$ is included for all values of N and is included in Figure 7-2.

An approximate model can be developed that can be used to explain much of the details of structure of the scattering patterns to be computed using the above more precise numerical analysis.

First, the fields radiated into the "earth" medium by an electric line source at the interface are given by

$$\overline{E}_{em} = \overline{E}_{homo}\ (1 + R_{\perp}) \quad .$$

where $\overline{E}_{homo}$ are the fields radiated into a homogeneous earth medium and

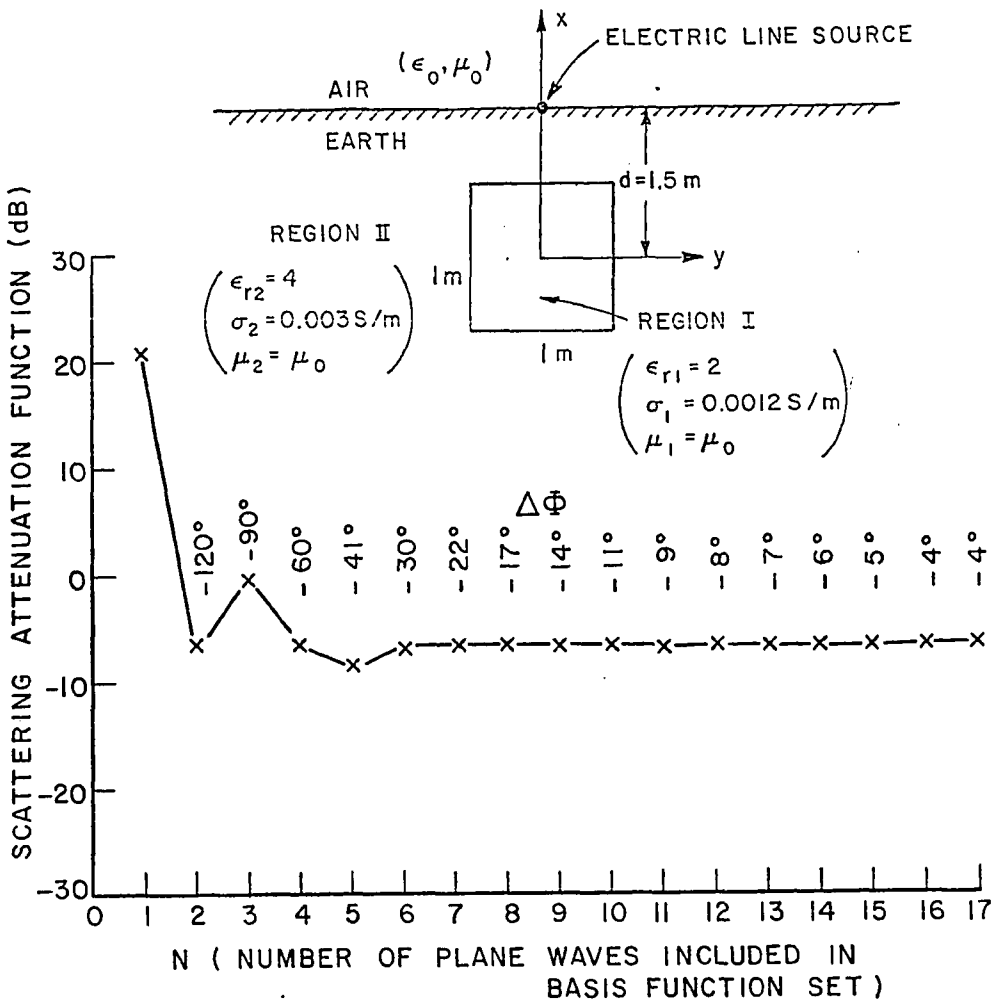

Figure 7-2. The convergence curve for computer program RTUNLE for a buried tunnel. Scattering Attenuation Function is calculated for increasing values of N, the number of plane waves in the expansion. The frequency used is 100 MHz.

$R_\perp$ is the plane wave reflection coefficient for incidence on the interface from the "earth" medium.

This approximation was confirmed in Chapter V.

Second, the fields scattered by the target are also incident on the interface. This requires that a second $(1+R_\perp)$ factor be introduced. Thus the SAF_I for the case for the interface could be approximated by

$$SAF_I = (SAF)_{homo} (1+R_\perp)^2$$

where $(SAF)_{homo}$ is the scattering attenuation function when the target and source are contained in a homogeneous medium. Note that the normalization used in this dissertation did not include the interface, i.e., the normalization factor was the fields of a line source at the image position in a homogeneous medium. If the interface had been included in the normalization procedure, the SAF would to a first approximation be dependent only on the target.

Another factor that appears in the appropriate forms are the scattering patterns of the "tunnels". Referring to Figure 3-4, it is seen that only a small lobe appears at ϕ=180°. This is the region for which we will be observing these targets. Thus if one considers the factors discussed above, the scattering pattern of the tunnel in a homogeneous medium and the scattering pattern of the line source on the interface, then the computed results to be shown are those that would be anticipated.

D. SCATTERING PATTERNS

Some examples of bistatic and backscattered patterns are given for a filled trench and some tunnel geometries. A family of curves is presented for increasing values of "d", the depth of the center of the tunnel. The trench or tunnel (see Figure 7-1) is modeled by a 1 m by .5 m rectangular cylinder of infinite length with $\varepsilon_{r_1}=2$, $\sigma_2=.0012$ s/m, and $\mu_1=\mu_0$. The earth is modeled by a medium with $\varepsilon_{r_2}=4$, $\sigma_2=.003$ s/m, and $\mu_2=\mu_0$. The frequency used is 100 MHz. The electromagnetic scattering model is shown in Figure 7-3. An electric line source is placed on the interface parallel to z-axis at $(x_s=d, y_s)$.

1. Backscattered Patterns

Figure 7-3 shows various backscattered patterns. When d=a=.5m, a trench geometry is modeled. The backscattered pattern for this trench geometry is shown in Figure 7-3, which indicates a strong backscattered field in regions directly above the trench. After a minimum at $|y|\approx.5$m region, the backscattered field increases slightly and then falls rapidly as $|y|$ is increased.

For values of d>a tunnel geometries are modeled. Some backscattered patterns are included in Figure 7-3 for tunnels buried at d=.75m, 1m, 1.25m, and 1.5m. These patterns, in general, follow the same shape as that of the trench, except that, the pattern is widened and reduced in magnitude for most regions close to the scatterer. This is caused by the scattering pattern of the tunnel and is not an

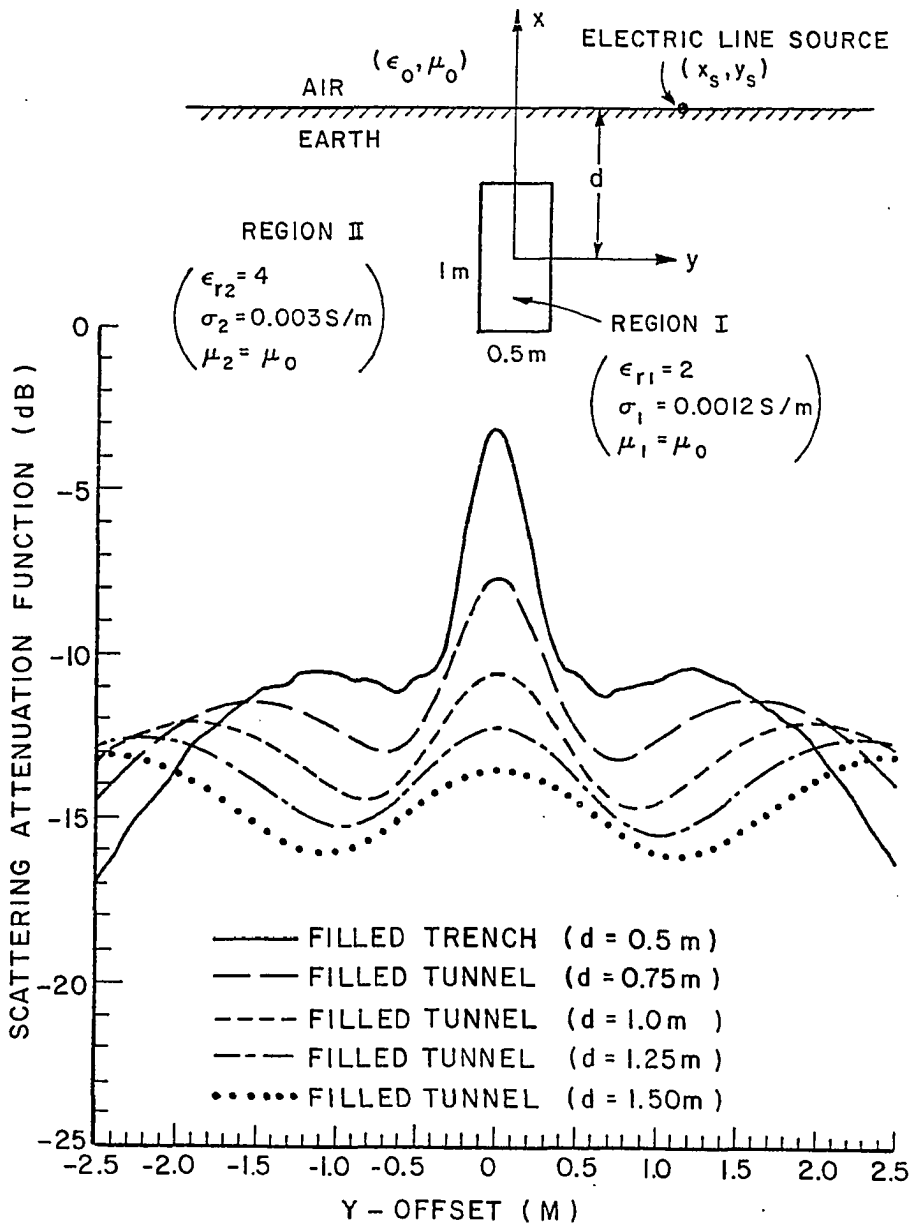

Figure 7-3. The backscattering patterns for trench and tunnel geometries. The electric line source is placed on the interface, parallel to z-axis, and moved from y=-2.5 m to y=2.5 m incrementally. The frequency is 100 MHz.

interface phenomena. Figure 7-3 suggests that (for the case under consideration) for deeply buried tunnels, there is not a distinct maximum above the tunnel, while for shallowly buried tunnel for this case, there is a definite maximum directly above the tunnel.

To investigate the effect of the air-earth interface on the backscattering patterns of a trench and a tunnel, Figures 7-4 and 7-5 are presented. Figure 7-4 shows the backscattered pattern for the trench geometry discussed in Figure 7-3. In addition, an analogous backscattered pattern is given for a case where the air-earth interface is removed (i.e., air region is replaced with Region II). This pattern shows that the air-earth interface changes the backscattered pattern considerably. For the case shown, Figure 7-4 suggests that the interface enhances the backscattered field in the vicinity of the trench. This is because the source and observation point are in the immediate vicinity of the top of the tunnel. Note that the increase in the Scattering Attenuation Function (SAF) level at when the source is at the top of the trench may be obtained by multiplying the SAF with no interface by $(1+R_{\perp})^2$ where $R_{\perp}$ is the plane wave reflection coefficient for a wave in the tunnel normally incident on the interface. The decay in the pattern as y increases is caused by the directional pattern of the line source on the interface as shown in Chapter V. For the case of the tunnel (Figure 7-5), the line source pattern is not significant. We also note that the presence of the interface is approximately accounted for by the $(1+R_{\perp})^2$ factor. In this case, the interface for which $R_{\perp}$ is computed is that between medium II and free space.

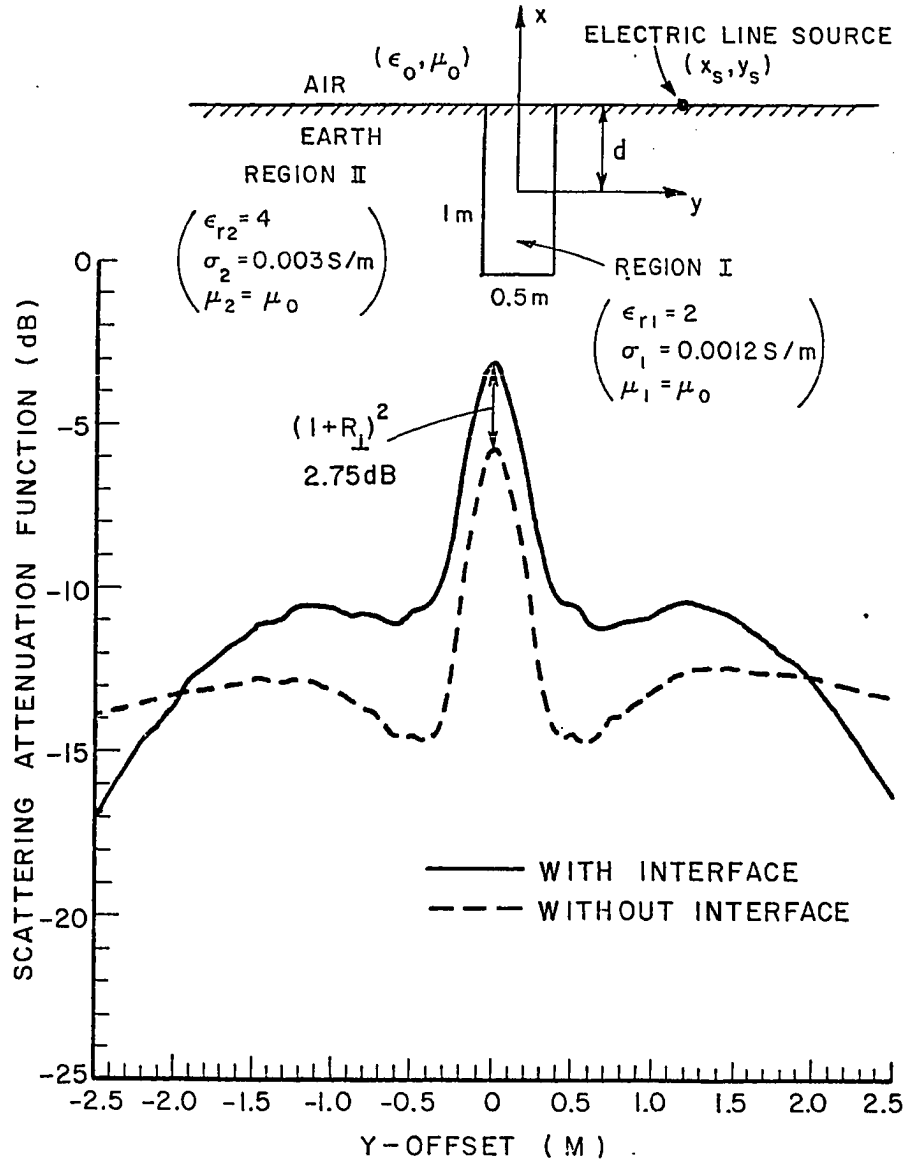

Figure 7-4. Comparison of backscattered field patterns of a trench geometry, with and without the air-earth interface. Frequency is 100 MHz.

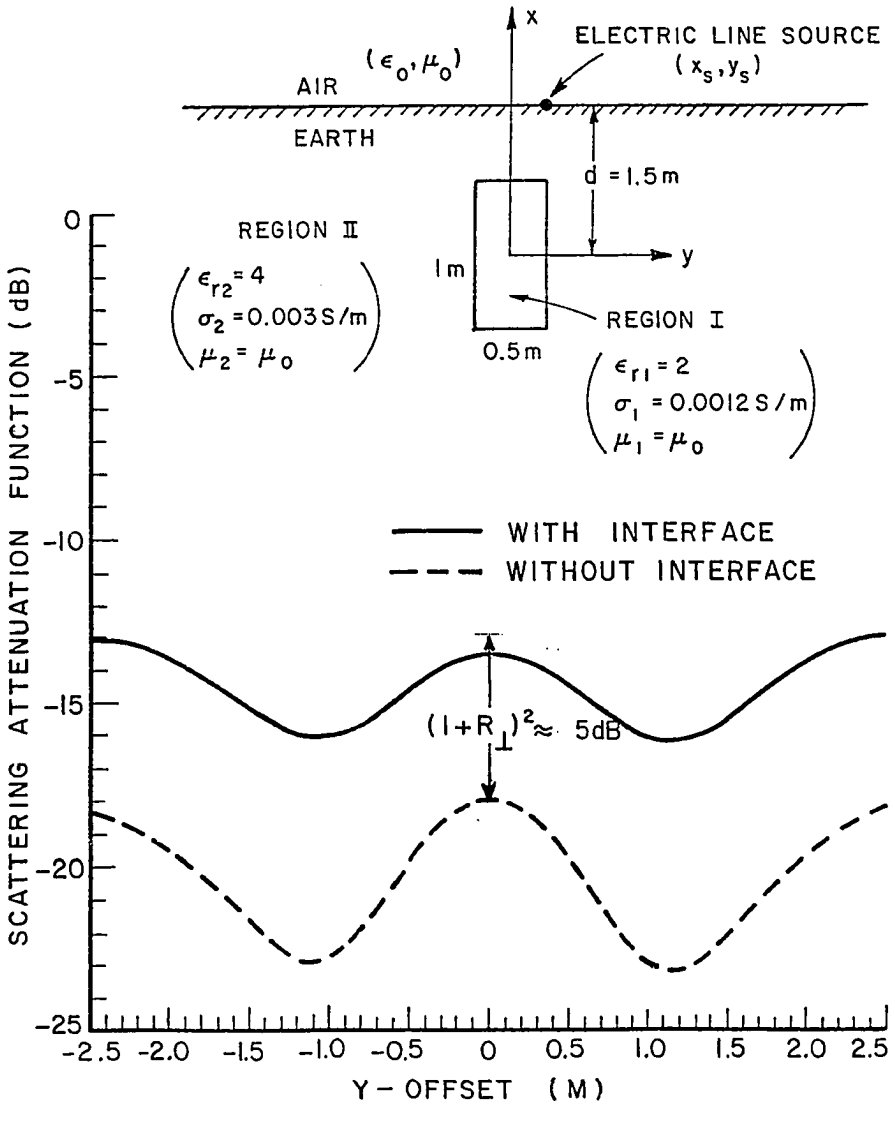

Figure 7-5. Comparison of backscattered field patterns of a tunnel geometry, with and without the air-earth interface. Frequency is 100 MHz.

This $(1+R_{\perp})^2$ factor is that suggested by Burrell and Peters [47]. The fields radiated by the line source into the medium are increased by $(1+R_{\perp})$ as was discussed in Chapter V. The total scattered fields are also increased by $(1+R_{\perp})$ on reflection at the interface.

2. Bistatic Scattering Patterns

As a first example of bistatic scattering pattern, an electric line source is placed on the interface at $(x_s,y_s)=(d,0)$ and the scattered field is observed on the interface at y=-2.5m to y=2.5m incrementally. This model is shown in Figure 7-6. Some bistatic scattering patterns are included in Figure 7-6 for a trench geometry and some tunnels buried at d=.75m, 1m, 1.25m, and 1.5m. For the trench case (d=a=.5m), the bistatic pattern is maximum directly above the trench and it falls rapidly as $|y|$ is increased. For tunnel geometries (d>a) the general shape of the bistatic pattern is similar to that of the trench and is reduced in amplitude and widened as d is increased. It is also noted that the bistatic pattern falls with a slower rate for deeper tunnels. This is primarily caused by the scattering angles becoming more restrictive as the depth increases.

To investigate the effect of the air-earth interface on the bistatic patterns of a trench and a tunnel, Figures 7-7 and 7-8 are presented. Figure 7-7 shows the bistatic scattering pattern for the trench geometry discussed in Figure 7-6. In addition, a similar bistatic scattering pattern is given for a case where the air-earth interface is removed (i.e., air region is replaced by Region II).

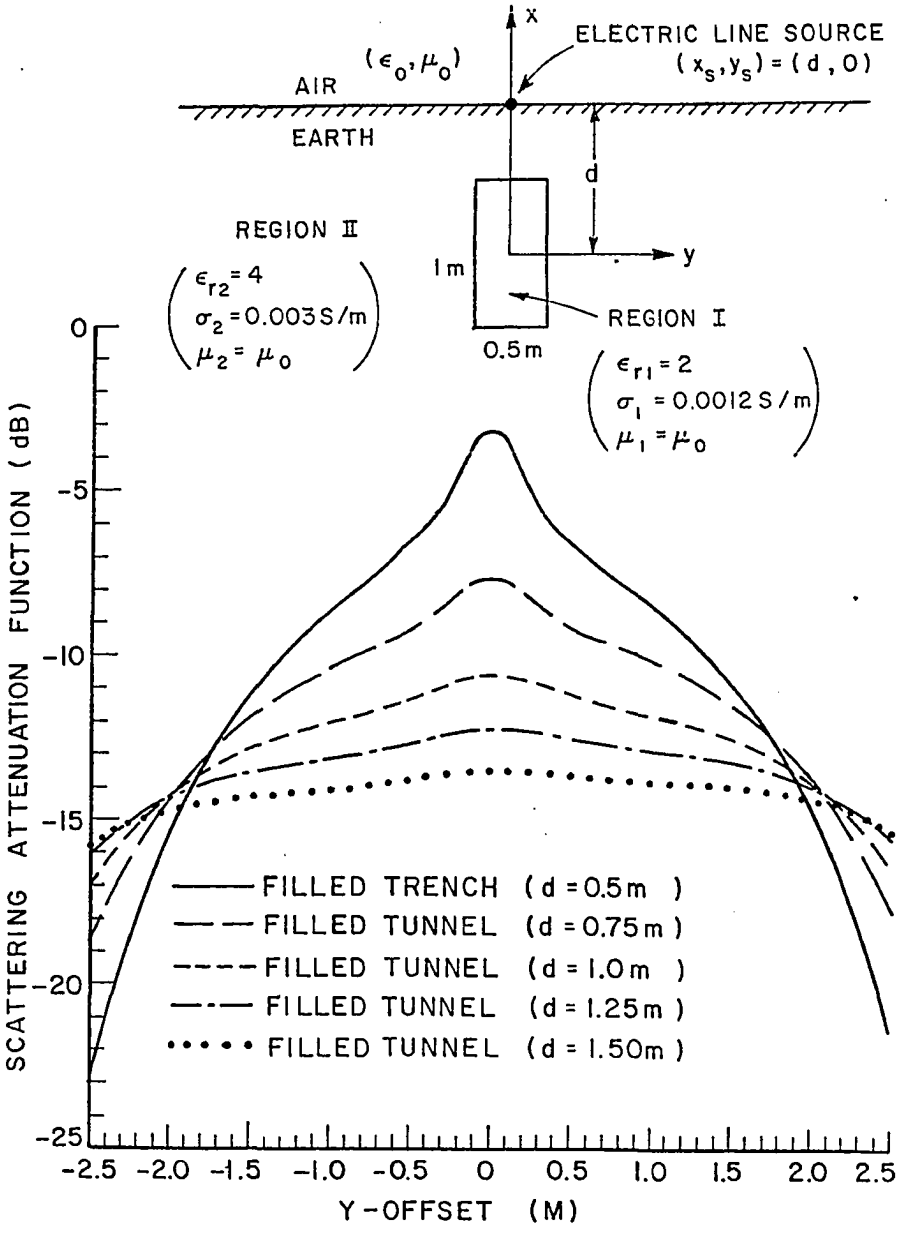

Figure 7-6. Bistatic scattering patterns for some trench and tunnel geometries. An electric line source is placed on the interface at $(x_S, y_S)=(d,0)$ parallel to z-axis, and the scattered field is observed at points on the interface along y-axis (from y=-2.5m to y=2.5m). The frequency is 100 MHz.

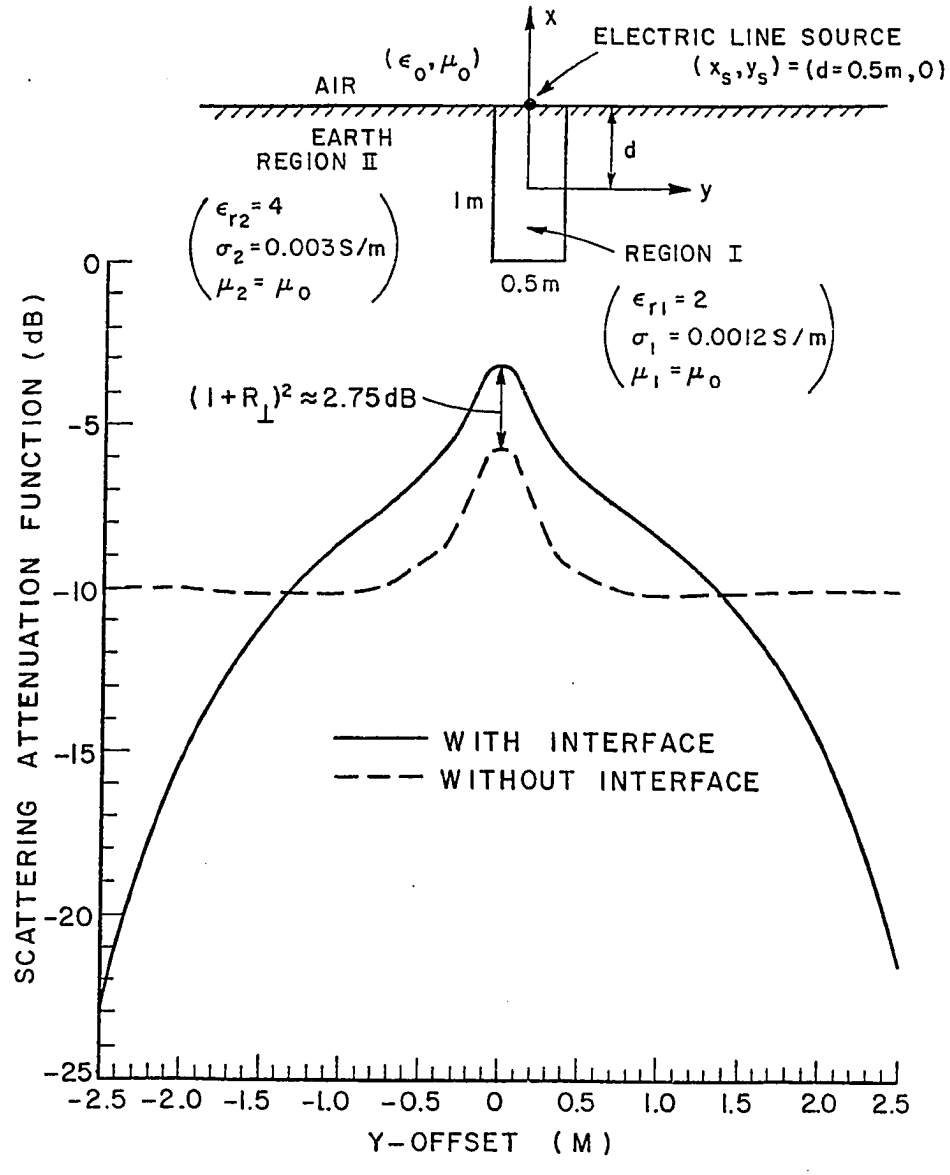

Figure 7-7. Comparison of the bistatic scattering patterns for a trench geometry, with and without the air-earth interface. Frequency is 100 MHz. $(1+R_\perp)^2$

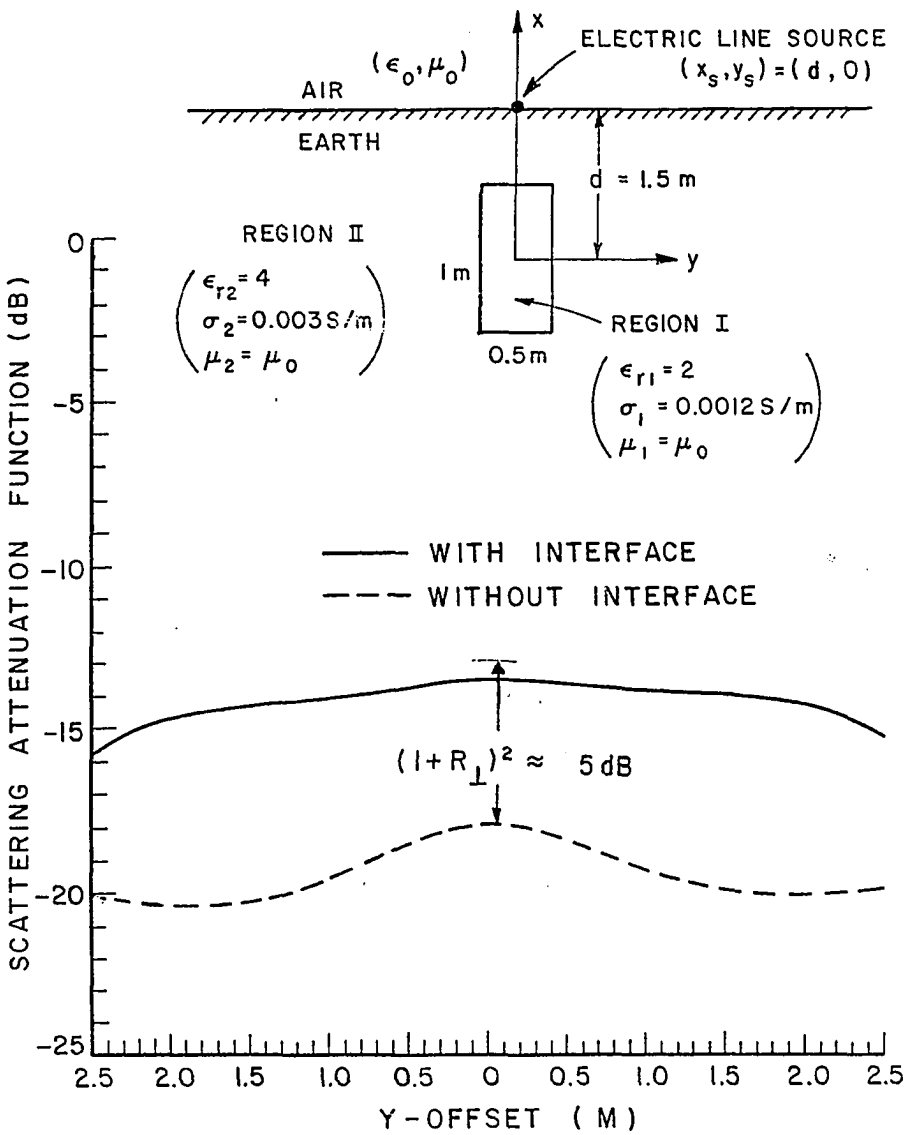

Figure 7-8. Comparison of the bistatic scattering patterns for a tunnel geometry, with and without the air-earth interface. Frequency is 100 MHz.

Figure 7-7 suggests that the bistatic pattern is enhanced by interface in the vicinity of the trench (i.e., $|y|<1.5m$) by a factor of $(1+R_\perp)^2$, where $R_\perp$ is the plane wave reflection coefficient between region I and air. As $|y|$ is increased, the pattern falls rapidly, partially because of the effect of the radiation pattern of the line source on the interface as discussed in Chapter V. The pattern for the no-interface case remains unchanged for large values of $|y|$ for the range shown. Figure 7-8 shows an analogous set of patterns for a tunnel buried at d=1.5m. It is apparent that the interface produces only minor changes in the bistatic scattering pattern. For this case $R_\perp$ in the $(1+R_\perp)^2$ factor is between regions II and air.

As a second example of bistatic scattering pattern, an electric line source is placed on the interface at $(x_s,y_s)=(d,1.5m)$ and the scattered field is calculated on the interface from y=-2.5m to y=2.5m. The bistatic scattering patterns are shown in Figure 7-9 for a trench geoemetry and for a tunnel buried at d=.75m, 1m, 1.25m, and 1.5m. It is noted that because of the none symmetrical physical situation, the patterns do not have any symmetry. It is apparent that the general shape of the pattern is basically the same for all cases, except that as the tunnel is buried deeper, the pattern widens and is reduced in magnitude as is expected.

E. BACKSCATTERING VERSUS FREQUENCY

In this section two sets of frequency curves are presented, one for a trench geometry, and the other for a tunnel geometry. In each case a

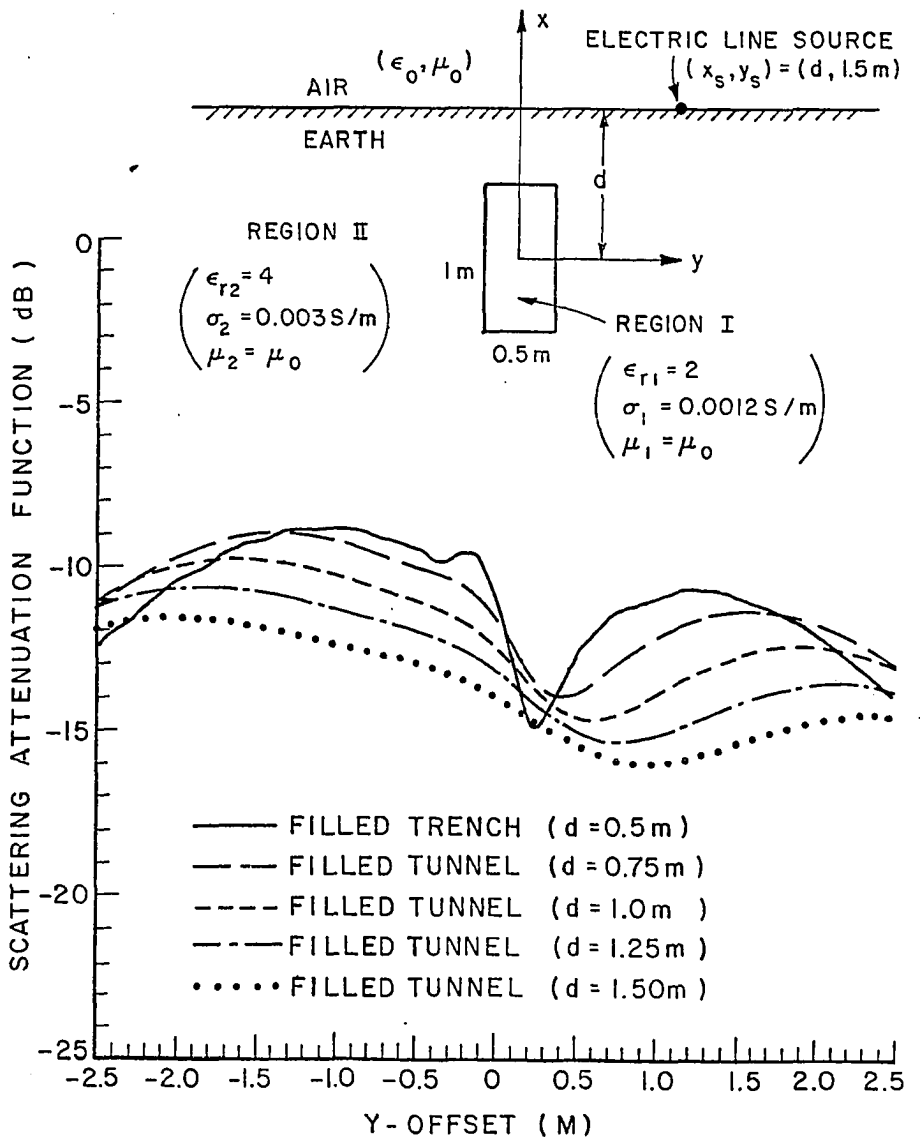

Figure 7-9. Bistatic scattering patterns for some trench and tunnel geometries. An electric line source is placed on the interface at $(x_s, y_s)=(d,1.5m)$ parallel to z-axis, and the scattered field is observed at points on the interface along y-axis (from y=-2.5m to y=2.5m). The frequency is 100 MHz.

curve for the no interface case is included for comparison. In addition, a set of frequency curves for an equivalent cross-section area circular cylinder is provided for testing the validity of the moment method solution.

The scattering model for a trench geometry is shown in Figure 7-10, where a 1 m by .5 m lossy rectangular trench of buried in an earth medium, is considered. For this model, a backscattered field versus frequency curve (solid line) is shown in Figure 7-10 which shows increases in relative scattering with frequency.

The dashed curve in Figure 7-10 is the relative scattering curve for the case where the interface is removed and the same source location is maintained. The two curves are related as has already been discussed. Similar results are shown in Figure 7-11 except that $R_{\perp 2}$ is used in lieu of $R_{\perp 1}$ where $R_{\perp 1}$ is the reflection coefficient between region I and air, and $R_{\perp 2}$ is the reflection coefficient between region II and air. It is again noted that the presence of the interface can be accounted for in a simple way and yet reasonably accurate results can be obtained.

Also included in Figure 7-11 are two analogous backscattered versus frequency curves, for an equivalent cross-section area circular cylinder. The circular cylinder is composed of the same medium (Region II). Comparing the corresponding curves for the rectangular and the circular cylinders, it is apparent that at low frequency regions (i.e., <50 MHz) the scattering curves that are the same for each corresponding case. As the frequency increases the corresponding scattering curves

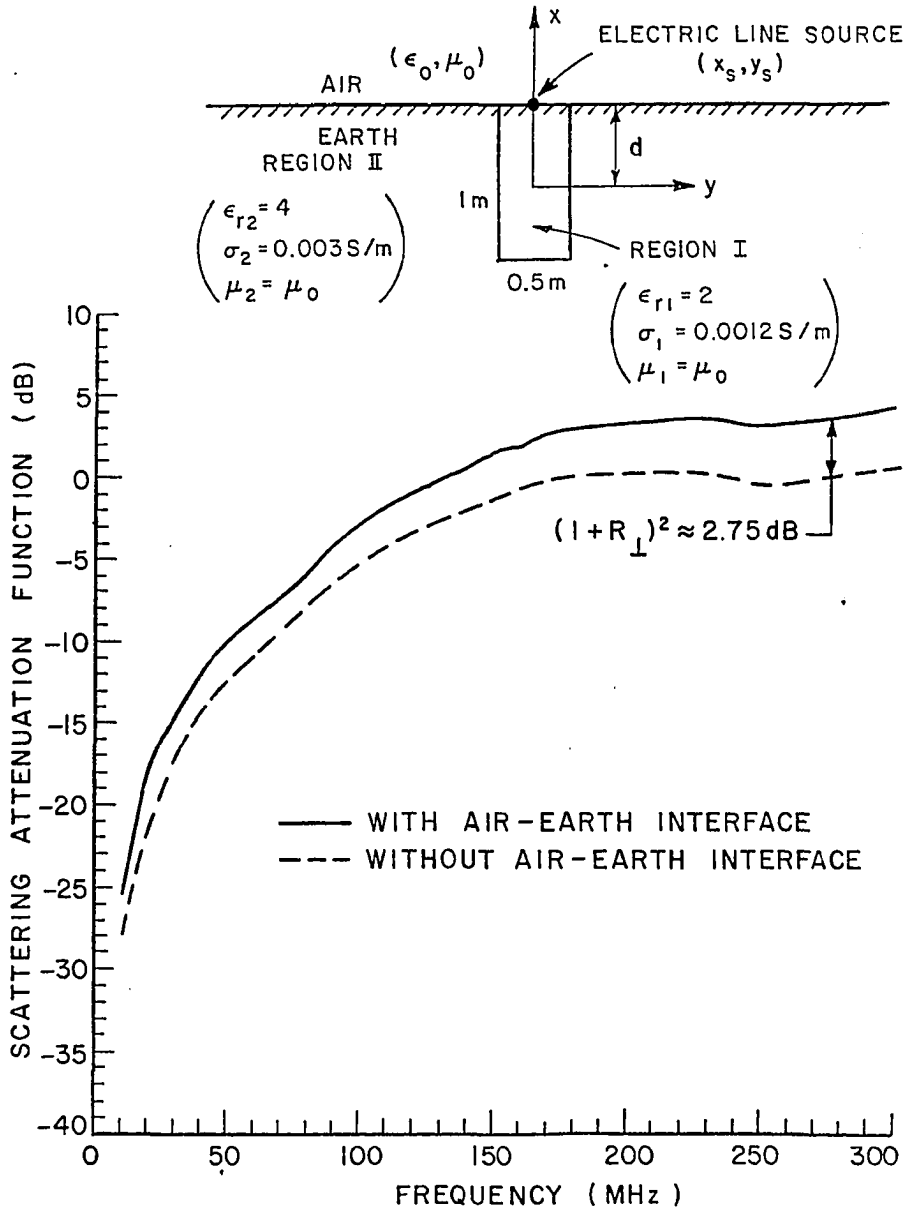

Figure 7-10. The backscattering versus frequency curve for a trench geometry, with and without the air-earth interface. An electric line source is placed at $(x_S, y_S)=(d,0)$.

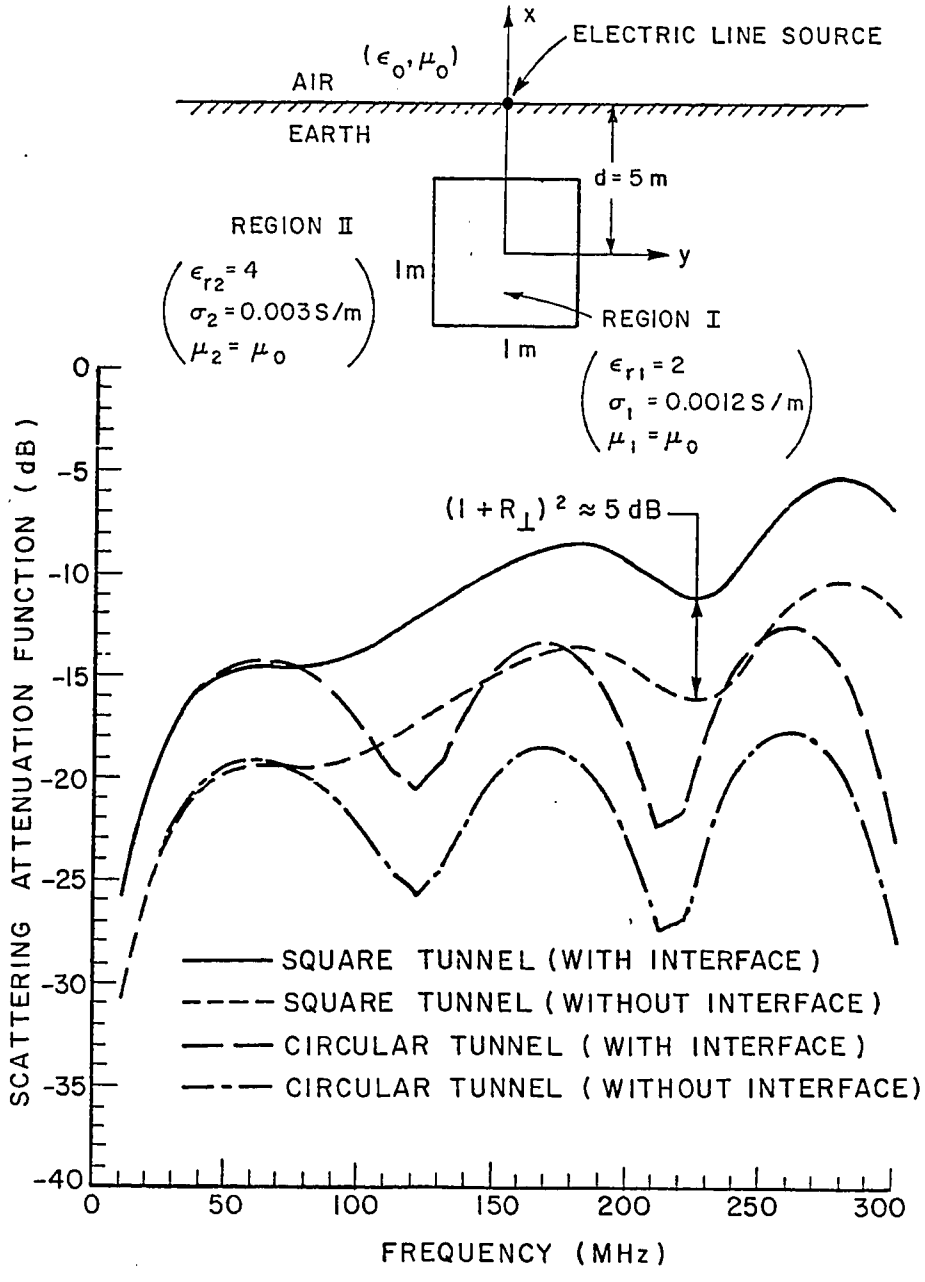

Figure 7-11. Backscattering versus frequency curves for a square tunnel with and without the air-earth interface and for an equivalent cross-section area circular cylinder tunnel, with and without the interface. The electric line source is placed at $(x_s, y_s)=(d,0)$.

diverge. These curves are a good test for the solution of moment method at low frequencies.

F. SUMMARY

In this chapter, the E-wave scattering by buried lossy dielectric rectangular cylinders was considered. Moment method formulations were presented and a convergence curve was included which showed excellent convergence. Some numerical results were also presented and discussed. It is again noted that the presence of the interface can be accounted for in a simple way and yet reasonably accurate results can be obtained. In the next chapter H-wave scattering by buried lossy dielectric rectangular cylinders is presented.

CHAPTER VIII

H-WAVE SCATTERING BY LOSSY DIELECTRIC RECTANGULAR CYLINDERS OF INFINITE LENGTH

A. INTRODUCTION

The electromagnetic scattering model developed in Chapter VI is specialized to a rectangular scatterer. Again a plane wave expansion is used in the moment method formulation as a set of basis functions. A convergence test similar to that used in Chapters VI and VII is applied and which gives comparable results for the moment method. Some numerical results are presented and discussed. The results can be explained in a manner similar to the interpretations of Chapter VII. The major difference is that the $(1+R_{\perp})^2$ factor is replaced by $(1+R_{\parallel})^2$ factor.

The H-wave electromagnetic scattering model is the same as that for E-wave as shown in Figure 7-1, except that the electric line source is replaced by a uniform time harmonic magnetic line source. Using this model, the moment method formulations are derived.

B. PLANE WAVE EXPANSION

The system of linear equation

$$(V_m + \Delta V_m) = \sum_{n=1}^{N} C_n (Z_{mn} + \Delta Z_{mn}) \qquad (8.1)$$

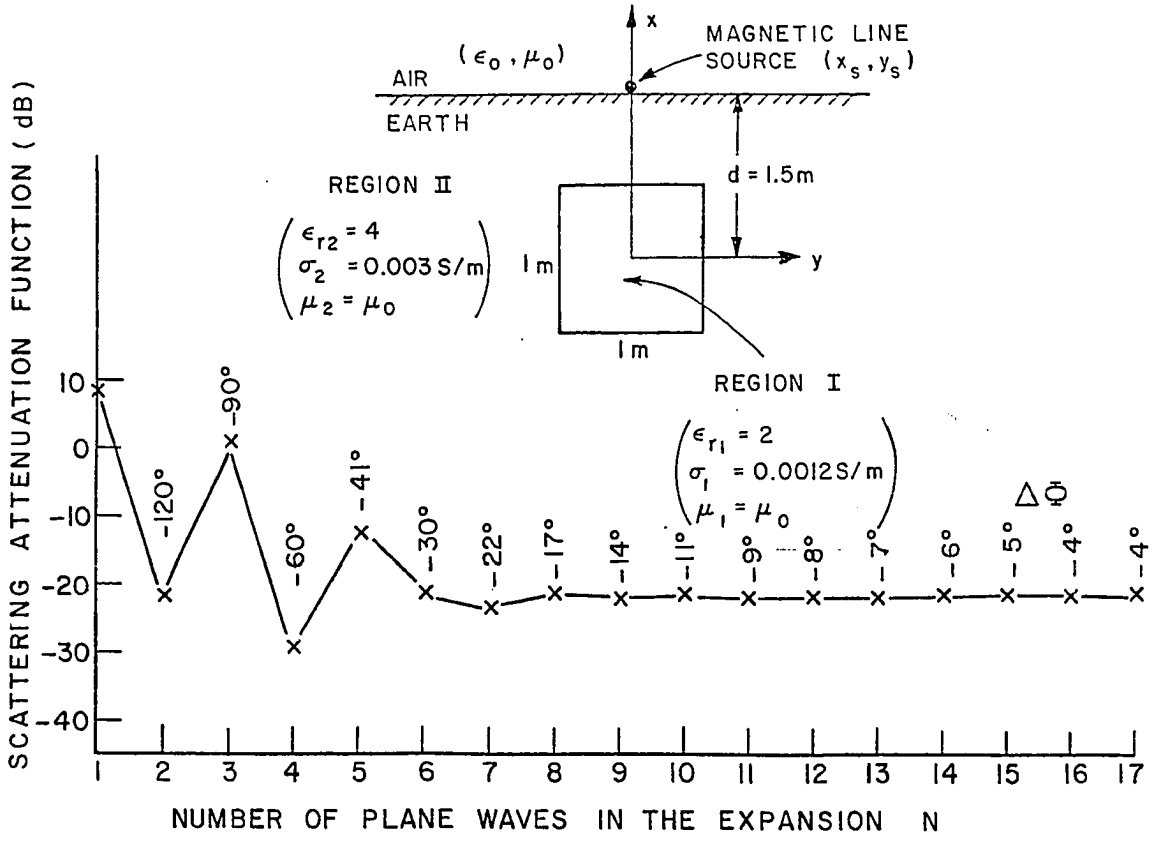

Figure 8-1. The convergence curve for computer program RTUNLH for a buried tunnel. Scattering Attenuation Function is calculated for increasing values of N, the number of plane waves in the expansion. The frequency used is 100 MHz.

was obtained by applying moment method to Integral Equation (6.23), where V_m and Z_{mn} are given by Equations (4.9) and (4.5) respectively, and ΔV_m and ΔZ_m are given by Equations (6.24c) and (6.26) respectively.

Using Equation (3.1) in Equation (6.24c) yields

$$\Delta V_m = -\frac{jk_1}{2\pi}\int_{-a}^{a}\int_{-b}^{b} e^{-jf_m x}\, e^{-jg_m y}\left[\int_0^\infty \frac{gR_\parallel\, e^{-f(2d-x-x_s)}}{f}\sin[g(y-y_s)]\,dg\,\sin\phi_m - \int_0^\infty \frac{fR_\parallel\, e^{-f(2d-x-x_s)}}{f}\cos[g(y-y_s)]\,dg\,\cos\phi_m\right]dxdy\,, \tag{8.2}$$

where Equation (3.2b) and (3.2c) has been used.

Substituting Equation (3.1) in Equation (6.26) yields

$$\Delta Z_{mn} = \frac{jk_1\,\eta_1(\hat{\varepsilon}_1-\hat{\varepsilon}_2)}{2\pi\hat{\varepsilon}_2}\int_{-a}^{a}\int_{-b}^{b}\int_{-a}^{a}\int_{-b}^{b} e^{-jf_n x'}\, e^{-jg_n y'}\, e^{-f_m x}\, e^{-jg_m y}\Bigg\{\sin\phi_m\sin\phi_n\int_0^\infty \frac{g^2R_\parallel\, e^{-f(2d-x-x')}}{f}\cos[g(y-y')]\,dg + (\sin\phi_m\cos\phi_n + \cos\phi_m\sin\phi_n)\int_0^\infty \frac{fgR_\parallel\, e^{-f(2d-x-x')}}{f}\sin[g(y-y')]\,dg - \cos\phi_m\cos\phi_n\int_0^\infty \frac{f^2R_\parallel e^{-f(2d-x-x')}}{f}\cos[g(y-y')]\,dg\Bigg\}dx'dy'dxdy, \tag{8.3}$$

where Equations (2.40c), (3.2b), and (3.2c) have been used to simplify the constant term. Interchanging the order of integration and rearranging terms in Equation (8.2) yields

$$\Delta V_m = \frac{-1}{2\pi\eta_1} \int_0^\infty \frac{R_\parallel \, e^{-f(2d-x_s)}}{f} \left\{ \left[\sin\phi_m g \int_{-b}^{b} e^{-jg_m y} \sin[g(y-y_s)]\, dy \right. \right.$$

$$\left. \left. - \cos\phi_m f \int_{-b}^{b} e^{-jg_m y} \cos[g(y-y_s)]\, dy \right] \int_{-a}^{a} e^{-jf_m x} e^{fx}\, dx \right\} dg \quad , \tag{8.4}$$

Or,

$$\Delta V_m = \frac{-1}{\pi\eta_1} \int_0^\infty \frac{R_\parallel \, e^{-f(2d-x_s)}}{f} \left[F_m (\sin\phi_m g \; GO_m^V - \cos\phi_m f \; GE_m^V) \right] dg \; . \tag{8.5}$$

F_m is given by Equation (7.4b). GE_m^V is given by Equation (3.8c) and GO_m^V is given by Equation (4.9b).

In a similar manner, Equation (8.3) is reduced to

$$\Delta Z_{mn} = \frac{(\hat{\epsilon}_1 - \hat{\epsilon}_2)}{2\pi\hat{\epsilon}_2} \int_0^\infty \frac{R_\parallel \, e^{-2df}}{f} \left\{ \left[(\sin\phi_m \sin\phi_n g^2 - \cos\phi_m \cos\phi_n f^2) \right. \right.$$

$$\left. \left. \int_{-b}^{b} \int_{-b}^{b} e^{-jg_n y} e^{-jg_m y} \cos[g(y-y')]\, dy'dy \right.$$

$$+ (\cos\phi_m \sin\phi_n + \sin\phi_m \cos\phi_n)\, fg \int_{-b}^{b}\int_{-b}^{b} e^{-jg_n y'} e^{-jg_m y} \sin[g(y-y')]dy'dy\Bigg]$$

$$\left.\int_{-a}^{a} e^{-jf_n x'} e^{fx'} dx' \int_{-a}^{a} e^{-jf_m x} e^{fx} dx\right\} dg \quad , \tag{8.6}$$

Or,

$$\Delta Z_{mn} = -\frac{4(\hat{\varepsilon}_1-\hat{\varepsilon}_2)}{\pi\hat{\varepsilon}_2} \int_0^\infty \frac{R_\parallel e^{-2df}}{f} \Bigg\{\Big[(\sin\phi_m \sin\phi_n g^2 - \cos\phi_m \cos\phi_n f^2)\, GE_{mn} + (\cos\phi_m \sin\phi_n + \sin\phi_m \cos\phi_n)\, fg\, GO_{mn}\Big] F_n \cdot F_m\Bigg\} dg \quad . \tag{8.7}$$

GE_{mn} is given by Equation (3.10c), GO_{mn} is given by Equation (4.19), and F_n and F_m are given by Equation (7.4b). In order to make ΔV_m and ΔZ_{mn} compatible with V_m and Z_{mn} derived in Chapter IV, ΔV_m and ΔZ_{mn} have been normalized to $-jk_1\eta_1$.

After solving Equation (8.1) for C_n's, the scattered field may be obtained by Equation (6.28) as

$$H_z^{sr}(x,y) = \frac{(\hat{\varepsilon}_1-\hat{\varepsilon}_2)}{2\pi\hat{\varepsilon}_1} \sum_{m=1}^{N} C_m \int_{-a}^{a}\int_{-b}^{b} \Bigg[\frac{\partial F_m(x',y')}{\partial y'} \int_0^\infty \frac{gR_\parallel e^{-f(2d-x-x')} \sin[g(y-y')]\, dg}{f} - \frac{\partial F_m(x',y')}{\partial x'} \int_0^\infty \frac{fR_\parallel e^{-f(2d-x-x')} \cos[g(y-y')]}{f} dg\Bigg] dx'dy' \quad . \tag{8.8}$$

Substituting for $F_m(x,y)$ from Equation (3.1), and simplifying, the scattered field is reduced to

$$H_z^{sr}(x,y) = \frac{-j\omega(\hat{\varepsilon}_1-\hat{\varepsilon}_2)\eta_1}{2\pi} \sum_{m=1}^{N} C_m \int_{-a}^{a}\int_{-b}^{b}$$

$$\left[e^{-jf_m x'} e^{-jg_m y'} \left(\sin\phi_m \int_0^\infty \frac{gR_\parallel e^{-f(2d-x-x')}\sin[g(y-y')]}{f}dy \right.\right.$$

$$\left.\left. - \cos\phi_m \int_0^\infty \frac{fR_\parallel e^{-f(2d-x-x')}\cos[g(y-y')]}{f}dg \right)\right] dx'dy' \quad . \tag{8.9}$$

Interchanging the order of integration and rearranging the terms and evaluating the cross-sectional integrals yields

$$H_z^{sr}(x,y) = \frac{-j\omega(\hat{\varepsilon}_1-\hat{\varepsilon}_2)\eta_1}{\pi} \sum_{m=1}^{N} C_m \int_0^\infty \frac{R_\parallel e^{-f(2d-x)}}{f}$$

$$\left[F_m\left(\sin\phi_m g\ GO_m^V - \cos\phi_m f\ GE_m^V\right)\right] dg \ ,$$

where F_m is given by Equation (7.4b). GE_m^V and GO_m^V are given by Equations (3.8c) and (4.9b) respectively, with y_s replaced by y.

For backscattered field, some computational time may be saved by using the elements of the voltage column. This may be verified by replacing (x,y) by (x_s,y_s) in Equation (8.9), and comparing the result with Equation (8.4).

$$H_z^{B.sr}(x_s,y_s) = j\omega\eta_1^2 (\hat{\varepsilon}_1-\hat{\varepsilon}_2) \sum_{m=1}^{N} C_m \Delta V_m \quad . \tag{8.11}$$

ΔV_m is given by Equation (8.5).

C. CONVERGENCE

A computer program was developed to model the air-earth interface and a buried scatterer. This program is called RTUNLH and it is included in the Appendix C. To check the convergence characteristic of this program, the program is used to calculated the relative scattering for increasing values of "N" the number of plane waves in the expansion. A typical curve is shown in Figure 8-1.

The scattering model used to obtain this curve is shown at top of Figure 8-1. This model is a 1m square filled cylindrical tunnel with $\varepsilon_{r_1}=2.$, and $\sigma_1=.0012$ s/m buried at d=1.5m in earth with $\varepsilon_{r_2}=4$ and $\sigma_2=.003$ s/m. The interface is the x=1.5m plane and the frequency is 100 MHz. As shown in Figure 8-1, the excitation line source is located at $(x_s,y_s)=(1.5m,0)$. As depicted in Figure 8-1, the solution seems to have converged for N>6. This convergence curve has the same behavior as the convergence curves presented in earlier chapters thus to avoid repetition, it is not discussed further. The $\Delta\Phi$ corresponding to every value of N is calculated from Equation (3.14), and is included in Figure 8-1.

D. SCATTERING PATTERNS

Some examples of bistatic and backscattered patterns are given for a filled trench and some filled tunnel geometries. A family of curves is presented for increasing values of "d", the depth of the center of the tunnel. The trench or tunnel (see Figure 7-1) is modeled by a 1m by .5m rectangular cylinder of infinite length with $\epsilon_{r_1}=2$, $\sigma_2=.0012$ s/m, and $\mu_1=\mu_0$. The earth is modeled by a medium with $\epsilon_{r_2}=4$, $\sigma_2=.003$ s/m, and $\mu_2=\mu_0$. The frequency used is 100 MHz. The electromagnetic scattering model is shown in Figure 8-2. A magnetic line source is placed on the interface parallel to z-axis at (x_s,y_s), and it can be moved in $\pm$y-direction to obtain various excitation cases.

1. Backscattering Patterns

Figure 8-2 shows various backscattering patterns for some trench and tunnel geometries. When d=.5m, a trench geometry is modeled. The backscattering pattern for this trench shows a strong relative backscattered field in regions directly above the trench. The relative scattered field decreases as the $|y|$-offset is increased until $|y|\approx 2.2$m, where an apparent null is obtained, beyond this point the field again increases for the range shown.

For values of d>.5m tunnel geometries are modeled. Some backscattering patterns are included in Figure 8-2 for tunnels buried at d=.75m, 1m, 1.25m, and 1.5m. Patterns for shallowly buried tunnels, i.e., d=.75m, 1.m, have the same general shape as that of the trench, but

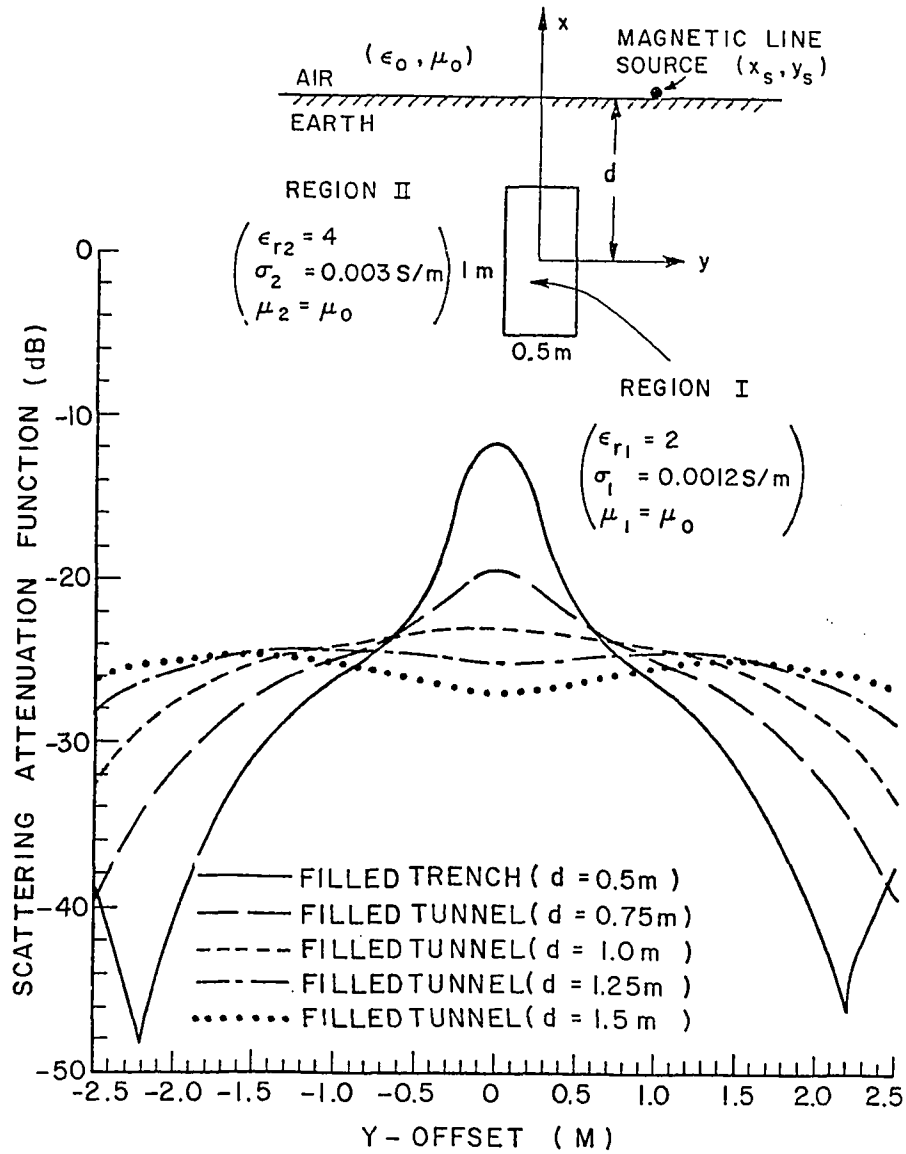

Figure 8-2. The backscattering patterns for trench and tunnel geometries. The magnetic line source is placed on the interface, parallel to z-axis, and moved from y=-2.5m to y=2.5m incrementally. The frequency is 100 MHz.

are widened and reduced in magnitude. As the tunnels are buried deeper, the backscattered field is no longer maximum directly above the tunnel, this case is shown in Figure 8-2 for tunnels buried at d=1.25m, and 1.5m.

To illustrate the effect of the air-earth interface on the backscattering patterns of a trench and a tunnel, Figures 8-3 and 8-4 are presented. Figure 8-3 shows the backscattered pattern for the trench geometry discussed in Figure 8-2. In addition, an analogous backscattered pattern is given for a case where the air-earth geometry is removed (i.e., air region is replaced with region II). This pattern shows the significant effect of air-earth interface on the backscattered fields at various points. However, the approximate model discussed in Chapter VII does not seem to fit as well for this polarization. As suggested by Figure 8-3, the air-earth interface not only changes the backscattering pattern of a trench more dramatically, but it also reduces the magnitude of the backscattered field as would be predicted. However the approximate solution is not as accurate as was the case for the electric line source. An analogous set of curves is shown in Figure 8-4 for a tunnel buried at d=1.5m. For this curve, the approximate model seems to work better than the trench case of Figure 8-3.

2. Bistatic Patterns

As a first example of bistatic scattering pattern, a magnetic line source is placed on the interface at $(x_s,y_s)=(d,0)$ and the scattered field is observed on the interface at y=-2.5m to y=2.5m incrementally. This model is shown in Figure 8-5, where bistatic scattering patterns are

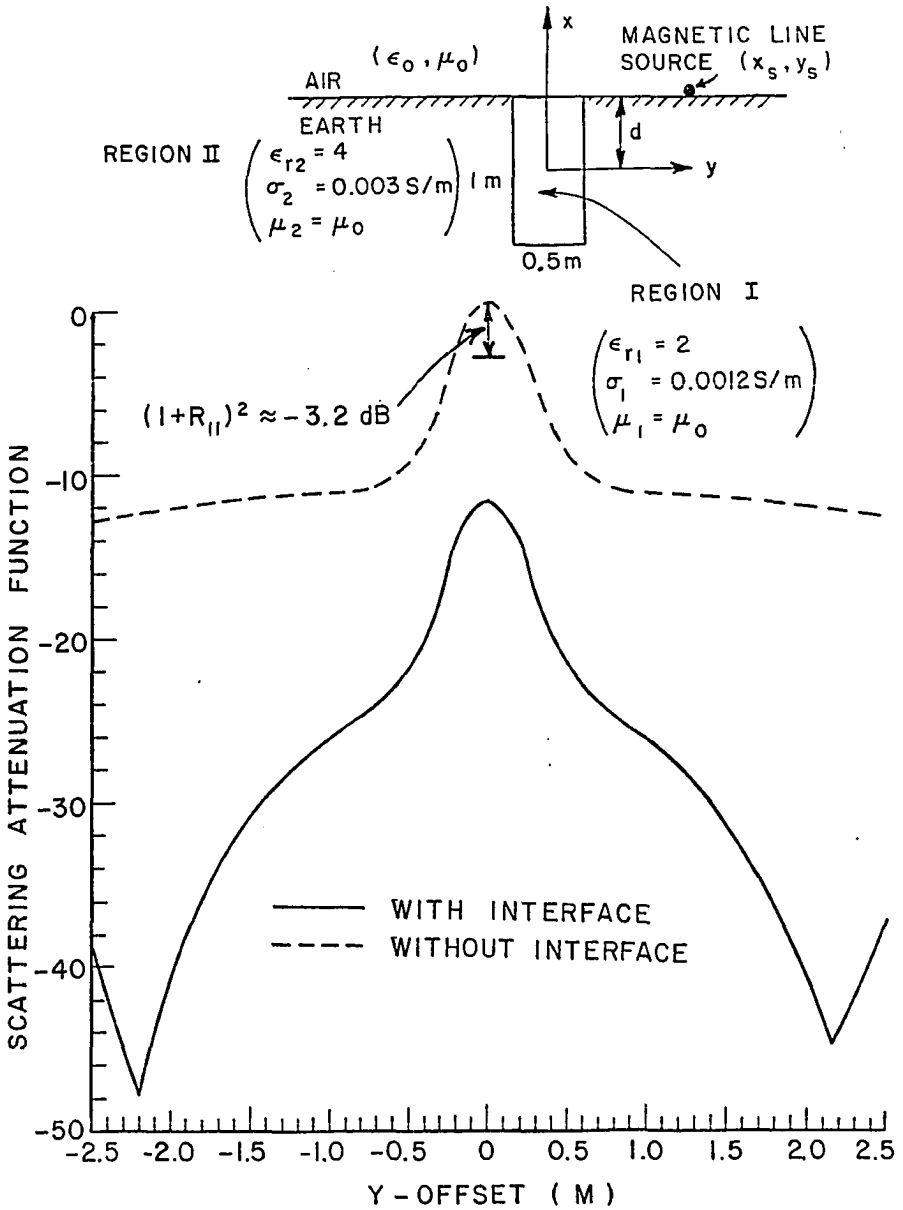

Figure 8-3. Comparison of backscattered field patterns of a trench geometry, with and without the air-earth interface. Frequency is 100 MHz.

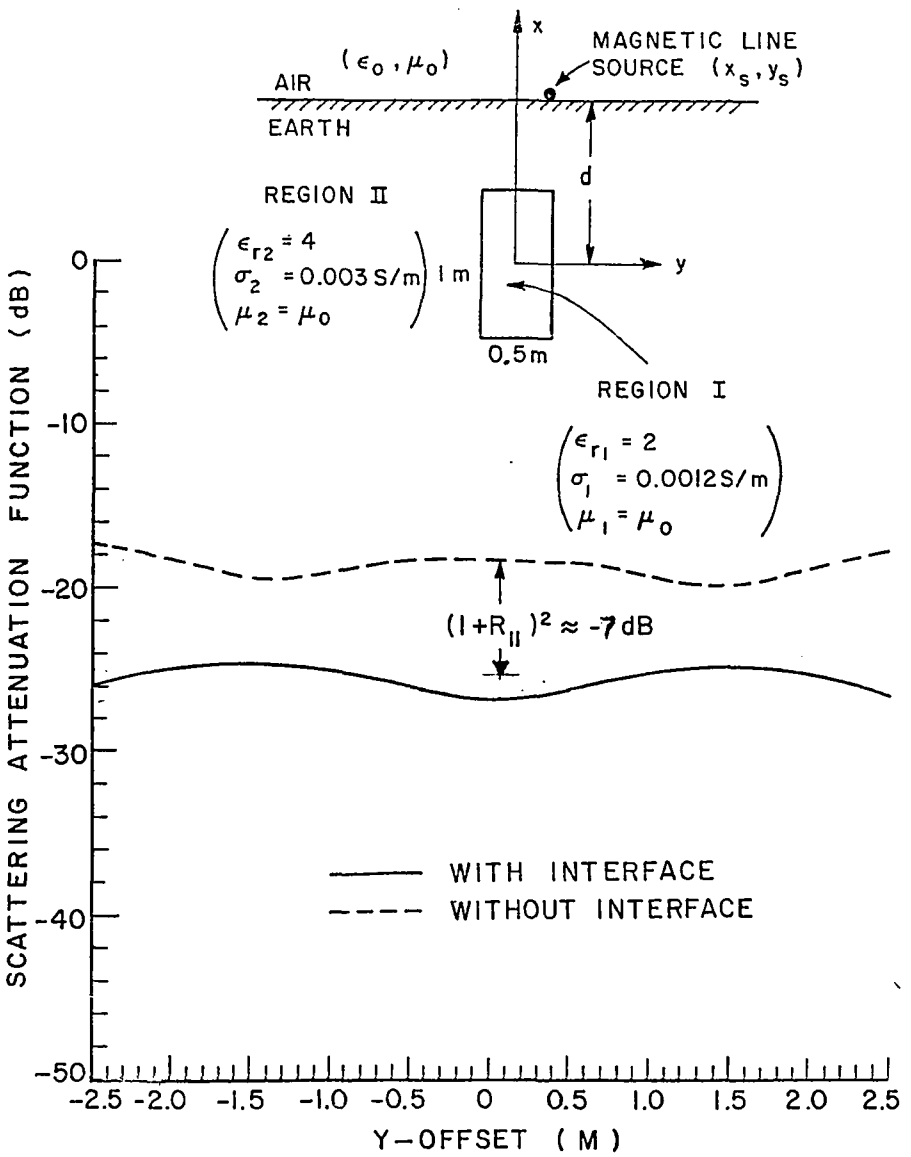

Figure 8-4. Comparison of backscattered field patterns of a tunnel geometry, with and without the air-earth interface. Frequency is 100 MHz.

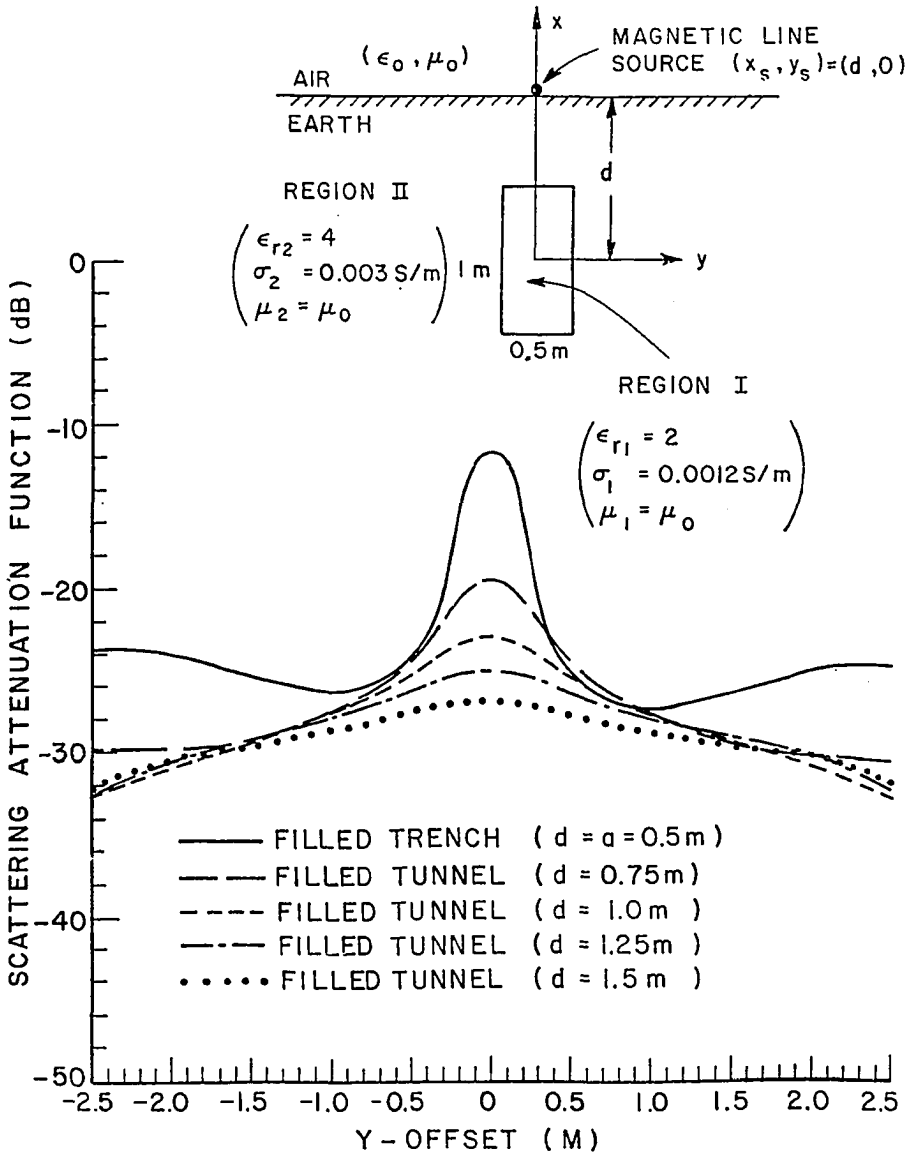

Figure 8-5. Bistatic scattering patterns for some trench and tunnel geometries. A magnetic line source is placed on the interface at $(x_S,y_S)=(d,0)$ parallel to z-axis, and the scattered field is observed at points on the interface along y-axis (from y=-2.5m to y=2.5m). The frequency is 100 MHz.

included for a trench and some tunnels buried at d=.75m, 1m, 1.25m, and 1.5m. For the trench model where d=.5m, a maximum is obtained directly above the trench. The scattered field is reduced for increased |y|-offsets up to |y|≈1, after which it smoothly increases for larger |y|-offsets. For tunnel geometries (d>.5m), the patterns shown in Figure 8-5 depicts maxima directly above the tunnel and smoothly decreasing scattered field for increasing |y|-offsets.

Figure 8-6 shows a comparison between the scattering pattern of a trench geometry and that of an analogous case with the air-earth interface removed (i.e., air region is replaced with region II), and Figure 8-7 shows an analogous sets of patterns for a tunnel geometry buried at d=1.5m.

A second example of bistatic scattering pattern is presented in Figure 8-8, where the scattering model of Figure 8-5 is used with the exception that the excitation line source is moved to $(x_s,y_s)=(d,1.5m)$. The patterns presented in Figure 8-8 are for a filled trench and some tunnels buried at d=.75m, 1m, 1.25m, and 1.5m. It is apparent that as the depth of burial of tunnel (d) is increased, the pattern is reduced and widened, and that the null directly above the tunnel remains very much in place, while the one to the left of tunnel gradually moves further away and becomes shallower.

E. BACKSCATTERING VERSUS FREQUENCY

In this section two sets of frequency curves are presented; one for a trench geometry and the other for a tunnel geometry. In each case an

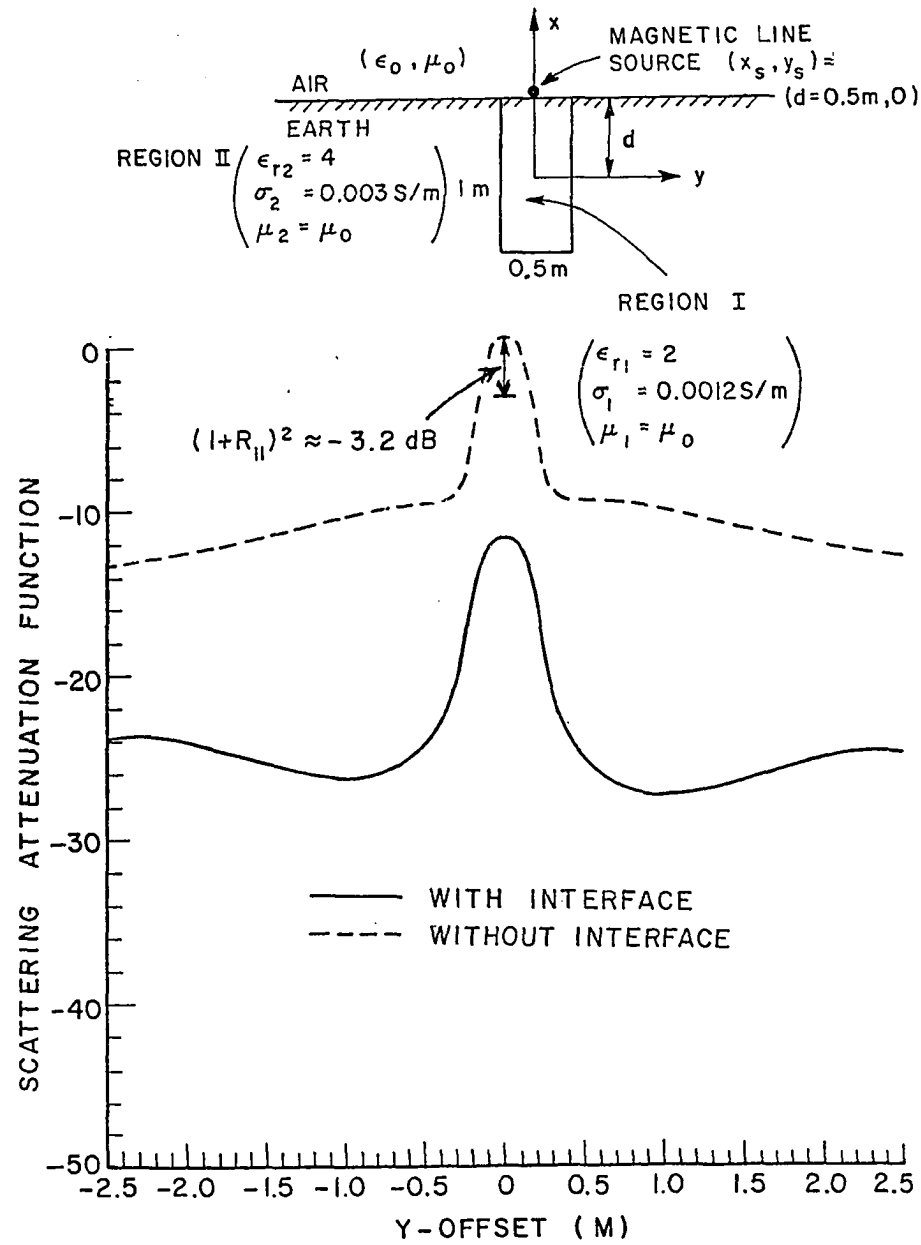

Figure 8-6. Comparison of the bistatic scattering patterns for a trench geometry, with and without the air-earth interface. Frequency is 100 MHz.

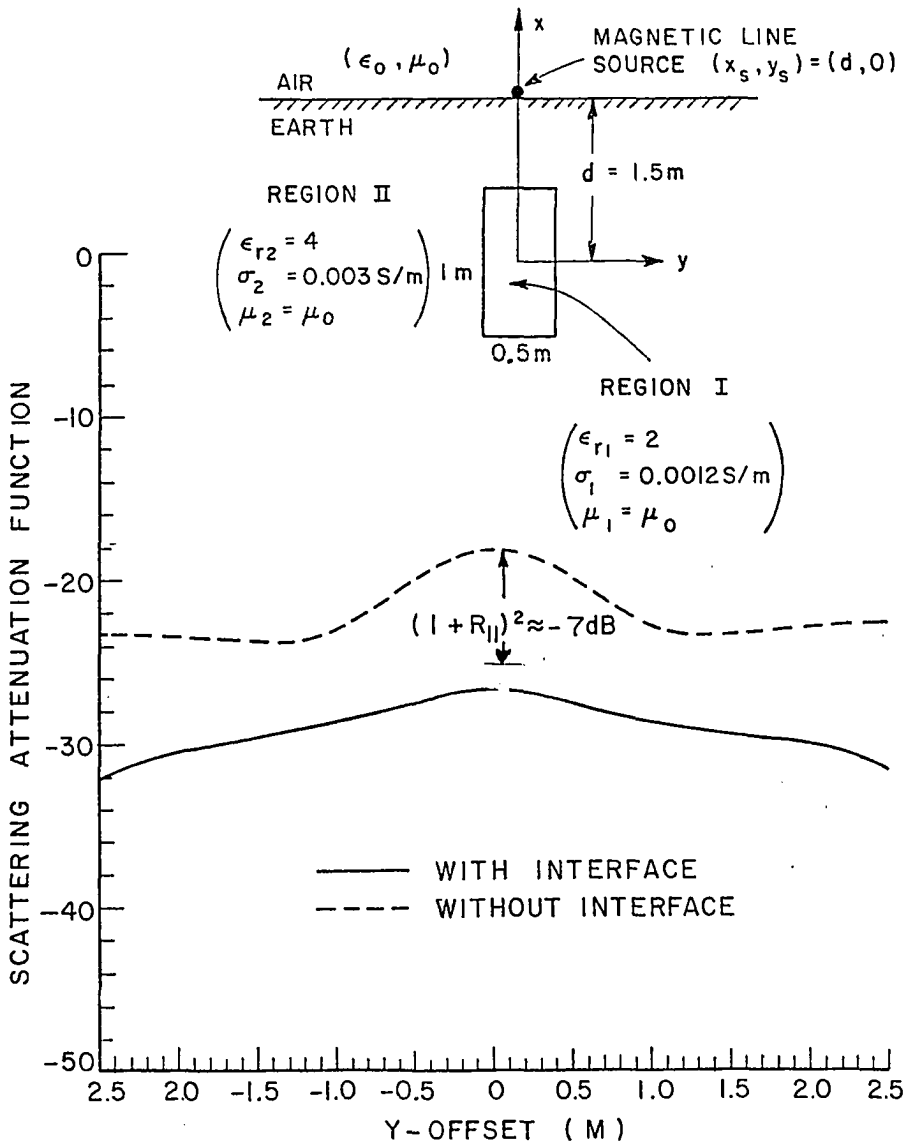

Figure 8-7. Comparison of bistatic scattering patterns for a tunnel geometry, with and without the air-earth interface. Frequency is 100 MHz.

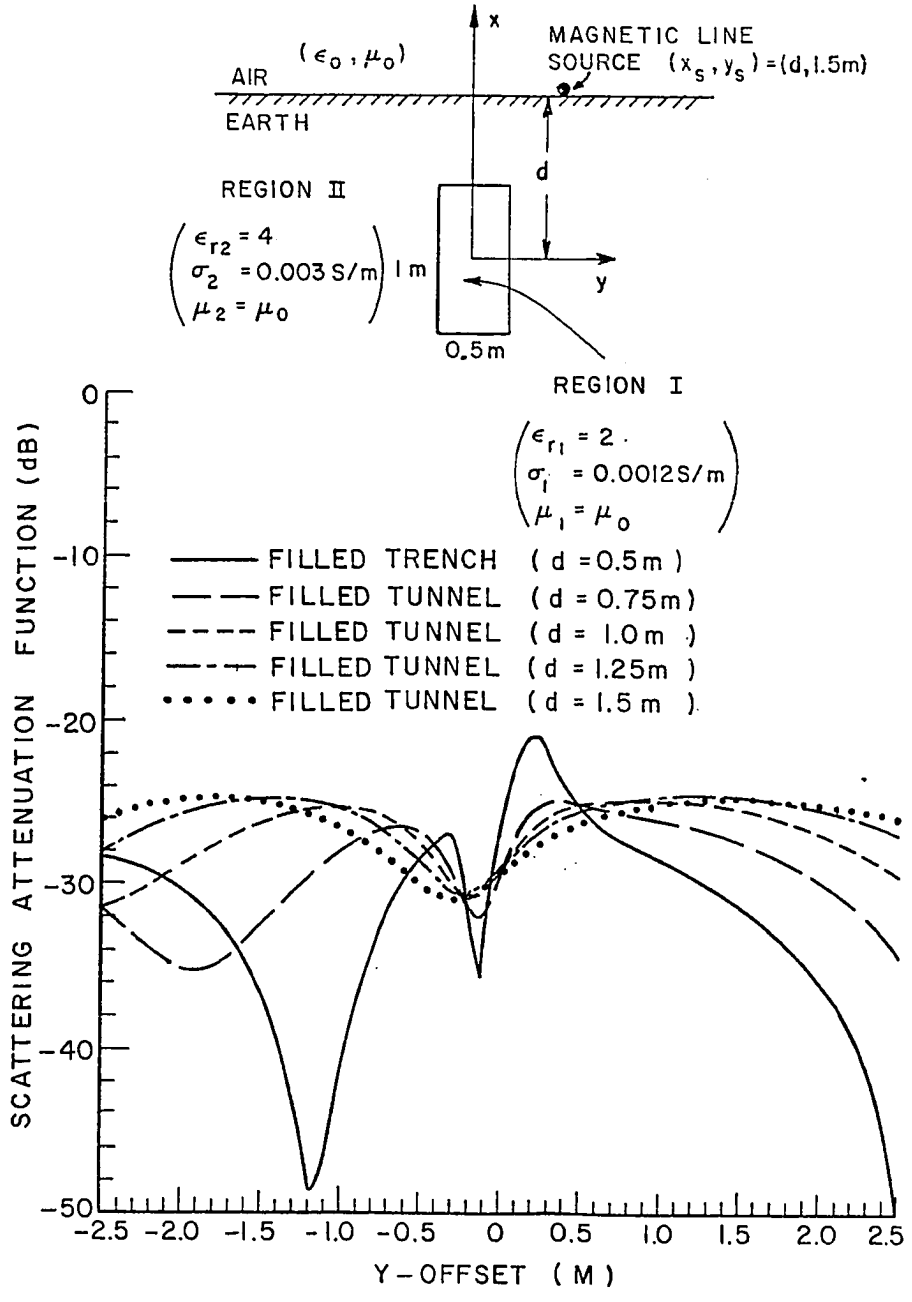

Figure 8-8. Bistatic scattering patterns for some trench and tunnel geometries. A magnetic line source is placed on the interface at $(x_s,y_s)=(d,1.5m)$ parallel to z-axis, and the scattered field is observed at points on the interface along y-axis (from y=-2.5m to y=2.5m). The frequency is 100 MHz.

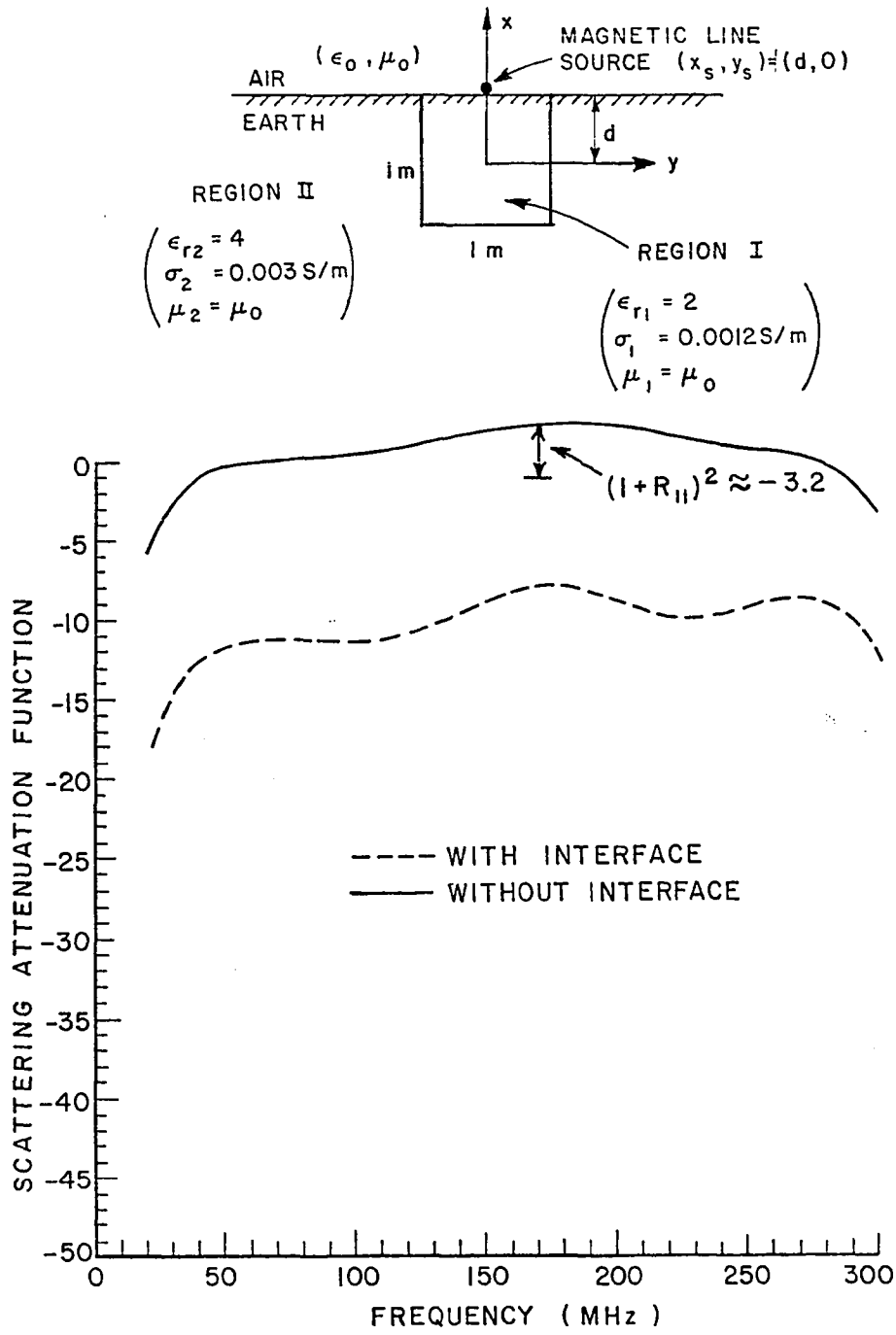

Figure 8-9. The backscattering versus frequency curves for a trench geometry, with and without the air-earth interface. The magnetic line source is placed at $(x_s,y_s)=(d,0)$.

analogous curve for no the interface case is included for comparison. A 1m square trench with $\varepsilon_{r_1}=2$, and $\sigma_1=.0012$ s/m in a earth medium with $\varepsilon_{r_2}=4$ and $\sigma_2=.003$ s/m for a magnetic line source placed on the interface at $(x_s,y_s)=(d,0)$ is shown in Figure 8-9. This geometry represents the electromagnetic scattering model of a filled trench.

The corresponding backscattering curves are shown in Figure 8-9. The dashed curve is the frequency curve for a trench, whereas, the solid curve is the frequency curve for the case where the air-earth interface is removed (i.e., air region is replaced by region II) and the same source geometry is retained. Comparing these two curves, it is apparent that the interface reduces the scattering as would be predicted and this reduction appears to be relatively nonuniform for various frequencies in contrast to the electric line source cases. The shape of the two curves appears to be almost the same for frequency range shown. Figure 8-10 shows a set of curves analogous to Figure 8-9 for a rectangular tunnel geometry. The electromagnetic scattering model is also shown. Comparing the curve for buried rectangular tunnel (dashed line) and the curve for the rectangular tunnel in the absence of air-earth interface (solid line), it is apparent that the two have the same shape for frequency range shown and that the interface effect, seems to be uniform at various frequencies. In fact, it seems like the interface shifted the solid curve by a -7.5 dB approximately. From a simplistic point of view, this factor may be approximated reasonably by a $(1+R_{\parallel})^2$ factor as discussed in Chapter VII, where $R_{\parallel}$ is the plane wave reflection coefficient at the interface. The first $(1+R_{\parallel})$ factor is due to the total incidence field

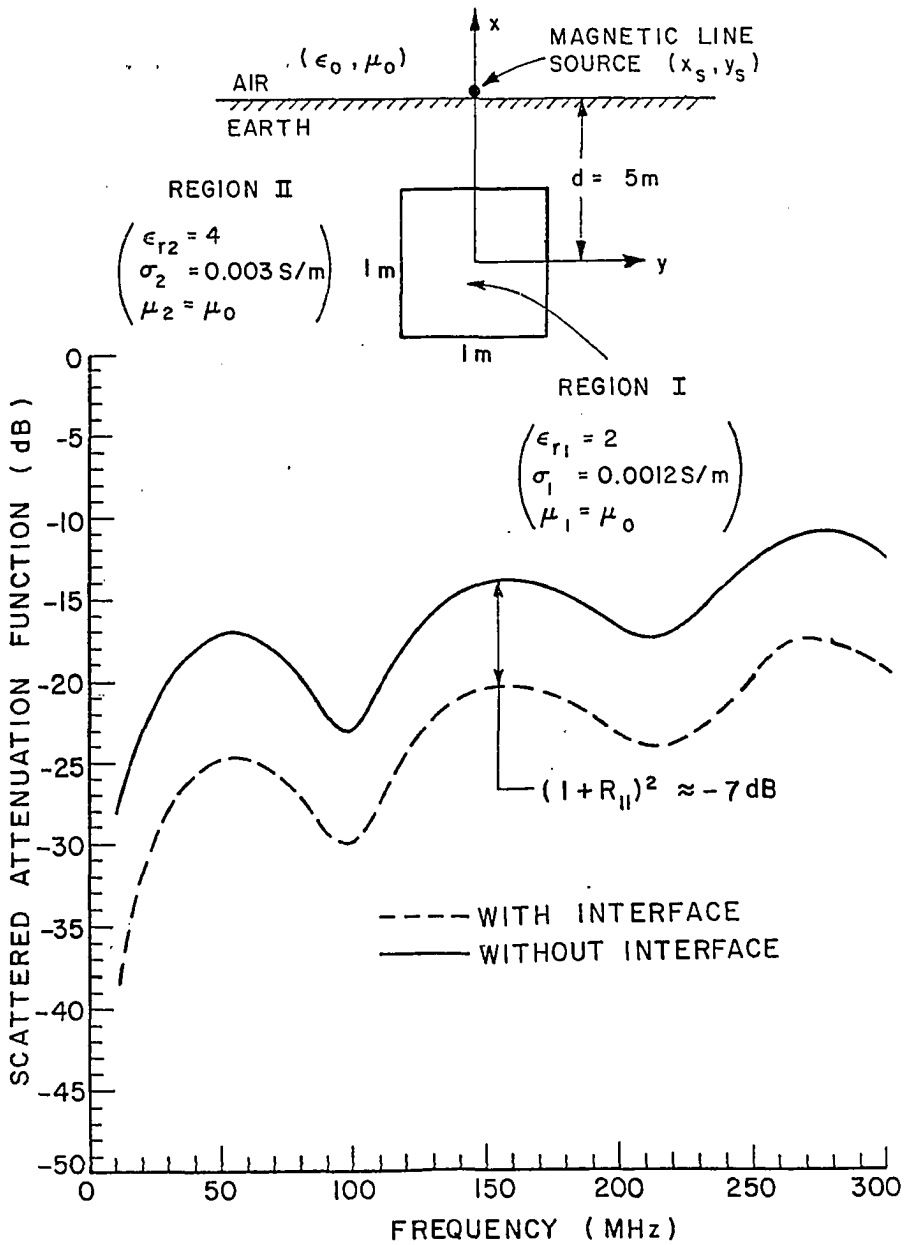

Figure 8-10. Backscattering versus frequency curves for a square tunnel with and without the air-earth interface. The magnetic line source is placed at $(x_S, y_S)=(d,0)$.

on the scatterer, and a second $(1+R_{\parallel})$ factor is due to the scattered field, due to the induced currents in the scatterer. For the model shown in Figure 8-10, $R_{\parallel} \approx -\frac{1}{3}$ (neglecting the effect of loss as suggested by curves of Figure 8-10) and $(1+R_{\parallel})^2 = (1 - \frac{1}{3})^2$ which implies approximately a -7 dB shift of the solid curve to obtain the dashed curve in Figure 8-10. This approach fails for the target at the surface. This simplistic approximation is sufficiently accurate for the case under consideration, thus the costly evaluation of the Sommerfeld integrals may not be necessary in this case. It is hypothesized that the approximate model gives better results as the scatterer is buried deeper.

F. SUMMARY

In this chapter, a moment method formulation for H-wave scattering by buried lossy dielectric rectangular cylinders was given. A convergence curve was presented, and various numerical results were included and discussed.

CHAPTER IX

CPU-TIME CONSIDERATIONS

One advantage offered by using the plane wave expansion is that the number of linear equations required to solve a given problem is considerably less than the number of linear equations required to solve the same problem via a pulse basis method. This is very critical in terms of the CPU-time required to solve a set of simultaneous linear equations, usually, a matrix inversion or a gauss elimination routine is required to solve such a system. Thus, the efficiency of the operation is highly dependent on the efficiency of the matrix inversion routine. For this reason, it is convenient to choose a matrix reduction technique such as triangulation or gauss's elimination. This usually requires a $\frac{1}{3}$ N^3 operations (one operation usually consists of an addition and a multiplication) to triangulate the matrix where N is the number of linearly independent equations to be solved, and $\frac{1}{2}$ N^2 operations are required to solve the matrix. It is possible to use a compact scheme for gaussian elimination [48] such as Crout's method to solve the system of the N linearly independent equations. The CPU-time required for solving N simultaneous linear equations by Crout's method is proportional to N^2. A subroutine implementing the Crout's method is included in the appendix (courtesy of Professor Richmond).

It is possible to subdivide a moment method computer program into four major parts in terms of the types of the operations involved, such as:

1) setting up the generalized impedance matrix

2) setting up the generalized voltage column

3) solving the matrix

4) calculating the final results, i.e., SAF or echowidth ... .

Parts 2 and 4 are not very critical in terms of the amount of the required CPU-time, whereas, parts 1 and 3 usually represent the time consuming operations.

Depending on how a moment method solution is formulated and the type of expansion and testing used, the four operational catagories are weighted differently in terms of the required CPU-time. For example: RCYLPWE program presented in Appendix A uses four fold symmetry and standing plane wave expansion and Galerkin testing, while, RTUNLE computer program presented in Appendix B uses traveling plane wave expansion and Galerkin testing. Thus, the former may require more time to set up the generalized impedance matrix than the latter, but the former is much faster in solving the matrix than the latter. In contrast, a simple pulse basis point matching requires a short set-up time, but it uses much longer time to invert the matrix. In fact, the time required for solving the matrix becomes so great for larger N's, that it becomes economically infeasible for larger geometries.

This is illustrated in Figure 9-1, where a comparison between the Pulse Basis Point Matching (PBPM) and a Plane Wave Expansion Galerkin

(PWEG) is given in form of the CPU-time and the number of required linear equations N as a function of frequency. The CPU-time values are the required time to obtain a convergent solution for the particular scatterer shown. These times are typical of the VAX-11/780 Computer in the ElectroScience Laboratory computing facilities, and may vary considerably on other computers. However, regardless of the computer speed, the relative speed of the PBPM and PWEG methods would be very similar to that of Figure 9-1.

For the PBPM computer program, the CPU-time increases very slowly for frequencies smaller than 80 MHz (see Figure 9-1), in fact, in this region, the PBPM program is faster than the PWEG program. The additional time required by PWEG program in this region is partially due to the time required to set up the generalized impedance matrix. As the frequency is increased beyond 80 MHz, the solution time for PBPM program increases rapidly as more equations are needed to obtain a convergent solution. In contrast to this, a much faster solution is obtained by PWEG program from fewer linear equations. The small rate of increase of the required CPU-time and the fewer needed linear equations makes the PWEG method very attractive for higher frequencies or larger geometries, while at low frequencies PBPM is more suitable. It is hypothesized that for larger values of N, the CPU-time becomes a function of N^2.

The excitation source used in the scattering model of Figure 9-1 is a uniform time harmonic electric line source. An analogous set of curves is given in Figure 9-2 for a magnetic line source excitation. The moment method formulation for this case is more involved and the

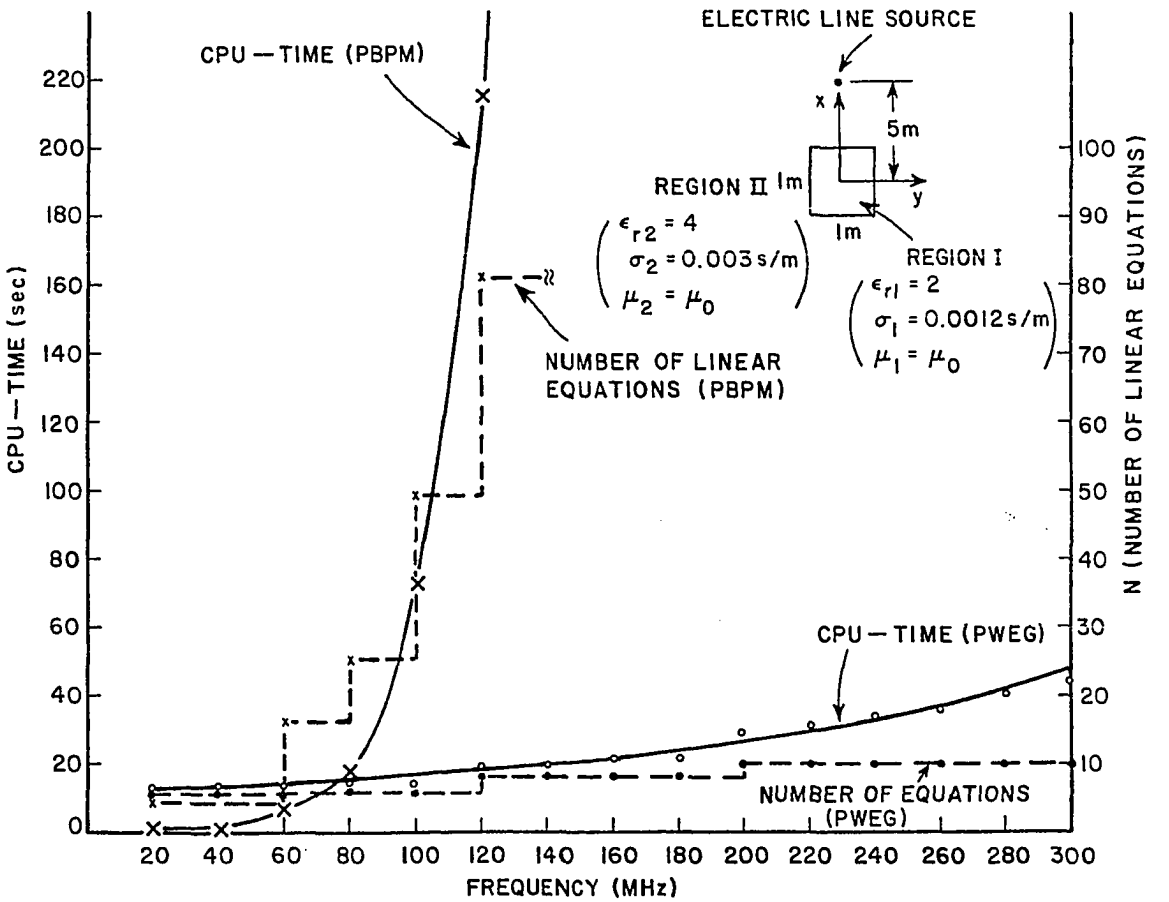

Figure 9-1. Comparison between the Pulse Basis Point Matching (PBPM) and a Plane Wave Expansion Galerkin (PWEG) methods. The CPU-time and the number of linear equations "N" needed to obtain a convergent solution is plotted for various frequencies. The excitation is due to a uniform electric line source and the computer programs used are RECTPPE and RTUNLE for PBPM and PWEG respectively.

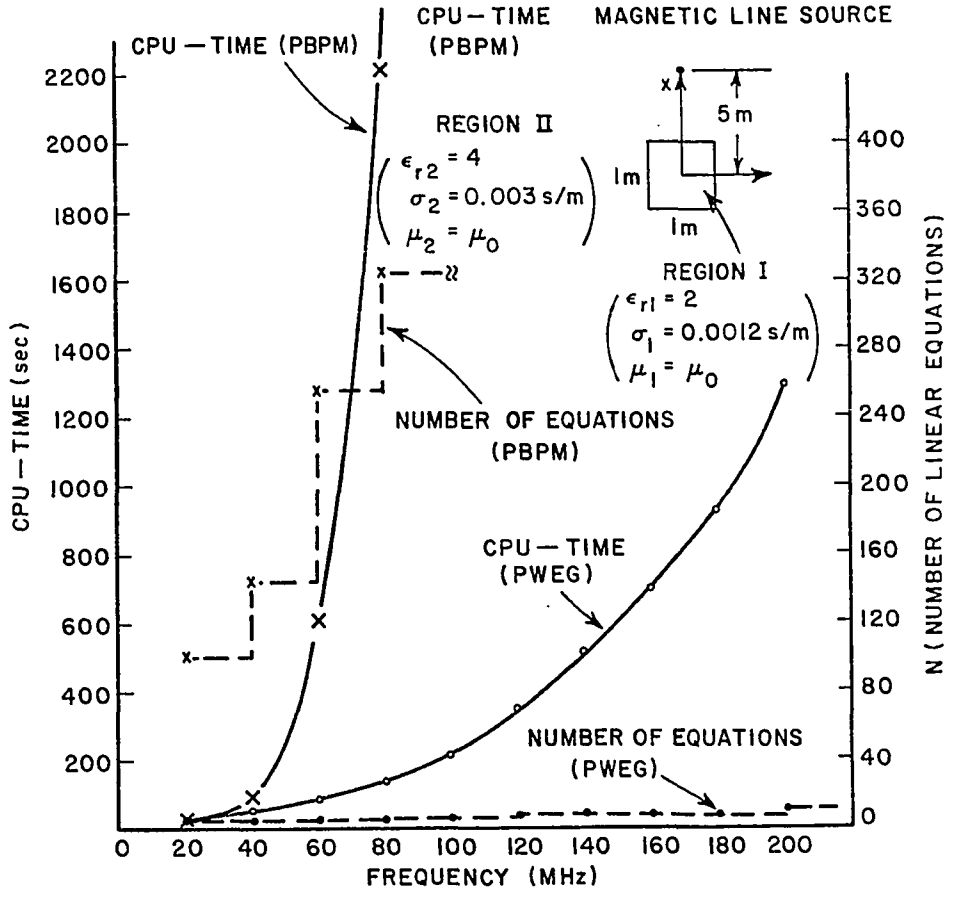

Figure 9-2. Comparison between the Pulse Basis Point Matching (PBPM) and a Plane Wave Expansion Galerkin (PWEG) methods. The CPU-time and the number of linear equations "N" needed to obtain a convergent solution is plotted for various frequencies. The excitation is due to a uniform magnetic line source and the computer programs used are SQCYLH and RTUNLH for PBPM and PWEG respectively.

execution time for the computer programs are longer than the electric line source case. Figure 9-2 basically shows the same relative CPU-time behavior for PBPM and PWEG as that of Figure 9-1, and similar conclusions may be drawn.

The maximum frequency or the size of the scatterer to be modeled by the PWEG technique may be limited by the economic considerations of CPU-execution time. Modern high density core memories in conjuction with added virtual memories may soon eliminate most of the limitations imposed by memory size. The VAX-11/780 computer can accommodate approximately a 1000 by 1000 matrix of complex elements in its addressable memory of about 2 Gbytes [50].

CHAPTER X

CONCLUSIONS

The object of this research has been to obtain an efficient computational model for the study of EM-scattering by buried, penetrable non-circular cylinder of infinite length. This model can be used to model two-dimensional scatterers in either a lossy half space or in a lossy homogeneous medium.

The Plane Wave Expansion Galerkin method presented here offers several advantages over the Pulse Basis Point Matching. It gives a stable convergence for a fewer number of linear equations, it provides reduced integration time for a rectangular based cylinder, where the cross-sectional integrals are evaluated in closed form. Additionally, the various optimizations provided by PWEG, enables modeling of larger scatterers that was not possible previously.

In Chapter III and IV, some numerical results were included for E-wave and H-wave scattering by a rectangular cylinder immersed in a homogeneous ambient medium. The scattering pattern obtained in Chapter III and IV were then used to develop an approximate model to explain much of the details of the structure of the scattering patterns obtained by the more exact solutions obtained by evaluating the Sommerfeld

integrals. In Chapter V the radiation patterns of a line sources placed on the air-interface were obtained. It was illustrated that these patterns may be approximated by $(1+R_{\perp})$ factor for an electric line source and $(1+R_{\parallel})$ factor for a magnetic line source. It is apparent that the simple approximation does not include the lateral type waves. Exclusion of the effect of lateral waves is more drastic for the case of the magnetic line source, because the lateral wave is more significant for this particular polarization because of its association with the Brewster angle [51]. It is also shown that the far field of a magnetic line source in a homogeneous lossless medium is proportional to $\varepsilon_r^{-1/4}$ and far field of a magnetic line source in that medium is proportional to $\varepsilon_r^{3/4}$.

In Chapter VII, E-wave, and in Chapter VIII, H-wave, scattering by buried lossy dielectric rectangular cylinders of infinite length were considered and some scattering patterns were presented. It was illustrated that a simple model may be used to obtain the effect of the air-earth interface. This approximate model suggests that SAF for a buried scatterer may be obtained by multiplying the SAF of scatterer immersed in homogeneous earth medium by $(1+R)^2$, where R is equal to $R_{\perp}$ for an electric line source excitation, and $R_{\parallel}$ for a magnetic line source excitation. The first (1+R) factor is introduced to account for the presence of the interface on the field radiated by the line source. The second (1+R) accounts for the reflection of the scattered fields by the interface. Thus the total of $(1+R)^2$ factor is required to approximate the effect of the interface on the scattered fields. This

approximation seems to work better for the electric line source excitation.

A. SUGGESTIONS

The EM-scattering models presented in this dissertation may by extended so that finite sources may by modeled. This would involve utilizing a Fourier transform and solving the above problem numerous times for various values of the transform argument. This however may be avoided by utilizing the method of Steepest descent for cases where the scatterer is located far enough so that the asymptotic evaluation of the pertinent integrals is possible.

A problem of interest in underground radar is the crossed dipole transmitter-receiver antenna pairs. This enables considerable isolation between the transmitter signal and the received signal. The EM-scattering results of the two different polarizations, the parallel and the perpendicular polarization may be combined to obtain a solution for such an antenna system [52].

Finally, the scattering models should be tested for various material case, i.e., good conductors and poor conductors. This would determine some of the limitations that the method may have.

APPENDICES

APPENDIX A

Computer program RCYLPWE uses Plane Wave Expansion Galerkin with four fold symmetry. The field inside the scatterer is expanded as

$$E^{I}_{(x,y)} = \sum_{n=1}^{N} \left[a_n F_n^{ee}(x,y) + b_n F_n^{oe}(x,y) + c_n F_n^{eo}(x,y) + d_n F_n^{oo}(x,y)\right] , \tag{A.1a}$$

where

$$F_n^{ee}(x,y) = \cos(f_n x)\cos(g_n y) \quad , \tag{A.1b}$$

$$F_n^{oe}(x,y) = \sin(f_n x)\cos(g_n y) \quad , \tag{A.1c}$$

$$F_n^{eo}(x,y) = \cos(f_n x)\sin(g_n y) \quad , \tag{A.1d}$$

and

$$F_n^{oo}(x,y) = \sin(f_n x)\sin(g_n y) \quad . \tag{A.1e}$$

The superscripts correspond to evenness or oddness w.r.t x and y.

From the wave equation it is shown that

$$f_n^2 + g_n^2 = k_1^2 \quad , \tag{A.2a}$$

where

$$f_n = k_1 \cos\phi_n \quad , \tag{A.2b}$$

$$g_n = k_1 \sin\phi_n \quad , \tag{A.2c}$$

$$\phi_n = \frac{(n-1)}{(N-1)} \frac{\pi}{2} \quad , \tag{A.2d}$$

and

$$k_1 = \omega\sqrt{\mu_o \hat{\epsilon}_1} \quad . \tag{A.2e}$$

Following the same derivation procedure as discussed in Chapter II, for the electric line source excitation we obtain an integral equation of the form of Equation (2.7) which can be reduced to four sets of decoupled systems of simultaneous linear equations. These system of equations are:

$$\sum_{n=1}^{N} a_n A_{mn} = V_m^{ee} \qquad m = 1, 2, 3, \ldots, N, \tag{A.3a}$$

$$\sum_{n=1}^{N} b_n B_{mn} = V_m^{oe} \qquad m = 1, 2, 3, \ldots, N, \tag{A.3b}$$

$$\sum_{n=1}^{N} c_n C_{mn} = V_m^{eo} \qquad m = 1, 2, 3, \ldots, N, \tag{A.3c}$$

and

$$\sum_{n=1}^{N} d_n D_{mn} = V_m^{oo} \qquad m = 1, 2, 3, \ldots, N, \tag{A.3d}$$

where $E_z^i(x,y)$ has been expressed as a sum of odd and even symmetrical functions of x and y

$$E_z^i(x,y) = E^{ee}(x,y) + E^{oe}(x,y) + E^{eo}(x,y) + E^{oo}(x,y) \quad , \tag{A.4}$$

for an electric line source excitation it was shown in Chapter II that

$$E_z^i(x,y) = I\, K_o(\gamma_2 \rho_1) \quad , \tag{A.5a}$$

ρ_1 is shown in Figure A-1, and

$$I = \frac{-j\omega\mu_o}{2\pi} \quad . \tag{A.5b}$$

thus from Equations (A.4) and (A.5) one can obtain the following:

$$E^{ee}(x,y) = \frac{I}{4}\left(K_o(\gamma_2\rho_1) + K_o(\gamma_2\rho_2) + K_o(\gamma_2\rho_3) + K_o(\gamma_2\rho_4)\right) , \tag{A.6a}$$

$$E^{oe}(x,y) = \frac{I}{4}\left(K_o(\gamma_2\rho_1) - K_o(\gamma_2\rho_2) - K_o(\gamma_2\rho_3) + K_o(\gamma_2\rho_4)\right) , \tag{A.6b}$$

$$E^{eo}(x,y) = \frac{I}{4}\left(K_o(\gamma_2\rho_1) + K_o(\gamma_2\rho_2) - K_o(\gamma_2\rho_3) - K_o(\gamma_2\rho_4)\right) , \tag{A.6c}$$

$$E^{oo}(x,y) = \frac{I}{4}\left(K_o(\gamma_2\rho_1) - K_o(\gamma_2\rho_2) + K_o(\gamma_2\rho_3) - K_o(\gamma_2\rho_4)\right) . \tag{A.6d}$$

For a uniform line source of unit current excitation placed at (x_1, y_1), Equations (A.4), (A.5), and (A.6) can be achieved by replacing the

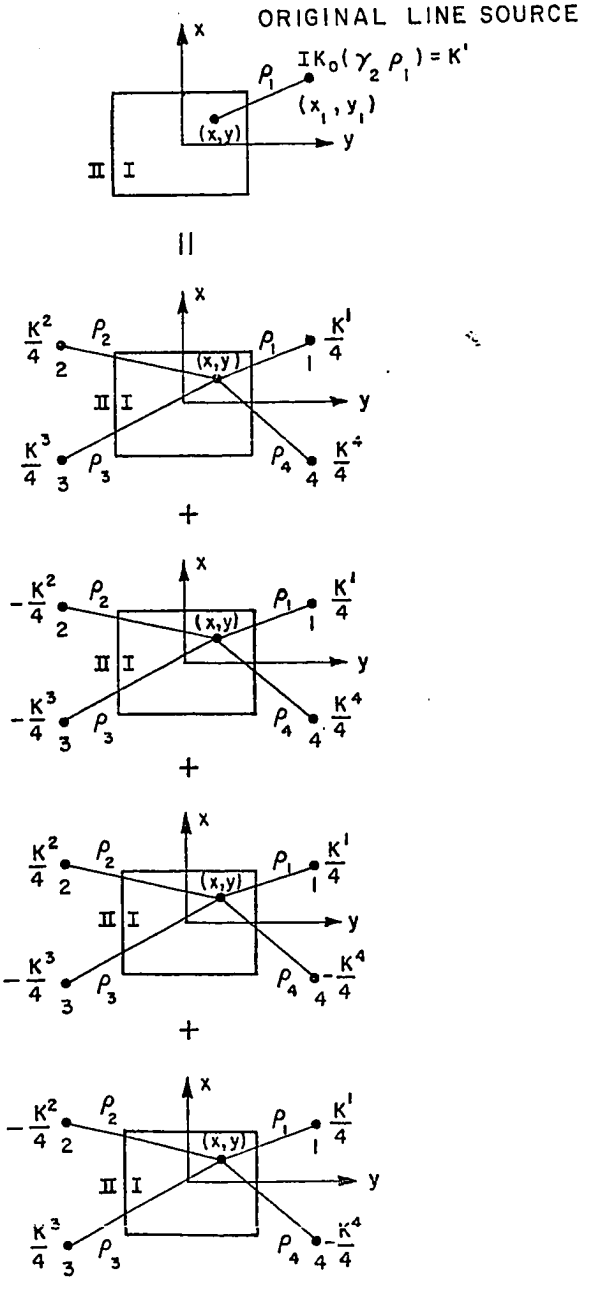

Figure A-1. Pictorial illustration of four fold symmetry where a line source is replaced by four line sources with desired symmetry.

this line source with four line sources of $\frac{1}{4}$ current strength at (x_1,y_1), (x_2,y_2), (x_3,y_3), and (x_4,y_4) respectively as illustrated in Figure A-1. The polarity of the currents is chosen so that the desired symmetries w.r.t x and y are obtained. This is illustrated pictorially in Figure A-1. To simplify this figure the points (x_1,y_1), (x_2,y_2), (x_3,y_3), and (x_4,y_4) are only designated by 1, 2, 3, and 4. Also the line source excitations are simplified as

$$I\ K_0(\gamma_2\rho_i) = K^i \qquad i = 1, 2, 3, 4.$$

The V_m's of the Equations (A.3) involve a cross-sectional integration which can be evaluated easily, because there is no singularity involved. These are given by

$$V_m^{ee} = \iint_{cs} F_m^{ee}(x,y)\ E^{ee}(x,y)\ ds \quad , \tag{A.7a}$$

$$V_m^{oe} = \iint_{cs} F_m^{oe}(x,y)\ E^{oe}(x,y)\ ds \quad , \tag{A.7b}$$

$$V_m^{eo} = \iint_{cs} F_m^{eo}(x,y)\ E^{oe}(x,y)\ ds \quad , \tag{A.7c}$$

$$V_m^{oo} = \iint_{cs} F_m^{oo}(x,y)\ E^{oo}(x,y)\ ds \quad , \tag{A.7d}$$

where F_m's are defined in Equation (A.1), and E's are defined in Equation (A.6).

The A_{mn}, B_{mn}, C_{mn}, and D_{mn} are given by

$$A_{mn} = \iint_{cs} F_m^{ee}(x,y)\, F_n^{ee}(x,y)\, ds + Q \iint_{cscs} F_m^{ee}(x,y)\, F_n^{ee}(x',y')\, K_o(\gamma_2\rho)\, ds'ds \,, \tag{A.8a}$$

$$B_{mn} = \iint_{cs} F_m^{oe}(x,y)\, F_n^{oe}(x,y)\, ds + Q \iint_{cscs} F_m^{oe}(x,y)\, F_n^{oe}(x',y')\, K_o(\gamma_2\rho)\, ds'ds \,, \tag{A.8b}$$

$$C_{mn} = \iint_{cs} F_m^{eo}(x,y)\, F_n^{eo}(x,y)\, ds + Q \iint_{cscs} F_m^{eo}(x,y)\, F_n^{eo}(x',y')\, K_o(\gamma_2\rho)\, ds'ds \,, \tag{A.8c}$$

$$D_{mn} = \iint_{cs} F_m^{oo}(x,y)\, F_n^{oo}(x,y)\, ds + Q \iint_{cscs} F_m^{oo}(x,y)\, F_n^{oo}(x',y')\, K_o(\gamma_2\rho)\, ds'ds \,, \tag{A.8d}$$

where

$$Q = \frac{\omega^2 \mu_o (\hat{\varepsilon}_1 - \hat{\varepsilon}_2)}{2\pi} \,. \tag{A.8e}$$

and

$$\rho = \sqrt{(x-x')^2 + (y-y')^2} \,.$$

in the Equations (A.8a)-(A.8d), the integrals of the first terms are evaluated in a closed form with no difficulty, but, the integrals of the second terms are difficult to evaluate because of the singularity point at which $\rho=0$. A method that has been introduced by Richmond [2] for the point matching is applied here to evaluate these integrals. The method involves dividing the cross-section over which the integration is to be carried out into many square cells, and approximating the integration

over the cross-section by a sum of the integration over the cross-section of each cell. A further approximation can be made if the sizes of the cells are chosen small enough so that F_n's of Equation (A.1) can be assumed to vary very slowly over the cross-section of a cell. These approximations reduce the integrations of the second terms of the equation (A.8a)-(A.8d)

$$\iint_{cscs} F_m(x,y)\, F_n(x',y')\, K_o(\gamma_2\rho)\, ds'ds$$

$$\approx \sum_{i=1}^{NC} \sum_{j=1}^{NC} F_m(x_i,y_i)\, F_n(x_j,y_j) \iint_{cell_i} \iint_{cell_j} K_o(\gamma_2 r_{ij})\, ds_i ds_j \quad . \tag{A.9}$$

Approximate superscripts for F_m and F_n may be used as if applies to each Equation (A.8), and NC is the number of cell in the cross-section.

Referring to Figure A-2, r_{ij} is defined as

$$r_{ij} = \sqrt{(x_i-x_j)^2 + (y_i-y_j)^2} \quad , \tag{A.10}$$

where (x_i,y_i) defines a point in cell i and (x_j,y_j) defines a point in cell j. The square cells may be replaced by a circular cell which has the same cross-section area and is centered at the center of the corresponding cell [2]. Without including the details the final form is given as follows

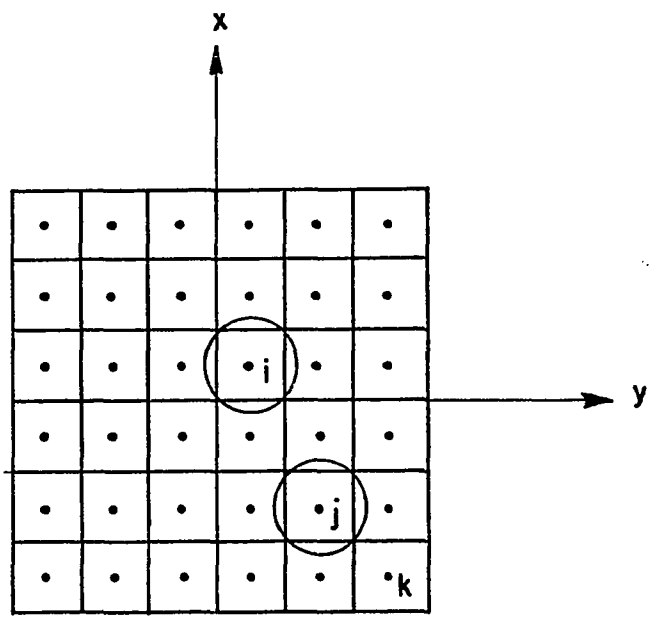

Figure A-2. Pictorial illustration for evaluating the cross sectional integrals.

$$\int_{cell_i}\int_{cell_j} K_o(\gamma_2 r_{ij})\, ds_i ds_j = \begin{cases} \frac{(2\pi)^2 C}{\gamma_2^3}\left(1 - \gamma_2 C K_1(\gamma_2 C) I_1(\gamma_2 C)\right) ; & i=j \\ \left[\frac{2\pi C}{\gamma_2} I_1(\gamma_2 C)\right]^2 K_o(\gamma_2 R_{ij}) ; & i \neq j \end{cases} \quad \text{(A.11a)}$$

C is the radius of the equivalent area circular cylinder and

$$R_{ij} = \sqrt{(X_i - X_j)^2 + (Y_i - Y_j)^2} \quad , \quad \text{(A.11b)}$$

where

(X_i, Y_i) and (X_j, Y_j) are the centers of $cell_i$ and $cell_j$ respectively. I_1 is the modified Bessel function of the first kind of order one, K_1 and K_o are the modified Bessel functions of the second kind and orders one and zero respectively.

RCYLPWE program is set up so that various outputs may be obtained selectively. It can be set so that to give single outputs or an array of numbers. Three major loops to be discussed are shown in Figure A-3. These are: frequency loop, backscattering loop, and bistatic scattering loop. The statement number of the start of the loop is also included in Figure A-3 for easy reference to the program listing in subsequent pages.

To obtain a frequency plot from 10 to 300 MHz. FMCMX is set equal to 300, and IFMC is set to desired number of points to be calculated. To obtain a backscattered patterns IBS is set equal to the number of

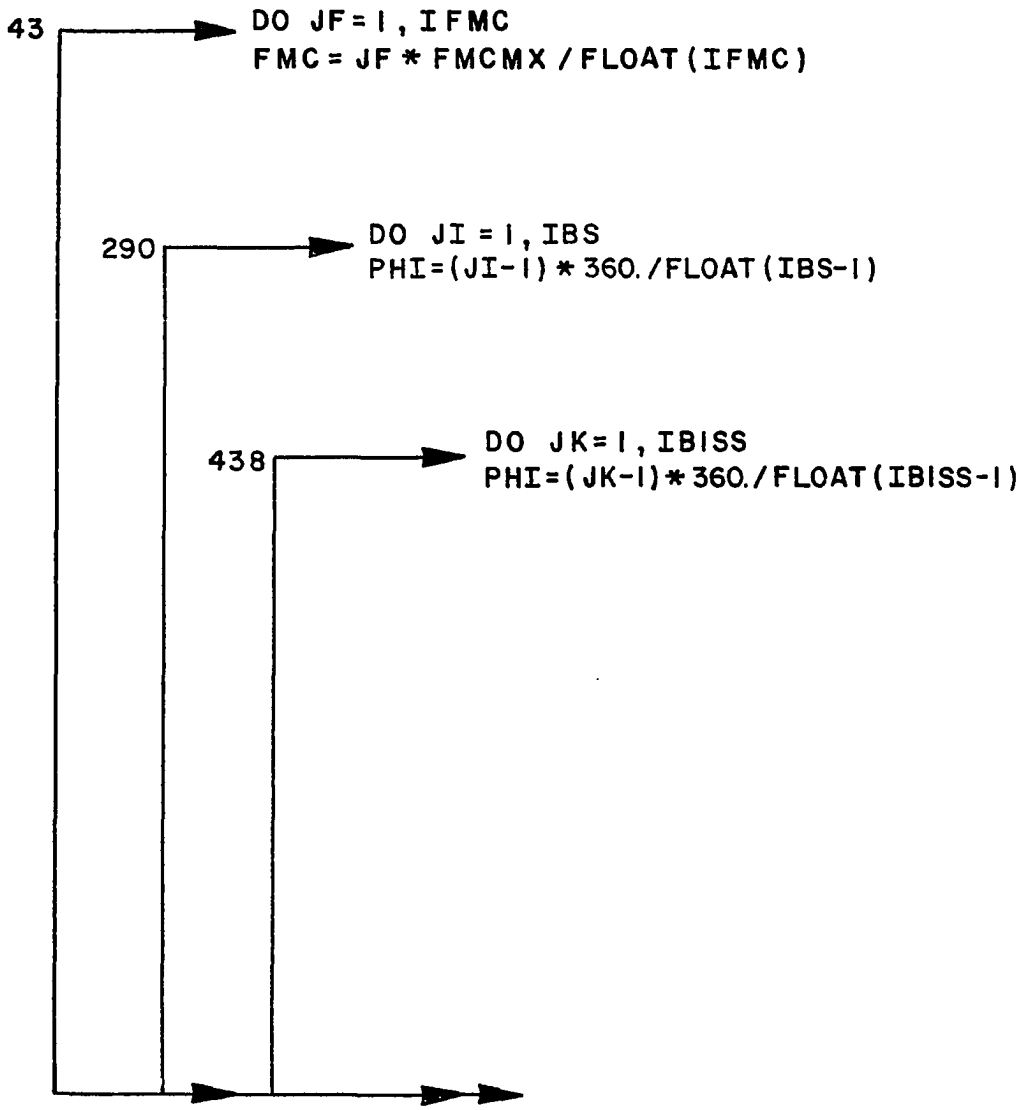

Figure A-3. Three major loops used in the computer program RCYLPWE.

points needed between 0° to 360°: for getting a Bistatic Scattering pattern IBISS is used similarly. It must be kept in mind that only one of the three inputs: IFMC, IBS, IBISS, may be used at a time. Other inputs may be used in combination to obtain desired outputs.

The RCYLPWE program can model an electric line source excitation or a plane wave excitation. If IPW=1, the plane wave excitation is used, and the output is the echowidth/λ_2, and if IPW=0, electric line source excitation is used and the output is the Scattering Attenuation Function (SAF).

The following is a list of the inputs for RCYLPWE program in the order they appear in line 29 of the listing:

ER1: Relative dielectric constant of region I.

SIG1: Conductivity of region I in s/m.

ER2: Relative dielectric constant of region I.

SIG2: Conductivity of region I in s/m.

FMCMX: Maximum frequency in MHz for the frequency plot.

AWM: The length (in meters) of the cross-section of the rectangular cylinders (see Figure 2-1b).

BWM: Width (in meters) of the rectangular cylinder (see Figure 2-1b).

PHI: The polar angle at which the line source is located or a plane wave is incident (Figure 2-1).

IWR: If 1, all the generalized impedance matrix element and the voltage column element are written in a file FOR010.DAT. In addition, to above, the solutions of the plane wave

coefficients are also written in the above file. IWR=0 otherwise.

IFILD: If 1, the field inside the scatterer is written in FOR010. DAT for various points in the first quadrant. Must be set to zero otherwise.

IWRC: If set to 1, the various elements in CROUT subroutine is printed on the screen for debugging purposes. Set to zero otherwise.

IPW: If set to 1, the plane wave excitation is used and the output is echowidth/λ_2, if set to zero, the line source excitation is used, and the output is (SAF).

IBS: If > 1, the backscattering pattern is calculated for IBS points, with angles divided equally. Otherwise it MUST BE SET TO 1.

IBISS: The same as above, except for Bistatic Scattering Patterns. If not needed, it MUST BE SET TO 1.

IFMC: Number of frequency points to be calculated for a frequency plot. If not used it MUST BE SET TO 1.

IEQ: If set to 1, the program automatically calculates NEQ the number of plane waves needed in the expansion to obtain a convergent solution, and NY the number of cells in y-direction for the integration routines. If set to zero, the program asks for the values of NEQ and NY to be input by the user.

RLS: Radial position of the line source (in meters).

RCYLPWE program uses various optimization techniques, one of which is the use of Gaussian interpolation technique. This is done by subroutine INTERP in line 216. Instead of calculating a value of a Bessel function many times, a table of required numbers is calculated only at a few points and is kept. The needed values as they are needed are then extraplated from this table. Another optimization is made in reducing the values of the Bessel function needed to a minimum by not calculating any values for redundant cases, i.e., cases where the same argument for Bessel functions occur over and over again.

```
0001    C       LINK WITH  CROUT & MBEZ10
0002    C
0003    C       THIS PROGRAM (RCYLPWE.FOR) USES PLANE WAVE EXPANSION AND
0004    C       GALERKIN METHOD TO CALCULATE THE SCATTERED FIELD BY
0005    C       A LOSSY DIELECTRIC INFINITE RECTANGULAR CYLINDER
0006    C       FOR AN ELECTRIC LINE SOURCE PARALLEL TO AXIS OF THE CYLINDER.
0007    C       THE CYLINDER IS LOCATED IN A LOSSY HOMOGINEOUS MEDIUM.
0008    C       THE PROGRAM USES FOUR FOLD SYMMETRY
0009    C
0010    C       WRITTEN BY JAMAL IZADIAN  NOVEMBER 1981.
0011    C
0012            COMPLEX BKK(25,25),FNEE(25),FNOE(25),FNEO(25),FNOO(25)
0013            COMPLEX FMEE(25),FMEO(25),FMOE(25),FMOO(25),FK(75)
0014            COMPLEX CMN(25,25),DMN(25,25),EMN(25,25),FMN(25,25)
0015            COMPLEX A(25),B(25),C(25),D(25),FA(25),GA(25)
0016            COMPLEX GC,VEE,VOE,VEO,VOO,CXP,CYP,SXP,SYP,CXL,CYL,SXL,SYL
0017            COMPLEX EGXP,EGYP,EGXL,EGYL,EGX1,EGX2,EGX3,EGX4,FN,FM,GN,GM
0018            COMPLEX EZI,FMF,FPF,GMG,GPG,S1,S2,S3,S4,SS1,SS2,SS3,SS4
0019            COMPLEX SFPF,SFMF,SGMG,SGPG,FMXP,GMYP,FNXL,GNYL
0020            COMPLEX CII,CIK,CV1,EP1,EP2,ETA2,CST,CSS,EZ1,EZS,SEE,SOE,SEO,SOO
0021            COMPLEX GAM1,GAM2,BI,BK,BI1,BK1,GR,K1,K2,SF,SG,REE,ROE,REO,ROO
0022            DIMENSION XM(450),YM(450)
0023            INTEGER P
0024            DATA FP,TD2/12.5663706144,0./
0025            DATA ETA,PI,TP/376.730366239,3.14159265359,6.28318530718/
0026            DATA ICC,NYX,ISIZE,NJ,ITBL/25,30,10,0,0/
0027            DATA E0,U0/8.85418533677E-12,1.25663706144E-6/
0028            call getcp(itl)
0029            READ(7,*)ER1,SIG1,ER2,SIG2,FMCMX,AWM,BWM,PHI,IWR,IFILD,IWRC
0030           &,IPW.IBS,IBISS,IFMC,IEQ,RLS
0031            IFRSCT=IBISS
0032            IBISS=IABS(IBISS)
0033            WRITE(10,*)IBS,IBISS,IFMC
0034            IC=(IBS-1)*(IBISS-1)+(IBS-1)*(IFMC-1)+(IBISS-1)*(IFMC-1)
0035            IF(IC.NE.0) GO TO 600
0036            WPH=PHI
0037            IF(IEQ.EQ.0)TYPE*,'GIVE NEQ & NY ='
0038            IF(IEQ.EQ.0)ACCEPT*,NEQ,NY
0039            IF(IFMC.GT.1) GO TO 41
0040    20      TYPE*,'GIVE FMC='
0041            ACCEPT*,FMC
0042            IF(FMC.LT.0) GO TO 600
0043    41      DO 500 JF=1,IFMC
0044            IF(IFMC.GT.1)FMC=JF*FMCMX/FLOAT(IFMC)
0045            I12=1
0046            AM=AWM/2 .
0047            BM=BWM/2.
0048            OMEGA=TP*FMC*1.E6
0049            BTS1=OMEGA*OMEGA*U0*ER1*E0
0050            BET1=SQRT(BTS1)
0051            EP1=CMPLX(ER1*E0,-SIG1/OMEGA)
0052            EP2=ER2*E0*(1.,.0)
0053            IF(TD2.GT.1.E-10)EP2=ER2*E0*CMPLX(1.,-TD2)
0054            IF(SIG2.GT.1.E-10)EP2=CMPLX(ER2*E0,-SIG2/OMEGA)
0055            ETA2=CSQRT(U0/EP2)
0056            GAM2=OMEGA*CSQRT(-U0*EP2)
0057            GAM1=OMEGA*CSQRT(-U0*EP1)
0058            K1=(0.,-1.)*GAM1
0059            K2=(0.,-1.)*GAM2
0060            BET2=AIMAG(GAM2)
0061            BTS2=BET2*BET2
0062            WAV1=TP/BET1
0063            WAV2=TP/BET2
```

```
0064            CPH=1.-PI/(14.*BET1*AM)
0065            IF(ABS(CPH).GT.1) GO TO 25
0066            DPH=ACOS(CPH)
0067            IF(IEQ.EQ.1)NEQ=1.+PI/(2.*DPH)
0068    25      IF(NEQ.LT.2) NEQ=2
0069            IF(NEQ.GT.ICC)GO TO 600
0070            IF(IEQ.EQ.1)NY=15.*BET1*BWM/PI
0071            IF(NY.LT.6.AND.IEQ.EQ.1)NY=6
0072            IF(NY.GT.NYX) NY=NYX
0073            NY=2*(NY/2)
0074            NX=INT(AM/EM)*NY
0075            NX=(NX/2)*2
0076            NY2=NY/2
0077            NX2=NX/2
0078            K4=NX2*NY2
0079            DPH=.5*PI/(NEQ-1)
0080            DO 90 J=1,NEQ
0081            PH=(J-1)*DPH
0082            FA(J)=K1*COS(PH)
0083            GA(J)=K1*SIN(PH)
0084    90      CONTINUE
0085            IX=NX/2
0086            IY=NY/2
0087            DX=AWM/NX
0088            DY=BWM/NY
0089            DX2=DX/2.
0090            DY2=DY/2.
0091    C       FIND THE RADIOUS OF EQUIVLANT CIRCULAR CELL
0092            CM=SQRT(DX*DY/PI)
0093            GC=GAM2*CM
0094            CALL MBEZ10(GAM2*CM,BI,BK,BI1,BK1,1,-1)
0095            CSS=(1.-GC*BK1)*(EP1-EP2)/EP2
0096            CST=GC*BI1*(EP1-EP2)/EP2
0097            CIK=CSS*2.*FP*CM*BI1/GAM2
0098            CII=CST*2.*FP*CM*BI1/GAM2
0099            CV1=-ETA2*CM*BI1
0100            RAB=SQRT(AWM*AWM+BWM*BWM)
0101    21      DELTR=(RAB-DX)/ISIZE
0102            IF(DX.GT.DELTR) GO TO 23
0103            ISIZE=ISIZE+5
0104            GO TO 21
0105    23      DO 22 I=1,ISIZE
0106            RR=I*DELTR
0107            CALL MBK0Z(GAM2*RR,BK,-1)
0108            FK(I)=BK*CII
0109    22      CONTINUE
0110            TYPE*,'ISIZE=',ISIZE
0111            M=0
0112            Y=DY2
0113    C       SET UP THE COORDINATES OF CENTERS OF CELL M
0114            DO 40 J=1,NY2
0115            X=DX2
0116            DO 30 I=1,NX2
0117            M=M+1
0118            XM(M)=X
0119            YM(M)=Y
0120    30      X=X+DX
0121    40      Y=Y+DY
0122            DO 42 J=1,25
0123            DO 42 I=1,25
0124    42      BKK(I,J)=(0.,0.)
0125    C       SET UP IMPEDANCE MATRIX
0126            DO 200 M=1,NEQ
```

```
0127            FM=FA(M)
0128            GM=GA(M)
0129            DO 160 N=M,NEQ
0130            FN=FA(N)
0131            GN=GA(N)
0132            FMF=FN-FM
0133            FPF=FN+FM
0134            GMG=GN-GM
0135            GPG=GN+GM
0136            IF(M.NE.N) GO TO 31
0137            SF=CSIN(2.*FN*AM)
0138            SG=CSIN(2.*GN*BM)
0139            S1=AM*BM
0140            IF(M.EQ.1)THEN
0141            S3=.5*BM*SF/FN
0142            REE=2.*(S1+S3)
0143            ROE=2.*(S1-S3)
0144            REO=(0.,0.)
0145            ROO=(0.,0.)
0146            GO TO 33
0147            END IF
0148            IF(M.EQ.NEQ) THEN
0149            S2=.5*AM*SG/GN
0150            REE=2.*(S1+S2)
0151            ROE=(0.,0.)
0152            REO=2.*(S1-S2)
0153            ROO=(0.,0.)
0154            GO TO 33
0155            END IF
0156            S2=.5*AM*SG/GN
0157            S3=.5*BM*SF/FN
0158            S4=.25*SF*SG/FN/GN
0159            REE=S1+S2+S3+S4
0160            ROE=S1+S2-S3-S4
0161            REO=S1-S2+S3-S4
0162            ROO=S1-S2-S3+S4
0163            GO TO 33
0164    31      SFMF=CSIN(FMF*AM)
0165            SFPF=CSIN(FPF*AM)
0166            SGMG=CSIN(GMG*BM)
0167            SGPG=CSIN(GPG*BM)
0168            SS1=SFMF*SGMG/FMF/GMG
0169            SS2=SFMF*SGPG/FMF/GPG
0170            SS3=SFPF*SGMG/FPF/GMG
0171            SS4=SFPF*SGPG/FPF/GPG
0172            REE=SS1+SS2+SS3+SS4
0173            ROE=SS1+SS2-SS3-SS4
0174            REO=SS1-SS2+SS3-SS4
0175            ROO=SS1-SS2-SS3+SS4
0176    33      CONTINUE
0177            CMN(M,N)=REE
0178            DMN(M,N)=ROE
0179            M1=M-1
0180            N1=N-1
0181            IF(M.GT.1)EMN(M1,N1)=REO
0182            IF(M.GT.1)FMN(M1,N1)=ROO
0183     180    CONTINUE
0184     200    CONTINUE
0185            DO 160 P=1,K4
0186            XP=XM(P)
0187            YP=YM(P)
0188            JPP=(P-1)/IX+1
0189            IPP=P-(JPP-1)*IX
```

```
0190            JP=JPP+IY
0191            IP=IPP+IX
0192            DO 140 L=1,K4
0193            XL=XM(L)
0194            YL=YM(L)
0195            JLP=(L-1)/IX+1
0196            ILP=L-(JLP-1)*IX
0197            XN=XL
0198            YN=YL
0199            IN=ILP
0200            JN=JLP
0201            SIGX=1.
0202            SIGY=1.
0203            DO 120 L1=1,2
0204            YY=YP-YL
0205            YS=YY*YY
0206            JL=IY+JLP+(L1-1)
0207            DO 100 L2=1,2
0208            XX=XP-XL
0209            XS=XX*XX
0210            IL=IX+ILP+(L2-1)
0211            II=1+IABS(IP-IL)
0212            JJ=1+IABS(JP-JL)
0213            ROH=SQRT(XS+YS)
0214            IF(ROH.LT.DX2) GO TO 79
0215            IF(BKK(II,JJ).EQ.(0.,0.))THEN
0216            CALL INTERP(ROH,BKK(II,JJ),DELTR,FK,ISIZE)
0217            BKK(JJ,II)=BKK(II,JJ)
0218            NJ=NJ+1
0219            END IF
0220    79      DO  80 M=1,NEQ
0221            IF(L.GT.1) GO TO 77
0222            FM=FA(M)
0223            GM=GA(M)
0224            FMXP=FM*XP*(0.,1.)
0225            GMYP=GM*YP*(0.,1.)
0226            EGXP=CEXP(FMXP)
0227            EGYP=CEXP(GMYP)
0228            CXP=.5*(EGXP+1./EGXP)
0229            CYP=.5*(EGYP+1./EGYP)
0230            SXP=(0.,-.5)*(EGXP-1./EGXP)
0231            SYP=(0.,-.5)*(EGYP-1./EGYP)
0232            FMEE(M)=CXP*CYP
0233            FMOE(M)=SXP*CYP
0234            FMEO(M)=CXP*SYP
0235            FMOO(M)=SXP*SYP
0236    77      DO 80 N=M,NEQ
0237            IF(L1.GT.1.OR.L2.GT.1) GO TO 75
0238            FN=FA(N)
0239            GN=GA(N)
0240            FNXL=FN*XL*(0.,1.)
0241            GNYL=GN*YL*(0.,1.)
0242            EGXL=CEXP(FNXL)
0243            EGYL=CEXP(GNYL)
0244            CXL=.5*(EGXL+1./EGXL)
0245            CYL=.5*(EGYL+1./EGYL)
0246            SXL=(0.,-.5)*(EGXL-1./EGXL)
0247            SYL=(0.,-.5)*(EGYL-1./EGYL)
0248            FNEE(N)=CXL*CYL
0249            FNOE(N)=SXL*CYL
0250            FNEO(N)=CXL*SYL
0251            FNOO(N)=SXL*SYL
0252    75      IF(ROH.GT.DX2)GO TO 35
```

```
0253            CMN(M,N)=CMN(M,N)+FMEE(M)*FNEE(N)*CIK
0254            DMN(M,N)=DMN(M,N)+FMOE(M)*FNOE(N)*CIK*SIGX
0255            M1=M-1
0256            N1=N-1
0257            IF(M.GT.1)EMN(M1,N1)=EMN(M1,N1)+FMEO(M)*FNEO(N)*CIK*SIGY
0258            IF(M.GT.1)FMN(M1,N1)=FMN(M1,N1)+FMOO(M)*FNOO(N)*CIK*SIGX*SIGY
0259            GO TO 80
0260    35      BK=BKK(II,JJ)
0261            CMN(M,N)=CMN(M,N)+FMEE(M)*FNEE(N)*BK
0262            DMN(M,N)=DMN(M,N)+FMOE(M)*FNOE(N)*BK*SIGX
0263            M1=M-1
0264            N1=N-1
0265            IF(M.GT.1)EMN(M1,N1)=EMN(M1,N1)+FMEO(M)*FNEO(N)*BK*SIGY
0266            IF(M.GT.1)FMN(M1,N1)=FMN(M1,N1)+FMOO(M)*FNOO(N)*BK*SIGX*SIGY
0267    80      CONTINUE
0268            SIGX=-1.
0269            ILP=-IN
0270    100     XL=-XN
0271            SIGX=1.
0272            SIGY=-1.
0273            XL=XN
0274            ILP=IN
0275            JLP=-JN
0276    120     YL=-YN
0277    140     CONTINUE
0278    160     CONTINUE
0279            TYPE*,'NJ=',NJ
0280            NJ=0
0281            IF(IWR.EQ.1) THEN
0282            WRITE(10,2)
0283            DO 210 M=1,NEQ
0284            DO 210 N=M,NEQ
0285            WRITE(10,3)M,N,CMN(M,N),DMN(M,N),EMN(M,N),FMN(M,N)
0286    210     CONTINUE
0287            END IF
0288            IF(IWR.EQ.1)WRITE(10,9)
0289            IF(IWR.EQ.1)WRITE(10,4)
0290            DO 500 JI=1,IBS
0291            IF(IBS.GT.1)PHI=(JI-1)*360./FLOAT(IBS-1)
0292            PH1=.0174533*PHI
0293            PH2=PI-PH1
0294            PH3=PI+PH1
0295            PH4=-PH1
0296            CS1=COS(PH1)
0297            SN1=SIN(PH1)
0298            CS2=COS(PH2)
0299            SN2=SIN(PH2)
0300            CS3=COS(PH3)
0301            SN3=SIN(PH3)
0302            CS4=COS(PH4)
0303            SN4=SIN(PH4)
0304            XLS1=RLS*CS1
0305            YLS1=RLS*SN1
0306            XLS2=RLS*CS2
0307            YLS2=RLS*SN2
0308            XLS3=RLS*CS3
0309            YLS3=RLS*SN3
0310            XLS4=RLS*CS4
0311            YLS4=RLS*SN4
0312    C       SET UP THE VOLTAGE MATRIX
0313            DO 240 M=1,NEQ
0314            FM=FA(M)
0315            GM=GA(M)
```

```
0316            SEE=(0.,0.)
0317            SOE=(0.,0.)
0318            SEO=(0.,0.)
0319            SOO=(0.,0.)
0320            DO 220 P=1,K4
0321            X=XM(P)
0322            Y=YM(P)
0323            FMXP=FM*X*(0.,1.)
0324            GMYP=GM*Y*(0.,1.)
0325            EGXP=CEXP(FMXP)
0326            EGYP=CEXP(GMYP)
0327            CXP=.5*(EGXP+1./EGXP)
0328            CYP=.5*(EGYP+1./EGYP)
0329            SXP=(0.,-.5)*(EGXP-1./EGXP)
0330            SYP=(0.,-.5)*(EGYP-1./EGYP)
0331            FMEE(M)=CXP*CYP
0332            FMOE(M)=SXP*CYP
0333            FMEO(M)=CXP*SYP
0334            FMOO(M)=SXP*SYP
0335            IF(IPW.EQ.1)THEN
0336            PSI1=X*CS1+Y*SN1
0337            PSI2=X*CS2+Y*SN2
0338            PSI3=X*CS3+Y*SN3
0339            PSI4=X*CS4+Y*SN4
0340            EGX1=CEXP(GAM2*PSI1)
0341            EGX2=CEXP(GAM2*PSI2)
0342            EGX3=CEXP(GAM2*PSI3)
0343            EGX4=CEXP(GAM2*PSI4)
0344            CV1=(1.,0.)*DX*DY
0345            GO TO 219
0346            END IF
0347            X1=XLS1-X
0348            Y1=YLS1-Y
0349            X2=XLS2-X
0350            Y2=YLS2-Y
0351            X3=XLS3-X
0352            Y3=YLS3-Y
0353            X4=XLS4-X
0354            Y4=YLS4-Y
0355            RH1=SQRT(X1*X1+Y1*Y1)
0356            RH2=SQRT(X2*X2+Y2*Y2)
0357            RH3=SQRT(X3*X3+Y3*Y3)
0358            RH4=SQRT(X4*X4+Y4*Y4)
0359            CALL MBK0Z(GAM2*RH1,EGX1,-1)
0360            CALL MBK0Z(GAM2*RH2,EGX2,-1)
0361            CALL MBK0Z(GAM2*RH3,EGX3,-1)
0362            CALL MBK0Z(GAM2*RH4,EGX4,-1)
0363    219     VEE=EGX1+EGX2+EGX3+EGX4
0364            VOE=EGX1-EGX2-EGX3+EGX4
0365            VEO=EGX1+EGX2-EGX3-EGX4
0366            VOO=EGX1-EGX2+EGX3-EGX4
0367            SEE=SEE+FMEE(M)*VEE
0368            SOE=SOE+FMOE(M)*VOE
0369            SEO=SEO+FMEO(M)*VEO
0370            SOO=SOO+FMOO(M)*VOO
0371    220     CONTINUE
0372            A(M)=SEE*CV1
0373            B(M)=SOE*CV1
0374            M1=M-1
0375            IF(M.GT.1)C(M1)=SEO*CV1
0376            IF(M.GT.1)D(M1)=SOO*CV1
0377    240     CONTINUE
0378            IF(IWR.EQ.1)THEN
```

```
0379            DO 202 M=1,NEQ
0380    202     WRITE(10,5)M,A(M),B(M),C(M),D(M)
0381            WRITE(10,9)
0382            END IF
0383            NN1=NEQ-1
0384            NN2=NEQ-2
0385            ISYM=0
0386            CALL CROUT(CMN,A,ICC,ISYM,IWRC,I12,NEQ)
0387            CALL CROUT(DMN,B,ICC,ISYM,IWRC,I12,NN1)
0388            CALL CROUT(EMN,C,ICC,ISYM,IWRC,I12,NN1)
0389            CALL CROUT(FMN,D,ICC,ISYM,IWRC,I12,NN2)
0390            IF(IWR.EQ.1)THEN
0391            WRITE(10,6)
0392            DO 244 M=1,NEQ
0393            WRITE(10,5)M,A(M),B(M),C(M),D(M)
0394    244     CONTINUE
0395            WRITE(10,9)
0396            END IF
0397            DO 242 J=1,NEQ-1
0398            I=NEQ-J
0399            C(I+1)=C(I)
0400    242     D(I+1)=D(I)
0401            C(1)=(0.,0.)
0402            D(1)=(0.,0.)
0403            D(NEQ)=(0.,0.)
0404    C       FIND THE FIELD IN CELLS OF FIRST QUADRANT
0405            IF(IFILD.NE.1) GO TO 45
0406            WRITE(10,8)
0407            DO 248 L=1,K4
0408            EZ1=(0.,0.)
0409            XL=XM(L)
0410            YL=YM(L)
0411            DO 246 N=1,NEQ
0412            FN=FA(N)
0413            GN=GA(N)
0414            FNXL=FN*XL*(0.,1.)
0415            GNYL=GN*YL*(0.,1.)
0416            EGXL=CEXP(FNXL)
0417            EGYL=CEXP(GNYL)
0418            CXL=.5*(EGXL+1./EGXL)
0419            CYL=.5*(EGYL+1./EGYL)
0420            SXL=(0.,-.5)*(EGXL-1./EGXL)
0421            SYL=(0.,-.5)*(EGYL-1./EGYL)
0422            FNEE(N)=CXL*CYL
0423            FNOE(N)=SXL*CYL
0424            FNEO(N)=CXL*SYL
0425            FNOO(N)=SXL*SYL
0426            EZ1=EZ1+(A(N)*FNEE(N)+B(N)*FNOE(N)+C(N)*FNEO(N)+D(N)*FNOO(N))
0427    246     CONTINUE
0428            CX=.0174533
0429            RE=REAL(EZ1)
0430            AIE=AIMAG(EZ1)
0431            AMP=CABS(EZ1)
0432            PHASE=ATAN2(AIE,RE)/CX
0433            WRITE(10,11)XL,YL,AMP,PHASE
0434    248     CONTINUE
0435    45      IF(IWR.EQ.1)WRITE(10,9)
0436            PHS=PH1
0437            IF(IFRSCT.EQ.-1)PHS=PHS+PI
0438            DO 500 JK=1,IBISS
0439            IF(IBISS.GT.1)THEN
0440            PHI=(JK-1)*360./FLOAT(IBISS-1)
0441            PHS=.0174533*PHI
```

```
0442            END IF
0443            XLS=RLS*COS(PHS)
0444            YLS=RLS*SIN(PHS)
0445    C       FIND THE BACKSCATTERED FIELD
0446            EZS=(.0,.0)
0447            DO 290 L=1,K4
0448            XL=XM(L)
0449            YL=YM(L)
0450            XN=XL
0451            YN=YL
0452            SIGX=1.
0453            SIGY=1.
0454            DO 260 L1=1,2
0455            YY=YLS-YL
0456            YS=YY*YY
0457            DO 270 L2=1,2
0458            XX=XLS-XL
0459            XS=XX*XX
0460            IF(IPW.EQ.1)THEN
0461            PSI=XL*COS(PHS)+YL*SIN(PHS)
0462            BK=CEXP(GAM2*PSI)
0463            GO TO 47
0464            END IF
0465            ROH=SQRT(XS+YS)
0466            CALL MBK0Z(GAM2*ROH,BK,-1)
0467    47      EZ1=(0.,0.)
0468            DO 260 N=1,NEQ
0469            IF(L1.GT.1.OR.L2.GT.1) GO TO 269
0470            FN=FA(N)
0471            GN=GA(N)
0472            FNXL=FN*XL*(0.,1.)
0473            GNYL=GN*YL*(0.,1.)
0474            EGXL=CEXP(FNXL)
0475            EGYL=CEXP(GNYL)
0476            CXL=.5*(EGXL+1./EGXL)
0477            CYL=.5*(EGYL+1./EGYL)
0478            SXL=(0.,-.5)*(EGXL-1./EGXL)
0479            SYL=(0.,-.5)*(EGYL-1./EGYL)
0480            FNEE(N)=CXL*CYL
0481            FNOE(N)=SXL*CYL
0482            FNEO(N)=CXL*SYL
0483            FNOO(N)=SXL*SYL
0484    269     EZ1=EZ1+(A(N)*FNEE(N)+B(N)*FNOE(N)*SIGX+C(N)*FNEO(N)*SIGY
0485           &+D(N)*FNOO(N)*SIGX*SIGY)
0486    260     CONTINUE
0487            EZS=EZS+EZ1*BK
0488            SIGX=-1.
0489    270     XL=-XN
0490            SIGX=1.
0491            SIGY=-1.
0492            XL=XN
0493    280     YL=-YN
0494    290     CONTINUE
0495            EZS=-CST*EZS
0496            IF(IPW.EQ.1)EZS=EZS*CSQRT(.5*PI/GAM2)
0497            AZS=CABS(EZS)
0498            IF(IWR.EQ.1)WRITE(10,*)'AZS=',AZS
0499            EWL=TP*AZS*AZS/WAV2
0500            DB=.0
0501    C       FIND THE NORMALIZED SCATTERING ATTENUATION FUNCTION
0502            IF(IPW.EQ.0)THEN
0503            GR=2.*GAM2*RLS
0504            CALL MBK0Z(GR,BK,-1)
```

```
0505            EZI=(.0,-1.)*OMEGA*U0*BK/TP
0506            AZI=CABS(EZI)
0507            IF(IWR.EQ.1)WRITE(10,*)'AZI=',AZI
0508            AZN=AZS/AZI
0509            DB=20.*ALOG10(AZN)
0510            TYPE1,NEQ,NX,NY,FMC,DB,PHI
0511            WRITE(10,1)NEQ,NX,NY,FMC,DB,PHI
0512            GO TO 599
0513            END IF
0514            TYPE1,NEQ,NX,NY,FMC,EWL,PHI
0515            WRITE(10,1)NEQ,NX,NY,FMC,EWL,PHI
0516    599     IF(IBS.EQ.1.AND.IBISS.EQ.1.AND.IFMC.EQ.1)GO TO 20
0517            I12=2
0518    500     CONTINUE
0519    600     CONTINUE
0520            IF(IPW.EQ.1)WRITE(10,14)
0521            IF(IPW.EQ.0)WRITE(10,13)
0522            WRITE(10,9)
0523            WRITE(10,*)' ER1 & SIG1 =',ER1,SIG1
0524            WRITE(10,*)' ER2 & SIG2 =',ER2,SIG2
0525            WRITE(10,*)' AWM & BWM =' ,AWM,BWM
0526            WRITE(10,*) 'RLS=',RLS,'PHI=',WPH
0527            call getcp(it2)
0528            time=(it2-it1)/100.
0529            WRITE(10,*) ' CPU TIME (SEC) =',TIME
0530            TYPE*,' CPU TIME (SEC) = ',TIME
0531            WRITE(10,*) 'RCYLPWE.FOR'
0532    1       FORMAT(1X,3I5,6F12.6)
0533    2       FORMAT(5X,'M',4X,'N',13X,'CMN',21X,'DMN',21X,'EMN',21X,'FMN')
0534    3       FORMAT(1X,2I5,8F12.6)
0535    4       FORMAT(5X,'M',18X,'VEE',21X,'VOE',21X,'VEO',21X,'VOO')
0536    5       FORMAT(1X,I5,5X,8F12.6)
0537    6       FORMAT(5X,'M',18X,' A ',21X,' B ',21X,' C ',21X,' D ')
0538    8       FORMAT(5X,'X',9X,'Y',11X,'AMPLITUDE',3X,'PHASE')
0539    9       FORMAT(1H0)
0540    11      FORMAT(1X,2F10.5,5X,2F12.6)
0541    13      FORMAT(3X,'NEQ',3X,'NX',3X,'NY',6X,'FMC',9X,'SAF',9X,'PHI')
0542    14      FORMAT(3X,'NEQ',3X,'NX',3X,'NY',6X,'FMC',9X,'EWL',9X,'PHI')
0543            CALL EXIT
0544            END
```

APPENDIX B

The computer program RTUNLE uses the formulation of Chapter III and Chapter VII. It is capable of treating a rectangular scatterer in a homogeneous ambient medium or in a lossy half space. To include the effects of the half space IGROND is set to one otherwise, it must be set to zero. All the inputs necessary to execute the program is shown in line 16 and 17 in the listing. This program has the same type of internal DO loops as described in Figure A-3 for RCYLPWE program. Here, only the new inputs are described.

NEQ: Number of plane waves to be included in the plane wave expansion, restricted to condition in line 53. This will be used by the program when line 24-25 and 48-52 are not to be executed.

DM: The x-coordinate of the air-earth interface plane parallel to yz-plane as shown in Figure 7-1. DM is in meters.

XLS: X-coordinate of the electric line source location (in meters) as shown in Figure 7-1. In this program the restriction $\frac{AWM}{2} \leq XLS \leq DM$ is made.

YLS: Y-coordinate of the electric line source (in meters) as shown in Figure 7-1.

IGROND: If set to one, the air-earth interface will be included in the model as shown in Figure 7-1. If set to zero only the homogeneous ambient medium is considered.

IZMN: If set to one, the elements of the generalized impedance matrix is stored in file FOR$\phi\phi$8.DAT for cases where these elements are needed again. If set to zero, the program does not calculate the elements of generalized impedance matrix, instead it reads them from file FOR$\phi\phi$8.DAT.

```
0001    C       This is program (RTUNLE.FOR) Rectangular TUNneL Ez-polarization.
0002    C       It uses Plane Wave Expansion Galerkin.
0003    C
0004    C       WRITTEN BY JAMAL IZADIAN DECEMBER 1981.
0005    C
0006            COMPLEX A(25),V(25),DV(25),VT(25),Z(25,25),DZ(25,25),ZT(25,25)
0007            COMPLEX FA(25),GA(25),B(25),EZ1,EZI,EZS
0008            COMPLEX SUM1,SUM2,SUMT,RMN,SMN,FN,FM,GN,GM,S1,S2,FNFM,GNGM
0009            COMPLEX C2,CST,C1,CJ,EP1,EP2,GAM1,GAM2,GAM2S,K1,K2,EXF,EXG,BK
0010            DIMENSION XM(100),YM(100)
0011            COMMON /JI/ GAM2S,GAM2,OMEGA,ER2,SIG2
0012            COMMON FN,FM,GN,GM,AM,BM,DM,XLS,YLS
0013            DATA PI,TP/3.14159265359,6.28318530718/
0014            DATA E0,U0/8.85418533677E-12,1.25663706144E-6/
0015            DATA IWRC,ICC,I12,ISYM/0,25,1,0/
0016            READ(7,*)ER1,SIG1,ER2,SIG2,FMCMX,NEQ,AWM,BWM,DM,XLS,YLS,IWR
0017           &,IFILD,IBS,IBISS,IFMC,IGROND,IZMN
0018            call getcp(it1)
0019            IF((AWM/2.).GT.DM.OR.XLS.GT.DM) GO TO 500
0020            WRITE(10,*)MAX(IBS,IBISS,IFMC)
0021            CJ=(0.,1.)
0022            CX=.0174533
0023            NY=1
0024    21      TYPE*,'GIVE FMC,NEQ,NY='
0025            ACCEPT*,FMC,NEQ,NY
0026            IF(FMC.LT.0)GO TO 500
0027            NX=(AWM/BWM)*NY
0028            AM=AWM/2.
0029            BM=BWM/2.
0030            DO 500 JF=1,IFMC
0031            IF(IFMC.GT.1)FMC=JF*FMCMX/FLOAT(IFMC)
0032            OMEGA=TP*FMC*1.E6
0033            EP1=CMPLX(ER1*E0,-SIG1/OMEGA)
0034            EP2=CMPLX(ER2*E0,-SIG2/OMEGA)
0035            GAM1=OMEGA*CSQRT(-U0*EP1)
0036            GAM2=OMEGA*CSQRT(-U0*EP2)
0037            BET1=AIMAG(GAM1)
0038            GAM2S=GAM2*GAM2
0039            K1=-CJ*GAM1
0040            K2=-CJ*GAM2
0041            CST=-OMEGA*OMEGA*U0*(EP1-EP2)/TP
0042            C1=-CJ*OMEGA*U0/TP
0043            C2=CJ*OMEGA*(EP1-EP2)
0044            DX=AWM/NX
0045            DY=BWM/NY
0046            DX2=DX/2.
0047            DY2=DY/2.
0048            CPH=1.-PI/(14.*BET1*AM)
0049            IF(ABS(CPH).GT.1)GO TO 19
0050            DPH=ACOS(CPH)
0051            NEQ=1.+PI/(2.*DPH)
0052            NEQ=2*NEQ
0053    19      IF(NEQ.LT.6)NEQ=6
0054            M=0
0055            Y=-BM+DY2
0056            DO 20 J=1,NY
0057            X=-AM+DX2
0058            DO 22 I=1,NX
0059            M=M+1
0060            XM(M)=X
0061            YM(M)=Y
0062    22      X=X+DX
0063    20      Y=Y+DY
```

```
0064            KK=M
0065            DPH=TP/NEQ
0066            DO 90 J=1,NEQ
0067            A(J)=(0.,0.)
0068            B(J)=(0.,0.)
0069            PH=(J-1)*DPH
0070            FA(J)=K1*COS(PH)
0071    90      GA(J)=K1*SIN(PH)
0072            IF(IWR.EQ.1)WRITE(10,1)
0073            IF(IZMN.EQ.0)THEN
0074            DO 92 M=1,NEQ
0075            DO 92 N=M,NEQ
0076    92      READ(8,2)I,J,Z(M,N),DZ(M,N),ZT(M,N)
0077            GO TO 404
0078            END IF
0079            DO 100 M=1,NEQ
0080            FM=FA(M)
0081            GM=GA(M)
0082            DO 200 N=M,NEQ
0083            FN=FA(N)
0084            GN=GA(N)
0085            FNFM=FN+FM
0086            GNGM=GN+GM
0087            S1=AM
0088            S2=BM
0089            IF(CABS(FNFM).GT.1.E-6)S1=CSIN(FNFM*AM)/FNFM
0090            IF(CABS(GNGM).GT.1.E-6)S2=CSIN(GNGM*BM)/GNGM
0091            RMN=4.*S1*S2
0092 .          CALL SPCIRM(SUMT,2,IGROND)
0093            SMN=4.*CST*SUMT
0094            Z(M,N)=RMN+SMN
0095            IF(IGROND.EQ.1)CALL SPCIRM(SUMT,3,IGROND)
0096            IF(IGROND.EQ.1)DZ(M,N)=8.*CST*SUMT
0097            IF(IGROND.EQ.1)ZT(M,N)=Z(M,N)+DZ(M,N)
0098            IF(IWR.EQ.1)WRITE(10,2)M,N,Z(M,N),DZ(M,N),ZT(M,N)
0099            WRITE(8,2)M,N,Z(M,N),DZ(M,N),ZT(M,N)
0100    200     CONTINUE
0101    100     CONTINUE
0102    404     CONTINUE
0103            IF(IGROND.EQ.1)THEN
0104            DO 106 M=1,NEQ
0105            DO 106 N=M,NEQ
0106    106     Z(M,N)=ZT(M,N)
0107            END IF
0108            IF(IWR.EQ.1)WRITE(10,3)
0109            IF(IWR.EQ.1)WRITE(10,4)
0110            DO 500 JI=1,IBS
0111            IF(IBS.GT.1)YLS=((IBS-1)/2+1-JI)*.0625
0112            YLSS=YLS
0113    C       SET UP THE VOLTAGE COLUMN
0114            DO 120 M=1,NEQ
0115            FM=FA(M)
0116            GM=GA(M)
0117            CALL SPCIRM(SUMT,0,IGROND)
0118            A(M)=SUMT
0119            V(M)=2.*C1*SUMT
0120            IF(IGROND.EQ.1)THEN
0121            CALL SPCIRM(SUMT,1,IGROND)
0122            B(M)=SUMT
0123            DV(M)=2.*C1*SUMT
0124            VT(M)=V(M)+DV(M)
0125            END IF
0126    120     IF(IWR.EQ.1)WRITE(10,5)M,V(M),DV(M),VT(M)
```

```
0127            IF(IWR.EQ.1)WRITE(10,3)
0128            IF(IGROND.EQ.1)THEN
0129            DO 104 M=1,NEQ
0130    104     V(M)=VT(M)
0131            END IF
0132            CALL CROUT(Z,V,ICC,ISYM,IWRC,I12,NEQ)
0133            IF(IFILD.EQ.0) GO TO 45
0134    C       FIND FIELD INSIDE THE TUNNEL
0135            WRITE(10,3)
0136            WRITE(10,6)
0137            DO 300 L=1,KK
0138            EZ1=(0.,0.)
0139            X=XM(L)
0140            Y=YM(L)
0141            IF(X.LT.0.OR.Y.LT.0) GO TO 300
0142            DO 400 N=1,NEQ
0143            FN=FA(N)
0144            GN=GA(N)
0145            EXF=CEXP(-CJ*FN*X)
0146            EXG=CEXP(-CJ*GN*Y)
0147    400     EZ1=EZ1+EXF*EXG*V(N)
0148            RE=REAL(EZ1)
0149            AIE=AIMAG(EZ1)
0150            PHASE=ATAN2(AIE,RE)/CX
0151            AMP=CABS(EZ1)
0152            WRITE(10,7)X,Y,AMP,PHASE
0153    300     CONTINUE
0154            WRITE(10,3)
0155    C       FIND SCATTERED FIELD
0156    45      DO 500 JK=1,IBISS
0157            IF(IBISS.GT.1)YLS=((IBISS-1)/2+1-JK)*.0625
0158            EZS=(0.,0.)
0159            DO 600 M=1,NEQ
0160            IF(IBISS.GT.1)THEN
0161            FM=FA(M)
0162            GM=GA(M)
0163            CALL SPCIRM(SUMT,0,IGROND)
0164            A(M)=SUMT
0165            IF(IGROND.EQ.1)CALL SPCIRM(SUMT,1,IGROND)
0166            IF(IGROND.EQ.1)B(M)=SUMT
0167            END IF
0168    600     EZS=EZS+V(M)*(A(M)+B(M))
0169            EZS=-CST*2.*EZS
0170            AZS=CABS(EZS)
0171    C       IF(IGROND.EQ.0)THEN
0172            RLSO=SQRT(XLS*XLS+YLS*YLS)
0173            RLSS=SQRT(XLS*XLS+YLSS*YLSS)
0174            CALL MBK0Z(GAM2*(RLSO+RLSS),BK,-1)
0175            EZI=BK*C1
0176            AZI=CABS(EZI)
0177            AZN=AZS/AZI
0178            DB=20.*ALOG10(AZN)
0179            TYPE8,NEQ,NX,NY,FMC,DB,YLS
0180            WRITE(10,8)NEQ,NX,NY,FMC,DB,YLS
0181    C       GO TO 499
0182    C       END IF
0183    C       TYPE8,NEQ,NX,NY,FMC,AZS,YLS
0184    C       WRITE(10,8)NEQ,NX,NY,FMC,AZS,YLS
0185    499     IF(IBS.GT.1)I12=2
0186            IF(IBS.EQ.1.AND.IBISS.EQ.1.AND.IFMC.EQ.1)GO TO 21
0187    500     CONTINUE
0188            IF(IGROND.EQ.1)WRITE(10,9)
0189            IF(IGROND.EQ.0)WRITE(10,10)
```

```
0190    1       FORMAT(5X,'M',4X,'N',13X,'ZMN',20X,'DZMN',20X,'ZTMN'25X)
0191    2       FORMAT(1X,2I5,8F12.6)
0192    3       FORMAT(1H0)
0193    4       FORMAT(5X,'M',12X,' VM ',21X,'DVM',21X,'VTM',21X)
0194    5       FORMAT(1X,I5,8F12.6)
0195    6       FORMAT(5X,'X',9X,'Y',13X,'AMPLITUDE',3X,'PHASE')
0196    7       FORMAT(1X,2F10.5,5X,2F12.6)
0197    8       FORMAT(1X,3I5,6F12.6)
0198    9       FORMAT(3X,'NEQ',3X,'NX',3X,'NY',6X,'FMC',9X,'SAF')
0199    10      FORMAT(3X,'NEQ',3X,'NX',3X,'NY',6X,'FMC',9X,'SAF')
0200            call getcp(it2)
0201            time=(it2-it1)/100.
0202            WRITE(10,*)'ER1 & SIG1=',ER1,SIG1
0203            WRITE(10,*)'ER2 & SIG2=',ER2,SIG2
0204            WRITE(10,*)'AWM,BWM,DM,XLS,YLS=',AWM,BWM,DM,XLS,YLS
0205            write(10,*) ' cpu time=',time,'sec'
0206            WRITE(10,*)'RTUNLE.FOR'
0207            write(10,*)ER1,SIG1,ER2,SIG2,FMC,NEQ,AWM,BWM,DM,XLS,YLS,IWR
0208         &,IFILD,IBS,IBISS
0209            STOP
0210            END
```

FUNCTIONS AND SUBROUTINES REFERENCED

```
0001    C
0002            SUBROUTINE SPCIRM(SUMT,I0123,IGROND)
0003            COMPLEX GAM2S,GAM2,GAM0S,FQ,RC,F,F0,FF,SUM1,SUM2,SUM3,SUMT
0004            COMPLEX FN,FM,GN,GM,CJ,FF1,FF2,FF3,DSUM
0005            REAL K0
0006            COMMON /J1/GAM2S,GAM2,OMEGA,ER2,SIG2
0007            COMMON FN,FM,GN,GM,AM,BM,DM,XLS,YLS
0008            DATA PI,TP/3.14159265359,6.28318530718/
0009            DATA E0,U0/8.85418533677E-12,1.25663706144E-6/
0010            CJ=(0.,1.)
0011            K0=OMEGA*SQRT(E0*U0)
0012            GAM0S=-K0*K0*(1.,0.)
0013            GC=OMEGA*SQRT(U0*ER2*E0)
0014            GCS=GC*GC
0015            G1=GC/SQRT(2.)
0016    C       SET UP FOR SUM1 & SUM2
0017            IF(I0123.LT.3)DEL=PI/10./(AM+BM)
0018            IF(I0123.EQ.3)DEL=PI/10./(AM+DM+BM)
0019            NS=G1/DEL
0020            IF(NS.LT.20) NS=20
0021            NP=2*(NS/2)
0022            DEL=G1/NP
0023            NP=NP+1
0024            DEL3=DEL/3.
0025            SUM1=(0.,0.)
0026            SUM2=(0.,0.)
0027            DO 100 I=1,2
0028            SIGN=1.
0029            DO 100 J=1,NP
0030            W=(3.-SIGN)*DEL3
0031            IF(J.EQ.1.OR.J.EQ.NP) W=DEL3
0032            IF(I.EQ.2)GO TO 31
0033            G=(J-1)*DEL
0034            GO TO 33
0035    31      B=(J-1)*DEL
0036            BS=B*B
```

```
0037            G=SQRT(GCS-BS)
0038    33      GS=G*G
0039            F=CSQRT(GAM2S+GS)
0040            F0=CSQRT(GAM0S+GS)
0041            IF(IGROND.EQ.1)RC=(F-F0)/(F+F0)
0042            IF(I0123.EQ.0)FF=FF1(G,F)*CEXP(-F*XLS)
0043            IF(I0123.EQ.1)FF=FF1(G,F)*RC*CEXP(F*(-2.*DM+XLS))
0044            IF(I0123.EQ.2)FF=FF2(G,F)
0045            IF(I0123.EQ.3)FF=FF3(G,F)*RC*CEXP(-2.*F*DM)
0046            IF(SIG2.NE.0.AND.I.EQ.2)FQ=B/F
0047            IF(SIG2.EQ.0.AND.I.EQ.2)FQ=(0.,-1.)
0048            IF(I.EQ.1)SUM1=SUM1+W*FF/F
0049            IF(I.EQ.2)SUM2=SUM2+W*FF*FQ/G
0050    100     SIGN=-SIGN
0051    C       type*,'npl=',np
0052            ALPH1=10.*AMAX1(K0,GC,CABS(GAM2))
0053    C       SET UP FOR SUM3 & SUM4
0054            DELAL=DEL
0055            NS=ALPH1/DELAL
0056            IF(NS.LT.20)NS=20
0057            NP=2*(NS/2)
0058            DELAL=ALPH1/NP
0059            NPT=NP/4
0060            NP=NP+1
0061            SUM3=(0.,0.)
0062            SIGN=1.
0063            DELA3=DELAL/3.
0064            IABORT=0
0065            DO 200 I=1,NP
0066            W1=3.-SIGN
0067            W=W1*DELA3
0068            IF(I.EQ.1.OR.I.EQ.NP)W=DELA3
0069    34      ALPHA=(I-1)*DELAL
0070            ALPHS=ALPHA*ALPHA
0071            G=SQRT(ALPHS+GCS)
0072            GS=G*G
0073            F=CSQRT(GAM2S+GS)
0074            F0=CSQRT(GAM0S+GS)
0075            IF(IGROND.EQ.1)RC=(F-F0)/(F+F0)
0076            IF(I0123.EQ.0)FF=FF1(G,F)*CEXP(-F*XLS)
0077            IF(I0123.EQ.1)FF=FF1(G,F)*RC*CEXP(F*(-2.*DM+XLS))
0078            IF(I0123.EQ.2)FF=FF2(G,F)
0079            IF(I0123.EQ.3)FF=FF3(G,F)*RC*CEXP(-2.*F*DM)
0080            IF(SIG2.NE.0)FQ=ALPHA/F
0081            IF(SIG2.EQ.0)FQ=(1.,0.)
0082            DSUM=W*FF*FQ/G
0083            SUM3=SUM3+DSUM
0084            IF(IABORT.EQ.1) GO TO 300
0085            IF(CABS(DSUM).LT.(CABS(SUM3)/1000.).AND.I.GT.NPT.AND.
0086         &W1.EQ.4.)THEN
0087            IABORT=1
0088            W=DELA3
0089            GO TO 34
0090            END IF
0091    200     SIGN=-SIGN
0092    C       type*,'np2=',np
0093    300     SUMT=SUM1+SUM2+SUM3
0094            RETURN
0095            END


0001    C
```

```
0002            COMPLEX FUNCTION FF1(G,F)
0003            COMPLEX FN,FM,GN,GM,F,CJ,T1,T2,T3,FMPF,GMMG,GMPG,S1,S2
0004            COMMON FN,FM,GN,GM,AM,BM,DM,XLS,YLS
0005            CJ=(0.,1.)
0006    C       TYPE*,'FF1,AM,BM,DM,XLS,YLS=',AM,BM,DM,XLS,YLS
0007            FMPF=FM+CJ*F
0008            GMMG=GM-G
0009            GMPG=GM+G
0010            S1=BM
0011            IF(CABS(GMMG).GT.1.E-6)S1=CSIN(GMMG*BM)/GMMG
0012            S2=BM
0013            IF(CABS(GMPG).GT.1.E-6)S2=CSIN(GMPG*BM)/GMPG
0014            T1=CSIN(FMPF*AM)/FMPF
0015            T2=CEXP(-CJ*G*YLS)*S1
0016            T3=CEXP(CJ*G*YLS)*S2
0017            FF1=T1*(T2+T3)
0018            RETURN
0019            END
```

```
0001    C
0002            COMPLEX FUNCTION FF2(G,F)
0003            COMPLEX FN,FM,GN,GM,F,SNK1,SNK2,SNK3,SNK4,SNK5,SNK6,SNK7,SNK8
0004            COMPLEX EX1,EX2,T1,T2,T3,T4,T5,T6,CJ
0005            COMPLEX GNPG,GNMG,GMPG,GMMG,FMFN,FNPF,FNMF,FMPF,FNMF
0006            COMMON FN,FM,GN,GM,AM,BM,DM,XLS,YLS
0007    C       TYPE*,'FF2,AM,BM,DM,XLS,YLS=',AM,BM,DM,XLS,YLS
0008            CJ=(0.,1.)
0009            GNPG=GN+G
0010            GNMG=GN-G
0011            GMPG=GM+G
0012            GMMG=GM-G
0013            FMFN=FM+FN
0014            FNPF=FN+CJ*F
0015            FNMF=FN-CJ*F
0016            FMPF=FM+CJ*F
0017            FNMF=FN-CJ*F
0018            SNK1=BM
0019            IF(CABS(GNPG).GT.1.E-6)SNK1=CSIN(GNPG*BM)/GNPG
0020            SNK2=BM
0021            IF(CABS(GMMG).GT.1.E-6)SNK2=CSIN(GMMG*BM)/GMMG
0022            SNK3=BM
0023            IF(CABS(GNMG).GT.1.E-6)SNK3=CSIN(GNMG*BM)/GNMG
0024            SNK4=BM
0025            IF(CABS(GMPG).GT.1.E-6)SNK4=CSIN(GMPG*BM)/GMPG
0026            SNK5=AM
0027            IF(CABS(FMFN).GT.1.E-6)SNK5=CSIN(FMFN*AM)/FMFN
0028            SNK6=AM
0029            IF(CABS(FNMF).GT.1.E-6)SNK6=CSIN(FNMF*AM)/FNMF
0030            SNK7=AM
0031            IF(CABS(FMPF).GT.1.E-6)SNK7=CSIN(FMPF*AM)/FMPF
0032            SNK8=SNK5
0033            EX1=AM
0034            IF(CABS(FNPF).GT.1.E-6)EX1=CEXP(CJ*FNPF*AM)/FNPF
0035            EX2=-AM
0036            IF(CABS(FNMF).GT.1.E-6)EX2=CEXP(-CJ*FNMF*AM)/FNMF
0037            T1=SNK1*SNK2
0038            T2=SNK3*SNK4
0039            T3=-SNK5/FNPF
0040            T4=EX1*SNK6
0041            T5=-EX2*SNK7
```

```
0042            T6=SNK8/FNMF
0043            FF2=-CJ*(T1+T2)*(T3+T4+T5+T6)
.C044           RETURN
0045            END
```

```
0001    C
0002            COMPLEX FUNCTION FF3(G,F)
0003            COMPLEX FN,FM,GN,GM,CJ,F
0004            COMPLEX SNK1,SNK2,SNK3,SNK4,SNK5,SNK6,T1,T2,T3
0005            COMPLEX FNPF,FMPF,GNPG,GMMG,GNMG,GMPG
0006            COMMON FN,FM,GN,GM,AM,BM,DM,XLS,YLS
0007    C       TYPE*,'FF3,AM,BM,DM,XLS,YLS=',AM,BM,DM,XLS,YLS
0008            CJ=(0.,1.)
0009            FNPF=FN+CJ*F
0010            FMPF=FM+CJ*F
0011            GNPG=GN+G
0012            GMMG=GM-G
0013            GNMG=GN-G
0014            GMPG=GM+G
0015    C       TYPE*,'G,F=',G,F
0016    C       TYPE*,'FNPF,FMPF',FNPF,FMPF
0017            SNK1=AM
0018            IF(CABS(FNPF).GT.1.E-6)SNK1=CSIN(FNPF*AM)/FNPF
0019            SNK2=AM
0020            IF(CABS(FMPF).GT.1.E-6)SNK2=CSIN(FMPF*AM)/FMPF
0021            SNK3=BM
0022            IF(CABS(GNPG).GT.1.E-6)SNK3=CSIN(GNPG*BM)/GNPG
0023            SNK4=BM
0024            IF(CABS(GMMG).GT.1.E-6)SNK4=CSIN(GMMG*BM)/GMMG
0025            SNK5=BM
0026            IF(CABS(GNMG).GT.1.E-6)SNK5=CSIN(GNMG*BM)/GNMG
0027            SNK6=BM
0028            IF(CABS(GMPG).GT.1.E-6)SNK6=CSIN(GMPG*BM)/GMPG
0029            T1=SNK1*SNK2
0030            T2=SNK3*SNK4
0031            T3=SNK5*SNK6
0032            FF3=T1*(T2+T3)
0033            RETURN
0034            END
```

APPENDIX C

The program RTUNLH is based on the formulation given in Chapters IV and VIII. All other descriptions are analogous to RTUNLE.

```
0001    C       This is program (RTUNLH.FOR) Rectangular TUNnel using
0002    C       Hz-polarization with electric field formulation.
0003    C       It uses Plane Wave Expansion Galerkin.
0004    C
0005    C       WRITTEN BY JAMAL S. IZADIAN MARCH 1982.
0006    C
0007            COMPLEX A(25),V(25),DV(25),VT(25),Z(25,25)
0008            COMPLEX FA(25),GA(25),B(25),HZ1,HZI,HZS,GR
0009            COMPLEX SUMT,RMN,SMN,FN,FM,GN,GM,S1,S2,FNFM,GNGM
0010            COMPLEX CST2,CST1,CV1,CJ,EP1,EP2,GAM1,GAM2,GAM2S
0011            COMPLEX C1,K1,K2,EXF,EXG,BK,BK1,ETA1,ETA2
0012            DIMENSION PHY(25),XM(500),YM(500)
0013            COMMON /JI/ GAM2S,GAM2,OMEGA,ER2,SIG2,EP2
0014            COMMON /JERK/ CST1,CST2,CSMN
0015            COMMON FN,FM,GN,GM,AM,BM,DM,XLS,YLS,CSN,SNN,CSM,SNM
0016            DATA PI,TP/3.14159265359,6.28318530718/
0017            DATA E0,U0/8.85418533677E-12,1.25663706144E-6/
0018            DATA IWRC,ICC,I12,ISYM/0,25,1,0/
0019            READ(7,*)ER1,SIG1,ER2,SIG2,FMCMX,NEQ,AWM,BWM,DM,XLS,YLS,IWR
0020           &,IFILD,IBS,IBISS,IFMC,IGROND,IZMN
0021            call getcp(itl)
0022            IF((AWM/2.).GT.DM.OR.XLS.GT.DM) GO TO 500
0023            WRITE(10,*)MAX(IBS,IBISS,IFMC)
0024            CJ=(0.,1.)
0025            CX=.0174533
0026            NY=1
0027    201     IF(IFMC.EQ.1)TYPE*,'GIVE FMC,NEQ,NY='
0028            IF(IFMC.EQ.1)ACCEPT*,FMC,NEQ,NY
0029.           IF(FMC.LT.0)GO TO 500
0030            DO 500 JF=1,IFMC
0031            IF(IFMC.GT.1)FMC=JF*FMCMX/FLOAT(IFMC)
0032            NX=(AWM/BWM)*NY
0033            AM=AWM/2.
0034            BM=BWM/2.
0035            OMEGA=TP*FMC*1.E6
0036            EP1=CMPLX(ER1*E0,-SIG1/OMEGA)
0037            EP2=CMPLX(ER2*E0,-SIG2/OMEGA)
0038            ETA1=CSQRT(U0/EP1)
0039            ETA2=CSQRT(U0/EP2)
0040            GAM1=OMEGA*CSQRT(-U0*EP1)
0041            BET1=AIMAG(GAM1)
0042            GAM2=OMEGA*CSQRT(-U0*EP2)
0043            GAM2S=GAM2*GAM2
0044            K1=-CJ*GAM1
0045            K2=-CJ*GAM2
0046            CST1=-OMEGA*OMEGA*U0*(EP1-EP2)/TP
0047            CST2=-(EP1-EP2)/(TP*EP2)
0048            CV1=-1./(ETA1*PI)
0049            C1=CJ*OMEGA*(EP1-EP2)*ETA1/PI
0050            DX=AWM/NX
0051            DY=BWM/NY
0052            DX2=DX/2.
0053            DY2=DY/2.
0054    C       CPH=1.-PI/(14.*BET1*AM)
0055    C       IF(ABS(CPH).GT.1)GO TO 19
0056    C       DPH=ACOS(CPH)
0057    C       NEQ=1.+PI/(2.*DPH)
0058    C       NEQ=NEQ*2
0059    C19     IF(NEQ.LT.6)NEQ=6
0060            M=0
0061            Y=-BM+DY2
0062            DO 20 J=1,NY
0063            X=-AM+DX2
```

```
0064            DO 22 I=1,NX
0065            M=M+1
0066            XM(M)=X
0067            YM(M)=Y
0068    22      X=X+DX
0069    20      Y=Y+DY
0070            KK=M
0071            DPH=TP/NEQ
0072            DO 90 J=1,NEQ
0073            A(J)=(0.,0.)
0074            B(J)=(0.,0.)
0075            PH=(J-1)*DPH
0076            PHY(J)=PH
0077            FA(J)=K1*COS(PH)
0078    90      GA(J)=K1*SIN(PH)
0079            IF(IWR.EQ.1)WRITE(10,1)
0080            IF(IZMN.EQ.0)THEN
0081            DO 92 M=1,NEQ
0082            DO 92 N=M,NEQ
0083    92      READ(8,2)I,J,Z(M,N)
0084            GO TO 404
0085            END IF
0086            DO 100 M=1,NEQ
0087            PHM=PHY(M)
0088            CSM=COS(PHM)
0089            SNM=SIN(PHM)
0090            FM=FA(M)
0091            GM=GA(M)
0092            DO 200 N=M,NEQ
0093            PHN=PHY(N)
0094            CSN=COS(PHN)
0095            SNN=SIN(PHN)
0096            CSMN=COS(PHM-PHN)
0097            FN=FA(N)
0098            GN=GA(N)
0099            FNFM=FN+FM
0100            GNGM=GN+GM
0101            S1=AM
0102            S2=BM
0103            IF(CABS(FNFM).GT.1.E-6)S1=CSIN(FNFM*AM)/FNFM
0104            IF(CABS(GNGM).GT.1.E-6)S2=CSIN(GNGM*BM)/GNGM
0105            RMN=4.*S1*S2*CSMN
0106            CALL SPCIRM(SMN,2,IGROND)
0107            Z(M,N)=RMN+SMN
0108            IF(IWR.EQ.1)WRITE(10,2)M,N,Z(M,N)
0109            IF(IZMN.EQ.1)WRITE(8,2)M,N,Z(M,N)
0110    200     CONTINUE
0111    100     CONTINUE
0112    404     CONTINUE
0113            IF(IWR.EQ.1)WRITE(10,3)
0114            IF(IWR.EQ.1)WRITE(10,4)
0115            DO 500 JI=1,IBS
0116            IF(IBS.GT.1)YLS=((IBS-1)/2+1-JI)*.0625
0117            YLSS=YLS
0118    C       SET UP THE VOLTAGE COLUMN
0119            DO 120 M=1,NEQ
0120            PH=PHY(M)
0121            CSM=COS(PH)
0122            SNM=SIN(PH)
0123            FM=FA(M)
0124            GM=GA(M)
0125            CALL SPCIRM(SUMT,1,IGROND)
0126            A(M)=SUMT
```

```
0127            V(M)=CV1*SUMT
0128    120     IF(IWR.EQ.1)WRITE(10,5)M,V(M),DV(M),VT(M)
0129            IF(IWR.EQ.1)WRITE(10,3)
0130            CALL CROUT(Z,V,ICC,ISYM,IWRC,I12,NEQ)
0131            IF(IWR.EQ.1)THEN
0132            WRITE(10,3)
0133            WRITE(10,10)
0134            DO 108 M=1,NEQ
0135    108     WRITE(10,5)M,V(M)
0136            WRITE(10,3)
0137            END IF
0138            IF(IFILD.EQ.0) GO TO 45
0139    C       FIND FIELD INSIDE THE TUNNEL
0140            WRITE(10,3)
0141            WRITE(10,6)
0142            DO 300 L=1,KK
0143            HZ1=(0.,0.)
0144            X=XM(L)
0145            Y=YM(L)
0146            IF(X.LT.0.OR.Y.LT.0) GO TO 300
0147            DO 400 N=1,NEQ
0148            FN=FA(N)
0149            GN=GA(N)
0150            EXF=CEXP(-CJ*FN*X)
0151            EXG=CEXP(-CJ*GN*Y)
0152    400     HZ1=HZ1+EXF*EXG*V(N)
0153            RE=REAL(HZ1)
0154            AIE=AIMAG(HZ1)
0155            PHASE=ATAN2(AIE,RE)/CX
0156            AMP=CABS(HZ1)
0157            WRITE(10,7)X,Y,AMP,PHASE
0158    300     CONTINUE
0159            WRITE(10,3)
0160    C       FIND SCATTERED FIELD
0161    45      DO 500 JK=1,IBISS
0162            IF(IBISS.GT.1)YLS=((IBISS-1)/2+1-JK)*.0625
0163            HZS=(0.,0.)
0164            DO 600 M=1,NEQ
0165            IF(IBISS.GT.1)THEN
0166            PH=PHY(M)
0167            CSN=COS(PH)
0168            SNM=SIN(PH)
0169            FM=FA(M)
0170            GM=GA(M)
0171            CALL SPCIRM(SUMT,1,IGRGND)
0172            A(M)=SUMT
0173            END IF
0174    600     HZS=HZS+V(M)*A(M)
0175            HZS=C1*HZS
0176            AZS=CABS(HZS)
0177            RLSO=SQRT(XLS*XLS+YLS*YLS)
0178            RLSS=SQRT(XLS*XLS+YLSS*YLSS)
0179            GR=(RLSO+RLSS)*GAM2
0180            IF(CABS(GR).GT.80.) THEN
0181            BK=CSQRT(.5*PI/GR)*CEXP(-GR)
0182            GO TO 47
0183            END IF
0184            CALL MBK0Z(GR,BK,-1)
0185    47      HZI=BK*(-GAM2/ETA2/TP)
0186            AZI=CABS(HZI)
0187            AZN=AZS/AZI
0188            IF(IWR.EQ.1)WRITE(10,*)'AZS=',AZS
0189            IF(IWR.EQ.1)WRITE(10,*)'AZI=',AZI
```

```
0190            DB=20.*ALOG10(AZN)
0191            IF(IBS.GT.1)I12=2
0192            TYPE8,NEQ,NX,NY,FMC,DB,YLS
0193            WRITE(10,8)NEQ,NX,NY,FMC,DB,YLS
0194            IF(IFMC.EQ.1.AND.IBS.EQ.1.AND.IBISS.EQ.1)GO TO 201
0195    500     CONTINUE
0196            WRITE(10,9)
0197    1       FORMAT(5X,'M',4X,'N',13X,'ZMN',24X,'DZMN',26X,'ZTMN'25X)
0198    2       FORMAT(1X,2I5,8(2X,G12.6))
0199    3       FORMAT(1H0)
0200    4       FORMAT(5X,'M',13X,' VM ',25X,'DVM',23X,'VTM',21X)
0201    5       FORMAT(1X,I5,6(2X,G12.6))
0202    6       FORMAT(9X,'X',9X,'Y',13X,'AMPLITUDE',3X,'PHASE')
0203    7       FORMAT(1X,2(2X,G10.5),5X,2(2X,G12.6))
0204    8       FORMAT(1X,3I5,6F12.6)
0205    9       FORMAT(3X,'NEQ',3X,'NX',3X,'NY',6X,'FMC',9X,'SAF')
0206    10      FORMAT(5X,'M',18X,' A ')
0207            call getcp(it2)
0208            time=(it2-it1)/100.
0209            WRITE(10,*)'ER1 & SIG1=',ER1,SIG1
0210            WRITE(10,*)'ER2 & SIG2=',ER2,SIG2
0211            WRITE(10,*)'AWM,BWM,DM,XLS,YLS=',AWM,BWM,DM,XLS,YLS
0212            write(10,*) ' cpu time=',time,'sec'
0213            WRITE(10,*)'RTUNLH.FOR'
0214            write(10,*)ER1,SIG1,ER2,SIG2,FMC,NEQ,AWM,BWM,DM,XLS,YLS,IWR
0215         &,IFILD,IBS,IBISS
0216            STOP
0217            END
```

FUNCTIONS AND SUBROUTINES REFERENCED

```
0001    C
0002            SUBROUTINE SPCIRM(SUMT,I12,IGROND)
0003            COMPLEX GAM2S,GAM2,GAM0S,FQ,RC,F,F0,FF,SUM1,SUM2,SUM3,SUMT
0004            COMPLEX FN,FM,GN,GM,CJ,FF1,FF2,FF3,EP2,DSUM
0005            REAL K0
0006            COMMON /J1/GAM2S,GAM2,OMEGA,ER2,SIG2,EP2
0007            COMMON FN,FM,GN,GM,AN,BM,DM,XLS,YLS,CSN,SNN,CSM,SNM
0008            DATA PI,TP/3.14159265359,6.28318530718/
0009            DATA E0,U0/8.85418533677E-12,1.25663706144E-6/
0010            CJ=(0.,1.)
0011            K0=OMEGA*SQRT(E0*U0)
0012            GAM0S=-K0*K0*(1.,0.)
0013            GC=OMEGA*SQRT(U0*ER2*E0)
0014            GCS=GC*GC
0015            G1=GC/SQRT(2.)
0016    C       SET UP FOR SUM1 & SUM2
0017    C       IF(I12.LT.3)DEL=PI/10./(AM+EM)
0018            DEL=PI/10./(AM+DM+EM)
0019            NS=G1/DEL
0020            IF(NS.LT.30) NS=30
0021            NP=2*(NS/2)
0022            DEL=G1/NP
0023            NP=NP+1
0024            DEL3=DEL/3.
0025            SUM1=(0.,0.)
0026            SUM2=(0.,0.)
0027            DO 100 I=1,2
0028            SIGN=1.
0029            DO 100 J=1,NP
0030            W=(3.-SIGN)*DEL3
```

```
0031            IF(J.EQ.1.OR.J.EQ.NP) W=DEL3
0032            IF(I.EQ.2)GO TO 31
0033            G=(J-1)*DEL
0034            GO TO 33
0035    31      B=(J-1)*DEL
0036            BS=B*B
0037            G=SQRT(GCS-BS)
0038    33      GS=G*G
0039            F=CSQRT(GAM2S+GS)
0040            F0=CSQRT(GAM0S+GS)
0041            RC=(E0*F-EP2*F0)/(E0*F+EP2*F0)
0042            IF(I12.EQ.1)FF=FF1(G,F)*(CEXP(-F*XLS)+IGROND*RC
0043           &*CEXP(F*(-2.*DM+XLS)))
0044            IF(I12.EQ.2.AND.IGROND.EQ.1)FF=FF3(G,F)*RC*CEXP(-2.*F*DM)
0045            IF(I12.EQ.2)FF=FF2(G,F)+IGROND*FF
0046            IF(SIG2.NE.0.AND.I.EQ.2)FQ=E/F
0047            IF(SIG2.EQ.0.AND.I.EQ.2)FQ=(0.,-1.)
0048            IF(I.EQ.1)SUM1=SUM1+W*FF/F
0049            IF(I.EQ.2)SUM2=SUM2+W*FF*FQ/G
0050    100     SIGN=-SIGN
0051    C       type*,'np1=',np
0052            ALPH1=10.*AMAX1(K0,GC,CABS(GAM2))
0053    C       SET UP FOR SUM3 & SUM4
0054            DELAL=DEL
0055            NS=ALPH1/DELAL
0056            IF(NS.LT.30) NS=30
0057            NP=2*(NS/2)
0058            DELAL=ALPH1/NP
0059            NP=NP+1
0060            SUM3=(0.,0.)
0061            SIGN=1.
0062            DELA3=DELAL/3.
0063            DO 200 I=1,NP
0064            W=(3.-SIGN)*DELA3
0065            IF(I.EQ.1.OR.I.EQ.NP)W=DELA3
0066            ALPHA=(I-1)*DELAL
0067            ALPHS=ALPHA*ALPHA
0068            G=SQRT(ALPHS+GCS)
0069            GS=G*G
0070            F=CSQRT(GAM2S+GS)
0071            F0=CSQRT(GAM0S+GS)
0072            RC=(E0*F-EP2*F0)/(E0*F+EP2*F0)
0073            IF(I12.EQ.1)FF=FF1(G,F)*(CEXP(-F*XLS)+IGROND*RC
0074           &*CEXP(F*(-2.*DM+XLS)))
0075            IF(I12.EQ.2.AND.IGROND.EQ.1)FF=FF3(G,F)*RC*CEXP(-2.*F*DM)
0076            IF(I12.EQ.2)FF=FF2(G,F)+IGROND*FF
0077            IF(SIG2.NE.0)FQ=ALPHA/F
0078            IF(SIG2.EQ.0)FQ=(1.,0.)
0079            DSUM=W*FF*FQ/G
0080            SUM3=SUM3+DSUM
0081    C       IF(CABS(DSUM).LT.(CABS(SUM3)/1000.))GO TO 300
0082    200     SIGN=-SIGN
0083    C       type*,'np2=',np
0084    300     SUMT=SUM1+SUM2+SUM3
0085            RETURN
0086            END



0001    C
0002            COMPLEX FUNCTION FF1(G,F)
0003            COMPLEX FN,FM,GN,GM,F,CJ,T1,T2,T3,FMPF,GMMG,GMPG,S1,S2
```

```
0004            COMPLEX CSY,SNY
0005            COMMON FN,FM,GN,GM,AM,BM,DM,XLS,YLS,CSN,SNN,CSM,SNM
0006            CJ=(0.,1.)
0007            FMPF=FM+CJ*F
0008            GMMG=GM-G
0009            GMPG=GM+G
0010            S1=BM
0011            IF(CABS(GMMG).GT.1.E-6)S1=CSIN(GMMG*BM)/GMMG
0012            S2=BM
0013            IF(CABS(GMPG).GT.1.E-6)S2=CSIN(GMPG*BM)/GMPG
0014            T1=CSIN(FMPF*AM)/FMPF
0015            T2=CEXP(-CJ*G*YLS)*S1
0016            T3=CEXP(CJ*G*YLS)*S2
0017            CSY=T2+T3
0018            SNY=-CJ*(T2-T3)
0019            FF1=T1*(SNM*G*SNY-CSM*F*CSY)
0020            RETURN
0021            END



0001    C
0002            COMPLEX FUNCTION FF2(G,F)
0003            COMPLEX FN,FM,GN,GM,F,SNK1,SNK2,SNK3,SNK4,SNK5,SNK6,SNK7,SNK8
0004            COMPLEX EX1,EX2,T1,T2,T3,T4,T5,T6,CJ,FXE,FXO,SNY,CSY,PEX,EXM
0005            COMPLEX EXBM,EXBP,SYBM,SYBP,CSBM,CSBP,S1,S2,S3,S4,S5,S6,S7,S8
0006            COMPLEX EXBMN,EXBPN,CST1,CST2,F1,F2
0007            COMPLEX GNPG,GNMG,GMPG,GMMG,FMFN,FNPF,FMMF,FMPF,FNMF
0008            COMMON FN,FM,GN,GM,AM,BM,DM,XLS,YLS,CSN,SNN,CSM,SNM
0009            COMMON /JERK/ CST1,CST2,CSMN
0010            CJ=(0.,1.)
0011            GNPG=GN+G
0012            GNMG=GN-G
0013            GMPG=GM+G
0014            GMMG=GM-G
0015            FMFN=FM+FN
0016            FNPF=FN+CJ*F
0017            FMMF=FM-CJ*F
0018            FMPF=FM+CJ*F
0019            FNMF=FN-CJ*F
0020            SNK1=BM
0021            IF(CABS(GNPG).GT.1.E-6)SNK1=CSIN(GNPG*BM)/GNPG
0022            SNK2=BM
0023            IF(CABS(GMMG).GT.1.E-6)SNK2=CSIN(GMMG*BM)/GMMG
0024            SNK3=BM
0025            IF(CABS(GNMG).GT.1.E-6)SNK3=CSIN(GNMG*BM)/GNMG
0026            SNK4=BM
0027            IF(CABS(GMPG).GT.1.E-6)SNK4=CSIN(GMPG*BM)/GMPG
0028            SNK5=AM
0029            IF(CABS(FMFN).GT.1.E-6)SNK5=CSIN(FMFN*AM)/FMFN
0030            SNK6=AM
0031            IF(CABS(FMMF).GT.1.E-6)SNK6=CSIN(FMMF*AM)/FMMF
0032            SNK7=AM
0033            IF(CABS(FMPF).GT.1.E-6)SNK7=CSIN(FMPF*AM)/FMPF
0034            SNK8=SNK5
0035            EX1=CEXP(CJ*FNPF*AM)/FNPF
0036            EX2=CEXP(-CJ*FNMF*AM)/FNMF
0037            T1=SNK1*SNK2
0038            T2=SNK3*SNK4
0039            T3=SNK5/FNPF
0040            T4=EX1*SNK6
0041            T5=EX2*SNK7
```

```
0042            T6=SNK8/FNMF
0043            FXE=CJ*(T3-T4+T5-T6)
0044            FXO=CJ*(T3-T4-T5+T6)
0045            CSY=T1+T2
0046            SNY=-CJ*(T1-T2)
0047            F1=FXE*CSY*CST1*CSMN*4.
0048            EXBMN=CEXP(-CJ*GN*BM)
0049            EXBPN=CEXP(CJ*GN*BM)
0050            EXBM=CEXP(-CJ*G*BM)
0051            EXBP=CEXP(CJ*G*BM)
0052            SYBM=-CJ*(EXBM*SNK2-EXBP*SNK4)
0053            SYBP=-CJ*(EXBP*SNK2-EXBM*SNK4)
0054            CSBM=EXBM*SNK2+EXBP*SNK4
0055            CSBP=EXBP*SNK2+EXBM*SNK4
0056            EXM=CEXP(-CJ*FNMF*AM)
0057            PEX=CEXP(CJ*FNPF*AM)
0058            S1=4.*EXM*SNK7*SNY
0059            S2=-4.*EXM*SNK7*CSY
0060            S3=2.*EXBMN*FXE*SYBM
0061            S4=2.*EXBMN*FXO*CSBM
0062            S5=4.*PEX*SNK6*SNY
0063            S6=4.*PEX*SNK6*CSY
0064            S7=2.*EXBPN*FXE*SYBP
0065            S8=2.*EXBPN*FXO*CSBP
0066    C       WRITE(8,*)'F,G,SNY=',F,G,SNY
0067    C       WRITE(8,*)'CSN,SNN,CSM,SNM=',CSN,SNN,CSM,SNM
0068    C       WRITE(8,*)'S1,S5=',S1,S5
0069    C       WRITE(8,*)'S2,S6=',S2,S6
0070    C       WRITE(8,*)'S3,S7=',S3,S7
0071    C       WRITE(8,*)'S4,S8=',S4,S8
0072            F2=-SNN*CSM*G*(S1-S5)+SNN*SNM*F*(S2-S6)+CSN*CSM*G*(S3-S7)
0073           &-CSN*SNM*F*(S4-S8)
0074            F2=F2*CST2
0075            FF2=F1+F2
0076    C       WRITE(8,*)'FF2=',FF2
0077            RETURN
0078            END
```

```
0001    C
0002            COMPLEX FUNCTION FF3(G,F)
0003            COMPLEX FN,FM,GN,GM,CJ,F,CST1,CST2
0004            COMPLEX SNK1,SNK2,SNK3,SNK4,SNK5,SNK6,T1,T2,T3
0005            COMPLEX FNPF,FMPF,GNPG,GMMG,GNMG,GMPG,SNY,CSY
0006            COMMON FN,FM,GN,GM,AM,BM,DM,XLS,YLS,CSN,SNN,CSM,SNM
0007            COMMON /JERK/ CST1,CST2,CSMN
0008            CJ=(0.,1.)
0009            FNPF=FN+CJ*F
0010            FMPF=FM+CJ*F
0011            GNPG=GN+G
0012            GMMG=GM-G
0013            GNMG=GN-G
0014            GMPG=GM+G
0015            SNK1=AM
0016            IF(CABS(FNPF).GT.1.E-6)SNK1=CSIN(FNPF*AM)/FNPF
0017            SNK2=AM
0018            IF(CABS(FMPF).GT.1.E-6)SNK2=CSIN(FMPF*AM)/FMPF
0019            SNK3=BM
0020            IF(CABS(GNPG).GT.1.E-6)SNK3=CSIN(GNPG*BM)/GNPG
0021            SNK4=BM
```

```
0022            IF(CABS(GMMG).GT.1.E-6)SNK4=CSIN(GMMG*BM)/GMMG
0023            SNK5=BM
0024            IF(CABS(GNMG).GT.1.E-6)SNK5=CSIN(GNMG*BM)/GNMG
0025            SNK6=BM
0026            IF(CABS(GMPG).GT.1.E-6)SNK6=CSIN(GMPG*BM)/GMPG
0027            T1=SNK1*SNK2
0028            T2=SNK3*SNK4
0029            T3=SNK5*SNK6
0030            CSY=T2+T3
0031            SNY=-CJ*(T2-T3)
0032            FF3=(SNN*SNM*G*G+CSN*CSM*F*F)*CSY
0033            FF3=FF3+(SNN*CSM-CSN*SNM)*F*G*SNY
0034            FF3=T1*FF3*CST2*8.
0035            RETURN
0036            END
```

APPENDIX D

Program RCYLHGP is the same as RTUNLH, except it does not include the air-earth interface, and it can model plane wave incidence.

```
0001    C       LINK WITH  CROUT & MBEZ10
0002    C
0003    C       THIS PROGRAM (RCYLHGP.FOR) USES TRAVELING PLANE WAVE EXPANSION AND
0004    C       GALERKIN METHOD TO CALCULATE THE SCATTERING ATTENUATION
0005    C       FUNCTION OF A LOSSY DIELECTRIC INFINITE RECTANGULAR CYLINDER,
0006    C       FOR A MAGNETIC LINE SOURCE PARALLEL TO AXIS OF THE CYLINDER.
0007    C       THE CYLINDER IS LOCATED IN A LOSSY HOMOGINEOUS MEDIUM.
0008    C
0009    C       WRITTEN BY JAMAL IZADIAN  MARCH. 1982.
0010    C
0011            COMPLEX C(25),A(25),FA(25),GA(25),FNEE(25),Z(25,25),V(25)
0012            COMPLEX FNEE(25),FMXP,GMYP,EGXP,EGYP,Sumc,Sums
0013            COMPLEX GC,VEE,EGYL,EGXL,EGX1,FNXL,GNYL,SEE,HZ1,HZS
0014            COMPLEX SUMT,RMN,SMN,FN,FM,GN,GM,S1,S2,FNFM,GNGM,HZI
0015            COMPLEX CST2,CST1,CV1,CJ,EP1,EP2,GAM1,GAM2,GAM2S,GR
0016            COMPLEX C1,CI,K1,K2,BI,BI1,BK,BK1,ETA1,ETA2,DET
0017            DIMENSION PHY(25),XM(1000),YM(1000),LL(25),MM(25)
0018            INTEGER P
0019            COMMON /JI/ GAM2S,GAM2,OMEGA,ER2,SIG2,EP2
0020            COMMON /JERK/ CST1,CST2,CSMN
0021            COMMON FN,FM,GN,GM,AM,BM,DM,XLS,YLS,CSN,SNN,CSM,SNM
0022            DATA PI,TP/3.14159265359,6.28316530718/
0023            DATA E0,U0/8.85418533677E-12,1.25663706144E-6/
0024            DATA IWRC,ICC,I12,ISYM/0,25,1,0/
0025            call getcp(it1)
0026            CJ=(0.,1.)
0027            READ(7,*)ER1,SIG1,ER2,SIG2,FMCMX,AWM,BWM,DM,XLS,YLS,IWR,IFILD,IWRC
0028           &,IPW.IBS,IBISS,IFMC,IEQ,IGROND,IZMN
0029            PHI=ATAN2(YLS,XLS)/.0174533
0030            RLS=SQRT(XLS*XLS+YLS*YLS)
0031            WPH=PHI
0032            WRITE(10,*)MAX(IBS,IBISS,IFMC)
0033            CX=.0174533
0034    201     IF(IEQ.EQ.0) TYPE*,'GIVE NEQ & NY='
0035            IF(IEQ.EQ.0) ACCEPT*,NEQ,NY
0036            IF(IFMC.EQ.1)TYPE*,'GIVE FMC='
0037            IF(IFMC.EQ.1)ACCEPT*,FMC
0038            IF(FMC.LT.0)GO TO 500
0039            DO 500 JF=1,IFMC
0040            IF(IFMC.GT.1)FMC=JF*FMCMX/FLOAT(IFMC)
0041            AM=AWM/2.
0042            BM=BWM/2.
0043            OMEGA=TP*FMC*1.E6
0044            EP1=CMPLX(ER1*E0,-SIG1/OMEGA)
0045            EP2=CMPLX(ER2*E0,-SIG2/OMEGA)
0046            ETA1=CSQRT(U0/EP1)
0047            ETA2=CSQRT(U0/EP2)
0048            GAM1=OMEGA*CSQRT(-U0*EP1)
0049            BET1=AIMAG(GAM1)
0050            GAM2=OMEGA*CSQRT(-U0*EP2)
0051            GAM2S=GAM2*GAM2
0052            WAV2=300./(SQRT(ER2)*FMC)
0053            WAV1=300./(SQRT(ER1)*FMC)
0054            K1=-CJ*GAM1
0055            K2=-CJ*GAM2
0056            CST1=-OMEGA*OMEGA*U0*(EP1-EP2)/TP
0057            CST2=-(EP1-EP2)/(TP*EP2)
0058            CV1=-GAM2/(ETA1*TP)
0059            C1=CJ*OMEGA*(EP1-EP2)*GAM2*ETA1/TP
0060            CI=-CJ*OMEGA*EP2/TP
0061            TYPE*,'AOL=',(AWM/WAV1)
0062            IF(IEQ.EQ.1)THEN
0063            NY=15.*BET1*AM/PI
```

```
0064            IF(NY.LT.8.AND.IEQ.EQ.1)NY=8
0065            CPH=1.-PI/(14.*BET1*AM)
0066            TYPE*,'CPH=',CPH
0067            IF(ABS(CPH).GT.1)GO TO 19
0068            DPH=ACOS(CPH)
0069            NEQ=1.+PI/(2.*DPH)
0070    19      IF(NEQ.LT.6)NEQ=6
0071            NEQ=NEQ*2+2
0072            END IF
0073            NY=2*(NY/2)
0074            NY=NY
0075            NX=INT(AM/BM)*NY
0076            NX=(NX/2)*2
0077            DX=AWM/NX
0078            DY=BWM/NY
0079            DX2=DX/2.
0080            DY2=DY/2.
0081            DXY=DX*DY
0082            M=0
0083            Y=-BM+DY2
0084            DO 20 J=1,NY
0085            X=-AM+DX2
0086            DO 22 I=1,NX
0087            M=M+1
0088            XM(M)=X
0089            YM(M)=Y
0090    22      X=X+DX
0091    20      Y=Y+DY
0092            KK=M
0093            IF(KK.GT.1000) GO TO 500
0094            DPH=TP/NEQ
0095            DO 90 J=1,NEQ
0096            PH=(J-1)*DPH
0097            PHY(J)=PH
0098            FA(J)=K1*COS(PH)
0099    90      GA(J)=K1*SIN(PH)
0100            IF(IZMN.EQ.0)THEN
0101            DO 92 M=1,NEQ
0102            DO 92 N=M,NEQ
0103    92      READ(8,2)I,J,Z(I,J)
0104            GO TO 404
0105            END IF
0106            IF(IWR.EQ.1)WRITE(10,1)
0107            DO 100 M=1,NEQ
0108            PHM=PHY(M)
0109            CSM=COS(PHM)
0110            SNM=SIN(PHM)
0111            FM=FA(M)
0112            GM=GA(M)
0113            DO 200 N=M,NEQ
0114            PHN=PHY(N)
0115            CSN=COS(PHN)
0116            SNN=SIN(PHN)
0117            CSMN=COS(PHM-PHN)
0118            FN=FA(N)
0119            GN=GA(N)
0120            FNFM=FN+FM
0121            GNGM=GN+GM
0122            S1=AM
0123            S2=BM
0124            IF(CABS(FNFM).GT.1.E-6)S1=CSIN(FNFM*AM)/FNFM
0125            IF(CABS(GNGM).GT.1.E-6)S2=CSIN(GNGM*BM)/GNGM
0126            RMN=4.*S1*S2*CSMN
```

```
0127            CALL SPCIRM(SMN,2)
0128            Z(M,N)=RMN+SMN
0129            IF(IWR.EQ.1)WRITE(10,2)M,N,Z(M,N)
0130            WRITE(8.2)M,N,Z(M,N)
0131    200     CONTINUE
0132    100     CONTINUE
0133            IF(IWR.EQ.1)WRITE(10,3)
0134    404     IF(IWR.EQ.1)WRITE(10,4)
0135            DO 500 JI=1,IBS
0136    C       SET UP THE VOLTAGE COLUMN
0137            RLS=SQRT(XLS*XLS+YLS*YLS)
0138            IF(IBS.GT.1)PHI=(JI-1)*360./FLOAT(IBS-1)
0139            PH1=CX*PHI
0140            CS1=COS(PH1)
0141            SN1=SIN(PH1)
0142            XLS1=RLS*CS1
0143            YLS1=RLS*SN1
0144            DO 240 M=1,NEQ
0145            FM=FA(M)
0146            GM=GA(M)
0147            PHM=PHY(M)
0148            SEE=(0.,0.)
0149            DO 220 P=1,KK
0150            X=XM(P)
0151            Y=YM(P)
0152            FMXP=-CJ*FM*X
0153            GMYP=-CJ*GM*Y
0154            EGXP=CEXP(FMXP)
0155            EGYP=CEXP(GMYP)
0156            FMEE(M)=EGXP*EGYP
0157            IF(IPW.EQ.1)THEN
0158            PSI1=X*CS1+Y*SN1
0159            EGX1=CEXP(GAM2*PSI1)
0160            CV1=-ETA2/ETA1
0161            PH=PH1
0162            GO TO 219
0163            END IF
0164            X1=X-XLS1
0165            Y1=Y-YLS1
0166            PH=ATAN2(Y1,X1)
0167            RH1=SQRT(X1*X1+Y1*Y1)
0168            CALL MBEZ10(GAM2*RH1,BI,BK,BI1,EGX1,1,-1)
0169    219     SEE=SEE+FMEE(M)*EGX1*COS(PHM-PH)
0170    220     CONTINUE
0171            A(M)=SEE
0172            V(M)=A(M)*CV1*DXY
0173    240     CONTINUE
0174            IF(IWR.EQ.1)THEN
0175            DO 202 M=1,NEQ
0176    202     WRITE(10,5)M,V(M)
0177            WRITE(10,3)
0178            END IF
0179            CALL CROUT(Z,V,ICC,ISYM,IWRC,I12,NEQ)
0180    C       CALL CMINV(A,V,Z,ICC,IWRC,I12,LL,MM,NEQ,DET)
0181    C       DO 242 M=1,NEQ
0182    C242    V(M)=A(M)
0183            IF(IWR.EQ.1)THEN
0184            WRITE(10,6)
0185            DO 244 M=1,NEQ
0186            WRITE(10,5)M,V(M)
0187    244     CONTINUE
0188            WRITE(10,3)
0189            END IF
```

```
0190    C       FIND THE FIELD IN CELLS OF FIRST QUADRANT
0191            IF(IFILD.NE.1) GO TO 45
0192            WRITE(10,8)
0193            DO 248 L=1,KK
0194            HZ1=(0.,0.)
0195            XL=XM(L)
0196            YL=YM(L)
0197            DO 246 N=1,NEQ
0198            FN=FA(N)
0199            GN=GA(N)
0200            FNXL=-CJ*FN*XL
0201            GNYL=-CJ*GN*YL
0202            EGXL=CEXP(FNXL)
0203            EGYL=CEXP(GNYL)
0204            FNEE(N)=EGXL*EGYL
0205            HZ1=HZ1+V(N)*FNEE(N)
0206    246     CONTINUE
0207            IF(XL.GT.0.AND.YL.GT.0) THEN
0208            RE=REAL(HZ1)
0209            AIE=AIMAG(HZ1)
0210            AMP=CABS(HZ1)
0211            PHASE=ATAN2(AIE,RE)/CX
0212            WRITE(10,11)XL,YL,AMP,PHASE
0213            END IF
0214    248     CONTINUE
0215    45      IF(IWR.EQ.1)WRITE(10,3)
0216            PHS=PH1
0217            DO 500 JK=1,IBISS
0218.           IF(IBISS.GT.1)THEN
0219            PHI=(JK-1)*360./FLOAT(IBISS-1)
0220            PHS=CX*PHI
0221            END IF
0222            XLS=RLS*COS(PHS)
0223            YLS=RLS*SIN(PHS)
0224    C       FIND THE BACKSCATTERED FIELD
0225            HZS=(.0,.0)
0226            DO 292 N=1,NEQ
0227            IF(IBISS.GT.1)THEN
0228            FN=FA(N)
0229            GN=GA(N)
0230            PHN=PHY(N)
0231            A(N)=(0.,0.)
0232            DO 290 L=1,KK
0233            XL=XM(L)
0234            YL=YM(L)
0235            IF(IPW.EQ.1)THEN
0236            PSI=XL*COS(PHS)+YL*SIN(PHS)
0237            BK1=CEXP(GAM2*PSI)
0238            PH=PHS
0239            GO TO 47
0240            END IF
0241            YY=YLS-YL
0242            YS=YY*YY
0243            XX=XLS-XL
0244            XS=XX*XX
0245            PH=ATAN2(YY,XX)
0246            ROH=SQRT(XS+YS)
0247            CALL MBEZ10(GAM2*ROH,BI,BK,BI1,BK1,1,-1)
0248    47      FNXL=-CJ*FN*XL
0249            GNYL=-CJ*GN*YL
0250            EGXL=CEXP(FNXL)
0251            EGYL=CEXP(GNYL)
0252            FNEE(N)=EGXL*EGYL
```

```
0253    290     A(N)=A(N)+BK1*FNEE(N)*COS(PHN-PH)
0254            END IF
0255    292     HZS=HZS+V(N)*A(N)
0256            HZS=C1*HZS*DXY
0257            IF(IPW.EQ.1)HZS=HZS*CSQRT(.5*PI/GAM2)
0258            AZS=CABS(HZS)
0259            IF(IWR.EQ.1)WRITE(10,*)'AZS=',AZS
0260            EWL=TP*AZS*AZS/WAV2
0261            DB=.0
0262    C       FIND THE NORMALIZED SCATTERING ATTENUATION FUNCTION
0263            IF(IPW.EQ.0)THEN
0264            GR=2.*GAM2*RLS
0265            IF(CABS(GR).GT.80) THEN
0266            BK=CSQRT(.5*PI/GR)*CEXP(-GR)
0267            GO TO 555
0268            END IF
0269            CALL MBESJ0(GR,BI,BK,BI1,BK1,0,-1)
0270    555     HZI=CI*BK
0271            TYPE*,'HZI=',HZI
0272            AZI=CABS(HZI)
0273            IF(IWR.EQ.1)WRITE(10,*)'AZI=',AZI
0274            AZN=AZS/AZI
0275            IF(AZN.NE.0.)DB=20.*ALOG10(AZN)
0276            TYPE9,NEQ,NX,NY,FMC,DB,PHI
0277            WRITE(10,9)NEQ,NX,NY,FMC,DB,PHI
0278            GO TO 599
0279            END IF
0280            TYPE9,NEQ,NX,NY,FMC,EWL,PHI
0281            WRITE(10,9)NEQ,NX,NY,FMC,EWL,PHI
0282    599     IF(IBS.EQ.1.AND.IBISS.EQ.1.AND.IFMC.EQ.1)GO TO 201
0283            IF(IBS.GT.1)I12=2
0284    500     CONTINUE
0285    600     CONTINUE
0286            IF(IPW.EQ.1)WRITE(10,14)
0287            IF(IPW.EQ.0)WRITE(10,13)
0288            WRITE(10,3)
0289            WRITE(10,*)' ER1 & SIG1 =',ER1,SIG1
0290            WRITE(10,*)' ER2 & SIG2 =',ER2,SIG2
0291            WRITE(10,*)' AWM & BWM =' ,AWM,BWM
0292            WRITE(10,*) 'RLS=',RLS,'PHI=',WPH
0293            call getcp(it2)
0294            time=(it2-it1)/100.
0295            WRITE(10,*) ' CPU TIME (SEC) =',TIME
0296            TYPE*,' CPU TIME (SEC) = ',TIME
0297            WRITE(10,*) 'RCYLHGP.FOR'
0298    1       FORMAT(5X,'M',4X,'N',13X,'ZMN',24X,'DZMN',26X,'ZTMN'25X)
0299    2       FORMAT(1X,2I5,8(2X,G12.6))
0300    3       FORMAT(1H0)
0301    4       FORMAT(5X,'M',13X,' VM ',25X,'DVM',23X,'VIM',21X)
0302    5       FORMAT(1X,I5,6(2X,G12.6))
0303    6       FORMAT(5X,'M',18X,' A ')
0304    8       FORMAT(5X,'X',9X,'Y',13X,'AMPLITUDE',3X,'PHASE')
0305    9       FORMAT(1X,3I5,6F12.6)
0306    11      FORMAT(1X,2(2X,G10.5),5X,2(2X,G12.6))
0307    13      FORMAT(3X,'NEQ',3X,'NX',3X,'NY',6X,'FMC',9X,'SAF',9X,'PHI')
0308    14      FORMAT(3X,'NEQ',3X,'NX',3X,'NY',6X,'FMC',9X,'EWL',9X,'PHI')
0309            CALL EXIT
0310            STOP
0311            END


0001    C
```

```
0002            SUBROUTINE SPCIRM(SUMT,I0123)
0003            COMPLEX GAM2S,GAM2,GAM0S,FQ,RC,F,F0,FF,SUM1,SUM2,SUM3,SUMT
0004            COMPLEX FN,FM,GN,GM,CJ,FF1,FF2,FF3,EP2,DSUM
0005            REAL K0
0006            COMMON /JI/GAM2S,GAM2,OMEGA,ER2,SIG2,EP2
0007            COMMON FN,FM,GN,GM,AN,BM,DM,XLS,YLS,CSN,SNN,CSM,SNM
0008            DATA PI,TP/3.14159265359,6.28318530718/
0009            DATA E0,U0/8.85418533677E-12,1.25663706144E-6/
0010            CJ=(0.,1.)
0011            K0=OMEGA*SQRT(E0*U0)
0012            GAM0S=-K0*K0*(1.,0.)
0013            GC=OMEGA*SQRT(U0*ER2*E0)
0014            GCS=GC*GC
0015            G1=GC/SQRT(2.)
0016    C       SET UP FOR SUM1 & SUM2
0017            IF(I0123.LT.3)DEL=PI/10./(AM+BM)
0018            IF(I0123.EQ.3)DEL=PI/10./(AM+BM+BM)
0019            NS=G1/DEL
0020            IF(NS.LT.20) NS=20
0021            NP=2*(NS/2)
0022            DEL=G1/NP
0023            NP=NP+1
0024            DEL3=DEL/3.
0025            SUM1=(0.,0.)
0026            SUM2=(0.,0.)
0027            DO 100 I=1,2
0028            SIGN=1.
0029            DO 100 J=1,NP
0030            W=(3.-SIGN)*DEL3
0031            IF(J.EQ.1.OR.J.EQ.NP) W=DEL3
0032            IF(I.EQ.2)GO TO 31
0033            G=(J-1)*DEL
0034            GO TO 33
0035    31      B=(J-1)*DEL
0036            BS=B*B
0037            G=SQRT(GCS-BS)
0038    33      GS=G*G
0039            F=CSQRT(GAM2S+GS)
0040            F0=CSQRT(GAM0S+GS)
0041            IF(I0123.EQ.2)FF=FF2(G,F)
0042            IF(SIG2.NE.0.AND.I.EQ.2)FQ=B/F
0043            IF(SIG2.EQ.0.AND.I.EQ.2)FQ=(0.,-1.)
0044            IF(I.EQ.1)SUM1=SUM1+W*FF/F
0045            IF(I.EQ.2)SUM2=SUM2+W*FF*FQ/G
0046    100     SIGN=-SIGN
0047    C       type*,'npl=',np
0048            FACT=5.
0049            ALPH1=FACT*AMAX1(K0,GC,CABS(GAM2))
0050    C       SET UP FOR SUM3 & SUM4
0051            DELAL=DEL
0052            NS=ALPH1/DELAL
0053            IF(NS.LT.20)NS=20
0054            NP=2*(NS/2)
0055            DELAL=ALPH1/NP
0056            NPT=NP/4
0057            NP=NP+1
0058    C       type*,'np & npt =',np,npt
0059            SUM3=(0.,0.)
0060            SIGN=1.
0061    C       IABORT=0
0062            DELA3=DELAL/3.
0063            DO 200 I=1,NP
0064            W1=3.-SIGN
```

```
0065            W=W1*DELA3
0066            IF(I.EQ.1.OR.I.EQ.NP)W=DELA3
0067    34      ALPHA=(I-1)*DELAL
0068    C       type*,'i & w =',i,w
0069            ALPHS=ALPHA*ALPHA
0070            G=SQRT(ALPHS+GCS)
0071            GS=G*G
0072            F=CSQRT(GAM2S+GS)
0073            F0=CSQRT(GAM0S+GS)
0074            IF(I0123.EQ.2)FF=FF2(G,F)
0075            IF(SIG2.NE.0)FQ=ALPHA/F
0076            IF(SIG2.EQ.0)FQ=(1.,0.)
0077            DSUM=W*FF*FQ/G
0078            SUM3=SUM3+DSUM
0079    C       IF(IABORT.EQ.1) GO TO 300
0080    C       IF(CABS(DSUM).LT.(CABS(SUM3)/1000.).AND.I.GT.NPT.AND.W1.EQ.4.
0081    C      &)THEN
0082    C       IABORT=1
0083    C       W=DELA3
0084    C       GO TO 34
0085    C       END IF
0086    200     SIGN=-SIGN
0087    C       type*,'np2=',np
0088    300     SUMT=SUM1+SUM2+SUM3
0089            RETURN
0090            END
```

FUNCTIONS AND SUBROUTINES REFERENCED

```
0001    C
0002    C
0003            COMPLEX FUNCTION FF2(G,F)
0004            COMPLEX FN,FM,GN,GM,F,SNK1,SNK2,SNK3,SNK4,SNK5,SNK6,SNK7,SNK8
0005            COMPLEX EX1,EX2,T1,T2,T3,T4,T5,T6,CJ.FXE,FXO,SNY,CSY,PEX,EXM
0006            COMPLEX EXBM,EXBP,SYBM,SYBP,CSBM,CSBP,S1,S2,S3,S4,S5,S6,S7,S8
0007            COMPLEX EXEMN,EXBPN,CST1,CST2,F1,F2
0008            COMPLEX GNPG,GNMG,GMPG,GMMG,FMFN,FNPF,FMMF,FMPF,FNMF
0009            COMMON FN,FM,GN,GM,AM,BM,DM,XLS,YLS,CSN,SNN,CSM,SNM
0010            COMMON /JERK/ CST1,CST2,CSMN
0011            CJ=(0.,1.)
0012            GNPG=GN+G
0013            GNMG=GN-G
0014            GMPG=GM+G
0015            GMMG=GM-G
0016            FMFN=FM+FN
0017            FNPF=FN+CJ*F
0018            FMMF=FM-CJ*F
0019            FMPF=FM+CJ*F
0020            FNMF=FN-CJ*F
0021            SNK1=BM
0022            IF(CABS(GNPG).GT.1.E-6)SNK1=CSIN(GNPG*BM)/GNPG
0023            SNK2=BM
0024            IF(CABS(GMMG).GT.1.E-6)SNK2=CSIN(GMMG*BM)/GMMG
0025            SNK3=BM
0026            IF(CABS(GNMG).GT.1.E-6)SNK3=CSIN(GNMG*BM)/GNMG
0027            SNK4=BM
0028            IF(CABS(GMPG).GT.1.E-6)SNK4=CSIN(GMPG*BM)/GMPG
0029            SNK5=AM
0030            IF(CABS(FMFN).GT.1.E-6)SNK5=CSIN(FMFN*AM)/FMFN
0031            SNK6=AM
0032            IF(CABS(FMMF).GT.1.E-6)SNK6=CSIN(FMMF*AM)/FMMF
```

```
0033            SNK7=AM
0034            IF(CABS(FMPF).GT.1.E-6)SNK7=CSIN(FMPF*AM)/FMPF
0035            SNK8=SNK5
0036            EX1=CEXP(CJ*FNPF*AM)/FNPF
0037            EX2=CEXP(-CJ*FNMF*AM)/FNMF
0038            T1=SNK1*SNK2
0039            T2=SNK3*SNK4
0040            T3=SNK5/FNPF
0041            T4=EX1*SNK6
0042            T5=EX2*SNK7
0043            T6=SNK8/FNMF
0044            FXE=CJ*(T3-T4+T5-T6)
0045            FXO=CJ*(T3-T4-T5+T6)
0046            CSY=T1+T2
0047            SNY=-CJ*(T1-T2)
0048            F1=4.*FXE*CSY*CST1*CSMN
0049            EXBMN=CEXP(-CJ*GN*BM)
0050            EXBPN=CEXP(CJ*GN*BM)
0051            EXBM=CEXP(-CJ*G*BM)
0052            EXBP=CEXP(CJ*G*BM)
0053            SYBM=-CJ*(EXBM*SNK2-EXBP*SNK4)
0054            SYBP=-CJ*(EXBP*SNK2-EXBM*SNK4)
0055            CSBM=EXBM*SNK2+EXBP*SNK4
0056            CSBP=EXBP*SNK2+EXBM*SNK4
0057            EXM=CEXP(-CJ*FNMF*AM)
0058            PEX=CEXP(CJ*FNPF*AM)
0059            S1=4.*EXM*SNK7*SNY
0060            S2=-4.*EXM*SNK7*CSY
0061            S3=2.*EXBMN*FXE*SYBM
0062            S4=2.*EXBMN*FXO*CSBM
0063            S5=4.*PEX*SNK6*SNY
0064            S6=4.*PEX*SNK6*CSY
0065            S7=2.*EXBPN*FXE*SYBP
0066            S8=2.*EXBPN*FXO*CSBP
0067    C       T1=SNN*CSM*G*(S1-S5)
0068    C       T2=SNN*SNM*F*(S2-S6)
0069    C       T3=CSN*CSM*G*(S3-S7)
0070    C       T4=CSN*SNM*F*(S4-S8)
0071    C       WRITE(8,*)'F,G,SNY=',F,G,SNY
0072    C       WRITE(8,*)'CSN,SNN,CSM,SNM=',CSN,SNN,CSM,SNM
0073    C       WRITE(8,*)'T1,T2=',T1,T2
0074    C       WRITE(8,*)'T3,T4=',T3,T4
0075    C       WRITE(8,*)'S3,S7=',S3,S7
0076    C       WRITE(8,*)'S4,S8=',S4,S8
0077            F2=-SNN*CSM*G*(S1-S5)+SNN*SNM*F*(S2-S6)+CSN*CSM*G*(S3-S7)
0078           &-CSN*SNM*F*(S4-S8)
0079            F2=F2*CST2
0080            FF2=F1+F2
0081    C       WRITE(8,*)'FF2=',FF2
0082            RETURN
0083            END
```

APPENDIX E

Subroutine SMRFLD2 is based on the formulation of Section E in Chapter V. The program uses Figure 5-3 as its model. The evaluated integral is output as SUMT. The rest of the inputs are self explanatory.

```
0001            SUBROUTINE SMRFLD2(X,Y,XP,YP,D,ER2,SIG2,FMC,I01,SUMT)
0002    C
0003    C       THIS IS PROGRAM (SMRFLD2.FOR) WHICH USES SIMPSON'S
0004    C       RULE TO INTEGRATE A SUMMERFELD INTEGRAL FROM ZERO TO INFINITY.
0005    C       IT CAN BE USED TO TEST A MODIFIED BESSEL FUNCTION K0(Z)
0006    C       IF I01= 1 RC IS THE ELECTRIC REF. COEF.
0007    C       IF I01=-1 RC IS THE MAGNETIC REF. COEF.
0008    C       IF I01= 0 RC IS = 1.
0009    C       IF I01> 1 RC IS =-1.
0010    C
0011    C       PROGRAM WRITTEN BY JAMAL S. IZADIAN NOV.-81
0012    C
0013            COMPLEX GAM2S,GAM2,F,FF,SUM1,SUM2,SUM3,SUM4,SUMT,EP2
0014            COMPLEX S1,S2,S3,GAM,GAM0S,FQ,C1,F0,RC,EF,C2,AA,EXAA,Z
0015            REAL K0
0016            DATA PI,TP/3.14159265359,6.28318530718/
0017            DATA E0,U0/8.85418533677E-12,1.25663706144E-6/
0018            IF(IABS(I01).GE.1)ARG=2.*D-X-XP
0019            IF(IABS(I01).EQ.0)ARG=ABS(X-XP)
0020            OMEGA=TP*FMC*1.E6
0021            K0=OMEGA*SQRT(E0*U0)
0022            GAM0S=-K0*K0*(1.,0.)
0023            EP2=CMPLX(ER2*E0,-SIG2/OMEGA)
0024            GAM2S=-OMEGA*OMEGA*U0*EP2
0025            GAM2=CSQRT(GAM2S)
0026            C1=(0.,-1.)*OMEGA*U0/TP
0027            GC=OMEGA*SQRT(U0*ER2*E0)
0028            GCS=GC*GC
0029            C2=((0.,1.)*OMEGA*U0*SIG2+GAM0S-GCS)/8.
0030            G1=GC/SQRT(2.)
0031    C       SET UP FOR SUM1 & SUM2
0032            DEL=PI/10./(ARG+Y-YP)
0033            NS=G1/DEL
0034            IF(NS.LT.40) NS=40
0035            NP=2*(NS/2)
0036            DEL=G1/NP
0037            NP=NP+1
0038            DEL3=DEL/3.
0039            SUM1=(0.,0.)
0040            SUM2=(0.,0.)
0041            DO 100 I=1,2
0042            SIGN=1.
0043            DO 100 J=1,NP
0044            W=(3.-SIGN)*DEL3
0045            IF(J.EQ.1.OR.J.EQ.NP) W=DEL3
0046            IF(I.EQ.2)GO TO 31
0047            G=(J-1)*DEL
0048            GO TO 33
0049    31      B=(J-1)*DEL
0050            BS=B*B
0051            G=SQRT(GCS-BS)
0052    33      GS=G*G
0053            F=CSQRT(GAM2S+GS)
0054            F0=CSQRT(GAM0S+GS)
0055            IF(I01.EQ.1)RC=(F-F0)/(F+F0)
0056            IF(I01.EQ.-1)RC=(E0*F-EP2*F0)/(E0*F+EP2*F0)
0057            IF(IABS(I01).EQ.0)RC=(1.,0.)
0058            IF(IABS(I01).GT.1)RC=(-1,0.)
0059            EF=CEXP(-F*ARG)
0060            CS=COS(G*(Y-YP))
0061            FF=RC*EF*CS
0062            IF(SIG2.NE.0.AND.I.EQ.2)FQ=B/F
0063            IF(SIG2.EQ.0.AND.I.EQ.2)FQ=(0.,-1.)
```

```
0064            IF(I.EQ.1)SUM1=SUM1+W*FF/F
0065            IF(I.EQ.2)SUM2=SUM2+W*FF*FQ/G
0066            SIGN=-SIGN
0067    100     CONTINUE
0068            ALPH1=15./ARG
0069    C       SET UP FOR SUM3 & SUM4
0070            DELAL=DEL
0071            NS=ALPH1/DELAL
0072            IF(NS.LT.40)NS=40
0073            NP=2*(NS/2)
0074            DELAL=ALPH1/NP
0075            NP=NP+1
0076            SUM3=(0.,0.)
0077            SIGN=1.
0078            DELA3=DELAL/3.
0079            DO 200 I=1,NP
0080            W=(3.-SIGN)*DELA3
0081            IF(I.EQ.1.OR.I.EQ.NP)W=DELA3
0082            ALPHA=(I-1)*DELAL
0083            ALPHS=ALPHA*ALPHA
0084            G=SQRT(ALPHS+GCS)
0085            GS=G*G
0086            F=CSQRT(GAM2S+GS)
0087            F0=CSQRT(GAM0S+GS)
0088            IF(IOI.EQ.1)RC=(F-F0)/(F+F0)
0089            IF(IOI.EQ.-1)RC=(E0*F-EP2*F0)/(E0*F+EP2*F0)
0090            IF(IABS(IOI).EQ.0)RC=(1.,0.)
0091            IF(IABS(IOI).GT.1)RC=(-1.,0.)
0092            EF=CEXP(-F*ARG)
0093            CS=COS(G*(Y-YP))
0094            FF=RC*EF*CS
0095            IF(SIG2.NE.0)FQ=ALPHA/F
0096            IF(SIG2.EQ.0)FQ=(1.,0.)
0097            SUM3=SUM3+W*FF*FQ/G
0098            SIGN=-SIGN
0099    200     CONTINUE
0100            SUM4=(0.,0.)
0101            SIGN=1.
0102            DO 300 J=1,2
0103            GAM=-ARG+(0.,1.)*SIGN*(Y-YP)
0104            AA=GAM*ALPH1
0105            Z=-AA
0106            EXAA=CEXP(AA)
0107            S1=.5*EXAA/ALPH1/ALPH1
0108            S2=.5*GAM*EXAA/ALPH1
0109            EI=.711093/(Z+.415775)
0110            EI=EI+.278518/(Z+2.29428)
0111            EI=EI+.010389/(Z+6.29)
0112            EI=EI*CEXP(-Z)
0113            S3=GAM*GAM*.5*EI
0114            SUM4=SUM4+S1+S2+S3
0115    300     SIGN=-1.
0116            SUM4=SUM4*C2
0117            SUMI=SUM1+SUM2+SUM3+SUM4
0118            RETURN
0119            END
```

APPENDIX F

Computer program RCYLEGP is the same as RTUNLE except, this has used Trapazoidal rule to integrate all the integrations over the cross section. The treatment is similar to RCYLPWE of Appendix A. In addition this program models the air-earth interface. When the interface is not modeled, the plane wave incidence excitation may also be used.

```
0001    C       LINK WITH  CROUT & MBEZ10
0002    C
0003    C       THIS PROGRAM (RCYLEGP.FOR) USES TRAVELING PLANE WAVE EXPANSION
0004    C       AND GALERKIN METHOD TO CALCULATE THE SCATTERED FIELD BY
0005    C       A LOSSY DIELECTRIC INFINITE RECTANGULAR CYLINDER, AND
0006    C       FOR AN ELECTRIC LINE SOURCE PARALLEL TO AXIS OF THE CYLINDER.
0007    C       THE CYLINDER MAY BE IMMERSED IN A LOSSY HOMOGENEOUS MEDIUM,
0008    C       OR IT MAY BE BURIED IN A LOSSY HOMOGENEOUS  EARTH.
0009    C
0010    C       WRITTEN BY JAMAL IZADIAN  JAN. 1982.
0011    C
0012            COMPLEX BKK(25,25),FNEE(25),FMEE(25),FK(75),CMN(25,25),B(25)
0013            COMPLEX A(25),FA(25),GA(25),DCMN(25,25),CIMN(25,25)
0014            COMPLEX EZSR,C1,GC,VEE,SUMT,SDD
0015            COMPLEX EGXP,EGYP,EGXL,EGYL,EGX1,FN,FM,GN,GM
0016            COMPLEX EZI,FPF,GPG,SS1,SS2
0017            COMPLEX SFPF,SGPG,FMXP,GMYP,FNXL,GNYL
0018            COMPLEX CSF,CII,CIK,CV1,EP1,EP2,ETA2,CST,CSS,EZ1,EZS,SEE
0019            COMPLEX GAM1,GAM2,BI,BK,BI1,BK1,GR,K1,K2,REE
0020            DIMENSION XM(450),YM(450)
0021            INTEGER P
0022            DATA FP,TD2,CX/12.5663706144,0.,.0174533/
0023            DATA ETA,PI,TP/376.730366239,3.14159265359,6.28318530718/
0024            DATA ICC,NYX,ISIZE,NJ,ITBL/25,30,10,0,0/
0025            DATA E0,U0/8.85418533677E-12,1.25663706144E-6/
0026            call getcp(itl)
0027            READ(7,*)ER1,SIG1,ER2,SIG2,FMCMX,AWM,BWM,DM,XLS,YLS,IWR,
0028           &IFILD,IWRC,IPW,IBS,IBISS,IFMC,IEQ,IGROND
0029            PHI=ATAN2(YLS,XLS)/.0174533
0030            RLS=SQRT(XLS*XLS+YLS*YLS)
0031            WPH=PHI
0032            IF(IEQ.EQ.0)TYPE*,'GIVE NEQ & NY ='
0033            IF(IEQ.EQ.0)ACCEPT*,NEQ,NY
0034            IF(IFMC.GT.1) GO TO 41
0035    20      TYPE*,'GIVE FMC='
0036            ACCEPT*,FMC
0037            IF(FMC.LT.0) GO TO 600
0038    41      DO 500 JF=1,IFMC
0039            IF(IFMC.GT.1)FMC=JF*FMCMX/FLOAT(IFMC)
0040            I12=1
0041            AM=AWM/2.
0042            BM=BWM/2.
0043            OMEGA=TP*FMC*1.E6
0044            BTS1=OMEGA*OMEGA*U0*ER1*E0
0045            BET1=SQRT(BTS1)
0046            EP1=CMPLX(ER1*E0,-SIG1/OMEGA)
0047            EP2=ER2*E0*(1.,.0)
0048            IF(TD2.GT.1.E-10)EP2=ER2*E0*CMPLX(1.,-TD2)
0049            IF(SIG2.GT.1.E-10)EP2=CMPLX(ER2*E0,-SIG2/OMEGA)
0050            ETA2=CSQRT(U0/EP2)
0051            GAM2=OMEGA*CSQRT(-U0*EP2)
0052            GAM1=OMEGA*CSQRT(-U0*EP1)
0053            K1=(0.,-1.)*GAM1
0054            K2=(0.,-1.)*GAM2
0055            BET2=AIMAG(GAM2)
0056            BTS2=BET2*BET2
0057            WAV1=TP/BET1
0058            WAV2=TP/BET2
0059            CPH=1.-PI/(14.*BET1*AM)
0060            DPH=ACOS(CPH)
0061            IF(IEQ.EQ.1)NEQ=(1.+PI/(2.*DPH))*2
0062            IF(NEQ.LT.4) NEQ=4
```

```
0063            IF(NEQ.GT.ICC)GO TO 600
0064            IF(IEQ.EQ.1)NY=15.*BETl*BWM/PI
0065            IF(NY.LT.6.AND.IEQ.EQ.1)NY=6
0066            IF(NY.GT.NYX) NY=NYX
0067            NY=2*(NY/2)
0068            NX=INT(AM/EM)*NY
0069            NX=(NX/2)*2
0070            NY2=NY/2
0071            NX2=NX/2
0072            KK=NX*NY
0073            DPH=TP/NEQ
0074            DO 90 J=1,NEQ
0075            PH=(J-1)*DPH
0076            FA(J)=K1*COS(PH)
0077            GA(J)=K1*SIN(PH)
0078    90      CONTINUE
0079            DX=AWM/NX
0080            DY=BWM/NY
0081            DXY=DX*DY
0082            DX2=DX/2.
0083            DY2=DY/2.
0084    C       FIND THE RADIOUS OF EQUIVLANT CIRCULAR CELL
0085            CM=SQRT(DX*DY/PI)
0086            GC=GAM2*CM
0087            CALL MBEZ10(GAM2*CM,BI,BK,BI1,BK1,1,-1)
0088            CSF=-OMEGA*OMEGA*U0*(EP1-EP2)*DXY*DXY/TP
0089            CSS=(1.-GC*BK1)*(EP1-EP2)/EP2
0090            CST=GC*BI1*(EP1-EP2)/EP2
0091.           CIK=CSS*2.*PI*CM*BI1/GAM2
0092            CII=CST*2.*PI*CM*BI1/GAM2
0093            CV1=-ETA2*CM*BI1
0094            C1=(0.,-1.)*OMEGA*U0/TP
0095            RAB=SQRT(AWM*AWM+BWM*BWM)
0096    21      DELTR=(RAB-DX)/ISIZE
0097            IF(DX.GT.DELTR) GO TO 23
0098            ISIZE=ISIZE+5
0099            GO TO 21
0100    23      DO 22 I=1,ISIZE
0101            RR=I*DELTR
0102            CALL MBK0Z(GAM2*RR,BK,-1)
0103            FK(I)=BK*CII
0104    22      CONTINUE
0105            TYPE*,'ISIZE=',ISIZE
0106            M=0
0107            Y=-EM+DY2
0108    C       SET UP THE COORDINATES OF CENTERS OF CELL M
0109            DO 40 J=1,NY
0110            X=-AM+DX2
0111            DO 30 I=1,NX
0112            M=M+1
0113            XM(M)=X
0114            YM(M)=Y
0115    30      X=X+DX
0116    40      Y=Y+DY
0117            DO 42 J=1,25
0118            DO 42 I=1,25
0119    42      BKK(I,J)=(0.,0.)
0120    C       SET UP IMPEDANCE MATRIX
0121            DO 200 M=1,NEQ
0122            FM=FA(M)
0123            GM=GA(M)
0124            DO 180 N=M,NEQ
0125            FN=FA(N)
```

```
0126            GN=GA(N)
0127            FPF=FN+FM
0128            GPG=GN+GM
0129            SFPF=CSIN(FPF*AM)
0130            SGPG=CSIN(GPG*BM)
0131            SS1=AM
0132            IF(CABS(FPF).GT.J.E-6)SS1=SFPF/FPF
0133            SS2=BM
0134            IF(CABS(GPG).GT.1.E-6)SS2=SGPG/GPG
0135            REE=4.*SS1*SS2
0136            DCMN(M,N)=(0.,0.)
0137            CMN(M,N)=REE
0138      180 CONTINUE
0139      200 CONTINUE
0140            DO 160 P=1,KK
0141            XP=XM(P)
0142            YP=YM(P)
0143            JP=(P-1)/NX+1
0144            IP=P-(JP-1)*NX
0145            DO 140 L=1,KK
0146            XL=XM(L)
0147            YL=YM(L)
0148            JL=(L-1)/NX+1
0149            IL=L-(JL-1)*NX
0150            YY=YP-YL
0151            YS=YY*YY
0152            XX=XP-XL
0153            XS=XX*XX
0154            II=1+IABS(IP-IL)
0155            JJ=1+IABS(JP-JL)
0156            ROH=SQRT(XS+YS)
0157            IF(ROH.LT.DX2) GO TO 79
0158            IF(EKK(II,JJ).EQ.(0.,0.))THEN
0159            CALL INTERP(ROH,BKK(II,JJ),DELTR,FK,ISIZE)
0160            BKK(JJ,II)=BKK(II,JJ)
0161            NJ=NJ+1
0162            END IF
0163     79     DO  80 M=1,NEQ
0164            FM=FA(M)
0165            GM=GA(M)
0166            FMXP=FM*XP*(0.,-1.)
0167            GMYP=GM*YP*(0.,-1.)
0168            EGXP=CEXP(FMXP)
0169            EGYP=CEXP(GMYP)
0170            FMEE(M)=EGXP*EGYP
0171            DO 80 N=M,NEQ
0172            FN=FA(N)
0173            GN=GA(N)
0174            FNXL=FN*XL*(0.,-1.)
0175            GNYL=GN*YL*(0.,-1.)
0176            EGXL=CEXP(FNXL)
0177            EGYL=CEXP(GNYL)
0178            FNEE(N)=EGXL*EGYL
0179            IF(IGROND.EQ.1)CALL SMRFLD2(XP,YP,XL,YL,DM,ER2,SIG2,FMC,1,SUMT)
0180            IF(IGROND.EQ.1)NI=NI+1
0181            IF(IGROND.EQ.1)DCMN(M,N)=DCMN(M,N)+FMEE(M)*FNEE(N)*SUMT*CSF
0182            IF(ROH.GT.DX2)GO TO 35
0183            CMN(M,N)=CMN(M,N)+FMEE(M)*FNEE(N)*CIK
0184            GO TO 75
0185     35     BK=BKK(II,JJ)
0186            CMN(M,N)=CMN(M,N)+FMEE(M)*FNEE(N)*BK
0187     75     IF(IGROND.EQ.1)CMN(M,N)=CMN(M,N)+DCMN(M,N)
0188     80     CONTINUE
```

```
0189    140     CONTINUE
0190    160     CONTINUE
0191            TYPE*,'NJ=',NJ,'NI=',NI
0192            NI=0
0193            NJ=0
0194            IF(IWR.EQ.1) THEN
0195            WRITE(10,2)
0196            DO 210 M=1,NEQ
0197            DO 210 N=M,NEQ
0198            WRITE(10,3)M,N,CMN(M,N),DCMN(M,N),CIMN(M,N)
0199    210     CONTINUE
0200            END IF
0201            IF(IWR.EQ.1)WRITE(10,9)
0202            IF(IWR.EQ.1)WRITE(10,4)
0203            DO 500 JI=1,IBS
0204            IF(IBS.GT.1)PHI=(JI-1)*360./FLOAT(IBS-1)
0205            PH1=CX*PHI
0206            CS1=COS(PH1)
0207            SN1=SIN(PH1)
0208            XLS1=RLS*CS1
0209            YLS1=RLS*SN1
0210    C       SET UP THE VOLTAGE MATRIX COLUMN
0211            DO 240 M=1,NEQ
0212            FM=FA(M)
0213            GM=GA(M)
0214            SDD=(0.,0.)
0215            SEE=(0.,0.)
0216            DO 220 P=1,KK
0217            X=XM(P)
0218            Y=YM(P)
0219            FMXP=FM*X*(0.,-1.)
0220            GMYP=GM*Y*(0.,-1.)
0221            EGXP=CEXP(FMXP)
0222            EGYP=CEXP(GMYP)
0223            FMEE(M)=EGXP*EGYP
0224            IF(IPW.EQ.1)THEN
0225            IF(IGROND.EQ.1)TYPE*,'NO FORMULATION FOR P.W.REFLECTION YET!!!'
0226            PSI1=X*CS1+Y*SN1
0227            EGX1=CEXP(GAM2*PSI1)
0228            CV1=(1.,0.)*DX*DY
0229            GO TO 219
0230            END IF
0231            X1=XLS1-X
0232            Y1=YLS1-Y
0233            RH1=SQRT(X1*X1+Y1*Y1)
0234            CALL MBK0Z(GAM2*RH1,EGX1,-1)
0235            IF(IGROND.EQ.1)CALL SMRFLD2(X,Y,XLS1,YLS1,DM,ER2,SIG2,FMC,1,SUMT)
0236    219     VEE=EGX1
0237            IF(IGROND.EQ.1)SDD=SDD+FMEE(M)*SUMT
0238            SEE=SEE+FMEE(M)*VEE
0239    220     CONTINUE
0240            A(M)=SEE*CV1
0241            IF(IGROND.EQ.1)B(M)=SDD*C1*DXY
0242    240     CONTINUE
0243            IF(IWR.EQ.1)THEN
0244            DO 202 M=1,NEQ
0245    202     WRITE(10,5)M,A(M),B(M),(A(M)+B(M))
0246            WRITE(10,9)
0247            END IF
0248            IF(IGROND.EQ.1)THEN
0249            DO 204 M=1,NEQ
0250            A(M)=A(M)+B(M)
0251            DO 204 N=M,NEQ
```

```
0252    204     CMN(M,N)=CTMN(M,N)
0253            END IF
0254            ISYM=0
0255            CALL CROUT(CMN,A,ICC,ISYM,IWRC,I12,NEQ)
0256            IF(IWR.EQ.1)THEN
0257            WRITE(10,6)
0258            DO 244 M=1,NEQ
0259            WRITE(10,5)M,A(M)
0260    244     CONTINUE
0261            WRITE(10,9)
0262            END IF
0263            WRITE(8,*)KK,NX
0264    C       FIND THE FIELD IN CELLS OF FIRST QUADRANT
0265            IF(IFILD.NE.1) GO TO 45
0266            WRITE(10,8)
0267            DO 248 L=1,KK
0268            EZ1=(0.,0.)
0269            XL=XM(L)
0270            YL=YM(L)
0271            DO 246 N=1,NEQ
0272            FN=FA(N)
0273            GN=GA(N)
0274            FNXL=FN*XL*(0.,-1.)
0275            GNYL=GN*YL*(0.,-1.)
0276            EGXL=CEXP(FNXL)
0277            EGYL=CEXP(GNYL)
0278            FNEE(N)=EGXL*EGYL
0279            EZ1=EZ1+A(N)*FNEE(N)
0280    246     CONTINUE
0281    C       IF(XL.GT.0.AND.YL.GT.0) THEN
0282            RE=REAL(EZ1)
0283            AIE=AIMAG(EZ1)
0284            AMP=CABS(EZ1)
0285            PHASE=ATAN2(AIE,RE)/CX
0286            WRITE(10,11)XL,YL,AMP,PHASE
0287            WRITE(8,*)L,AMP,PHASE
0288    C       END IF
0289    248     CONTINUE
0290    45      IF(IWR.EQ.1)WRITE(10,9)
0291            PHS=PH1
0292            DO 500 JK=1,IBISS
0293            IF(IBISS.GT.1)THEN
0294            PHI=(JK-1)*360./FLOAT(IBISS-1)
0295            PHS=CX*PHI
0296            END IF
0297            XLS=RLS*COS(PHS)
0298            YLS=RLS*SIN(PHS)
0299    C       FIND THE BACKSCATTERED FIELD
0300            EZS=(.0,.0)
0301            EZSR=(0.,0.)
0302            DO 290 L=1,KK
0303            XL=XM(L)
0304            YL=YM(L)
0305            YY=YLS-YL
0306            YS=YY*YY
0307            XX=XLS-XL
0308            XS=XX*XX
0309            IF(IPW.EQ.1)THEN
0310            PSI=XL*COS(PHS)+YL*SIN(PHS)
0311            BK=CEXP(GAM2*PSI)
0312            GO TO 47
0313            END IF
0314            ROH=SQRT(XS+YS)
```

```
0315            CALL MBK0Z(GAM2*ROH,BK,-1)
0316            IF(IGROND.EQ.1)CALL SMRFLD2(XL,YL,XLS,YLS,DM,ER2,SIG2,FMC,1,SUMT)
0317    47      EZ1=(0.,0.)
0318            DO 260 N=1,NEQ
0319            FN=FA(N)
0320            GN=GA(N)
0321            FNXL=FN*XL*(0.,-1.)
0322            GNYL=GN*YL*(0.,-1.)
0323            EGXL=CEXP(FNXL)
0324            EGYL=CEXP(GNYL)
0325            FNEE(N)=EGXL*EGYL
0326            EZ1=EZ1+A(N)*FNEE(N)
0327    260     CONTINUE
0328            EZS=EZS+EZ1*BK
0329            IF(IGROND.EQ.1)EZSR=EZSR+EZ1*SUMT
0330    290     CONTINUE
0331            EZS=-CST*EZS
0332            EZSR=EZSR*C1*(0.,1.)*(EP1-EP2)*OMEGA*DXY
0333            EZS=EZS+EZSR
0334            IF(IPW.EQ.1)EZS=EZS*CSQRT(.5*PI/GAM2)
0335            AZS=CABS(EZS)
0336            IF(IWR.EQ.1)WRITE(10,*)'AZS=',AZS
0337            EWL=TP*AZS*AZS/WAV2
0338            DB=.0
0339    C       FIND THE NORMALIZED SCATTERING ATTENUATION FUNCTION
0340            IF(IPW.EQ.0)THEN
0341            GR=2.*GAM2*RLS
0342            CALL MBK0Z(GR,BK,-1)
0343            EZI=C1*BK
0344            AZI=CABS(EZI)
0345            IF(IWR.EQ.1)WRITE(10,*)'AZI=',AZI
0346            AZN=AZS/AZI
0347            DB=20.*ALOG10(AZN)
0348            TYPE1,NEQ,NX,NY,FMC,DB,PHI
0349            WRITE(10,1)NEQ,NX,NY,FMC,DB,PHI
0350            GO TO 599
0351            END IF
0352            TYPE1,NEQ,NX,NY,FMC,EWL,PHI
0353            WRITE(10,1)NEQ,NX,NY,FMC,EWL,PHI
0354    599     IF(IBS.EQ.1.AND.IBISS.EQ.1.AND.IFMC.EQ.1)GO TO 20
0355            I12=2
0356    500     CONTINUE
0357    600     CONTINUE
0358            IF(IPW.EQ.1)WRITE(10,14)
0359            IF(IPW.EQ.0)WRITE(10,13)
0360            WRITE(10,9)
0361            WRITE(10,*)' ER1 & SIG1 =',ER1,SIG1
0362            WRITE(10,*)' ER2 & SIG2 =',ER2,SIG2
0363            WRITE(10,*)' AWM & BWM =' ,AWM,BWM
0364            WRITE(10,*) 'RLS=',RLS,'PHI=',WPH
0365            call getcp(it2)
0366            time=(it2-it1)/100.
0367            WRITE(10,*) ' CPU TIME (SEC) =',TIME
0368            TYPE*,' CPU TIME (SEC) = ',TIME
0369            WRITE(10,*) 'RCYLEGP.FOR'
0370            WRITE(10,*)ER1,SIG1,ER2,SIG2,FMCMX,AWM,BWM,DM,XLS,YLS,IWR,IFILD,IWRC
0371          &,IPW,IBS,IBISS,IFMC,IEQ,IGROND
0372    1       FORMAT(1X,3I5,6F12.6)
0373    2       FORMAT(5X,'M',4X,'N',13X,'ZMN',21X,'DZMN',21X,'ZTMN')
0374    3       FORMAT(1X,2I5,8F12.6)
0375    4       FORMAT(5X,'M',18X,'VM',21X,'DVM',21X,'VTM')
0376    5       FORMAT(1X,I5,5X,8F12.6)
0377    6       FORMAT(5X,'M',18X,' A ')
```

```
0378    8       FORMAT(5X,'X',9X,'Y',13X,'AMPLITUDE',3X,'PHASE')
0379    9       FORMAT(1H0)
0380    11      FORMAT(1X,2F10.5,5X,2F12.6)
0381    13      FORMAT(3X,'NEQ',3X,'NX',3X,'NY',6X,'FMC',9X,'SAF',9X,'PHI')
0382    14      FORMAT(3X,'NEQ',3X,'NX',3X,'NY',6X,'FMC',9X,'EWL',9X,'PHI')
0383            CALL EXIT
0384            END
```

APPENDIX G

Program LSOIFP calculates near field patterns of electric or magnetic line sources on or off an interface between media I and II. The model for this program is Figure 5-3, except region I is not restricted to free space. The program always assumes the line source is in medium II, where in the limit it can be moved to be placed on the interface.

```
0001    C       PROGRAM (LSOIFP.FOR) CALCULATES THE PATTERN OF A UNIFORM
0002    C       ELECTRIC OR MAGNETIC LINE SOURCE ON OR OFF THE INTERFACE
0003    C       BETWWEN MEDIUM I (ABOVE I.F.) AND MEDIUM II (BELOW I.F.).
0004    C
0005    C  ------------------------------------------------------------------
0006    C       I01 = 1  ELECTRIC REF. COEF.
0007    C            -1  MAGNETIC REF. COEF.
0008    C             0  RC=1
0009    C            >1  RC=-1
0010    C       NANG =   NUMBER OF POINTS IN THE PATTERN.
0011    C       XP,YP=   LOCATION OF THE LINE SOURCE.
0012    C       D    =   X-LOCATIONS OF THE INTERFACE.
0013    C       R    =   RADIAL DISTANCE OF THE OBSERVATION POINT W.R.T.
0014    C                LINE SOURCE.
0015    C  ------------------------------------------------------------------
0016    C    WRITTEN BY JAMAL S. IZADIAN MARCH 1982
0017    C
0018            COMPLEX CJ,ET,SUMT,BK,BI,BK1,BI1,GAM1,GAM2,EP1,EP2
0019            COMPLEX CST1,CST2,BKI,BKII
0020            DATA PI,TP/3.14159265359,6.28318530718/
0021            DATA E0,U0/8.85418533677E-12,1.25663706144E-6/
0022            CJ=(0.,1.)
0023            READ(1,*)ER1,SIG1,ER2,SIG2,XP,YP,D,R,FMC,NANG,I01
0024            WRITE(10,*)NANG
0025            OMEGA=TP*FMC*1.E6
0026            EP1=CMPLX(E0*ER1,-SIG1/OMEGA)
0027            EP2=CMPLX(E0*ER2,-SIG2/OMEGA)
0028            GAM1=CJ*CSQRT(EP1*U0)*OMEGA
0029            GAM2=CJ*CSQRT(EP2*U0)*OMEGA
0030            IF(I01.EQ.1) CST2=(1.,0.)
0031            IF(I01.EQ.-1)CST2=EP2/E0
0032            IF(I01.EQ.1)CST1=(1.,0.)
0033            IF(I01.EQ.-1)CST1=EP1/E0
0034            PHI=0.
0035            CALL MBEZ10(GAM2*R,BI,BKII,BI1,BK1,0,-1)
0036            CALL MBEZ10(GAM1*R,BI,BKI,BI1,BK1,0,-1)
0037            DO 100 J=1,NANG
0038            IF(NANG.GT.1)PHI=FLOAT(J-1)*(TP/(NANG-1))
0039            XB=R*COS(PHI)
0040            YB=R*SIN(PHI)
0041            X=XP+XB
0042            Y=YP+YB
0043            IF(X.LT.D)THEN
0044            CALL SMRFLD(X,Y,XP,YP,D,ER2,SIG2,ER1,SIG1,FMC,I01,SUMT)
0045            ET=(BKII+SUMT)
0046            GO TO 101
0047            END IF
0048            CALL SMRFLD(X,Y,XP,YP,D,ER2,SIG2,ER1,SIG1,FMC,I01,SUMT)
0049            ET=SUMT
0050    101     PHY=PHI/.0174533
0051            WRITE(10,6)PHY,CABS(ET*CST2),CABS(EKI*CST1),CABS(EKII*CST2)
0052    100     CONTINUE
0053    6       FORMAT(1X,6F12.6)
0054            STOP
0055            END


0001    C
0002            SUBROUTINE SMRFLD(X,Y,XP,YP,D,ER2,SIG2,ER1,SIG1,FMC,I01,SUMT)
0003    C
0004    C       PROGRAM WRITTEN BY JAMAL S. IZADIAN NOV.-81
0005    C
0006            COMPLEX GAM2S,GAM2,F,FF,SUM1,SUM2,SUM3,SUM4,SUMT,EP2
```

```
0007            COMPLEX EP1,GAM0S,FQ,F0,RC,EF,BI,BK,BI1,BK1
0008            DATA PI,TP/3.14159265359,6.28318530718/
0009            DATA E0,U0/8.85418533677E-12,1.25663706144E-6/
0010    C       TYPE*,'ER1,SIG1,ER2,SIG2=',ER1,SIG1,ER2,SIG2
0011            D1=D-XP
0012            IF(X.GT.D)E=X-D
0013            ARG=2.*D-X-XP
0014            OMEGA=TP*FMC*1.E6
0015            EP2=CMPLX(ER2*E0,-SIG2/OMEGA)
0016            EP1=CMPLX(ER1*E0,-SIG1/OMEGA)
0017            GAM2S=-OMEGA*OMEGA*U0*EP2
0018            GAM2=CSQRT(GAM2S)
0019            GAM0S=-OMEGA*OMEGA*U0*EP1
0020            GC=OMEGA*SQRT(U0*ER2*E0)
0021            GCS=GC*GC
0022            G1=GC/SQRT(2.)
0023    C       SET UP FOR SUM1 & SUM2
0024            DEL=PI/10./(ARG+Y-YP)
0025            NS=G1/DEL
0026            IF(NS.LT.40) NS=40
0027            NP=2*(NS/2)
0028            DEL=G1/NP
0029            NP=NP+1
0030            DEL3=DEL/3.
0031            SUM1=(0.,0.)
0032            SUM2=(0.,0.)
0033            DO 100 I=1,2
0034            SIGN=1.
0035            DO 100 J=1,NP
0036            W=(3.-SIGN)*DEL3
0037            IF(J.EQ.1.OR.J.EQ.NP) W=DEL3
0038            IF(I.EQ.2)GO TO 31
0039            G=(J-1)*DEL
0040            GO TO 33
0041    31      B=(J-1)*DEL
0042            BS=B*B
0043            G=SQRT(GCS-BS)
0044    33      GS=G*G
0045            F=CSQRT(GAM2S+GS)
0046            F0=CSQRT(GAM0S+GS)
0047            IF(I01.EQ.1)RC=(F-F0)/(F+F0)
0048            IF(I01.EQ.-1)RC=(EP1*F-EP2*F0)/(EP1*F+EP2*F0)
0049            WRITE(8,*)'G,F,F0,RC=',G,F,F0,RC
0050            IF(IABS(I01).EQ.0)RC=(1.,0.)
0051            IF(IABS(I01).GT.1)RC=(-1,0.)
0052            IF(X.GT.D)RC=1.+RC
0053            IF(X.LE.D)EF=CEXP(-F*ARG)
0054            IF(X.GT.D)EF=CEXP(-F*D1-F0*H)
0055            CS=COS(G*(Y-YP))
0056            FF=RC*EF*CS
0057            IF(SIG2.NE.0.AND.I.EQ.2)FQ=B/F
0058            IF(SIG2.EQ.0.AND.I.EQ.2)FQ=(0.,-1.)
0059            IF(I.EQ.1)SUM1=SUM1+W*FF/F
0060            IF(I.EQ.2)SUM2=SUM2+W*FF*FQ/G
0061            SIGN=-SIGN
0062    100     CONTINUE
0063            ALPH1=5.*ANAX1(GC,CABS(GAM2),CABS(CSQRT(GAM0S)))
0064    C       SET UP FOR SUM3 & SUM4
0065            DELAL=DEL
0066            NS=ALPH1/DELAL
0067            IF(NS.LT.40)NS=40
0068            NP=2*(NS/2)
0069            DELAL=ALPH1/NP
```

```
0070            NP=NP+1
0071            SUM3=(0.,0.)
0072            SIGN=1.
0073            DELA3=DELAL/3.
0074            DO 200 I=1,NP
0075            W=(3.-SIGN)*DELA3
0076            IF(I.EQ.1.OR.I.EQ.NP)W=DELA3
0077            ALPHA=(I-1)*DELAL
0078            ALPHS=ALPHA*ALPHA
0079            G=SQRT(ALPHS+GCS)
0080            GS=G*G
0081            F=CSQRT(GAM2S+GS)
0082            F0=CSQRT(GAM0S+GS)
0083            IF(I01.EQ.1)RC=(F-F0)/(F+F0)
0084            IF(I01.EQ.-1)RC=(EP1*F-EP2*F0)/(EP1*F+EP2*F0)
0085            IF(IABS(I01).EQ.0)RC=(1.,0.)
0086            IF(IABS(I01).GT.1)RC=(-1.,0.)
0087            IF(X.GT.D)RC=1.+RC
0088            IF(X.LE.D)EF=CEXP(-F*ARG)
0089            IF(X.GT.D)EF=CEXP(-F*D1-F0*H)
0090            CS=COS(G*(Y-YP))
0091            FF=RC*EF*CS
0092            IF(SIG2.NE.0)FQ=ALPHA/F
0093            IF(SIG2.EQ.0)FQ=(1.,0.)
0094            SUM3=SUM3+W*FF*FQ/G
0095            SIGN=-SIGN
0096    200     CONTINUE
0097            SUMT=SUM1+SUM2+SUM3
0098    C       HH=2.*D1+(X-XP)
0099    C       ROH2=SQRT(HH*HH+(Y-YP)*(Y-YP))
0100    C       CALL MBEZ10(GAM2*ROH2,BI,BK,BI1,BK1,0,-1)
0101    C       TYPE*,'BK,SUMT=',BK,SUMT
0102            RETURN
0103            END
```

APPENDIX H

Subroutine MBEZ1ϕ (courtesy of Professor Richmond) is used to calculate the modified Bessel functions of order zero and one.

SZ: is the complex argument of the Modified Bessel Function to be calculated.

SBI: the calculated Modified Bessel Function of first kind of order zero.

SBK: the calculated Modified Bessel Function of second kind of order zero.

SBI1: the same as SBI except of order one.

SBK1: the same as SBK except of order one.

ID: if zero, only zero order functions are calculated. If one, only functions of order one are calculated. IF > 1, both orders of zeros and ones are calculated.

```
0001          SUBROUTINE MBEZ10(SZ,SBI,SBK,SBI1,SBK1,ID,ISC)
0002      C   DOUBLE PERCISION
0003      C   MODIFIED BESSEL FUNCTIONS WITH COMPLEX ARGUMENT
0004      C   ORDER ZERO AND ONE
0005      C   SET ISC=-1 TO AVOID SCALING.
0006      C   SET ISC=1 FOR SCALED FUNCTIONS.
0007      C   IF  ISC=1  AND REAL(Z).GE.0,  I(Z) = BI*CEXP(Z).
0008      C   IF  ISC=1  AND REAL(Z).LT.0,  I(Z) = BI/CEXP(Z).
0009      C   IF  ISC=1,  K(Z)= BK/CEXP(Z).
0010            REAL*8 ABT,ALG,AY,CT2,ST2,T1,X,Y,YP,AC2,AM,C,CY2,EMX2
0011            REAL*8 R2,STPR,XI,AC21,ARE,C2,DX,EPX2,R4,S,SY2,THETA
0012            REAL*8 XM,C57,PI,YT,AS2,PSI,RB,S2,T,TK,XP,YM
0013            REAL*8 IMIZ,IMKZ,R,REKZ,REIZ,ZRE,ZIM,Y2,T2
0014            COMPLEX SZ,SBI,SBK,SBI1,SBK1
0015          COMPLEX*16  BI0,BK0,FIZ,FKZ,Z,EZ
0016          COMPLEX*16  BI,BK,BI1,BK1
0017          COMPLEX*16  BIA,BIB,BIC,BKA,BKB,BKC,EA,EB,FA,AI
0018          DATA PI/3.1415926535897932/
0019          DATA FMX/1.E16/
0020            DATA C57/.5772156649015328/
0021            Z=SZ
0022          R=CDABS(Z)
0023          ZRE=DREAL(Z)
0024          ZIM=DIMAG(Z)
0025          THETA=DATAN2(ZIM,ZRE)
0026          C=ZRE/R
0027          S=ZIM/R
0028          BI=(.0,.0)
0029          BK=(.0,.0)
0030          BI1=(.0,.0)
0031          BK1=(.0,.0)
0032          IF(R.GT.9.)GO TO 10
0033          IF(ISC.LE.0)GO TO 8
0034          EX=DEXP(ZRE)
0035          EZ=EX*DCMPLX(DCOS(ZIM),DSIN(ZIM))
0036        8 ALG=DLOG(R/2.)+C57
0037          C2=2.*C*C-1.
0038          S2=2.*C*S
0039          R2=R/2.
0040          R4=R*R/4.
0041          GO TO 15
0042       10 R8=8.*R
0043          ARE=DABS(ZRE)
0044          EMX2=.0
0045          EPX2=.0
0046          IF(ARE.GT.40.)GO TO 11
0047          IF(ZRE.GE..0)EMX2=DEXP(-2.*ZRE)
0048          IF(ZRE.LT..0)EPX2=DEXP(2.*ZRE)
0049       11 IF(ISC.GT.0)GO TO 14
0050          IF(R.LT.80.)GO TO 12
0051            TYPE*,' ARGUMENT MAGNITUDE EXCEEDED 80 !!!'
0052            GO TO 81
0053       12   EX=DEXP(ZRE)
0054          EZ=EX*DCMPLX(DCOS(ZIM),DSIN(ZIM))
0055       14 Y2=2.*ZIM
0056          CY2=DCOS(Y2)
0057          SY2=DSIN(Y2)
0058          STPR=DSQRT(2.*PI*R)
0059          T2=THETA/2.
0060          CT2=DCOS(T2)
0061          ST2=DSIN(T2)
0062          TK=DSQRT(PI/(2.*R))
0063       15 NA=1
```

```
0064          NB=2
0065          IF(ID.EQ.0)NB=1
0066          IF(ID.EQ.1)NA=2
0067          DO 80 NP1=NA,NB
0068          N=NP1-1
0069          IF(R.GT.9.)GO TO 50
0070          AC2=C2
0071          AS2=S2
0072          T=1.
0073          X=1.
0074          Y=.0
0075          DO 20 J=1,1000
0076          T=T*R4/(J*(N+J))
0077          X=X+T*AC2
0078          Y=Y+T*AS2
0079          AY=DABS(Y)
0080          AM=DABS(X)
0081          IF(AY.GT.AM)AM=AY
0082          IF(T.LT.AM/FMX)GO TO 21
0083          AC21=AC2
0084          AC2=AC21*C2-AS2*S2
0085       20 AS2=AS2*C2+AC21*S2
0086       21 REIZ=X
0087          IMIZ=Y
0088          IF(N.EQ.0)GO TO 25
0089          REIZ=R2*(X*C-Y*S)
0090          IMIZ=R2*(X*S+Y*C)
0091       25 AC2=C2
0092          AS2=S2
0093          T=1.
0094          PSI=-ALG
0095          IF(N.EQ.1)PSI=.5-ALG
0096          X=PSI
0097          Y=-THETA
0098          DO 40 J=1,1000
0099          IF(N.EQ.1)GO TO 30
0100          PSI=PSI+1./J
0101          T=T*R4/(J*J)
0102          GO TO 35
0103       30 JP=(J+1)*J
0104          PSI=PSI+(J+.5)/JP
0105          T=T*R4/JP
0106       35 DX=T*(AC2*PSI+AS2*THETA)
0107          X=X+DX
0108          Y=Y+T*(AS2*PSI-AC2*THETA)
0109          AY=DABS(Y)
0110          AM=DABS(X)
0111          IF(AY.GT.AM)AM=AY
0112          IF(DABS(T*PSI).LT.AM/FMX)GO TO 41
0113          AC21=AC2
0114          AC2=AC21*C2-AS2*S2
0115       40 AS2=AS2*C2+AC21*S2
0116       41 REKZ=X
0117          IMKZ=Y
0118          IF(N.EQ.0)GO TO 70
0119          REKZ=C/R-(X*ZRE-Y*ZIM)/2.
0120          IMKZ=-S/R-(Y*ZRE+X*ZIM)/2.
0121          GO TO 70
0122       50 AC2=C
0123          AS2=S
0124          MU=4*N*N
0125          I=-1
0126          T=1.
```

```
0127          XM=1.
0128          YM=.0
0129          XP=1.
0130          YP=.0
0131          T1=1.
0132          DO 60 J=1,1000
0133          K=2*J-1
0134          T=(MU-K*K)*T/(J*R8)
0135          ABT=DABS(T)
0136          IF(ABT.LT.1.E-30)GO TO 61
0137          IF(ABT.GT.T1)GO TO 61
0138          T1=ABT
0139          XM=XM+I*T*AC2
0140          YM=YM-I*T*AS2
0141          XP=XP+I*AC2
0142          YP=YP-T*AS2
0143          AC21=AC2
0144          AC2=AC21*C-AS2*S
0145          AS2=AS2*C+AC21*S
0146       60 I=-I
0147       61 I=1
0148          IF(N.EQ.1)I=-1
0149          J=1
0150          IF(ZIM.LE.0)J=-1
0151          K=I*J
0152          IF(ZRE.GE..0)GO TO 66
0153          XI=-K*YP+(XM*CY2-YM*SY2)*EPX2
0154          YI= K*XP+(XM*SY2+YM*CY2)*EPX2
0155          GO TO 68
0156       66 XI=XM+K*(XP*SY2-YP*CY2)*EMX2
0157          YI=YM+K*(XP*CY2+YP*SY2)*EMX2
0158       68 REIZ=(XI*CT2+YI*ST2)/STPR
0159          IMIZ=(YI*CT2-XI*ST2)/STPR
0160          REKZ=TK*(XP*CT2+YP*ST2)
0161          IMKZ=TK*(YP*CT2-XP*ST2)
0162       70 FIZ=DCMPLX(REIZ,IMIZ)
0163          FKZ=DCMPLX(REKZ,IMKZ)
0164          IF(ISC.GT.0)GO TO 74
0165          IF(R.LE.9.)GO TO 78
0166          IF(ZRE.LT..0)FIZ=FIZ/EZ
0167          IF(ZRE.GE..0)FIZ=FIZ*EZ
0168          FKZ=FKZ/EZ
0169          GO TO 78
0170       74 IF(R.GT.9.)GO TO 78
0171          IF(ZRE.LT..0)FIZ=FIZ*EZ
0172          IF(ZRE.GE..0)FIZ=FIZ/EZ
0173          FKZ=FKZ*EZ
0174       78 IF(N.EQ.1)GO TO 79
0175          BI=FIZ
0176          BK=FKZ
0177          GO TO 80
0178       79 BI1=FIZ
0179          BK1=FKZ
0180       80 CONTINUE
0181       81    SBI=BI
0182             SBK=BK
0183             SBI1=BI1
0184             SBK1=BK1
0185          RETURN
0186          END
```

APPENDIX I

Subroutine CROUT (courtesy of Professor Richmond) uses Crout's method to solve a system of simultaneous linear equations.

C: the NxN matrix to be solved.

S: the excitation column as input, and the solution as output.

ICC: maximum number of linear equations or unknowns.

ISYM: set to zero if C is symmetric, otherwise set to 1.

IWR: if one, the subroutine prints some numerical values for debugging purposes, otherwise set to zero.

I12: if 1, inverts and solves, if 2, it only solves.

N: number of unknowns or linear equations to be solved.

```
0001          SUBROUTINE CROUT(C,S,ICC,ISYM,IWR,I12,N)
0002          COMPLEX C(ICC,ICC),S(1)
0003          COMPLEX F,P,SS,T
0004      1   FORMAT(15X,'LIST OF THE LOOP CURRENTS CJ(I)')
0005      2   FORMAT(5X,'I',3X,'MAGNITUDE',3X,'PHASE',5X,'REAL'
0006         2,5X,'IMAGINARY')
0007      3   FORMAT(1X,I5,F10.4,F10.1,2E12.4)
0008      5   FORMAT(1H0)
0009          IF(I12.NE.1)GO TO 22
0010          IF(N.EQ.1)S(1)=S(1)/C(1,1)
0011          IF(N.EQ.1)GO TO 39
0012          IF(ISYM.NE.0)GO TO 8
0013          DO 6 I=1,N
0014          DO 6 J=I,N
0015      6   C(J,I)=C(I,J)
0016      8   F=C(1,1)
0017          DO 10 L=2,N
0018      10  C(1,L)=C(1,L)/F
0019          DO 20 L=2,N
0020          LLL=L-1
0021          DO 20 I=L,N
0022          F=C(I,L)
0023          DO 11 K=1,LLL
0024      11  F=F-C(I,K)*C(K,L)
0025          C(I,L)=F
0026          IF(L.EQ.I)GO TO 20
0027          P=C(L,L)
0028          IF(ISYM.EQ.0)GO TO 15
0029          F=C(L,I)
0030          DO 12 K=1,LLL
0031      12  F=F-C(L,K)*C(K,I)
0032          C(L,I)=F/P
0033          GO TO 20
0034      15  F=C(I,L)
0035          C(L,I)=F/P
0036      20  CONTINUE
0037      22  DO 30 L=1,N
0038          P=C(L,L)
0039          T=S(L)
0040          IF(L.EQ.1)GO TO 30
0041          LLL=L-1
0042          DO 25 K=1,LLL
0043      25  T=T-C(L,K)*S(K)
0044      30  S(L)=T/P
0045          DO 38 L=2,N
0046          I=N-L+1
0047          II=I+1
0048          T=S(I)
0049          DO 35 K=II,N
0050      35  T=T-C(I,K)*S(K)
0051      38  S(I)=T
0052      39  IF(IWR.LE.0) GO TO 100
0053          WRITE(6,5)
0054          WRITE(6,1)
0055          WRITE(6,2)
0056          CNOR=.0
0057          DO 40 I=1,N
0058          SA=CABS(S(I))
0059      40  IF(SA.GT.CNOR)CNOR=SA
0060          IF(CNOR.LE.0.)CNOR=1.
0061          DO 44 I=1,N
0062          SS=S(I)
```

```
0063          SA=CABS(SS)
0064          SNOR=SA/CNOR
0065          PH=.0
0066          IF(SA.GT.0.)PH=57.29578*ATAN2(AIMAG(SS),REAL(SS))
0067       44 WRITE(6,3)I,SNOR,PH,SS
0068          WRITE(6,5)
0069      100 RETURN
0070          END
```

APPENDIX J

Program RECT (courtesy of Professor Richmond) modified slightly to calculate some curves for checking the results of some of the programs. It calculates the scattered electric field from a rectangular cylindrical scatterer considered throughout the dissertation. Some of the outputs of this program are included in Chapter III. This program uses Pusle Basis Point Matching (PBPM).

```
0001    C     LINK WITH CROUT & HANK
0002    C       THIS IS PROGRAM RECT.FOR FOR EZ POLARIZATION
0003    C
0004          COMPLEX H0,H1,ECM,EP,EZ,CII,CST
0005          COMPLEX C(500,500),V(500)
0006          DIMENSION X(500),Y(500)
0007          DATA ETA,PI,TP,E0/376.727,3.14159,6.28318,8.85E-12/
0008       1  FORMAT(1X,8E15.4)
0009       2  FORMAT(1X,3I5,8F12.6)
0010       5  FORMAT(1H0)
0011       7  FORMAT(7F10.5)
0012      11  FORMAT(1H1)
0013            call getcp(it1)
0014          IDM=500
0015            TYPE*,'GIVE IBS,IBISS,PHI='
0016            ACCEPT*,IBS,IBISS,PHI
0017            IFRSCT=IBISS
0018            IBISS=IABS(IBISS)
0019            WRITE(10,*)IBS,IBISS,IFMC
0020     201    TYPE*,'GIVE FMC,NY'
0021            ACCEPT*,FMC,NY
0022            IF(FMC.LT.0) GO TO 300
0023            SIG=.3E-3
0024          ER=4.
0025            OMEGA=TP*FMC*1.E6
0026          TD=SIG/(OMEGA*ER*E0)
0027          EP=ER*CMPLX(1.,-TD)
0028          ECM=EP-1.
0029            IFMC=1
0030            AM=1.
0031            BM=.5
0032            NX=(AM/BM)*NY
0033            WAV=300./FMC
0034            AL=AM/WAV
0035            TYPE*,'AL=',AL
0036            BL=BM/WAV
0037          AK=TP*AL
0038          BK=TP*BL
0039          DX=AK/NX
0040          DY=BK/NY
0041          K=0
0042          YY=DY/2.
0043          DO 20 J=1,NY
0044          XX=DX/2.
0045          DO 18 I=1,NX
0046          K=K+1
0047          X(K)=XX
0048          Y(K)=YY
0049       18 XX=XX+DX
0050       20 YY=YY+DY
0051          N=NX*NY
0052          CK=SQRT(DX*DY/PI)
0053          CALL HANK(CK,H0,H1,1)
0054          CII=1.+ECM*(.0,.5)*(PI*CK*H1-(.0,2.))
0055          B1=REAL(H1)
0056          CST=-(.0,1.)*(1.,1.)*CK*B1*ECM/(2.*1.414214)
0057          DO 200 I=1,N
0058          XI=X(I)
0059          YI=Y(I)
0060          C(I,I)=CII
0061          DO 200 J=I,N
0062          IF(J.EQ.I)GO TO 200
```

```
0063          XJ=X(J)
0064          YJ=Y(J)
0065          R=SQRT((XJ-XI)**2+(YJ-YI)**2)
0066          CALL HANK(R,H0,H1,0)
0067          C(I,J)=.5*PI*CK*(.0,1.)*ECM*B1*H0
0068        200 CONTINUE
0069          I12=1
0070            DO 600 JI=1,IBS
0071            IF(IBS.GT.1)PHI=(JI-1)*360./FLOAT(IBS-1)
0072          PHR=.0174533*PHI
0073          CPH=COS(PHR)
0074          SPH=SIN(PHR)
0075            DO 202 I=1,N
0076          XI=X(I)
0077          YI=Y(I)
0078          PSI=XI*CPH+YI*SPH
0079          V(I)=CMPLX(COS(PSI),SIN(PSI))
0080        202   CONTINUE
0081          IWR=0
0082          ISYM=0
0083          CALL CROUT(C,V,IDM,ISYM,IWR,I12,N)
0084            I12=2
0085        C     DO 220 J=1,4
0086        C     NS=55+J*10
0087        C     DO 220 I=NS,NS+5
0088        C     FACT=WAV/TP
0089        C     WRITE(10,*)'X=',(X(I)*FACT),'Y=',(Y(I)*FACT)
0090        C     RE=REAL(V(I))
0091        C     AIE=AIMAG(V(I))
0092        C     AMP=CABS(V(I))
0093        C     PHAS=ATAN2(AIE,RE)/.0174533
0094        C     WRITE(10,*)'EZ1=',AMP,'PHASE=',PHAS
0095        C220  CONTINUE
0096            IF(IFRSCT.EQ.-1)PHR=PHR+PI
0097            DO 600 JK=1,IBISS
0098            IF(IBISS.GT.1)THEN
0099            PHI=(JK-1)*360./FLOAT(IBISS-1)
0100            PHR=.0174533*PHI
0101            END IF
0102          CPH=COS(PHR)
0103          SPH=SIN(PHR)
0104          EZ=(.0,.0)
0105          DO 250 I=1,N
0106          PSI=X(I)*CPH+Y(I)*SPH
0107        250 EZ=EZ+V(I)*CMPLX(COS(PSI),SIN(PSI))
0108          EZ=CST*EZ
0109          EZA=CABS(EZ)
0110          EWL=TP*EZA*EZA
0111          WRITE(10,2)N,NX,NY,FMC,EWL,PHI
0112          TYPE2,N,NX,NY,FMC,EWL,PHI
0113          IF(IBS.EQ.1.AND.IBISS.EQ.1)GO TO 201
0114        600   CONTINUE
0115            WRITE(10,*)'      FMC        EWL    NX   XY   '
0116        300   call getcp(it2)
0117            WRITE(10,*)'PHI=',PHI
0118            WRITE(10,*)'AWM=',AM,'EWM=',EM
0119            time=(it2-it1)/100.
0120            type*,'cpu time secs=',time
0121          CALL EXIT
0122          END
```

APPENDIX K

Program SQCYLH (courtesy of Professor Richmond) modified slightly to calculate magnetic scattered field from a rectangular cylindrical geometry considered in this dissertation. Some of the outputs of this program is included in Chapter IV. It uses Pulse Basis Point Matching (PBPM).

```
0001    C       LINK WITH CROUT & DMBEZ10
0002            COMPLEX CMN(500,500),A(500)
0003            COMPLEX EGR,GP,GR,HZI,HZS,CJX,CJY,BKK,BKX,BKY
0004            COMPLEX EP1,EP2,ETA2,GAM2,CST,BI,BK,BI1,BK1
0005            DIMENSION XM(500),YM(500)
0006            DATA FP/12.5663706144/
0007            DATA ETA,PI,TP/376.730366239,3.14159265359,6.28318530718/
0008            DATA E0,U0/8.85418533677E-12,1.25663706144E-6/
0009      1     FORMAT(1X,2I5,6F12.3)
0010      2     FORMAT(1X,F12.6,I5,6F12.6)
0011      5     FORMAT(1H0)
0012    9         FORMAT(1X,3I5,6F12.6)
0013              READ(7,*)ER1,SIG1,ER2,SIG2,FMCMX,AWM,BWM,DM,XLS,YLS,IWR,
0014           &IFILD,IWRC,IPW,IBS,IBISS,IFMC,ICMN
0015              WRITE(10,*)MAX(IBS,IBISS,IFMC)
0016              CALL GETCP(IT1)
0017      20    TYPE*,'GIVE FMC,NYY'
0018              ACCEPT*,FMC,NYY
0019              I12=1
0020            ICC=500
0021              CX=.0174533
0022              PHI=ATAN2(YLS,XLS)/CX
0023              RLS=SQRT(XLS*XLS+YLS*YLS)
0024            PH=CX*PHI
0025            AM=AWM/2.
0026            BM=BWM/2.
0027              DO 500 JF=1,IFMC
0028              IF(IFMC.GT.1)FMC=JF*FMCMX/FLOAT(IFMC)
0029            OMEGA=TP*FMC*1.E6
0030            BET1=OMEGA*SQRT(U0*ER1*E0)
0031            EP1=CMPLX(ER1*E0,-SIG1/OMEGA)
0032            EP2=ER2*E0*(1.,.0)
0033            IF(SIG2.GT.1.E-10)EP2=CMPLX(ER2*E0,-SIG2/OMEGA)
0034            ETA2=CSQRT(U0/EP2)
0035            GAM2=OMEGA*CSQRT(-U0*EP2)
0036              WAV2=300./FMC/SQRT(ER2)
0037    C        NY=5.*BET1*AWM/TP
0038            NY=NYY
0039              NY2=NY/2
0040              NY=2*NY2
0041            IF(NY.LT.2)NY=2
0042              NX=INT(AM/BM)*NY
0043            NX2=NX/2
0044            NX=2*NX2
0045            NEQ=NX*NY
0046            IF(NEQ.GT.ICC)GO TO 600
0047            DX=AWM/NX
0048            DY=BWM/NY
0049            DX2=DX/2.
0050              DY2=DY/2.
0051            CM=DX/SQRT(PI)
0052            CALL MBEZ10(GAM2*CM,BI,BK,BI1,BK1,1,0)
0053            CST=-CM*(EP1-EP2)*BI1/(DX*EP1)
0054            M=0
0055            Y=-BM+DY2
0056            DO 40 J=1,NY
0057            X=-AM+DX2
0058            DO 30 I=1,NX
0059            M=M+1
0060            XM(M)=X
0061            YM(M)=Y
0062      30    X=X+DX
0063      40    Y=Y+DY
```

```
0064           IF(ICMN.EQ.0)GO TO 299
0065         DO 50 J=1,NEQ
0066         DO 45 I=1,NEQ
0067      45 CMN(I,J)=(.0,.0)
0068      50 CMN(J,J)=(1.,.0)
0069         DO 200 M=1,NEQ
0070         X=XM(M)
0071         Y=YM(M)
0072         DO 180 N=1,NEQ
0073         IF(M.EQ.N)GO TO 180
0074         XN=XM(N)
0075         YN=YM(N)
0076         XX=X-XN
0077         YY=Y-YN
0078         RH=SQRT(XX*XX+YY*YY)
0079         CALL MBEZ10(GAM2*RH,BI,BK,BI1,BK1,1,0)
0080         BK1=CST*BK1/RH
0081         J=1+(N-1)/NX
0082         I=N-(J-1)*NX
0083         NP=N
0084         IF(I.GT.NX2)NP=N-1
0085         NU=N
0086         IF(J.GT.NY2)NU=N-NX
0087         NV=NU+NX
0088         NQ=NP+1
0089         CMN(M,NP)=CMN(M,NP)-XX*BK1
0090         CMN(M,NQ)=CMN(M,NQ)+XX*BK1
0091         CMN(M,NU)=CMN(M,NU)-YY*BK1
0092         CMN(M,NV)=CMN(M,NV)+YY*BK1
0093     180 CONTINUE
0094     200 CONTINUE
0095     299   CONTINUE
0096           DO 500 JI=1,IBS
0097           IF(IBS.GT.1)PHI=(JI-1)*360./FLOAT(IBS-1)
0098           PH=CX*PHI
0099           CPH=COS(PH)
0100           SPH=SIN(PH)
0101           XLS=RLS*CPH
0102           YLS=RLS*SPH
0103         DO 240 M=1,NEQ
0104         X=XM(M)
0105         Y=YM(M)
0106         IF(IPW.EQ.0)GO TO 238
0107         PSI=X*CPH+Y*SPH
0108         GP=GAM2*PSI
0109         EGR=CEXP(GP)
0110         GO TO 240
0111     238 XX=XLS-X
0112         YY=YLS-Y
0113         YS=YY*YY
0114         RH=SQRT(XX*XX+YS)
0115         GR=GAM2*RH
0116         CALL MBEZ10(GR,BI,BK,BI1,BK1,0,0)
0117         EGR=BK
0118     240 A(M)=EGR
0119         IWRC=0
0120         ISYM=1
0121           IF(ICMN.EQ.0.AND.JI.EQ.1)THEN
0122           DO 298 M=1,NEQ
0123           DO 298 N=1,NEQ
0124     298   READ(8,*)CMN(M,N)
0125           I12=2
0126           END IF
```

```
0127          CALL CROUT(CMN,A,ICC,ISYM,IWRC,I12,NEQ)
0128            IF(ICMN.EQ.1.AND.JI.EQ.1)THEN
0129            DO 300 M=1,NEQ
0130            DO 300 N=1,NEQ
0131    300     WRITE(6,*)CMN(M,N)
0132            END IF
0133            DO  500 JK=1,IBISS
0134            IF(IBISS.GT.1)THEN
0135            PHI=(JK-1)*360./FLOAT(IBISS-1)
0136            PHS=CX*PHI
0137            CPH=COS(PHS)
0138            SPH=SIN(PHS)
0139            XLS=RLS*CPH
0140            YLS=RLS*SPH
0141            END IF
0142          HZS=(.0,.0)
0143          DO 280 N=1,NEQ
0144          X=XM(N)
0145          Y=YM(N)
0146            IF(IFILD.EQ.1)THEN
0147            RE=REAL(A(N))
0148            AIE=AIMAG(A(N))
0149            PHASE=ATAN2(AIE,RE)/.0174533
0150            AMP=CABS(A(N))
0151            WRITE(10,*)'X,Y,AMP,PHASE=',X,Y,AMP,PHASE
0152            END IF
0153          J=1+(N-1)/NX
0154          I=N-(J-1)*NX
0155          NP=N
0156          IF(I.GT.NX2)NP=N-1
0157          NQ=NP+1
0158          NU=N
0159          IF(J.GT.NY2)NU=N-NX
0160          NV=NU+NX
0161          CJX=A(NV)-A(NU)
0162          CJY=A(NQ)-A(NP)
0163          IF(IPW.EQ.0)GO TO 270
0164          PSI=X*CPH+Y*SPH
0165          GP=CEXP(GAM2*PSI)
0166          HZS=HZS+GP*(CJX*SPH+CJY*CPH)
0167          GO TO 280
0168      270 XX=XLS-X
0169          YY=YLS-Y
0170          RH=SQRT(XX*XX+YY*YY)
0171          GR=GAM2*RH
0172          CALL MBEZ10(GR,BI,BK,BI1,BK1,1,0)
0173          HZS=HZS+(YY*CJX+XX*CJY)*BK1/RH
0174      280 CONTINUE
0175          HZS=-CST*HZS
0176          IF(IPW.EQ.1)THEN
0177            HZS=HZS*CSQRT(.5*PI/GAM2)
0178          AZS=CABS(HZS)
0179          EWL=TP*AZS*AZS/WAV2
0180            TYPE9,NEQ,NX,NY,FMC,EWL,PHI
0181            WRITE(10,9)NEQ,NX,NY,FMC,EWL,PHI
0182            GO TO 400
0183            END IF
0184          GR=2.*GAM2*RLS
0185          CALL MBEZ10(GR,BI,BK,BI1,BK1,0,0)
0186          AZS=CABS(HZS)
0187          HZI=BK
0188          AZI=CABS(HZI)
0189          AZN=AZS/AZI
```

```
0190          DB=20.*ALOG10(AZN)
0191            TYPE9,NEQ,NX,NY,FMC,DB,PHI
0192            WRITE(10,9)NEQ,NX,NY,FMC,DB,PHI
0193    C      IF(NYY.LT.100)GO TO 20
0194    400     IF(IBS.GT.1)I12=2
0195    500     CONTINUE
0196            CALL GETCP(IT2)
0197            TIME=(IT2-IT1)/100.
0198            WRITE(10,*)'ER1 & SIG1=', ER1,SIG1
0199            WRITE(10,*)'ER2 & SIG2=',ER2,SIG2
0200            WRITE(10,*)'FMC ,XLS ,PHI  =',FMC,XLS,PHI
0201            WRITE(10,*)'AM=',AM
0202            WRITE(10,*)'CPU TIME=',TIME,'SEC'
0203            WRITE(10,*)'SQCYLH.FOR'
0204      600 CALL EXIT
0205          END
```

LIST OF REFERENCES

[1] Harrington, R.F., "Field Computation by Moment Methods", MacMillan Company, New York, New York, 1968.

[2] Richmond, J.H., "Scattering by a Dielectric Cylinder of Arbitrary Cross Section", IEEE Trans. Antennas and Propagation, 13(3), pp. 334-341, 1965.

[3] Richmond, J.H., "T.E. Scattering by a Dielectric Cylinder of Arbitrary Shape", IEEE Trans. Antennas and Propagation, 14(4), pp. 460-464, 1966.

[4] Ward, S.H., "Electrical Electromagnetic and Magnetotelluric Methods", Geophysics, 45(1), pp. 1659-1666, 1980.

[5] Parry, J.R. and S.H. Ward, "Electromagnetic Scattering from Cylinders of Arbitrary Cross Section in a Conducting Half Space", Geophysics, 36(1), pp. 67-100, 1971.

[6] D'Yakonov, B.P., "The Diffraction of Electromagnetic Waves by a Circular Cylinder in a Homogeneous Half Space", Bull. Acad. Sci. USSR, Geophys. Ser., 11, pp. 1120-1125, 1959.

[7] Howard, A.Q., "The Electromagnetic Fields of a Subterranean Cylindrical Inhomogeneity Excited by a Line Source", Geophysics, 37(6), pp. 975-984, 1972.

[8] Ogunade, S.O., "Electromagnetic response of an Embedded Cylinder for Line Current Excitation", Geophysics, 46(1), pp. 45-52, 1981.

[9] Peters, L., Jr. and J.H. Richmond, "Scattering from Cylindrical Inhomogeneities in a Lossy Medium", Radio Science, 17(5), pp. 973-987, 1982.

[10] Ogunade, S.O. and H.W. Dosso, "The Inductive Response of a Horizontal Conducting Cylinder Buried in a Uniform Earth for a Uniform Inducing Field", Geophysical Prospecting, 28, pp. 601-609, 1980.

[11] Mei, K. and J. VanBladel, "Low-frequency Scattering by Rectangular Cylinder", IEEE Trans. Antennas and Propagation, pp. 52-56, January 1963.

[12] Hohmann, G.W., "Electromagnetic Scattering by Two-Dimensional Inhomogeneities in the Earth", Ph.D. dissertation, University of California at Berkeley.

[13] Chang, S.K. and K.K. Mei, "Application of the Unimoment Method to Electromagnetic Scattering of Dielectric Cylinders", IEEE Trans. Antennas and Propagation, 24(1), pp. 35-42, 1976.

[14] Chang, S.K., "On EM-Wave Scattering by Buried Obstacles", Ph.D. dissertation, University of California at Berkeley, June 1977.

[15] Mei, K.K., J.F. Hunka and S.K. Chang, "Recent Developments in the Unimoment Method", Acoustic Electromagnetic and Elastic Waves Scattering-Focus on the T-Matrix Approach, edited by V.K. and V.V. Varadan, pp. 485-506, Pergamon, New York, 1979.

[16] Young, J.D., "A Transient Underground Radar for Buried Pipe Location", 1975 USNC/URSI meeting, Boulder, Colorado, October 23, 1975.

[17] Young, J.D. and R. Caldecott, "Underground Pipe Detector", U.S. Patent 3,967,282, June 29, 1976.

[18] Burrell, G.A. and L. Peters, Jr., "Design of Electromagnetic Pulse (EMP) Radars for Geological Exploration at Depths of Several Kilometers", The Ohio State University ElectroScience Laboratory, Department of Electrical Engineering, February 1976.

[19] Davis, C.W., III, "The Design and Analysis of a Transient Electromagnetic Antenna for Subsurface Radar Applications", M.Sc. Thesis, The Ohio State University ElectroScience Laboratory, Department of Electrical Engineering, June 1975.

[20] Burrell, G.A., L. Peters, Jr., and A.J. Terzuoli, Jr., "The Propagation of Electromagnetic Video Pulse with Application to Subsurface Radar for Tunnel Application", Report 784460-2, The Ohio State University ElectroScience Laboratory, Department of Electrical Engineering; prepared under Contract DAAG53-76-C-0179 for U.S. Army Mobility Equipment Research and Development Command, Ft. Belvoir, Virginia, October 1976.

[21] Peters, L., Jr., G.A. Burrell, and H.B. Tran, "A Scattering Model for Detection of Tunnels Using Video Pulse Systems", Report 784460-3, The Ohio State University ElectroScience Laboratory,

Department of Electrical Engineering; prepared under Contract DAAG53-76-C-0179 for U.S. Army Mobility Equipment Research and Development Command, Ft. Belvoir, Virginia, February 1977.

[22] Peters, Jr., L. and D.L. Moffatt, "Electromagnetic Pulse Soundings for Geological Surveying with Application in Rock Mechanics and Rapid Excavation Program", Report 3190-2, The Ohio State University ElectroScience Laboratory, Department of Electrical Engineering; prepared under Contract H0210042 for U.S. Department of Interior, Bureau of Mines, September 1972.

[23] Moffatt, D.L., R.J. Puskar, and L. Peters, Jr., "Electromagnetic Pulse Sounding for Geological Surveying with Applications in Rock Mechanics and the Rapid Excavation Program", Report 3408-1, The Ohio State University ElectroScience Laboratory, Department of Electrical Engineering; prepared under Contract H0230009 for U.S. Department of Interior, Bureau of Mines, April 1973.

[24] Moffatt, D.L. and L. Peters, Jr., "An Electromagnetic Pulse Hazard Detection System", The Ohio State University ElectroScience Laboratory, reprinted from the Proceedings of the 1972 North American Rapid Excavation and Tunnelling Conference, June 1972.

[25] Caldecott, R., D.A. Irons, Jr., D.L. Moffatt, L. Peters, Jr., R.J. Puskar, J.F. Toth, and J.D. Young, "Electromagnetic Pulse Sounding for Surveying Underground Water", Report 401X-1, The Ohio State University ElectroScience Laboratory, Department of Electrical Engineering; prepared under Contract N00019-72-C-0184 for Naval Air Systems Command, October 1972.

[26] Puskar, R.J., "The Use of Electromagnetic Video Pulses in Subsurface Remote Sensing", M.Sc. Thesis, The Ohio State University ElectroScience Laboratory, Department of Electrical Engineering, 1973.

[27] Hayes, P.K., "An On-Site Method of Measuring the Dielectric Constant and Conductivity of Soils over a One Gigahertz Bandwidth", M.Sc. Thesis, The Ohio State University ElectroScience Laboratory, Department of Electrical Engineering, June 1979.

[28] Izadian, J.S., "An Underground Near-Field Antenna Pattern Range", Quarterly Report 529081-3, The Ohio State University ElectroScience Laboratory, Department of Electrical Engineering; prepared under Contract No. 5014-352-0234 for Gas Research Institute, July 1980.

[29] Izadian, J.S. and J.D. Young, "Measurement of Surface Coupled Antennas for Subsurface Radar Probing", proceedings of AMTA meeting, Los Cruces, New Mexico, October 1982.

[30] Young, J.D., D.L. Moffatt, and E.M. Kennaugh, "Time-Domain Radar Signature Measurement Techniques", Report 2467-3, The Ohio State University ElectroScience Laboratory, Department of Electrical Engineering; prepared under Contract F33620-67-C-0095 for Air Force Cambridge Research Laboratories, July 30, 1969.

[31] Young, J.D., "Target Imaging from Multiple-Frequency Radar Returns", Report 2768-6, The Ohio State University ElectroScience Laboratory, Department of Electrical Engineering; prepared under Grant AFOSR-69-1710 for Air Force Office of Scientific Research, June 1971.

[32] Chan, L.C., "Subsurface Electromagnetic Target Characterization and Identification", Ph.D. dissertation, The Ohio State University ElectroScience Laboratory, Department of Electrical Engineering, June 1979.

[33] Chan, L.C., D.L. Moffatt, and L. Peters, Jr., "Surface Radar Target Imaging Estimates", IEEE Trans. Antennas and Propagation, 29(2), pp. 413-417, 1981.

[34] Chan, L.C., D.L. Moffatt, and L. Peters, Jr., "Estimation of Complex Natural Resonances of a Class of Subsurface Targets", Acoustic, Electromagnetic and Elastic Wave Scattering-Focus on the T-Matrix Approach, edited by V.K. and V.V. Varadan, Pergamon, New York, 1982.

[35] Young, J.D., "Approximate Image Reconstruction from Transient Signature", Acoustic, Electromagnetic and Elastic Wave Scattering-Focus on the T-Matrix Approach, edited by V.K. and V.V. Varadan, Pergamon, New York, 1982.

[36] Davis, C.W., III, "A Computational Model for Subsurface Propagation and Scattering for Antennas in the Presence of a Conducting Half Space", Report 479X-7, The Ohio State University ElectroScience Laboratory, Department of Electrical Engineering; prepared for Columbia Gas System Service Corporation, October 1979.

[37] Rhodes, D.R., "On the Theory of Scattering by Dielectric Bodies", Rep. 475-1, Antenna Laboratory, The Ohio State University, Columbus, Ohio, 1953.

[38] Peters, L., Jr. and J.H. Richmond, "Scattering from Cylindrical Inhomogeneities in a Lossy Medium", Radio Science, 17(5), pp. 973-987, 1982.

[39] Harrington, R.F., "Time-Harmonic Electromagnetic Fields", McGraw-Hill, p. 126, 1961.

[40] Richmond, J.H., "Scattering by a Dielectric Cylinder of Arbitrary Cross Section", IEEE Trans. Antennas and Propagation, 13(3), pp. 334-341, 1965.

[41] Tyras, G., "Radiation and Propagation of Electromagnetic Waves", Academic Press, p. 115, 1969.

[42] Peters, L., Jr., G.A. Burrell, and H.B. Tran, "A Scattering Model for Detection of Tunnels Using Video Pulse Systems", Report 784460-3, The Ohio State University ElectroScience Laboratory, Department of Electrical Engineering; prepared under Contract DAAG53-76-C-0179 for U.S. Army Mobility Equipment Research and Development Command, Ft. Belvoir, Virginia, February 1977.

[43] Richmond, J.H., "Scattering by a Dielectric Cylinder of Arbitrary Cross Section", IEEE Trans. Antennas and Propagation, 13(3), pp. 334-341, 1965.

[44] Schelkunoff, S.A., "On Diffraction and Radiation of Electromagnetic Waves", Physical Review, Vol. 56, pp. 308-316, August 15, 1939.

[45] Richmond, J.H., "Scattering by a Dielectric Cylinder of Arbitrary Cross Section", IEEE Trans. Antennas and Propagation, 13(3), pp. 334-341, 1965.

[46] Banos, A., Jr., Dipole Radiation in the Presence of a Conducting Half-Space", Pergamon Press, 1966.

[47] Peters, L., Jr., G.A. Burrell, and H.B. Tran, "A Scattering Model for Detection of Tunnels Using Video Pulse Systems", Report 784460-3, The Ohio State University ElectroScience Laboratory, Department of Electrical Engineering; prepared under Contract DAAG53-76-C-0179 for U.S. Army Mobility Equipment Research and Development Command, Ft. Belvoir, Virginia, February 1977.

[48] Dahlquist, G., A. Bjork, translated by N. Anderson, "Numerical Methods", Prentice-Hall, Englewood Cliff, New Jersey, pp. 157-158, 1974.

[49] Stutzman, W.L., and G.A. Thiele, "Antenna Theory and Design", John Wiley and Sons, pp. 140-141, 1981.

[50] Digital Equipment Corportation, "VAX-Architecture Handbook 1981-82", Maynard, Massachusetts, 1981.

[51] Collines, R.E., "Field Theory of the Guided Waves", McGraw-Hill, New York, p. 454, 1960.

[52] Davis, C.W., III, "A Computational Model for Subsurface Propagation and Scattering for Antennas in the Presence of a Conducting Half Space", Report 479X-7, The Ohio State University ElectroScience Laboratory, Department of Electrical Engineering; prepared for Columbia Gas System Service Corporation, October 1979.